THE ROLE OF CALNEXIN, CALRETICULIN AND HEAVY CHAIN GLYCOSYLATION IN MHC CLASS I ASSEMBLY

Thesis submitted in partial fulfilment of the requirements for the degree of

Doctor of Philosophy, University of Oxford

Raju Adhikari

Christ Church College
Oxford
&
Molecular Immunology Group
Nuffield Department of Clinical Medicine
John Radcliffe Hospital
University of Oxford
Oxford OX3 9DS

Hillary Term, May 2002

AUTHORSHIP DECLARATION

**I declare that this thesis represents entirely my work,
except where acknowledged below.
This thesis has not been submitted for any other degree.**

The antigen presentation experiments described in Chapter 3 Section 3.5 of the text were performed by Drs Ann Hill and Marielle Gold (Oregon Health Sciences University, Oregon, USA), and Mark Howarth and Dr Awen Gallimore (University of Oxford, UK). Dr. Bin Gao (University of Oxford, UK) performed the TAP coimmunoprecipitation experiments.

The CTL experiments performed to study the effect of MHC class I heavy chain glycosylation on antigen presentation was done in collaboration with Mr Andy King, FRCS (University of Southampton, UK). The results are described in Chapter 5, Section 5.5.

The calcium measurement experiments described in Chapter 6, Section 6.5 were carried out in collaboration with Dr Grant Churchill (Department of Pharmacology, University of Oxford, UK).

The Biacore results described in Chapter 5, Section 5.6 were carried out in collaboration with Dr Paul Eggleton (Department of Biochemistry, University of Oxford, UK)

Publications resulting from this work include:

*Gao B, **R Adhikari***, *Howarth M, Nakamura K, Gold MC, Hill AB, Knee R, Michalak M, Elliott T. Assembly and antigen-presenting function of MHC class I molecules in cells lacking the ER chaperone calreticulin. Immunity16: 99-109, 2002.*
(A copy of the article is attached to the thesis).

***Joint first author**

Raju Adhikari and Tim Elliott. Assembly of major histocompatibility complex class I and class II molecules. Recent Res. Devel. Immunology, 2 (2000): 323-346.
(A copy of the article is attached to the thesis).

Raju Adhikari and Tim Elliott. The role of calnexin and calreticulin in MHC class I assembly. Calreticulin, 2nd Edition (Landes Bioscience. Edited by Paul Eggleton and Marek Michalak.
(This will be published in December 2002, and a copy of the article is attached to the thesis)

D. Phil Thesis Hillary 2002 **Raju Adhikari**

Nuffield Department of Clinical Medicine and Christ Church College

ABSTRACT

THE ROLE OF CALNEXIN, CALRETICULIN AND HEAVY CHAIN GLYCOSYLATION IN MHC CLASS I ASSEMBLY

Class I heavy chain (HC) must assemble with β2-microglobulin (β2m) and acquire optimal peptide in order to be presented to cytotoxic T cells (CTLs). Calnexin is involved in the initial folding of class I HC and subsequent assembly with β2m. Incorporation of "empty" or suboptimally loaded class I molecules into the multimolecular loading complex is essential for them to acquire optimal peptides. The loading complex consists of several cofactors: TAP, tapasin, ERp57 and calreticulin. The precise role of calnexin and calreticulin in the regulated assembly and peptide loading and the significance of their physical interaction with other cofactors of the loading as well as preloading complex still remains unclear.

Using mouse fibroblasts that lack calreticulin, I have studied the role of calreticulin in the assembly and loading of H2-K^b and H2-D^b expressed in these cells. MHC class I molecules in calreticulin-deficient cells are able to assemble with β2m normally, but their subsequent loading with optimal, stabilising peptides is defective despite their ability to interact with the TAP complex. The "empty" or suboptimally loaded class I molecules exit the ER rapidly. Reflecting the loading defect, presentation of endogenously processed antigens by class I molecules in calreticulin-deficient cells is impaired.

I have used a human calnexin-deficient cell line CEM.NK^R to study assembly of class I in the absence of calnexin. The results demonstrate that contrary to current understanding, calnexin has an important role in class I HC assembly with β2-microglobulin.

The role of heavy chain glycosylation in class I biogenesis is still controversial. My findings suggest asparagine (N)-linked glycosylation of human class I heavy chain at position 86 is optimal and any deviations from "normal" glycosylation results in poor loading with peptides and some defect in the assembly with β2m. Despite affecting the loading function, glycosylation did not have significant effect on presentation of a high affinity binding epitope to HLA-A*0201 specific CTLs.

Finally, I show that co-operation from all domains of calreticulin is essential in order to generate a fully functional calreticulin. Interestingly, proline-rich (P) –domain of calreticulin downregulated expression of a number of cellular proteins including MHC class I HC, despite restoring the cytosolic calcium levels in calreticulin-deficient cells. The effect of P-domain on class I expression was at the level of transcription.

ACKNOWLEDGEMENTS

I would like to thank my supervisor Professor Tim Elliott for allowing me to undertake the research in his lab. Tim was a constant inspiration for me, both in and outside of work. In the lab, I thank him for his dedicated supervision and for sharing his enthusiasm about Immunology. Outside work, I thank him for listening to my own personal problems, guidance and his continual support. I also thank Tim for reading drafts of this thesis and for his suggestions for improvements. I would also like to thank Professor Andrew McMichael for being my second supervisor and for all the help and guidance.

Thank you to all the members of the group, past and present, especially to Cheryl, Bin, Mark, Denise, Nasia, Tony, Chen Au, Angela and Manita, for creating an amazing research environment. Thank you Mark for organising fruitful lab meetings and interesting journal clubs. Special thanks are due to Cheryl Bailey for training me in tissue culture and to Dr Bin Gac for his expertise in Molecular Biology techniques in the early days of my DPhil.

A huge debt of gratitude is owed to Professor Marek Michalak and Dr Kim Nakamura for supplying calreticulin-deficient cell line and for allowing me to work in their laboratories in Edmonton, Canada for a month at a later stage of my DPhil. I also thank them for their comments during discussions of my work while there.

I am very grateful to the Wellcome Trust of the United Kingdom and Overseas Research Student award scheme for generously financially supporting this work.

I would not have come this far without the love of my parents and my sisters. Special thanks are also due to my in-laws: Dad, Mum, Punam Dijju, Keshav Dai, Sohan and Sulaja. They have been an enormous moral and emotional support over the past two years.

Finally, I would like to dedicate this thesis and give a big thank you to my beautiful wife Sanu. I would like to thank her for putting up with so many of my problems during the write-up period especially the long hours away from home. I definitely couldn't have got anywhere without the love, moral and financial support I received from her. Thank you Sanu for making my life mean something. I quite simply couldn't be happy without you.

TABLE OF CONTENTS

CHAPTER 1- INTRODUCTION **1**

1.1 The innate immune system 1
1.2 The adaptive immune system 2
1.2.1 MHC class I and class II molecules 4
1.3 MHC class I restricted antigen presentation to cytotoxic T cells 5
1.3.1 The Major Histocompatibility Complex 5
1.3.2 Chain structure of MHC class I molecules 10
1.3.3 T cells are MHC restricted 10
1.3.4 Antigenic peptides are stably bound to MHC molecules 12
1.3.4.1 Peptides are presented to T cells in a MHC-restricted way 12
1.3.4.2 MHC class I structure determined by X-ray crystallography 13
1.3.4.3 Properties of peptides ligands stably bound to MHC class I 14
1.4 Generation of MHC class I peptide epitopes 16
1.4.1 Proteasome and peptide generation 17
1.4.2 Transport of peptides into the endoplasmic reticulum 19
1.4.2.1 TAP-dependent translocation 19
1.4.2.2 Structure of TAP 21
1.4.2.3 TAP transporter has specificity for the peptides it transports 21
1.4.2.4 ER processing of TAP transported peptides 23
1.4.2.5 TAP physically associates with class I molecules 24
1.5 Assembly of class I molecules with peptides *in vitro* 24
1.5.1 Co-operative binding of peptides with β2m and class I heavy chains 25
1.5.2 Assembly assay and peptide binding to class I 25
1.6 Assembly of class I molecules *in vivo* 26
1.6.1 Calnexin and calreticulin as ER chaperones 26
1.6.1.1 Calnexin 26
1.6.1.2 Structure 28
1.6.1.3 Calnexin: a chaperone 28
1.6.2 Calreticulin 29
1.6.2.1 Structure of calreticulin 30
1.6.2.1 Functions of calreticulin 31
1.6.3 Role of calnexin and calreticulin in the folding of glycoproteins 34
1.6.4 Assembly of MHC class I molecules in the ER 39
1.6.5 Release of MHC class I molecules from the ER 42
1.7 Subject of the thesis 42

CHAPTER 2 – MATERIALS AND METHODS **44**

2.1 Chemicals 44
2.2 General tissue culture 44
2.3 Cell lines 44
2.4 Antibodies 45
2.5 Purification of antibodies 48
2.5.1 Production of hybridoma supernatant 48
2.5.2 Protein A-Sepharose affinity purification of antibodies 49

2.6 Peptides and recombinant vaccinia virus 49
2.7 Techniques used to study the biochemistry of class I molecules 50
2.7.1 Flow cytometry (FACS) 50
2.7.2 Western blot 50
2.7.3 Immunoprecipitation and pulse chase 51
2.7.3.1 Immunoprecipitation 52
2.7.3.2 Pulse chase 52
2.7.4 Cell fractionation and scintillation counting 53
2.7.5 SDS-polyacrylamide electrophoresis and autoradiography 53
2.8 Stability of class I complexes *in vitro* 55
2.9 Co-immunoprecipitation 56
2.10 Pharmacological treatment of cells 56
2.11 Construction of plasmid vectors 57
2.11.1 pUB6/V5-His as expression vector 57
2.11.1.1 Choice of vector 57
2.11.2 cDNAs 58
2.11.3 Subcloning 59
2.12 Transformation of chemical competent *E coli* cells 59
2.12.1 Screening for positive colonies 60
2.13 Large scale preparation of plasmid DNA suitable for transfection 60
2.14 Site-directed mutagenesis 61
2.15 Viruses 62
2.15.1 Vaccinia expansion by transfection of tk-143 cells 62
2.15.2 Infection of cells with recombinant vaccinia virus 63
2.16 Stable transfection of mouse fibroblast cell lines 63
2.17 Confocal microscopy 64
2.18 TAP transport assay 65
2.19 Protein determination (Bradford) assay 66
2.20 Enzyme-linked ImmunoSPOT (ELISPOT) and Cytotoxicity (CTL) assay 66
2.20.1 Cell isolation 66
2.20.2 T cells 67
2.20.3 Dendritic cells 67
2.20.4 Generation of influenza-specific CTL 68
2.20.5 Influenza A virus infection 68
2.20.6 ELISPOT assay for IFN-gamma release 68
2.20.7 Cytotoxicity (CTL) Assay 69
2.21 Real Time Polymerase Chain Reaction (RTPCR) 69

CHAPTER 3 – EFFECTS OF CALRETICULIN KNOCKOUT ON MHC CLASS I ASSEMBLY AND ANTIGEN PRESENTATION 71

3.1 Background 71
3.2 Calreticulin-deficient cells express reduced cell surface levels of class I MHC 72
3.2.1 Fewer class I molecules are expressed on the surface of K42 72
3.2.2 Synthesis of class I heavy chain is not affected by the absence of calreticulin 74
3.2.3 Class I molecules can be stabilised on the surface by incubating K42 with stabilising peptides 77

3.2.4 Class I molecules can be stabilised on the surface by incubating K42 with β2m 79
3.2.5 H2-K^b molecules rapidly traffic to the cell surface in the absence of calreticulin 81
3.3 ER peptide supply is not affected in the absence of calreticulin 83
3.3.1 Rate of cytosolic degradation of a model antigen is the same in K41 and K42 85
3.3.2 ATP-dependent TAP transport is unaffected in the absence of calreticulin 85
3.4 Transfection of full-length calreticulin gene restores class I surface expression 87
3.5 Antigen presentation is impaired in K42 cells 89
3.6 Peptide loading of class I molecules is a specific function of calreticulin 91
3.7 Expression, assembly and transport of class I in cells overexpressing calnexin and calreticulin 95
3.7.1 MHC class I cell surface expression is increased in HeLa cells overexpressing calnexin and calreticulin 95
3.7.2 Assembly and export of class I from the ER in cells overexpressing calnexin and calreticulin 97
3.8 Assembly of class I when interaction of calnexin and calreticulin with the carbohydrate moiety is pharmacologically blocked 100
3.8.1 H2-K^b cell surface expression is reduced in the presence of castanospermine 101
3.8.2 Peptide loading is impaired in castanospermine treated cells 101
3.9 Intracellular distribution of class I in calreticulin-deficient cells 103
3.10 Chapter summary and discussions 105

CHAPTER 4 – ROLE OF CALNEXIN IN CLASS I ASSEMBLY 107

4.1 Background 107
4.2 Assembly of HLA-A2.1 and A2.1T134K in cells that lack calnexin 109
4.2.1 Assembly of A2.1 in CEM and CEM.NK^R 110
4.2.2 Assembly of A2.1T134K in CEM and CEM.NK^R cells 113
4.3 Chapter summary and discussion 115

CHAPTER 5- ROLE OF HEAVY CHAIN GLYCOSYLATION ON CLASS I ASSEMBLY AND ANTIGEN PRESENTATION 119

5.1 Background 119
5.1.1 Glycosylation and the assembly of class I 119
5.1.2 Glycosylation and antigen presentation 123
5.2 Generation of A2.1 glycosylation mutants 125
5.3 Role of heavy chain glycosylation in the expression of A2.1 molecules 126
5.3.1 Reduced cell surface expression of aglycosylated A2.1 molecules 126
5.3.2 Cell surface expression of di- and hyper- glycosylated A2.1 129
5.4 Assembly of A2.1 glycosylation mutants 130
5.4.1 Glycosylation mutants are unstable at the cell surface 131
5.4.2 A2.1 glycosylation mutants have loading defect 133
5.4.3 Glycosylation mutants associate with the TAP loading complex 133

5.4.4 Existence of a greater proportion of non-transported subpopulation of A2.1^{+++} molecules 137
5.4.5 Glycosylation mutants appear on the cell surface at a similar rate to wild-type A2.1 molecules 139
5.5 Antigen presentation by A2.1 glycosylation mutants 141
5.6 Non-glycosylated heavy chain binds to lectin chaperone calreticulin 145
5.7 Chapter summary and discussions 149

CHAPTER 6- P-DOMAIN OF CALRETICULIN DOWNREGULATES PROTEINEXPRESSION SPECIFICALLY 153

6.1 Background 153
6.2 Analysis of roles of different domains of calreticulin on the restoration of MHC class I surface expression 155
6.2.1 NP- domain does not restore MHC class I surface expression 156
6.2.2 PC- and P- domains downregulate MHC class I surface expression 156
6.2.3 P- domain has a dominant negative effect on MHC class I expression 160
6.3 P- domain reduces class I heavy chain expression in a dominant fashion 162
6.4 P- domain does not produce an unfolded protein response 162
6.5 P- domain is functional in K42 164
6.6 Affect of P- domain on protein synthesis and degradation 168
6.6.1 P- domain affects the synthesis of membrane proteins 168
6.6.2 P- domain does not affect degradation of membrane proteins 170
6.6.3 Rate of ER degradation of a model antigen is the same in K41 and K41-P 170
6.7 P- domain downregulates expression of specific proteins 173
6.7.1 Affect of P- domain on the expression of membrane proteins 173
6.7.2 Affect of P- domain on the expression of ER resident proteins 174
6.8 Mechanisms for downregulation of specific proteins 177
6.8.1 Competition for substrates and /or upset on ER calcium store 177
6.8.2 Transcriptional regulation 178
6.9 Chapter summary and discussion 181

CHAPTER 7- SUMMARY AND GENERAL DISCUSSIONS 185

7.1 Calreticulin 185
7.2 Calnexin 188
7.3 Heavy chain glycosylation 192
7.4 A model for class I assembly 194
7.5 What may be the function of P- domain? 196
7.6 Concluding remarks 199

APPENDIX 201

REFERENCES 207

Abbreviations and Acronyms

C	Degree(s) Celsius
α	Alpha
Å	Armstrong
aa	Amino acid
ABC	ATP-binding cassette
Amp	Ampicillin
APC	Antigen presenting cell
APS	Ammonium Persulphate
ATP	Adenosine Tri-phosphate
bp	Base pair
B Cells	Bone Marrow Derived Cells
BM36.1	TAP-deficient cell line
β2m	β2-microglubulin
BSA	Bovine Serum Albumen
Ca^{2+}	Calcium
cDNA	Complementary Deoxyribonucleic acid
CD	Cluster of Differentiation
cm	Centimetre
CNX	Calnexin
CRT	Calreticulin
CTL	Cytotoxic T lymphocytes
DMEM	Dulbecco's Modified Eagles Medium

DMSO	Dimethyl Sulphoxide
DNA	Deoxyribose nucleic acid
dNTP	Deoxynucleoside triphosphate
DriPs	Defective Ribosomal Products
DTT	Dithiothreitol
EDTA	Ethylenediaminetetra acetic acid
ER	Endoplasmic Reticulum
ES	Embryonic Stem
Fig	Figure
FCS	Foetal Calf Serum
GS	Glucosidase
HA	Hemagglutinin
HACBP	High Affinity Calcium Binding Protein
HC	MHC class I heavy chain
HLA	Human Leukocyte Antigen
HPLC	High Performance Liquid Chromatography
Ig	Immunoglobulin
kb	Kilobase
kDa	KiloDaltons
kV	Kilo Volts
l	Litre
LBL721.174	TAP-deficient B Cell Line
LCMV	Lymphocytic choreomeningitis virus
LMP	Large Multifunctional Protease
M	Molar

μCi	Micro Curie
μg	Microgram
mg	Milligram
$MgCl_2$	Magnesium chloride
MHC	Major Histocompatiblity Complex
min	Minute(s)
μl	Microlitre
ml	Millilitre
μm	Micrometer
MOI	Multiplicity of infection
mRNA	Messenger Ribonucleic Acid
N- linked	Asparagine-linked
NaCl	Sodium chloride
NaOH	Sodium hydroxide
NBD	Nucleotide-binding domain
ng	Nano gram
nmol	Nano mole
NMR	Nuclear Magnetic Resonance
NP	Nucleoprotein
NP40	Nonidet P40
PAS	Protein A-Sepharose
PBS	Phosphate Buffered Saline
PCR	Polymerase Chain Reaction
PDI	Protein Disulphide Isomerase

RMAS	Murine TAP-deficient lymphoma line
RNA	Ribonucleic Acid
RNaseA	Ribonuclease A
rpm	Revolutions per minute
RT	Room Temperature
RT-PCR	Reverse Transcriptase PCR
SDS	Sodium Dodecyl Sulphate
SDS-PAGE	SDS-Ploy acrylamide Gel Electrophoresis
sec	Second(s)
SERCA	Sarco-Endoplasmic reticulum Ca^{2+}-ATPases
SLE	Systemic lupus erythematosus
ss	Single stranded
T cells	Thymus derived cells
T2	TAP-deficient human cell line
TAE	Tris-acetate EDTA
TAP	Transporter associated with antigen processing
Taq	*Thermus aquaticus* DNA polymerase
TCR	T cell receptor
TEMED	N,N,N',N'-tetramethylethylenediamine
Tet	Tetracyclin
Th	T helper
TMD	Transmembrane Domain
Tris	2-amino-2-(hydromethyl) propane-1, 3 diol

UGGT	UDP-Glucose:glyprotein glucosyltransferase
UV	Ultraviolet
V	Volt
VDM	Virus dilution medium
VSV	Vesicular stomatitis virus

Chapter 1

INTRODUCTION

We live in an environment surrounded by microorganisms- viruses, bacteria and other pathogenic agents. Despite continual exposure to potential pathogens, we are taken ill only relatively rarely. This is because whenever pathogens infect us by penetrating our natural physical barriers, such as the skin or mucous membranes, our immune systems detects the presence of foreign antigens in the body and eliminates them [1]. The study of the body's defence against infection by pathogens is therefore called immunology.

1.1 THE INNATE IMMUNE SYSTEM

The early phases of the host responses to pathogenic infection depends on "innate" arm of the immune system in which a variety of innate resistance mechanisms respond to presence of pathogens. Recognition of pathogens is mainly through their characteristic chemical composition that distinguishes them from our own "self" characteristics. For example, prokaryotic proteins have formyl-methionine at the N-terminus of polypeptide, which can be recognised by neutrophils via their F-met-leu-phe receptor [2]. Once activated, neutrophils become highly phagocytic and are able to engulf and destroy pathogens or the "non-self" antigens. Moreover, repeating polysaccharides in the cell walls of yeast and certain bacteria activate alternative pathway of complement. Other effector cells, like macrophages and eosinophils, are also phagocytic cells. Macrophages are migratory cells derived from bone marrow

precursors and are found in most tissues of the body. Eosinophils have cell-surface receptors for IgE that allow them to attack parasites.

Innate immunity is present in all individuals at all times, does not increase with repeated exposure to a given pathogen, and does not discriminate between pathogens. Therefore, in the "innate" arm of the immune system, no attempt is made to selectively discriminate between all the possible types of invading organisms that the host may encounter. It is, therefore, likely that some intruders may remain undetected. In order to overcome this limitation in recognition of foreign pathogens, vertebrates have developed an "adaptive" immune response. "Adaptive" response is the response of antigen-specific lymphocytes to antigen, and also includes the development of immunological memory.

1.2 THE ADAPTIVE IMMUNE SYSTEM

The induction of a specific immune response, such as the production of antibodies to a particular pathogen, is called the "adaptive" or "acquired" immune response, because it is acquired during the lifetime of an individual as an adaptive response to a specific pathogen. The adaptive immune system has evolved to detect and eliminate foreign pathogens, providing defence mechanism against invading microorganisms. One of the many mechanisms that are utilised to detect the presence of invading microorganisms is based on a simple fact: all pathogens differ from their hosts by at least one protein. The unique specificity that characterises the adaptive immune response derives from the clonal reactivity patterns of two main cell types in the system, namely Bone marrow derived (B) and Thymocyte derived (T) lymphocytes. B and T cells recognise foreign antigens through their surface receptors but unlike the

effector cells in the "innate" arm of the immune system, B and T cells express specific receptors that are able to recognise specific antigenic determinants. The ability of the B and T cells to generate such highly diverse and specific surface receptors follows the 'shuffling' of their antigen receptor genes.

B and T cells respond to pathogenic invasion in a different manner. The antigen receptor on B cells is a cell-surface immunoglobulin (Ig) molecule. The antibody (Ig) molecule secreted by B cells can also act as receptor for antigen. These receptors recognise antigen in its intact (native) form. Once antigen has been recognised by the receptors, B cells are activated and differentiate into cells called plasma cells producing antibody of the same specificity as their initial receptor. Antibodies produced in this way can effectively recognise and neutralise invading pathogens such as bacteria. Immunological response through antibody production by B cells in this way is called humoral response.

B cell response cannot combat invasions by microorganisms such as viruses, which penetrate inside the cells of higher eukaryotes and multiply within. T cells take the job of combating these kinds of penetrative invasions. T cells act on cells of the body that contain foreign proteins, usually proteins produced by the pathogens (like viruses) that are infecting the cells. They do this by means of receptors (called T cell receptors or TCRs) that recognise antigen not in its intact form, as it is recognised by B cells, but rather as peptide fragments derived from the foreign proteins and bound to specialised cell surface membrane proteins. The molecules that bind peptide fragments are called MHC molecules as they are encoded within the Major Histocompatibility Complex (MHC).

During their synthesis inside the cell, MHC molecules trap peptide fragments and report their findings by displaying the trapped fragments on the cell surface. Each MHC molecule can bind any one of many different peptides and can thus display peptide fragments from a wide range of different pathogens at the cell surface as well as peptides derived from degraded fragments of the cell's own proteins. However, T cells that are able to recognise the self peptide-MHC complex are either deleted or inactivated before they mature to ensure self tolerance, and thus T cells are only able to detect cells displaying 'non-self' peptide-MHC complexes. When non-self peptides are displayed by MHC molecules, this will initiate a specific T cell mediated immune response to eliminate the infected cell from the population. Any alterations from this recognition or breaking of self-tolerance will lead to a variety of opportunistic infections or attacks of self tissues leading to autoimmune diseases.

1.2.1 MHC CLASS I AND CLASS II MOLECULES

Not only do T cells need to detect non-self peptide-MHC complexes on the surface of cells, but also respond appropriately; i.e., virally infected cells must be killed but B cells that have bound foreign antigen on their surface immunoglobulin as well as macrophages harbouring intracellular bacteria must be activated. Different classes of T cells mediate these distinct functions by recognising antigens displayed on two different classes of MHC molecules. T cells that kill infected cells are called cytotoxic T lymphocytes (CTLs) or $CD8^+$ T cells as they are distinguished by the cell-surface molecule CD8 [3] and recognise peptides bound to MHC class I molecules. T cells that mediate activation of macrophages and B cells are called T helper (Th) cells or $CD4^+$ T cells as they are distinguished by surface expression of the molecule CD4. $CD4^+$ T cells recognise peptides bound to MHC class II molecules.

This thesis mainly focuses on MHC class I antigen presentation pathway involved mainly in the presentation of viral and other intracellular antigens to $CD8^+$ T cells. MHC class I assembly and loading with antigenic peptides is an important step in this presentation pathway. Assembly and peptide loading occurs in the endoplasmic reticulum (ER) and involves participation of a range of assembly and loading factors, which reside within the ER [4-7]. The remainder of the chapter will form an introduction to the work that follows.

1.3 MHC CLASS I RESTRICTED ANTIGEN PRESENTATION TO CYTOTOXIC T CELLS

Viruses and some bacteria replicate in the cytosol. To produce an appropriate response to such an infection, viral or bacterial proteins are first degraded in the cytosol (additional degradation can occur in the ER) into smaller protein fragments. Because the generation of peptide fragments involves modifications of the native protein, it is commonly refereed to as "antigen processing". Antigen fragments are then bound to MHC class I molecules to be presented to $CD8^+$ T at the cell surface. Because peptides are displayed at the cell surface by the MHC molecules, the process is referred to as "antigen presentation".

1.3.1 The Major Histocompatibility Complex

The MHC, located on chromosome 6 (in humans) [8] and chromosome 17 (in mouse) extends over 2-3 centimorgans of DNA, and contains extended collections of genes. Figure 1.3.1a (more detailed version shown in figure 1.3.1b) shows the basic arrangement of genes of the region of human chromosome 6 containing the MHC. The region is gene dense and is subdivided into three classes, based on functional characteristics of the genes within each class. The most centromeric part is the class II

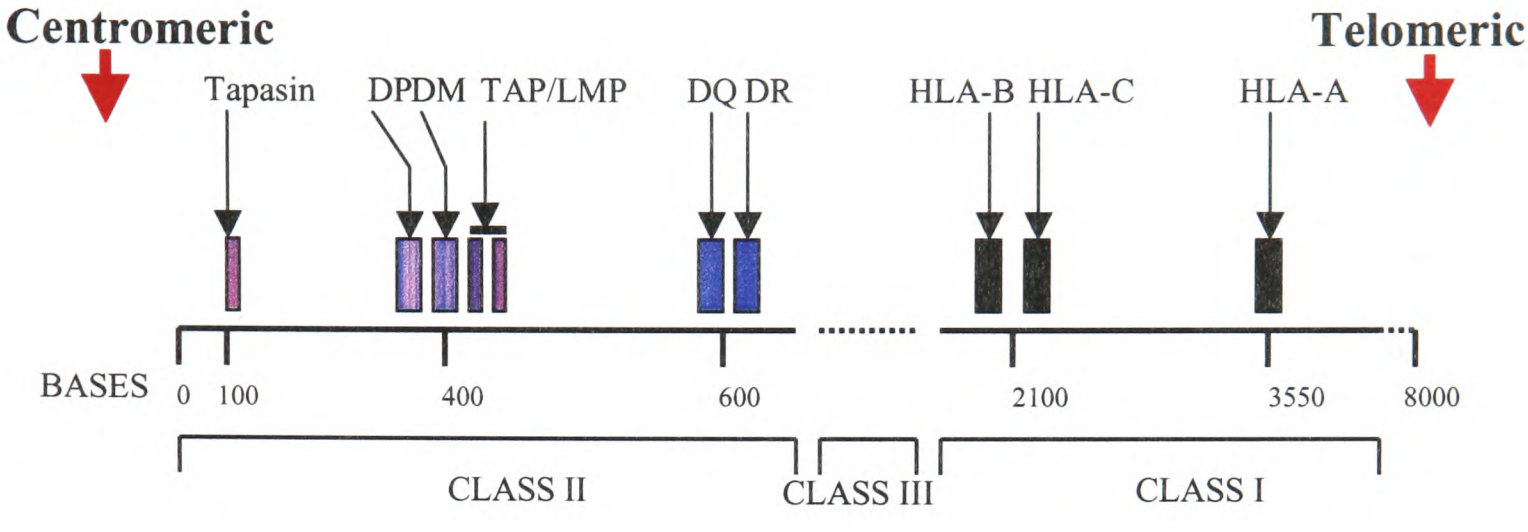

Figure 1.3.1a Basic arrangement of genes of the region of human chromosome 6 containing the MHC. This highly simplified diagram shows gene content within the three regions of the MHC.

Figure 1.3.1b Detailed map of the MHC class I, II and III regions. Class III region is very dense, packed with genes involved in activities such as complement and inflammation. Class II region is the most exhaustively studied region of the MHC and contains genes associated with antigen processing and presentation. Class I region contains further antigen presentation genes and is less gene-rich than class II and III regions with large gaps between genes. Gene map extracted from http://www.path.cam.ac.uk/~mhc/map/Fig1MED.jpg.

region, containing the HLA-DP, DQ and DR loci, which are found as pairs, encoding the α and β chains which form the heterodimeric class II protein molecules expressed at the cell surface of antigen presenting cells. Telomeric and next to the class II region is the class III region which contains a disparate collection of densely packed genes which have been characterised predominantly by sequencing studies [9, 10]. Many of the genes in this region have not been characterised fully at the functional level, but a role in the innate immune response and inflammation has been suggested for some. The class I region at the telomeric end contains the classical HLA-A, B and C and related loci, spread over a region of 2 mega bases.

The genes encoding the heavy chains of MHC class I molecules are linked within the MHC complex while the genes for β2-microglobulin (β2m) lie on separate chromosome (chromosome 15 in humans and chromosome 2 in mouse). Two separate mechanisms participate in combating intracellular invasion from pathogens. First, the MHC class I is polygenic (HLA-A, -B, and –C in humans, and H2-D, -K and –L in mouse) encoding proteins with different ranges of peptide. Second, the MHC is highly polymorphic- there are multiple alleles of each gene [11]. Since the products of the MHC genes are co-dominantly expressed, each human individual can express up to 6 different HLA class I alleles, two from each of the HLA-A, -B, and –C loci.

The majority of genes located in the human MHC class I and class II are devoted to generating peptide antigens and expressing them on the cell surface- thereby providing extracellular representation of intracellular invasion. The two **T**ransporter associated with **A**ntigen **P**rocessing (TAP) genes, TAP1 and TAP2, lie in close association with the LMP genes that encode components of the proteasome. The

proteasome functions as a general proteolytic device for proteins within the cell [12]. It produces the antigenic peptides for presentation on class I molecules at the cell surface. The TAP proteins, as will be discussed later, form a heterodimer localised to the membrane of the endoplasmic reticulum (reviewed in [13]) where they are responsible for the transport of antigenic peptide, by forming a channel through which peptides pass from the cytoplasm into the ER [14, 15]. The centromeric boundary of the MHC has been extended beyond the class II HLA-DP loci to encompass the tapasin region [16]. As will be discussed later, tapasin facilitates peptide loading and bridges TAP and class I molecule. The linkage of tapasin, TAP and class I genes alludes to a possible relationship, at the molecular genetic and functional level, between linked gene loci within the MHC.

The chicken MHC is roughly 20-fold smaller than the human MHC region [17]. Despite being smaller, all the genes have counterparts in the human MHC, defining a minimal essential set of MHC genes conserved over 200 million years of divergence between birds and mammals. They are organized differently, with the class III region genes located outside the class II and class I region genes. Interestingly, genes associated with the proteasome complex are absent and this might explain unusual peptide-binding specificities of chicken class I molecules. Moreover, presence of putative natural killer receptor gene(s) has been identified.

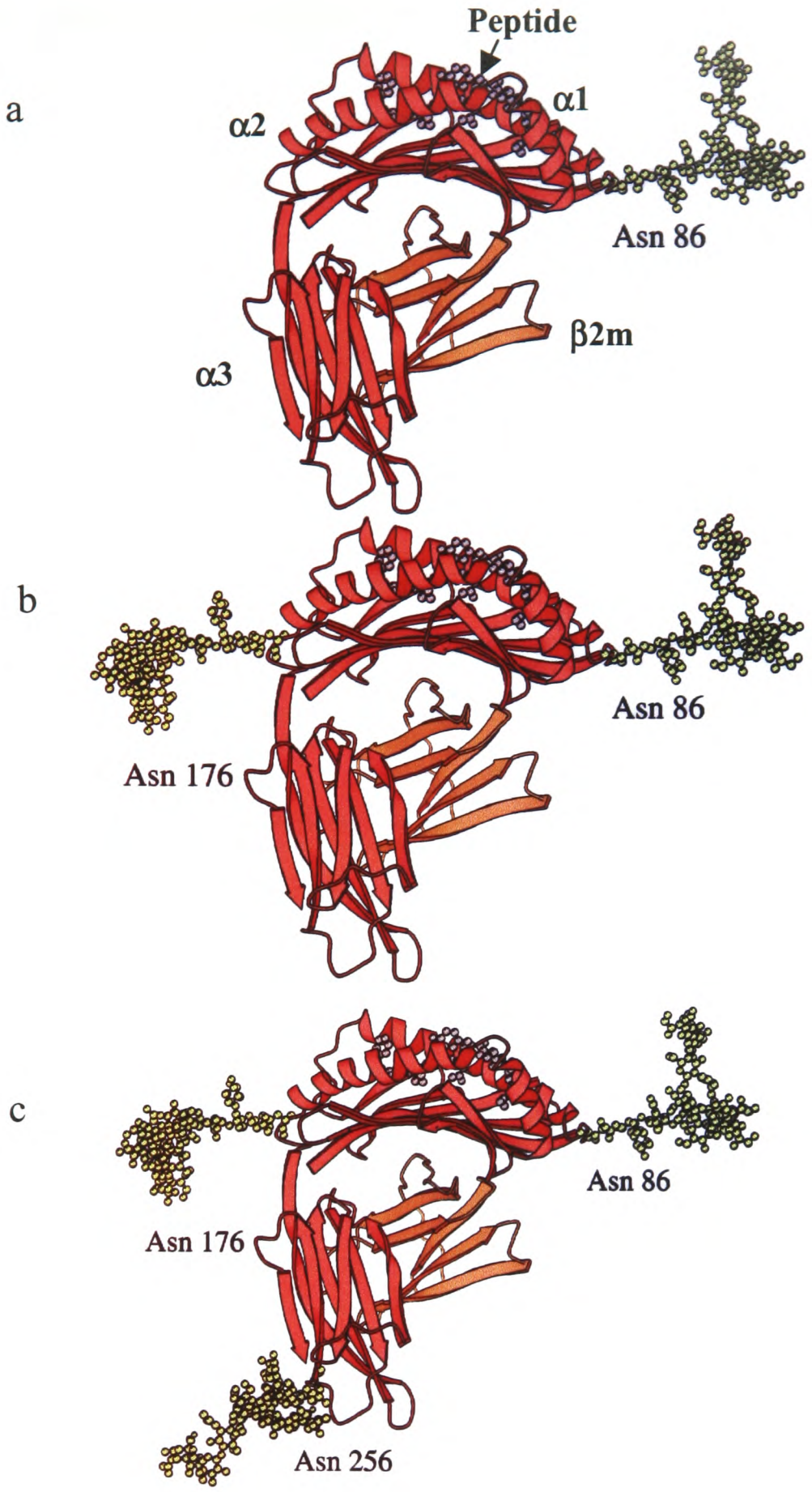

Figure 1.3.2 Structure of a class I molecule complexed with peptide.

Extracellular portion of the molecule is shown. The class I heavy chain (HC) (light pink) contains three extracellular domains: α1, α2, α3, and depending on the species may possess one (e.g., HLA-A*0201), two (e.g., H2-K^b) or three (e.g., H2-D^b) asparagine (N)-linked carbohydrate (yellow) at positions 86,176 and 256 of the HC. The α1 and α2 domains form the peptide-binding groove and most of the HC polymorphic residues that are different between class I alleles are concentrated within the groove. The peptide-binding groove rests on the base formed by α3 domain and the β2-microglobulin (β2m subunit) (light orange) – both of which are homologous to immunoglobulin constant domains. The peptide (light blue) is also shown. Carbohydrate modelling was done by Dr Mark Wormald, University of Oxford.

1.3.2 Chain structure of MHC class I molecules

MHC class I molecule is a cell surface glycoprotein. It consists of two polypeptide chains, a ~ 43 kDa heavy (α) chain encoded within the MHC, and a smaller non-covalently associated 12 kDa chain, β2-microglobulin (β2m), which is not encoded in the MHC (reviewed in [18]). The structure of MHC class I has been determined by X-ray crystallography. As shown in figure 1.3.2, MHC class I has four domains, three formed from the MHC-encoded heavy chain and one contributed by β2m. The α1, α2 and α3 domains of the heavy chain are extracellular followed by a transmembrane segment and a cytoplasmic tail that anchors the molecule in the ER membrane. Whilst the membrane distal α1 and α2 domains are polymorphic, the membrane proximal α3 domain is highly conserved across species [18]. The α3 domain and β2m have a folded structure that closely resembles that of an immunoglobulin domain. MHC class I is N-glycosylated at position 86 in humans while murine class I have additional glycosylation site at position 176. Some murine class I molecules are triply glycosylated, the third glycosylation site being at position 256 (H2-L^d, D^d, K^d). As will be discussed later, heavy chain glycosylation is important and is thought to contribute to ER quality control so that only optimally loaded and assembled molecules leave the ER.

1.3.3 T cells are MHC restricted

When an organism is infected with a virus, it generates cytotoxic T cells that kill self cells infected with the virus, while sparing uninfected cells or cells infected with unrelated viruses. In 1973, Rosenthal and Schevach, using inbred guinea pigs, demonstrated that T helper cells only proliferate in response to antigen when

presented by macrophages that share MHC alleles [19]. In the two years that followed, Zinkernagel and Doherty were able to show that $CD8^+$ T cells from mice of the H2-d haplotype infected with lymphocytic choreomeningitis virus (LCMV) only kill LCMV infected cells derived from any H2-d haplotype strain but not cells from H2-k or indeed any other haplotype, even when they were infected with the same LCMV virus [20-22]. Subsequently, using recombinant strains of mice, it was demonstrated that not only must target cells and CTLs share same MHC haplotype alleles, but also that the virus-specific CTLs only recognise viral antigens in association with class I MHC molecules [23]. Because the MHC genotype restricts the antigen specificity of T cells, this effect is called MHC restriction and this phenomenon is a critical feature of antigen recognition by all functional classes of T cells [24, 25].

1.3.4 Antigenic peptides are stably bound to MHC molecules

1.3.4.1 Peptides are presented to T cells in a MHC-restricted way

When the MHC-restriction phenomenon was discovered, it was initially assumed that CTL recognised viral glycoproteins that were inserted alongside MHC class I molecules on the surface of infected cells (for example haemagglutinin (HA) for influenza virus) [26]. It was to be demonstrated later that it was actually the peptide fragments to which MHC molecules bound which is presented to the CTLs. Work from Townsend and Bennink demonstrated that reactivity of influenza virus specific CTLs are directed against internally located proteins of influenza (e.g., nucleoprotein (NP)) and not HA expressed at the surface of infected cells [27-29]. Townsend and co-workers then showed that influenza specific CTL population could recognise

distinct fragments within internal NP molecule that were transported independently of one another to the cell surface for presentation through different MHC class I alleles (H2-k, H2-b) [30, 31]. They further showed that genetically engineered HA molecule without ER leader sequence that was rapidly degraded in the cytoplasm by proteasome complex, was as good as native HA in sensitising target cells for lysis by HA-specific CTLs [32]. When pure synthetic versions of peptides corresponding to the CTL epitopes of internal antigens were incubated with target cells, the cells were recognised and lysed by the CTLs just as well as class I matched target cells that had been infected with virus [33-37]. These experiments strongly suggested that MHC class I molecules associated with antigenic peptide fragments generated in the cytosol, which are presented to the CTLs at the cell surface.

1.3.4.2 MHC class I structure determined by X-ray crystallography

Results of these experiments were confirmed when Bjorkman and colleagues solved the crystal structure of MHC class I HLA-A*0201 (HLA-A2) in 1987 [38]. This and other structures of class I molecule revealed the most remarkable pairing of α1 and α2 domains of heavy chain to generate a cleft on the surface of the molecule that forms the peptide- binding site [38-42]. The α1 and α2 domains of the heavy chain form a β-sheet platform spanned by two long α-helices that comprise the floor and sides, respectively, of the peptide binding groove. The peptide-binding site is 30 Å long, 10 Å wide and 11 Å deep [38, 43]. Structure of class I co-crystallised with peptide fragments revealed details of the contacts between the MHC molecule and the peptide. The peptide binding cleft of class I molecule is large enough to accommodate an extended peptide fragment of 8-9 amino acids. The peptide normally lies in an

elongated conformation in the groove; a kinking in the peptide backbone accommodates small variations in the peptide length. The structure of the peptide-binding site also revealed that this site is lined with six depressions called "pockets" (reviewed in [44]). Of the six pockets (named A-F), A and F are the most conserved pockets and stabilise peptide fragments at N- and C- termini, respectively, by contacts between atoms in the free termini common to most short peptides. Pockets B through to E have distinct sizes and characters in different allelic variants of class I (reviewed in [44]) and it is here that many of the polymorphic residues lie [39, 40, 45]. Because the amino acid side chains of peptide participate in hydrogen bonding with residues in these pockets to stabilise the structure of the whole class I molecule [41, 46-48], the individual nature of the pockets directly dictate peptide binding selectivity of each class I allele (reviewed in [18, 49]). Evidence that these pockets are involved in peptide selectivity also comes from genetic studies. For example, when the pockets are mutated, peptides either fail to bind or bind with less efficiency [50-53]. Moreover, if pockets from one class I allele is transferred to another class I allele, the resulting chimeric class I molecule displays a new peptide-binding specificity [54].

The crystal structure of class I has also revealed that the peptide binding groove faces up towards the T cell receptor (TCR) suggesting that the residues in the peptide fragment as well as the residues around the groove make contacts with the TCR [38, 39].

1.3.4.3 Properties of peptide ligands stably bound to MHC class I

When MHC class I are purified from cells, their bound peptides co-purify with them, illustrating the tight association between the MHC molecules and their peptide

ligands. The peptides can then be eluted from the MHC class I molecules by denaturing the complex in acid, releasing the bound low molecular weight peptides, which can be purified and then sequenced. Using this approach, van Bleek and Rammensee affinity purified MHC-peptide complexes from detergent cell lysates and extracted the bound peptides by acid extraction followed by ultra centrifugation [55, 56]. When peptides eluted from MHC class I purified from virally infected cells were run on a HPLC column, dominant peptide epitopes were identified which comigrated with short synthetic peptides of 8 or 9 amino acids [55, 57]. These peptides were able to sensitise uninfected targets for lysis by CTL raised against the virus. These experiments therefore confirmed that peptide fragments are indeed the antigenic determinants and TCR recognise these determinants in the context of MHC class I molecules.

In order to further characterise the peptide determinants, Falk *et al.,* sequenced all peptides eluted from specific class I allele [56, 58]. They found that the length of the peptides was typically between 8 and 10 amino acids. An interesting observation was that certain amino acid residues were commonly found at particular positions in all peptides. These residues are called "anchor" residues because the binding of these residues side chains into the pockets of peptide binding groove anchors the peptide to the MHC molecule. There are at least two anchor residues in a peptide fragment, one is always a C-terminal residue and this residue is frequently a hydrophobic or a basic residue. The other anchor residue is usually at position 2, but can be at 3 or 5 [59, 60]. Changing any anchor residue can prevent the peptide from binding, and conversely, most synthetic peptides of correct length that contain these anchor residues will bind the appropriate MHC class I molecule, irrespective of the sequence of the peptide at other positions [54]. Thus, the characteristics and biochemical properties of the

anchor residues in peptide fragments and pockets in the peptide binding groove [40-42, 46, 47, 61-65] allow MHC class I molecules to bind a wide variety of different peptides of suitable length [59, 60]. For example, natural ligand of HLA-A2 is a nonamer peptide fragment ILKEPVHGV of HIV-pol (476-484). Leucine at position 2 (P2) and Valine at the C-terminus (P9) anchor the peptide epitope by binding to B and F pockets respectively, of HLA-A2 binding groove [56, 66, 67]. Similarly, H2-D^b binds to ASNENMDAM fragment from influenza NP (366-374). In this case, asparagine at P5 anchors into C pocket and methionine at P9 anchors into the F pocket of H2-D^b peptide binding groove. "Secondary anchor" residues have been described for HLA-A2.1 binding peptides in addition to the main anchor residues [68]. It is likely secondary anchor residues have prominent role in maintaining the stability of the class I complex.

1.4 Generation of MHC class I peptide epitopes

Protein degradation is a normal process that occurs in every cell. Proteins are degraded continuously in the cytosol and replaced with newly synthesised proteins. A large, multicatalytic protease complex called the proteasome plays a major part in cytosolic protein degradation. Various lines of evidence implicate cytosolic degradation in the generation of peptide ligands for MHC class I molecules. For example, proteins lacking ER targeting signal sequence and minigene-encoded peptide fragments of a full-length protein synthesised in the cytosol can both contribute peptide epitopes for MHC class I presentation at the cell surface [31, 32, 69, 70]. This led to the suggestion that because MHC class I is assembled in the ER, peptide fragments generated by cytosolic degradation are delivered to the lumen of

the ER independent of sec 61 pathway but by a mechanism that does not require signal sequence [71-73]. This idea was boosted by the identification of peptide transporter and named the **T**ransporter associated with **A**ntigen **P**rocessing (TAP). TAP translocated peptide fragments from the cytosol to the ER [74, 75] and in its absence antigen presentation was severely impaired (reviewed in [6]).

1.4.1 Proteasome and peptide generation

Proteasome is involved in the degradation of most cell proteins including regulatory and defective ribosomal proteins (DriPs) and requires covalent linking of proteins to multiple molecules of the polypeptide ubiquitin [76-78] [79] [80]. Proteasome complex forms a large structure of 26 S (200 kDa) generated through a combination of proteolytically active core of 20 S (673 kDa) and a19 S complex containing several ATPases and a binding site for ubiquitin chains [81]. The role of this 19S particle, which "caps" each extremity of the 20S proteasome, is to unfold the protein substrates to inject them into the 20S proteasome and to stimulate the proteolytic activity.

Various lines of evidence implicate the proteasome in the production of peptide ligands for MHC class I molecule. The proteasome takes part in the ubiquitin-dependent degradation pathway for cytosolic proteins and experimentally increasing cytosolic degradation by tagging with ubiquitin results in the more efficient presentation of their peptides by MHC class I molecules. For example, Townsend *et al.,* added N-terminal arginine to influenza nucleoprotein in order to accelerate its ubiquitin-dependent degradation in the cytosol. This resulted in enhanced presentation of its NP (366-374) D^b-restricted epitope in vaccinia-infected target cells [82]. Several

other studies also provided evidence that the proteasome is involved in the generation of peptides for presentation through MHC class I [81, 83-85].

Specific inhibitors of the proteolytic activity of the proteasome also inhibit antigen presentation by class I molecules [86-88]. Cerundolo *et al.,* have demonstrated that cells treated with lactacystine, a specific inhibitor of proteasome, no longer present influenza from full-length influenza nucleoprotein (NP) [89]. However, these cells are able to present the same epitope when expressed intracellularly using recombinant vaccinia virus, indicating the involvement of proteasome in the intracellular peptide generation [89, 90]. Using other inhibitors to block proteasome activity also results in the defective antigen presentation by class I molecules. Yang *et al.,* treated cells with the inhibitor MG132, a peptide aldehyde, to inhibit proteasome activity. The result was that inhibitor treated cells failed to present influenza HA epitope from a long precursor but not from the short precursor peptide expressed in the cytosol [91].

Moreover, purified proteasomes generate antigenic peptides of 5-15 amino acids in length suitable for binding to MHC class I [92, 93]. In addition, expression of two catalytic β subunits of the proteasome, LMP2 and LMP7, which are encoded within the MHC near the TAP1 and TAP2 genes [94-98], can alter the cleavage specificity of the proteasome to increase cleavage of polypeptides after basic or hydrophobic residue and to inhibit cleavage after acidic residues [99, 100]. This produces peptides with carboxyl-terminal residues that are the preferred anchor residues for peptide binding to most MHC class I molecules and are also the preferred structures for transport by TAP [59, 101]. Lactacystine has been shown to inhibit the LMP2 and

LMP7-specific proteasome cleavage sites in peptides and this directly correlates with the decrease in the formation of stable class I complexes in intact cells [102].

The 20 S proteasome can also associate at both ends with another regulatory complex, the 11S regulator (28.7 kDa) (known as REG or PA28) [103, 104]. This complex is different from the 26 S proteasome complex. 11 S regulator also stimulates proteasome peptidase activity and enhances the production of antigenic peptides for presentation by class I molecules [105]. Moreover, *in vitro* studies with purified 20 S proteasome-PA28 complex have shown to alter the nature and amount of peptide fragments generated from a 25-mer polypeptide [106]. In addition, Groettrup *et al.*, have shown that the same proteasome complex can enhance class I antigen presentation of two epitopes from murine cytomegalovirus pp89 to CTL in mouse fibroblasts [107].

Thus it is likely that the proteasome plays a significant role in generating peptide precursors and other "trimmases" may complement proteasomal activity in the generation of correct epitope. In support of this, puromycin-sensitive aminopeptidase and bleomycin hydrolase have been identified in the cytosol recently [108, 109]. Calpains, or calcium-dependent thiol-proteases, also constitute the other cytosolic proteolytic system [110].

1.4.2 Transport of peptides into the ER

1.4.2.1 Tap-dependent translocation

Since the peptide-binding site of the MHC class I molecule is first formed in the lumen of the ER, peptides derived from viral proteins in the cytosol need to be

translocated into the ER in order to bind to MHC class I molecule. The first insight into how peptide fragments cross the ER membrane before binding to the newly synthesised class I molecules came from the study of mutant cell lines with a defect in antigen presentation by MHC class I molecules. RMA-S [111, 112], LBL721.174 (.174) [113, 114], T2 [115] and BM36.1 [116] are examples of mutant cell lines with a defect in antigen presentation. Although class I heavy chains are synthesised normally in these cells, they are expressed only at very low levels at the cell surface. For example, only about 5% of normal class I is expressed on the surface of RMA-S cells [71] while 70-80% reduction in HLA-A2 is observed with .174 [113, 114, 117, 118]. Townsend and co-workers corrected the defect in class I surface expression in RMA-S and .174 cells by incubating these cells with synthetic peptides (derived from viral sequences) [71, 117] suggesting that the mutation affects the supply of peptides to the MHC class I molecules and that peptide is required for their normal cell surface expression.

Analysis of the affected DNA in .174 provided insight into why peptides in this cell line failed to be delivered into the ER: two genes encoding members of the ATP-binding cassette (ABC) family of proteins located in the class II region of the MHC (see figure 1b) on chromosome 6, were mutant or absent [119] (reviewed in [120]). The proteins encoded by these genes are now called **T**ransporters associated with **A**ntigen **P**rocessing-**1** and –**2** (TAP-1 and TAP-2). It is now clear that the two TAP proteins form a heterodimer and mutations in either TAP gene prevent antigen presentation by MHC class I molecule [116, 121, 122].

1.4.2.2 Structure of TAP

TAP1 (70kDa) and TAP2 (72kDa) encode an amino-terminal hydrophobic multiple spanning transmembrane domain (TMD) and a carboxy-terminal hydrophilic ATP-binding domain (NBD) located on the cytosolic side of the ER [123, 124]. A pore in the ER membrane is formed when TAP1 and TAP2 assemble into a heterodimer to form four-domain transporter [116, 121, 125]. Models for the structure of TAP have been based on the sequences of multiple transmembrane-spanning regions in the transmembrane domains [123, 126], the location of point mutations or naturally occurring polymorphisms affecting peptide selection and transport [126, 127] [128, 129] or the cytosolic or ER lumenal orientation of TAPs engineered to contain reporter molecules [130, 131]. Expression of truncated TAP polypeptides has suggested interactions between both the TMDs and NBDs of TAP1 and TAP2 [132-134]. More recently, detergent-solubilized immunopurified particles of TAP have been studied by electron microscopy and reveal TAP as a single heterodimeric complex, with the TAP1 and TAP2 subunits combining to create a central 3-nm-diameter pocket on the predicted ER-lumenal side [135].

1.4.2.3 TAP transporter has specificity for the peptides it transports

Several *in vitro* translocation assays have been described to study the nature of peptides transported by TAP [136-139]. These assays have demonstrated TAP favours peptides of 8-12 amino acids in length although longer peptides up to 40 amino acids in length could also be transported albeit with less efficiency [136, 140-144]. Moreover, transport of peptides into the ER is coupled to ATP hydrolysis [136-139].

The TAP transporter generally prefers peptides with hydrophobic or basic residues at the carboxy-terminus, the exact features of peptides that bind MHC class I molecules [59]. Human TAP is permissive of all TAP proteins studied, allowing transport of all carboxy-terminal amino acids except proline [143, 145]. Murine TAP, on the other hand, prefers peptides with hydrophobic amino acids at the carboxy-terminus [141, 145]. In the rat, there are two allelic variants of the TAP2 transporter [129, 146] that differ in their capacity to transport peptides. One variant ($TAP2^a$) is promiscuous and allows transport of peptides with most amino acids (except proline) at the C terminus, while the other ($TAP2^u$) is restrictive and transports only those peptides with hydrophobic carboxy-terminal residues [145, 147]. It has also been shown that $TAP2^u$ is also able to transport longer peptides more efficiently than $TAP2^a$ [143]. Functional polymorphism in TAP proteins can thus affect the repertoire of peptides available for binding by rat MHC class I molecule, $RT1.A^a$, in a set of phenomena called class I modification, or *cim* [148]. In *cim*, intracellular assembly of $RT1.A^a$ is much slower in cells homozygous for $TAP2^u$ (cim^u) compared to cells homozygous for $TAP2^a$ (cim^a) [148]. Moreover, alloreactive cytotoxic T lymphocyte responses can be generated that distinguishes between $RT1.A^a$ expressed by cim^a and cim^b cells [149]. It has been shown that *cim* effect is due to the loading of different peptide sets, that the key variable is the preference of arginine at the C-terminus of peptide by $RT1.A^a$ and that the limiting step in the supply of peptides with the appropriate C- terminus for class I binding occurs at the level of TAP [129, 150].

Whether the nature of amino acids other than at the carboxy-terminus of peptides affect TAP translocation efficiency has also been investigated [151, 152]. These studies have shown that TAP does not prefer proline residue at the first three positions of a potential substrate. This finding is significant as many human class I alleles

studied to date, including more than 50% of the B locus alleles, require proline at position 2 of a peptide to bind. This finding together with the fact that TAP is able to transport longer peptides suggests that further processing of TAP transported peptides occurs in the ER, which then leads to the generation of optimal peptides for binding to class I molecules.

1.4.2.4 ER processing of TAP transported peptides

Several other lines of evidence support further processing or "trimming" of TAP transported peptides in the ER. Snyder *et al.,* have shown that the C-terminal (but not the N-terminal) epitope could be released and presented to CTL in TAP-negative T2 cells infected with a vaccinia construct encoding the two epitopes in tandem [153]. Moreover, Elliott *et al.,* introduced a 170 amino acids long peptide precursor (residues 328-498), containing the D^b-restricted epitope ASNENMDAM (residues 366-374), from influenza A nucleoprotein (NP) into T2 cells expressing D^b. These cells were able to generate the D^b restricted epitope and present to CTL if the minigene encoding the extended precursor fragment was preceded by an ER translocation signal sequence, thus bypassing the need for TAP [154].

More direct evidence of the existence of ER trimmases has come recently. gp96, an abundant peptide-binding chaperone of the lumen of the ER has been shown to be an aminopeptidase capable of trimming a precursor T cell epitope *in vitro* [155]. Moreover, Serwold *et al.*, have identified leucinethiol-inhibited ER proteases, which can efficiently trim all amino acid residues except proline that flank the NH_2-termini of antigenic precursors in the ER [156] and the aminopeptidase activity is dependent on presence of appropriate class I molecules [157].

1.4.3.5 TAP physically associates with class I molecules

When weak detergents (e.g., 1% digitonin) are used to lyse cells, weak interactions between intracellular proteins is preserved. Using such cell lysates, when anti-TAP antibody was used to precipitate TAP, MHC class I molecules co-precipitated with TAP [158, 159] indicating that a fraction of mouse and human class I molecules physically associate with TAP in the ER of living cells. It is now well established that both TAP1 and TAP2 subunits can associate with class I molecules [160]. In human and mouse cells, the association of MHC class I molecules with TAP is mediated by a third 48 kDa type I glycoprotein termed TAP-A [161] or more commonly tapasin (TAP-associated glycoprotein) [14, 162-166].

1.5 Assembly of class I molecules with peptides *in vitro*

Optimal peptide binding to class I molecules is essential for the generation of a fully folded and stable class I complex. With the availability of TAP-deficient cells, which are unable to supply peptides into the ER, it is possible to study binding of peptides to class I *in vitro*. As discussed earlier, class I heavy chains assemble poorly with β2m in TAP-deficient cells. Unlike normal cells, when TAP-deficient cells, such as RMA-S or .174/T2, are lysed in detergent, most class I heavy chain:β2m complexes formed dissociate after an overnight incubation at 4^0C. However, if a stabilising synthetic peptide is added at the time of lysis, a significant increase in the number of assembled heavy chains:β2m is observed, recognised by conformational sensitive antibodies [71, 167-169].

1.5.1 Co-operative binding of peptides with β2m and class I heavy chains

Several studies have demonstrated that equilibrium exists between peptides and β2m bound to class I heavy chains and both peptides and β2m interact with the class I heavy chain co-operatively (for review see [170]). *In vitro*, both peptide and β2m can interact with the heavy chain to induce a conformational change and to partially stabilise the complex [167-169, 171-177]. Peptide:HC and HC:β2m complex remain unstable, however, and it is only when the co-operative interaction takes place between all three components, a stable class I complex with a high affinity peptide in the peptide binding groove, is generated. This explains why majority of class I complexes in TAP-deficient cells are unstable. This is because there is no supply of high affinity peptides into the ER by TAP in order to stabilise the class I HC:β2m complexes. Although peptides can associate with class I heavy chain before β2m binding *in vitro*, peptides seem to bind to class I only after class I heavy chain has associated with β2m *in vivo* [178] as will be discussed later.

1.5.2 Assembly assay and peptide binding to class I

Upon β2m and peptide binding, class I HC undergoes a conformational change to acquire specific serological epitopes, which can be detected with conformational-sensitive antibodies [167, 179]. This approach, commonly called as "assembly assay" can be used to understand and also quantify the ability of peptides to stabilise class I HC:β2m complexes. For example, if metabolically labelled cell lysates are aliquoted and each sample incubated overnight at 4^0C with an increasing concentration of stabilising peptide, the amount of material that can be precipitated with conformational sensitive antibodies is directly proportional to the amount of peptide

added to the lysates. Like wise, the increase in the amount of class I precipitated with the conformation-sensitive antibodies in the presence of added peptide is directly related to the amount of peptide-receptive class I in the cell [180].

Dissociation rate measurements also provide an indication of class I stability where the off-rate (k_{off}) of bound radio-iodinated peptide is measured in the presence of a large excess of unlabelled "cold" peptide [172, 179] *in vitro*. For example, the k_{off} values of 9-mer peptides at 37^0C correspond to a half-life ($t_{1/2}$) of about 3 to 7 hours [172], whilst the $t_{1/2}$ for 17-mer peptides is only about 30 minutes [181]. Recently, Springer *et al.*, have expressed empty soluble H-2D^b class I molecules in Chinese hamster ovary (CHO) cells and generated complete sets of association, dissociation, and equilibrium constants of unmodified peptides [182]. Their findings suggest that peptide binding occurs in several steps, most likely via a conformational rearrangement of the peptide-binding groove.

1.6 ASSEMBLY OF CLASS I MOLECULES *IN VIVO*

1.6.1 Calnexin and calreticulin as ER chaperones

1.6.1.1 Calnexin

Calnexin (CNX) is an important molecular chaperone in the ER assisting in protein folding and as part of quality control apparatus, retains unfolded proteins in the ER destined for degradation. CNX is 65 kDa type I membrane glycoprotein with its substrate-binding domain in the lumen of the ER (figures 1.6.1.1). The 89-residue cytoplasmic tail carries a carboxy-terminal RKPRRE sequence that serves as an ER-retention signal [183]. The lumenal region of CNX (amino acids 1-463) is involved in calcium binding and contains the proline-rich (P) homology region to calreticulin.

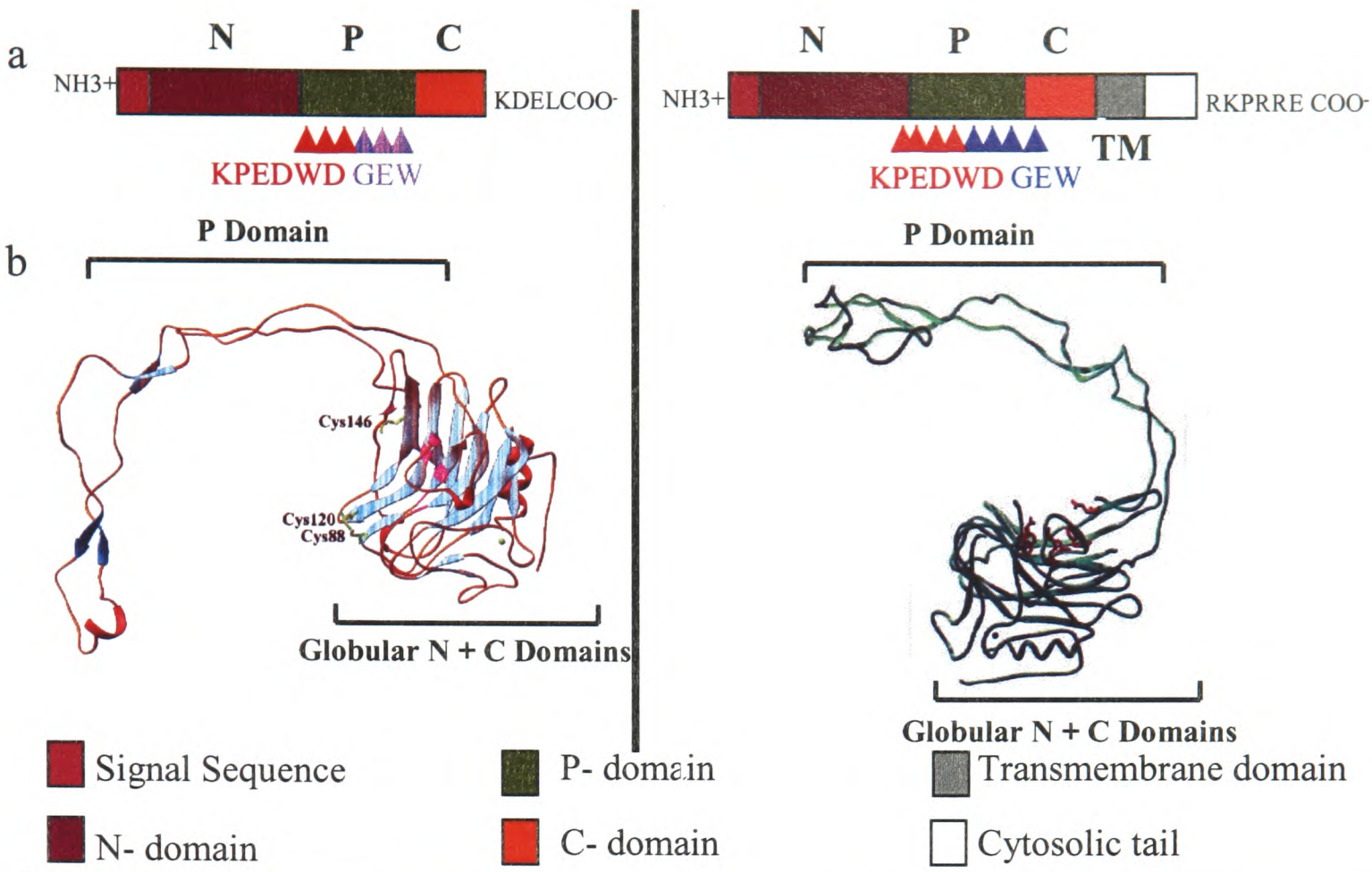

c

Residues in Calreticulin	Residues in Calnexin	Significance in Calnexin structure
1-189 284-358	67-275 410-482	Globular lectin domain – homologous to the legume lectin fold.
190-283	276-409	Large hairpin formed by the P-domain.
92-111, 143, 300	165-186, 217, 426	Putative carbohydrate binding site. Highly conserved between CRT and CNX.
44, 311	118, 437	Putative calcium binding sites.

Figure 1.6.1.1 (a) Schematic representation of calreticulin (CRT) and calnexin (CNX). CRT and CNX are divided into three domains: the N-, P- and C- domain. In the P-domain, KPEDWD and GEW repeats are repeated three times in calreticulin and four times in calnexin. (b) X-ray crystal structure of CNX (right hand panel) and model of calreticulin (left hand panel). The P- domain extends outwards from the central globular structure formed by the N- and the C- domains. A bound calcium ion is depicted as a green (CRT) or black (CNX) sphere in the globular domain. Residues within the lectin site that contact glucose are shown in pink (CRT) and red (CNX). CRT model with permission from Ron Landes, and CNX model extracted from http://bioinfo.med.utoronto.ca/Biochemistry/Faculty/D_Williams/chaperone.html. (c) Comparison of residues in CRT with CNX residues and their significance in the CNX structure. Table obtained from Dr Steven Johnson with permission.

1.6.1.1 Structure

Recently, structure of the lumenal domain of calnexin has been determined [184] and reveals much similarity with legume lectins (figure 1.6.1.1). The structure shows that P- domain forms a long extended arm of 140 Å folding back on itself and inserting into the mostly β-sheet composed globular N- domain. Moreover, the structure has established that the lectin domain comprising parts of the P- and N-domain forms the carbohydrate-binding site.

1.6.1.3 Calnexin: a chaperone

CNX was first identified as an 88kDa protein (p88) in transient association with newly synthesised murine class I molecules in the ER of lymphoma cells [185]. A human homologue ER resident calcium binding protein, IP90, was identified simultaneously in human cells and sequencing results showed p88 and IP90 were identical [186-190]. A common name "calnexin" was give to the protein to acknowledge its calcium-binding ability.

A large body of data exists to support the role of calnexin first as a molecular chaperone assisting in protein folding and as part of quality control apparatus that retains unfolded proteins in the ER destined for degradation. Calnexin has been shown to associate only with partially folded transferrin when not all disulphide bonds have formed [191]. It is transiently associated with incompletely assembled subunits of the T cell receptor [192] membrane immunoglobulin [192], achetylcholine receptors [193], integrin [194] and unassembled MHC class I and class II molecules [195].

Calnexin protects polypeptides from degradation allowing more time for folding. Co-expression of calnexin with K^b and D^b in *Drosophila* cells has been shown to extend half-lives class I molecules by four- and five-fold, respectively [196]. In another experiment, using technique of radiolabelling followed by pulse-chase analysis, class I HCs were rapidly degraded in the ER with a half-life of 10 minutes in β2m-deficient cells, while the HCs were stabilized (half-life of 30 minutes) in .174 cells [197]. This experiment suggests an important equilibrium between calnexin and β2m, where calnexin prevents class I HC from degradation in the presence of β2m and possibly ensures class I HC acquire a suitable conformation for binding to β2m. Wilson *et al.*, have recently used semipermeabilized cell system and elegantly shown class I HC is protected from proteasomal degradation in the presence of calnexin [198].

1.6.2 Calreticulin

Calreticulin (CRT) shares a high degree of homology with calnexin (figures 1.6.1.1). It was first identified as a 46kDa soluble high-affinity calcium binding protein from the sarcoplasmic reticulum of rabbit muscle and given the name HACBP (High Affinity Calcium Binding Protein). However, it took more than a decade to show that HACBP was in fact a major calcium binding protein in the ER [199] and was named "cal-reticulin" to acknowledge the fact that it bound calcium and it was localised in the ER.

Calreticulin cDNA from different organisms have been sequenced [200-204] and reveals a remarkable conservation at genomic and amino acid sequence level across species. For example, comparison of human and mouse calreticulin genes demonstrates high homology (70% identity) indicating strong evolutionary

conservations. At protein level, degree of conservation is even higher: there is more than 90% amino acid identity between human, rat, mouse and rabbit calreticulins.

1.6.2.1 Structure of calreticulin

Structural predictions of calreticulin suggest that the protein has at least three domains [186, 205-207]. Residues 1 to 180 of the mature protein form the N- domain and are predicted to form the globular β-sheet structure, containing 8 anti-parallel β-strands and two short α-helices. When modelled with the crystal structure of CNX [184], it is likely the N- domain forms the carbohydrate-binding site (figure 1.6.1.1). This is also the site where the most strongly conserved residues are clustered.

The proline-rich (P) domain encompasses residues 181-290. This domain is extremely rich in proline residues (17% of the residues are proline). It is the most highly conserved region of calreticulin, both across species and with its homologue calnexin. Most striking is the existence of two sequence repeats of 17 [P-x-x-I-x-D-P-D-A-x-K-P-E-D-W-D-x] (type 1) and 14 residues [G-x-W-X-P-P-x-I-x-N-P-x-Y-x] (type 2). Calreticulin comprises three copies of each repeat type in an "111222" arrangement while calnexin has four copies in an "11112222" arrangement [183, 186, 187, 208]. This domain has been implicated in high affinity calcium binding to calreticulin (K_d = 1 μM, Binding Capacity = 1 mol Ca^{2+} /mol protein) [209, 210]. It has a putative glycosylation site and also contains a putative nuclear localisation signal.

The three dimensional structure of rat calreticulin P- domain, encompassing residues 189-288, has now been determined using NMR [211, 212]. The P- domain region shows a hairpin fold that involves the entire polypeptide chain, has the two chain ends

in close spatial proximity, and does not fold back on itself. This long and extended structure is stabilized by the presence of three antiparallel β-sheets. The hairpin loop residues and the connecting regions between the β-sheets contain a hydrophobic cluster. The three β-sheets and the three hydrophobic clusters reflect the periodicity of the amino acid sequence consisting of three 17-residue repeats followed by three 14-residue repeats. The structural features of the P- domain region of calnexin, as determined by X-ray crystallography, is similar to the structure of calreticulin P-domain determined by NMR [184, 211, 212].

The C- domain (residues 291-400) of calreticulin is highly acidic (pI=4). This domain binds calcium with low affinity but high capacity (K_d = 2mM, Binding Capacity = 20-30 mol Ca^{2+} /mol protein) [209] and terminates with a KDEL sequence responsible for its retention in the ER [208]. This is the least conserved domain in calreticulin across species.

1.6.2.2 Functions of calreticulin

Many functions have been proposed for calreticulin [213] and it is beginning to emerge that all these functions are a direct or indirect result of its two major functions: its role as a classical chaperone and in controlling intracellular calcium homeostasis. Calreticulin-deficient mouse embryonic stem cells [214] and more recently, calreticulin-deficient cell lines and mice [215, 216] have made possible to dissect the functions of calreticulin in greater detail.

1) *Calcium homeostasis*: It is well established that calreticulin is involved in intracellular Ca^{2+} storage [186, 217-220]. In addition to storing Ca^{2+}, studies of

calreticulin-deficient embryonic stem cells [214] and mouse embryonic fibroblasts [215] have demonstrated the importance of calreticulin in calcium signalling. Several studies have demonstrated interaction of Sarco-Endoplasmic reticulum Ca^{2+}-ATPases (SERCA) with calreticulin and calnexin via the P-domain and this interaction is proposed to control Ca^{2+} uptake into the ER [221-225]. Similarly, CRT can modulate $InsP_3$-dependent Ca^{2+} release [215, 218]. For example, Mesaeli *et al.*, using calreticulin-deficient embryonic mouse fibroblast cells, have shown diminished $InsP_3$-dependent Ca^{2+} release from the ER in the absence of calreticulin [215]. The mechanism of calreticulin-dependent release of Ca^{2+} is far from clear but it may modulate $InsP_3$ and ryanodine receptors through direct interactions.

Not only calreticulin has a role in cytosolic calcium signalling, it is now emerging it modulates ER calcium signalling by altering free ER [Ca^{2+}] [226] (for review see [227]). It is becoming clear that free ER Ca^{2+} affects ER to Golgi trafficking, nuclear transport [228-230] and activity and interactions of chaperones within the ER [231]. For example, interaction of calreticulin with protein disulphide isomerase (PDI) and ERp57 has been shown to be dependent on free ER [Ca^{2+}] level [226].

As a consequence of its role in Ca^{2+}-homeostasis, calreticulin also plays an important role in the development of an organism. calreticulin-deficient mouse is embryonically lethal at 14.5-16.5 days post coitus [215, 216]. Gross morphological and histological examination of calreticulin- deficient embryos revealed several prominent defects, in the heart and body wall [215, 216]. Calreticulin has also been shown to modulate expression of steroid-sensitive genes. Normally, binding of steroids (such as progesterone, oestrogen and glucocorticoids) to their receptors promotes translocation

of the receptor from the cytoplasm to the nucleus, where it binds to the DNA response elements of a particular gene, and regulates expression of the gene. However, calreticulin can also bind to steroid receptors disabling them from binding to DNA response elements [232, 233]. Calreticulin over-expressing cells show inhibition of glucocorticoid, androgen, retinoic acid and vitamin D_3 dependent transcriptional activation of genes [234-236]. More recently, Holaska *et al.,* have demonstrated nuclear export of the glucocorticoid receptor mediated by calreticulin *in vivo* [237].

Calreticulin is also vitally important in regulating integrin-mediated cell adhesion and integrin-mediated Ca^{2+}-signalling [220, 233, 238]. Calreticulin-deficient embryonic stem (ES) cells are severely impaired in their ability to adhere to fibronectin and laminin via cell surface integrins [214]. Whether calreticulin directly interacts with surface integrins is still controversial [231, 237, 239]. However, it is clear that calreticulin can regulate integrin-mediated adhesion indirectly from within the ER by controlling gene expression of molecules involved in adhesion and/or by regulating integrin-dependent Ca^{2+}-signalling [220, 238].

2) *Chaperoning*: There is now overwhelming body of evidence to suggest that like calnexin, calreticulin is a molecular chaperone that binds transiently to many glycoproteins in the ER. Calnexin and calreticulin both function as monomers and are part of larger dynamic network of proteins that includes other ER chaperones and folding enzymes. Details of the molecular mechanisms of protein folding involving the chaperones calnexin and calreticulin are now emerging and will be discussed in the following section.

Calreticulin has been identified in granules of cytotoxic T lymphocytes, where it is proposed to regulate perforin-mediated lysis of target cells [240]. However, recent work of Fraser *et al.,* has suggested calreticulin may play a more active role in preventing autolysis of the CTL [241]. Another study has shown that activated, rather than resting T cells express higher levels of calreticulin on the cell surface [242]. The same study also found that β2m-free class I associated with calreticulin on the surface of T cells. The significance of this interaction is not clear and remains to be verified by an independent study.

Calreticulin is also the receptor for C1q, the first component of the classical complement cascade [243, 244]. *In vitro*, calreticulin binds to both the collagen-like region and globular head of C1q [245]. Calreticulin is also associated as having pathological roles in autoimmunity. For example, a series of studies have identified calreticulin as an autoantigen in a variety of autoimmune diseases, including systemic lupus erythematosus (SLE) [245-248], rheumatoid arthritis [249], celiac disease [250] and mixed connective tissue disease [251]. Consequently, autoantibodies against calreticulin have been detected in SLE patients and patients with secondary Sjogrens syndrome [252].

1.6.3 Role of calnexin and calreticulin in the folding of glycoproteins

The underpinning molecular mechanism involved in glycoprotein folding is beginning to emerge where calreticulin and calnexin participate in a cycle of binding and release to newly folded glycoproteins ([253, 254] see figure 1.6.3). Each oligosaccharide moiety, which is to be added to nascent polypeptide chain, is preformed by the sequential addition of sugars and is held on the ER membrane by a special lipid

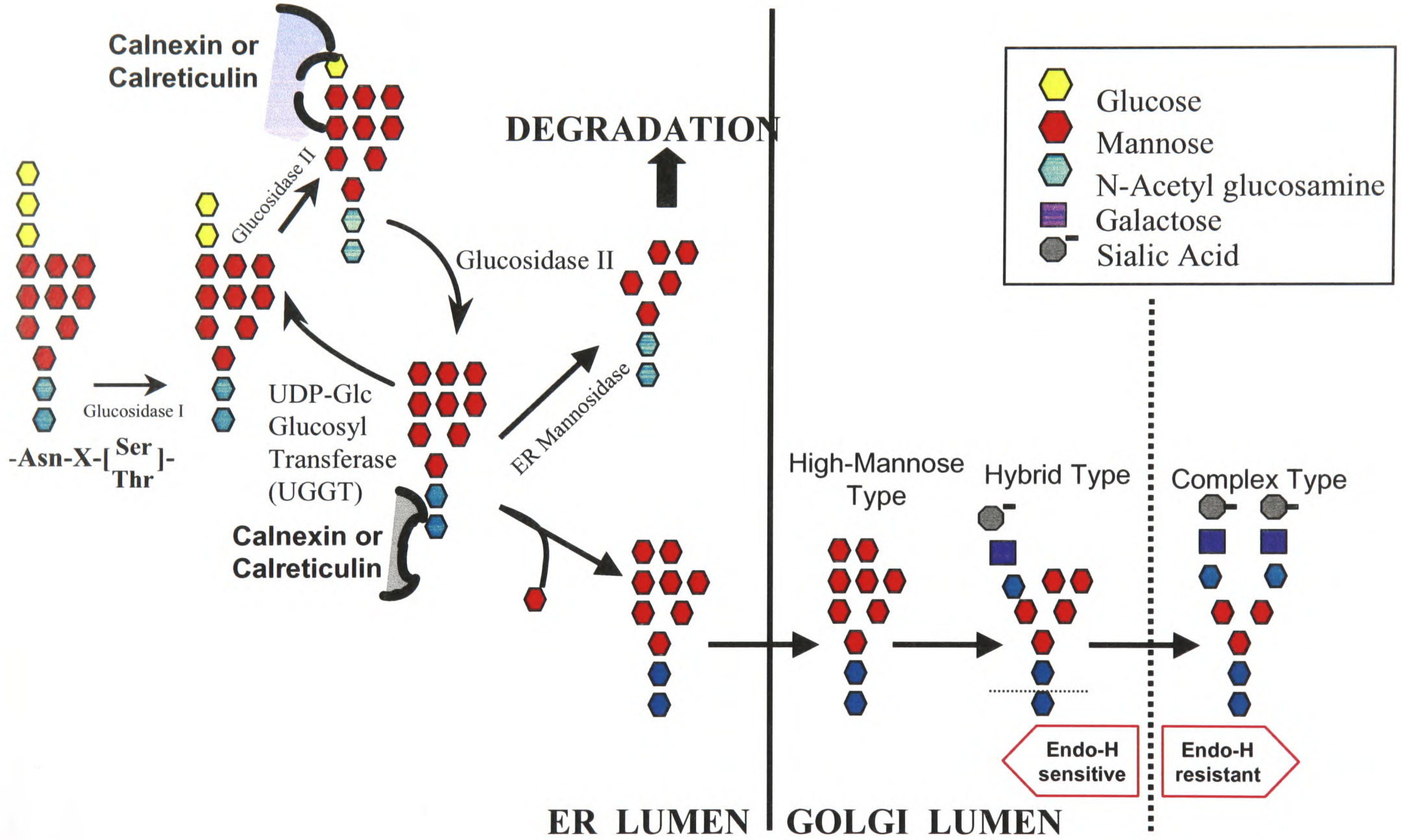

Figure 1.6.3 N-linked glycosylation in the ER. The core oligosaccharide ($Glc_3Man_9GlcNAc_2$) is synthesised in the ER membrane and transferred to the consensus N-glycosylation sequon (Asn-X-Ser/Thr) on nascent polypeptide chains. Immediately after transfer, the glucose residues are removed by Glucosidase I and II. Calnexin and calreticulin bind to Glc_1oligosaccharides. Fully glucose-trimmed high mannose glycans can be re-glucosylated by UGGT if present on incompletely folded proteins. Further oligosaccharide processing occurs in the Golgi, resulting in different carbohydrate moieties. Complex-type carbohydrates are not digested by Endoglycosidase H (Endo-H).

molecule called dolicol. When nascent polypeptide chain with an appropriate motif for N-linked glycosylation (Asn-X-Ser/Thr, where X is any amino acid except proline) emerges into the ER lumen during protein translocation, the preformed 14-residue oligosaccharides ($Glc_3Man_9GlcNAc_2$) is transferred to the side chain NH2-group of asparagines by an enzyme called oligosaccharyltransferase associated with the Sec61 protein translocator complex which translocates nascent polypeptides from the cytosol to the ER [255, 256].

The newly transferred glycans contain three glucose residues (figure 1.6.3). An ER-resident enzyme, Glucosidase I (GSI) removes the terminal α1,2-linked glucose, followed by elimination of the two remaining α1,3-linked glucoses by yet another ER-resident enzyme Glucosidase II (GSII) [257, 258]. It is this monoglucosylated $Glc_1Man_9GlcNAc_2$ trimming intermediate to which both calnexin and calreticulin bind [259-262]. More recently, Vassilakos *et al.*, have shown that the entire Glcα1-3Manα1-2Manα1-2Man structure extending from the α1-3 branch point of the oligosaccharide core is recognised by calnexin and calreticulin [231]. Analysis of binding of monoglucosylated oligosaccharides containing progressively fewer mannose residues suggests that for both chaperones, the α1-6 mannose branch point of oligosaccharide core is also essential for recognition. The proteins bind to fewer mannose containing structure with relatively same affinities as they bind to $Glc_1Man_{5-9}GlcNAc_2$.

The monoglucosylated glycans that bind to calnexin and calreticulin are intermediates during the stepwise removal of glucoses by GSI and GSII. The same structure is also formed by re-glucosylation of fully glucose-trimmed oligosaccharides. A 170 kDa

ER-luminal enzyme called UDP-Glucose:glyprotein glucosyltransferase (UGGT) reglucosylates by adding glucose residues back to the oligosaccharides, thus regenerating monoglucosylated glycans [263-267]. UGGT is special in that it only adds glucose residues only to a misfolded protein. The mechanism by which it recognises such proteins is not known but the existence of de- and re-glucosylation reactions introduces the possibility of a cycle that involves association with, and dissociation from, calnexin and calreticulin. Temperature-sensitive 045 VSV G protein has been used to demonstrate the possibility of the existence of the cycle in intact cell. At the nonpermissive temperature, the G protein undergoes continuous de- and re-glucosylation in the ER of infected cells and it remains calnexin associated. This quality control mechanism ensures that only proteins that reach the "correct" folding state, and would not be seen by UGGT, are allowed beyond this point [260, 268-270].

Recently, it has emerged that the ER chaperones compete for binding sites on a newly synthesised polypeptide. Using viral glycoproteins, Molinari and Helenius have demonstrated that glycoproteins that are glycosylated in their first 50 residues enter the calreticulin/calnexin/Erp57 pathway, and those that are more carboxy-terminally glycosylated enter the BiP/PDI pathway [271]. For calnexin and calreticulin associated glycoproteins, their final release occurs when the polypeptides have reached a fully folded conformation. Misfolded proteins remain trapped in the "GSII-UGGT" cycle of de- and re-glucosylation and calnexin and calreticulin continue to associate until the protein is degraded.

The currently accepted model of calnexin and calreticulin interaction with glycoproteins is the "dual-binding model" [272]. This model proposes that these chaperones bind unfolded glycoproteins through interactions with both carbohydrate and exposed hydrophobic polypeptide sequences. Binding to carbohydrate may initiate the more stable binding of chaperone with hydrophobic polypeptide sequences of a glycosubstrate [272-274].

Diverse range of N-linked oligosaccharide structures is found on mature glycoproteins. These are a result from later modifications made by other ER resident enzymes, which include glucosidases, mannosidases and glucosyltransferases [275, 276]. In essence, three main types of oligosaccharide structures are generated: a) high-mannose oligosaccharides, b) hybrid oligosaccharides, and c) complex oligosaccharides. Hybrid and complex oligosaccharides are generated by a process, which involves trimming of original oligosaccharides added in the ER and the addition of sugars like N-acetylglucosamine, galactose and sialic acid (N-acetylneuraminate). High-mannose-type and hybrid oligosaccharides are found in the ER/cis-Golgi network. However, the complex type oligosaccharides are only found once the proteins reach the medial-Golgi. Here, the complex acquires endoglycosidase-H (endo-H) (enzyme from *Streptomyces plicatus*) resistance, and this can be a useful tool to follow the rate of progress of glycoprotein maturation and traffic of glycoproteins from the ER to Golgi apparatus [277].

Class I HC is glycosylated at position 86 in human, and at positions 86 and 176 on murine H-2 antigens. An additional glycan is present at residue 256 (α3 domain) on murine H-2K^d, D^b, and L^d antigens [278]. Whether glycosylation of class I is essential

for its function is still very much controversial. A large body of evidence based on studies done in human and mouse class I alleles, suggests that glycosylation is probably not essential for class I function. I have explored this further in chapter five.

1.6.4 Assembly of MHC class I molecules in the ER

Assembly of MHC class I molecule is a two stage process which begins in the ER soon after the synthesis of class I heavy chain. A schematic model of MHC class I peptide loading and transport is shown in figure 1.6.4. In the earlier stage, the predominant molecular chaperone involved in MHC class I assembly is calnexin. Cell lines [279] or mice [280, 281], which lack β2m fail to express MHC class I molecules on the cell surface and prolonged association of calnexin with class I heavy chain (HC) followed by degradation of HC is observed [282]. Moreover, several studies have demonstrated transient association of calnexin with newly synthesised class I heavy chain (HC) [283]. It has been suggested that calnexin recruits Erp57, a protein disulphide isomerase (PDI) ortholog [284], which is predicted to promote class I heavy chain disulphide bond formation [283, 285]. Calnexin also protects class I heavy chain from degradation [196, 198] until β2-microglobulin (β2m) has associated.

In the second stage of assembly, calnexin dissociates from the class I HC probably as a result of class I HC undergoing a conformational change [168] upon binding to β2m and at least in human cells, is replaced by calreticulin [162, 286, 287], an important constituent of the multimolecular loading complex, which includes other cofactors like TAP, tapasin and Erp57 [288, 289]. Assembly of class I molecules is not sufficient at this stage for cell surface expression as class I molecules are retained in

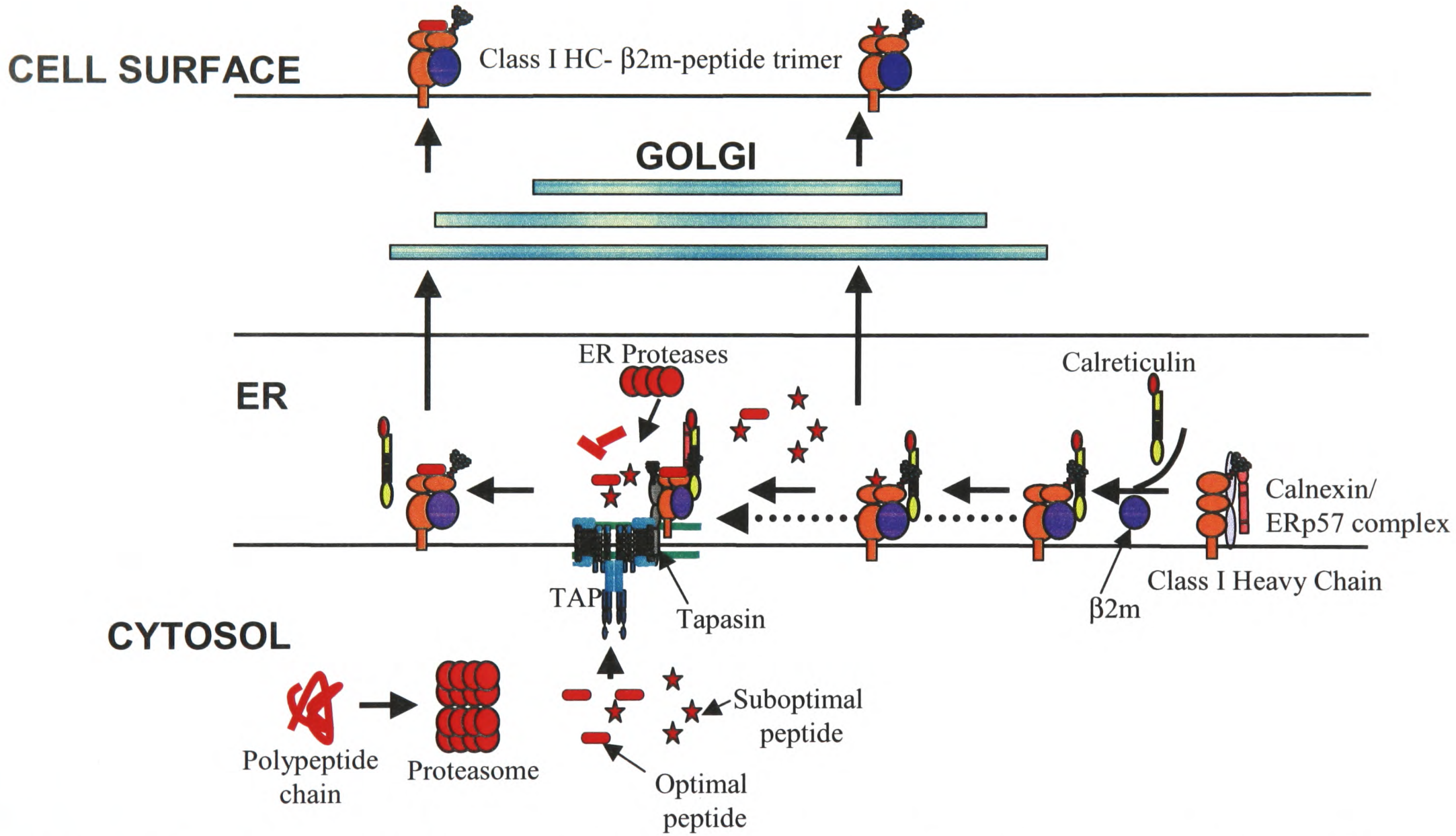

Figure 1.6.4 A Schematic model of MHC class I peptide loading and transport. Newly synthesised class I heavy chain (HC) associate with calnexin/ERp57 complex. Upon β2m binding, the HC dissociates from calnexin/ERp57 complex and the HC:β2m heterodimer associates with calreticulin. The HC:β2m heterodimer at this stage can either exit to the cell surface with a suboptimally loaded peptide or get incorporated into the multimolecular "loaing complex" consisting of TAP, tapasin, calreticulin and ERp57 and acquire optimal peptide. Proteasome in the cytosol degrades polypeptide chains into peptides and are transported into the ER through TAP. ER resident "trimases" may also trim longer peptides delivered by TAP or generate TAP-independent peptides. Upon peptide binding, the MHC class I molecule is released and transported via the Golgi to the cell surface to be scanned by cytotoxic T cells (CTLs)

the ER in Transporter associated with Antigen Processing (TAP)- deficient cells [290] suggesting that association of antigenic peptides with class I molecules may be required for correct folding of the heavy chain. Indeed this is the case as class I molecules with non-conservative threonine to lysine mutation at position 134 (T134K), which fail to interact with TAP, Erp57 and tapasin [291] [180] (Tim Elliott, unpublished data) assemble normally with β2m but fail to get loaded with optimal peptides [180]. As a result T134K molecules are unable to present endogenous viral epitopes to T cells [180, 292]. Other studies have also suggested that the release of peptide-receptive class I molecules from the ER is dependent on a TAP-dependent supply of peptides to the ER [293, 294].

Little is known how peptides are loaded onto class I, but it seems likely that other components of the loading complex are involved. There is accumulating evidence to support a role of tapasin in class I peptide loading and optimisation [14, 165, 295, 296]. Moreover, by comparing tapasin-deficient .220 cells (human B cell line) with the ones transfected with normal tapasin, it has been shown to increase steady-state TAP levels [161] as well as the rate of peptide translocation by TAP (2.5 to 3 fold) [165]. Tapasin-dependent loading and optimisation has been shown to be dependent on the type of class I allele [14, 162-165].

Apart from its function in peptide loading and optimisation, other ascribed functions of tapasin include retention of empty but not loaded class I molecules in the ER [297] and chaperoning of peptides from TAP to the peptide-binding groove of class I [296, 298].

1.6.5 Release of MHC class I molecules from the ER

It is not clear exactly what initiates the release of peptide-bound class I molecule from the loading complex. Release could be triggered by peptide-induced conformational change in the class I molecule itself [170]. Such a conformational change in heavy chain is seen in the absence of β_2m [168] and has been implicated when peptide binds to empty HC-β_2m heterodimers [177]. Alternatively, or in addition to this, conformational change in TAP could trigger the dissociation of the MHC class I molecule from the loading complex [299]. Such conformational change could be mediated by nucleotides binding to TAP, which would also results in the transport of peptides across the ER membrane [300]. Moreover, recycling of incompletely assembled class I molecules from Golgi apparatus into the ER [301] could also induce release of peptide-loaded class I from the loading complex.

1.7 SUBJECT OF THE THESIS

Assembly of class I HC with β2m and acquisition of optimal peptide is essential for appropriate CTL response. Following synthesis, class I HC associates transiently with calnexin/Erp57 complex. Class I HC is folded and disulphide bonds are formed during the association process, resulting in class I HC that is competent to assemble with β2m. At least in humans, calnexin/Erp57 complex dissociates after class I HC assembles with β2m. At this stage, assembled class I molecules are either "empty" or loaded with suboptimal peptide. Class I molecules acquire optimal peptides when they are incorporated into the loading complex, which consists of TAP, tapasin, ERp57 and calreticulin. The precise role of calnexin in the initial assembly of class I, the role of the components of the loading complex in optimal peptide loading and the significance of their physical interactions remain unclear still. Moreover, role of class

I HC glycosylation in the regulated assembly, loading and antigen presentation function is also unclear.

I have made use of calreticulin- and calnexin-deficient cells to dissect the role(s) of the chaperones in class I assembly and peptide loading. By introducing different domains of calreticulin into calreticulin-deficient cells, I have tried to understand the roles of different domains of calreticulin in class I expression and assembly. I have also generated a number of class I HC glycosylation mutants in order to further understand the role of HC glycosylation in the assembly and antigen presentation function of class I.

I show that calnexin plays an important role in the assembly of class I molecules. Calreticulin is critical in class I peptide loading and that co-operation from all domains is essential to generate a fully functional calreticulin. P- domain downregulated the expression of several ER proteins and glycoproteins including class I despite its ability to restore basal cytosolic calcium levels in calreticulin-deficient cells. I also show that glycosylation in class I is optimal and any alterations of glycosylation from normal results in defective peptide loading of class I.

Chapter 2

MATERIALS AND METHODS

2.1 CHEMICALS

Sigma, UK supplied all chemicals used unless otherwise stated.

2.2 GENERAL TISSUE CULTURE

All cells were grown at 37^0C in a water-saturated hood of 5% CO_2 in air. Media for tissue culture were purchased from Sigma, UK or from Gibco BRL, UK. Cells were grown in either Dulbecco's Modified Eagles Medium (DMEM) or in RPMI 1640 medium, supplemented with 10%FCS, 50U/ml Penicillin, 50 μg/ml Streptomycin and 2mM L-Glutamine (referred to either as D10 or R10) unless otherwise stated. Tissue culture materials were supplied by Falcon (Becton Dickinson, USA) or Nunc, UK. Stocks of all cells were prepared by freezing cells in FCS containing 10% sterile DMSO. Cells were aliquoted into Nalgene Cryovial and kept in Mr Frosty in -80^0C freezer, which allows slow cooling at the rate of 1^0C per minute. These stocks were then transferred to liquid nitrogen and the stocks were regularly checked for mycoplasma infection. Cells were discarded or mycoplasma treated if found infected.

2.3 CELL LINES

C1R [302] is a human B-lymphoblastoid cell line, derived from Hym2 [303]. It has one copy of chromosome 6 deleted and does not express HLA-A or –B alleles from the intact chromosome 6. HLA-Cw4 is however, expressed by this cell line [304]. C1R cells were transfected with the genes for wild-type HLA-A*0201 (I will call this C1R-A2.1) and HLA-A*0201 with a single coding change resulting in a threonine to

lysine substitution at position 134 (C1R-T134K) by Dr M. Matsui (Duke University, USA; [305]) and were a kind gif from Dr J. Frelinger (University of North Carolina, USA).

tk-143 cells are thymidine kinase (tk)-negative human cell line (line 143). They were derived by C. Croce and K. Huebner (Wistar Institute, Philadelphia, USA) and were grown in D10 and trypsinised as for K41 and K42 cells (see below).

K41 and K42 Wild-type (K41) and calreticulin-deficient (K42) fibroblasts were derived by SV40 transformation of primary fibroblast cultures from mouse embryos carrying a targeted knockout of the calreticulin gene [215]. The cells were passaged in R10 and grown to 80% confluency before harvesting by trypsinising using a 10% Trypsin:EDTA solution. After quenching trypsin activity using excess R10, cells were centrifuged and re-seeded as required. For experiments, cells at around 60-70% confluency were used.

CEM and CEM.NK^R CEM is a human T lymphoblastoid cell line. CEM.NK^R was generated by subjecting CEM to immunoselection by co-culture with peripheral blood mononuclear cells (PBMC) and selecting for resistance to natural killer (NK) cell-mediated lysis [306].

2.4 ANTIBODIES

Following is a description of antibodies that were used for immunoprecipitation studies, flow cytometry, confocal microscopy or western blotting.

BB7.2 It is a monoclonal antibody (mAb) that recognises a conformation dependent epitope on the α1 domain of HLA-A*0201 [307]. Purification of antibody from hybridoma supernatant was carried out as described below (section 2.5.1). The antibody was used at a final concentration of either 15 μg/ml (for immunoprecipitation studies) or 5 μg/ml (for flow cytometry).

ABR2 It is a rabbit polyclonal antiserum raised against a peptide with sequence identity to 10 amino acids of the cytoplasmic tail of HLA class I heavy chains. It reacts strongly with HLA class I free heavy chains but poorly with beta 2-microglobulin (beta 2-m)-associated heavy chains [308]. For immunoprecipitation studies 5 μl of ABR2 serum was used.

W6/32 It is a mAb that recognises a conformational epitope on properly folded HLA-A, -B, -C molecules [309, 310]. For flow cytometry, W6/32 was used at a concentration of 5 μg/ml.

B22.249 (B22) It is a mAb specific for a conformational epitope on the α1 domain of H-2D^b [311], requiring proper folding of the peptide-binding domain. The antibody also stabilises the interaction between H-2D^b heavy chain and β_2m [168, 312]. Moreover studies have shown that it slows the dissociation of bound peptides by around 10-fold [172]. Purification of antibody from hybridoma supernatant was carried out as described below (section 2.5.1). B22 was used either at a final concentration of 15 μg/ml (for immunoprecipitation studies) or at 5 μg/ml (for flow cytometry).

Y3 It is a mAb that recognises a conformation dependent epitope on α1 domain of H-2K^b. Purification of antibody from hybridoma supernatant was carried out as described below (section 2.5.1). Y3 was used either at a final concentration of 15 μg/ml (for immunoprecipitation studies) or at 5 μg/ml (for flow cytometry and confocal microscopy).

PA3-900 The rabbit polyclonal antibody raised against human calreticulin (Stendahl O science 1994) was purchased from Affinity Bioreagents, Inc (Golden, USA) and was supplied as 100 μl of diluted reagent. For immunoprecipitation studies it was used as a 1:100 dilution as suggested by the supplier.

SPA-860 This is a rabbit polyclonal antibody raised against canine calnexin synthetic peptide (amino acids 575-593, C- terminus) and was purchased from StressGen Biotechnologies Corp., USA). This antibody was supplied as 200 μl of diluted reagent and was used at a dilution of 1:200 for immunoprecipitation and confocal microscopy studies.

Oswald Rabbit anti-calnexin serum was generated by Dr B. Gao (Institute of Molecular Medicine, University of Oxford, UK) using a synthetic peptide (CAEEDEILNRSPRNRKPRRE) conjugated to the carrier protein KLH (haemocyanin) corresponding to the 20 C-terminal residues of human calnexin. For western blot, this was used at a dilution of 1:2000.

Tons Rabbit Anti-human calreticulin antiserum, which cross-reacts with the mouse protein was kindly provided by Dr B. Sim (University of Oxford, UK). For western blot, this was used at a dilution of 1:1500.

T18 Murine MHC heavy chain specific antiserum T18 was generated against a recombinant fragment of D^b molecule from residues 1 to 270 [313].

25-D1.16 Monoclonal antibody 25-D1.16 recognising the Kb/SIINFEKL complex was kindly provided by Dr Ron Germain (Bethesda, USA).

HA-probe The rabbit polyclonal anti-HA was purchased from Santa Cruz Biotechnologies Inc., USA. The antibody is against an epitope mapping to an internal region of the influenza hemagglutinin (HA) protein. The antibody was supplied at a concentration of 200 μg/ml and was used at a dilution of 1:200 for western blot.

HCA2 Mouse monoclonal antibody, which recognises heavy chain of A2.1 molecules. This antibody was used 1:1000 for western blot.

2.5 PURIFICATION OF ANTIBODIES

2.5.1 Production of hybridoma supernatant

BB7.2, B22 and Y3 hybridomas were thawed and cultured at 37^0C, 5%CO_2 in roller bottles holding a final volume of approximately 1500 ml R10 per bottle. About 200 ml of confluent hybridoma culture was used to seed the roller bottle cultures. The culture medium was harvested (5-7 litres) and centrifuged in 1-litre cylinders in a

Beckman J-6B centrifuge (3000 rpm, 30 min, no brakes, 4^0C). The supernatant was then carefully decanted and filtered through Whatman size 4 filter cups followed by Whatman GFC filter cups and stored at 4^0C containing 0.02% sodium azide, until purification of IgG.

2.5.2 Protein A-Sepharose affinity purification of antibodies

The following procedures were performed at 4^0C. The pH of the hybridoma culture supernatant was adjusted to 8.0 by addition of 1/10 volume of 1 M TrisHCl, pH 8.0. This was then passed through a 10 ml column packed with Protein A-Sepharose (PAS) beads equilibrated with 100mM TrisHCl, pH 8.0. The PAS column was then washed with approximately 20 column volumes of 100mM TrisHCl, pH 8.0. IgG fractions were eluted with 100mM GlycineHCl, pH3.0. 1 ml elute was collected stepwise into eppendorf tubes containing 100 µl 1 M TrisHCl, pH 8.0 for instant pH neutralisation of the elute. The tubes containing the eluted IgG were identified by spectroscopy at 280 nm (1 OD = 0.8 mg/ml) and pooled together. After dialysing overnight, antibody was aliquoted into eppendorfs and stored at -20^0C.

2.6 PEPTIDES AND RECOMBINANT VACCINIA VIRUS

The following peptides were used during the course of the study: a) HLA-A*0201 binding peptides ILKEPVHGV (corresponding to residues 476-484 of the naturally processed HIV-pol epitope) [314, 315] and GILGFVFTL (Influenza A matrix protein (MP) corresponding to residues 58-66) [316]; b) H-$2D^b$ binding peptide ASNENMDAM (corresponding to residues 366-374 of influenza A nucleoprotein from strain A/NT/60/68) [173] and c) H-$2K^b$ binding peptide SIINFEKL (derived from Ovalbumin). All peptides were synthesised commercially by Research Genetics,

Inc. (Huntsville, AL, USA) and supplied as lyophilised powder. The peptides were more than 95% pure judged by HPLC profile supplied with the product. Recombinant vaccinia virus expressing ovalbumin was kindly provided by Dr Jon Yewdell (Bethesda, USA). KAVYNFATC the immunodominant GP33 peptide derived from the glycoprotein of lymphocytic choriomeningitis virus (LCMV) and recombinant vaccinia virus expressing the same glycoprotein of LCMV and GP33-specific murine CTL were generous gifts from Dr A Gallimore (University of Oxford, UK).

2.7 TECHNIQUES USED TO STUDY THE BIOCHEMISTRY OF CLASS I MOLECULES

2.7.1 Flow Cytometry (FACS)

$1x10^6$ cells were washed in PBS and incubated with hybridoma culture supernatant (for 25-D1.16) at a ratio of 1:1 or mAb antibody at a final concentration of 5 μg/ml (for BB7.2, Y3, W6/32 and B22) in FACS solution (200 μl of PBS with 0.5% FCS and 0.5% Sodium Azide) on ice for 30 minutes, then washed two times with 200 μl cold FACS solution. The cells were stained for 45 minutes at 4°C in 200 μl of FACS solution containing a 150 fold of dilution of goat anti-mouse Ig-FITC conjugate (Sigma). The cells were then washed three times with 200 μl of FACS solution and resuspended in 500 μl of FACS solution containing 0.7% formaldehyde. A minimum of 20,000 cells was counted using the FACSCalibre flow cytometer (Becton Dickinson & Co. Mountain View CA, USA).

2.7.2 Western Blot

1×10^7 cells were washed once with PBS and lysed in 1 ml of 0.5% NP40 on ice for 30 minutes. The lysates were clarified by micro centrifugation at 13,000 rpm for 5

minutes. The supernatant was mixed with equivalent volume of 2-x SDS-PAGE loading buffer, boiled, and fractionated by SDS-PAGE on a 12.5% acrylamide gel. After separation, the proteins were blotted onto Hybond-C Extra membrane (Amersham) by electrophoretic transfer. The transferred membrane was blocked with PBS containing 2.5% fat-free milk for at least 1 hour. The first antibody in PBS with 0.02% Tween 20 (PBST) and 2.5% fat-free milk was added and incubated for one hour at room temperature. The membrane was then washed two times with PBST and incubated with an appropriate secondary antibody conjugated to horseradish peroxidase for further one hour. The membrane was washed three times with PBST and the signal was developed with a SuperSignal Dura West (Pierce) chemiluminescence kit and the membrane was exposed either to CCD camera on a phosphoimager for 30 seconds to 10 minutes or onto Kodak Xomat film for 2-10 minutes.

2.7.3 Immunoprecipitation and pulse chase

5×10^6 - 1×10^7 cells per time-point were washed once in PBS and incubated for 40 minutes in 2 ml of warm methionine/cysteine-free RPMI 1640 medium supplemented with 10% FCS and 1% glutamine and Penicillin and Streptomycin (M^-C^-R10) at 37^0C. The cells were then spun down at 1400 rpm and metabolically labelled at 37^0C in 1 ml fresh warm M^-C^-R10 with [^{35}S]-Promix (which consists of 70% L- [^{35}S]-methionine and 30% L-[^{35}S]-cysteine trans-label; supplied by Amersham, UK) at a concentration of 100 μCi per 1×10^7 cells.

2.7.3.1 Immunoprecipitation

For immunoprecipitation, cells were labelled for 40 minutes, at which point the cells were spun down and lysed on ice for 30 minutes in 1 ml ice-cold NP40 lysis buffer (0.5% Nonidet P40, 150mM NaCl, 5mM EDTA, 20mM TrisHCl, 2mM PMSF, 5mM Iodoacetamide). For cells lysed in the presence of stabilising peptide, 20 μM peptide was added at this stage to the lysis mix. The lysed cell samples were then centrifuged for 5 minutes at 13000rpm at 4^0C to remove nuclear debris before preclearing by rotating overnight at 4^0C with 100 μl of fixed *Staphylococcus aureus* (Staph A) in PBS. The Staph A was removed by centrifugation at 13000rpm for 5 minutes and the supernatant decanted into a fresh tube. Assembled class I molecules were then immunoprecipitated by first incubating with the relevant antibody by rotating for 90 minutes at 4^0C and then with 10% (w/v) suspension of purified Protein A-Sepharose (PAS) in PBS for a further 40 minutes. Samples were then washed three times in NP40 lysis buffer by repeated resuspension in lysis buffer and centrifugation (7000 rpm 40 seconds)

2.7.3.2 Pulse chase

For pulse-chase experiments cells were labelled for 10 minutes, after which cells were immediately quenched with pre-warmed "cold" R10 supplemented with 2mM methionine and 2mM cysteine (Sigma Ultra). Cells were then incubated at 37^0C for the duration of the chase and cell aliquots removed at specific time-intervals.

Where digestion with Endoglycosidase- H (Endo-H) was performed, the immunoprecipitated pellets were resuspended in 25 μl of Endo-H buffer (50mM sodium citrate buffer, pH 5.6 containing 0.2% SDS), vortexed briefly and heated to

100^0C for 5 minutes. The resuspension was then cooled to 37^0C and 3 U (1.5 μl) of Endo-H (Boehringer Mannheim, Germany) was added to each sample before incubating overnight at 37^0C. Endo-H treated samples were then analysed by 12.5% SDS-PAGE

2.7.4 Cell fractionation and scintillation counting

Cell fractionation was carried out after pulse labelling for 10 minutes. At the end of the labelling period cells were lysed with 20μM digitonin in the presence of protease inhibitors on ice for 30 minutes. At the end of the lysis, cells were spun down at 13000 rpm for 5 minutes and supernatant collected into fresh microfuge tubes. This fraction consisted of cytoplasmic proteins. The pellet was further lysed with NP40 lysis buffer on ice for further 30 minutes. The lysed mix was spun down at 13000 rpm for 5 minutes and supernatant collected into fresh microfuge tubes. This fraction will consist of membrane proteins. The pellet containing the nuclear fraction was lysed in 2.5% SDS.

β-radiation counter was used for the scintillation counting. The inherent protocol contained in the computer was used to count β-radiation in different fractions isolated.

2.7.5 SDS-polyacrylamide electrophoresis and autoradiography

Immunoprecipitated samples were resolved using SDS-polyacrylamide electrophoresis (SDS-PAGE) under reducing conditions. Equal volume of 2X SDS-PAGE loading buffer (30% glycerol, 10%SDS, 5% β-mercaptoethanol (2-ME), 50mM Tries (pH 6.8), 0.005% (w/v) bromophenol blue) was added to the Endo-H digested material and the samples heated to 95^0C for 5 minutes and centrifuged

briefly prior to loading onto 12.5% SDS-polyacrylamide gels. For immunoprecipitations not requiring Endo-H digestion, samples were mixed with 30 µl of 1X SDS-PAGE loading buffer and heated as above.

12.5% SDS-polyacrylamide gels were made using pre-mixed acrylamide/ N,N'-methylene bisacrylamide (National Diagnostics, USA) at 30% (w/v) and 0.8% (w/v), respectively (ratio = 37.5:1). Polymerisation of gels was performed under anaerobic conditions and catalysed using 10% ammonium persulphate (freshly made) and TEMED (National Diagnostics, USA). Samples, together with SDS-PAGE broad range (or low range as appropriate) molecular weight markers (BioRad) were loaded into wells formed in a stacking gel (0.125 M Tris pH6.8, 13% (v/v) acrylamide/bisacrylamide, 0.1% (w/v) SDS) which then were resolved on a 12.5% gel (0.125 M Tris pH6.8, 37.5% (v/v) acrylamide/bisacrylamide, 0.1% (w/v) SDS) buffered with standard running buffer (10 X running buffer: 30g Tris, 143g Glycine, 10g SDS in 1 L distilled water) and run at constant voltage of 200V using Novex X-Cell SureLock™ Mini-Cell system

Once the gels were resolved, they were first fixed in fixing solution (10% (v/v) acetic acid, 5% (v/v) methanol) for 5 minutes before staining with Coomassie Blue stain (0.1% (w/v) Coomassie Blue, 45% (v/v) methanol, 10% (v/v) acetic acid in distilled water) for 30 minutes to visualise antibody bands. Gels were then destained overnight using fixing solution (10% (v/v) acetic acid, 5% (v/v) methanol). They were then soaked in Amplify™ liquid scintillant (Amersham, UK) for 20 minutes before drying onto 3mm Whatman filter paper using heat/vacuum dryer. The dried gel was exposed to either phosphoimager or Biomax film (Kodak, UK) at – 80^0C for autoradiography.

Autoradiographs were quantified using the Aida programme (for images from Phosphoimager) or Quantity One software (BioRad, UK) both of which express band intensities as an integrated optical density (IOD).

2.8 STABILITY OF CLASS I COMPLEXES *IN VITRO*

Assembly assay [179] is based on peptide-dependent stabilisation of unstable class I complexes after lysis of cells and the detection by immunoprecipitation with the conformation-specific antibodies. Briefly, cells were labelled with [^{35}S]-methionine/cysteine for 20-30 minutes. Cells were then aliquoted (5 x 10^6 per sample) and lysed in 1 ml ice-cold 0.5% NP-40 in the presence of excess amount of stabilising peptide. Samples were then pre-cleared overnight with 100 µl Staph A or pre-cleared for 30 minutes with 40 µl 50% slurry of Protein-A Sepharose beads and immunoprecipitated using 15 µg/ml BB7.2 (HLA-A*0201), B22 (H-2Db), Y3 (H-2Kb) or 7 µl ABR2 (HLA-A*0201). Samples were washed four times, digested with Endo-H overnight (for pulse-chase experiments) and analysed by 12.5% SDS-PAGE. The intensity of class I heavy chains (HCs) was then determined either by phosphoimager or by autoradiography as described above.

For pulse-chase quantification, the fraction of a pulse-labelled cohort of class I molecules which leave the ER (A) and those that are retained and degraded in the ER (B) was calculated at each time point from IOD of Endo-H-resistance and Endo-H-sensitive class I HC bands precipitated by conformation-sensitive antibodies. A and B data was plotted with IOD on the Y-axis and time points on the X-axis.

2.9 CO-IMMUNOPRECIPITATION

Co-immunoprecipitation studies were carried out to study association of class I molecules with TAP and other ER-resident chaperones and co-factors. 1 x 10^7 cells per experimental point were washed in sterile PBS, starved in R10 medium lacking methionine and Cysteine (M^-C^- R10) for 40 minutes, and metabolically labelled with [^{35}S]-methionine/cysteine for 30-40 minutes at 37^0C. Cells were spun down, media aspirated and the pellet lysed in 1 ml of 1% digitonin lysis buffer (1% (w/v) digitonin (BDH, AnalaR), 50mM Tris-HCl (pH 7.5), 5mM $MgCl_2$ and 150mM NaCl) for 30 minutes on ice. The lysates were pre-cleared overnight at 4^0C with 60 µl Staph A and 2 µl normal rabbit serum (NRS) (Gibco BRL). The Staph A was removed by centrifugation at 14000rpm for 5 minutes. The supernatant was again pre-cleared in 45 µl of 50% slurry of Protein A Sepharose (PAS) for 40 minutes. PAS was removed by centrifugation at 7000 for 5 minutes. Supernatant was then immunoprecipitated with relevant antibodies. Samples were then washed four times in 0.5% digitonin lysis buffer and analysed by autoradiography as described earlier.

2.10 PHARMACOLOGICAL TREATMENT OF CELLS

In experiments designed to interfere with glycosylation, castanospermine (CAS), Thapsigargin (TG), Cyclopiazonic acid (CPA) and Tertiary butylhydroquinone (TBHQ) were added to cells at concentrations indicated. The drugs were continuously present during metabolic labelling with [^{35}S]-methionine/cysteine. For retention of HLAA*0201 molecules in the ER-*cis*Golgi, 10 µM Brefeldin A (BFA) was added.

2.11 CONSTRUCTION OF PLASMID VECTORS

All reagents required for construction of plasmid vectors (e.g., restriction endonucleases and their appropriate buffers) were purchased from New England Biolabs (NEB) or Promega (UK). Ready-to-Go T4 DNA ligase kit was purchased from Amersham (UK).

2.11.1 PUB6/V5-His as expression vector (Appendix 2.14)

2.11.1.1 Choice of vector

The mammalian expression vector pUB6/V5-His was purchased from Invitrogen and was chosen for a number of reasons:

a) PUbC (human ubiquitin C promoter)- This promoter allows recombinant proteins to be expressed in a wide range of mammalian cell lines. The ubiquitin C protein is highly conserved in eukaryotic cells and it can easily be introduced into a variety of cells.

b) V5 epitope- this epitope is recognized by the Anti-V5 Antibody. This epitope is translated as a part of the gene of interest. Such epitope tags are helpful when discriminating between a wild type protein and a re-engineered protein of interest.

c) C-terminal polyhistidine tag (6XHis)- This epitope is recognized by the Anti-His(C-term) Antibody. These six tandem histidine residues also aid in the purification of the recombinant proteins.

d) SV40 early promoter and origin (SV40 ori)- Cells that are infected with the simian virus express the SV40 large T antigen. This antigen prohibits the replication of the gene of interest. The SV40 origin permits replication in such cells, assuring overexpression of the recombinant gene.

e) Blasticidin Resistance Gene (BSD)- This gene confers resistance to cells in which blasticidin is present. Blasticidin is a nucleoside antibiotic that inhibits the formation of proteins in all cell types (prokaryotic and eukaryotic). This feature can be used to generate and maintain stable cell lines. The vector also contains the Ampicillin Resistance Gene, but by providing both of these resistance genes, the vector allows selection in *E. coli* and mammalian cells as well as increases the accuracy of cell selection.

2.11.2 cDNAs

Full-length rabbit calreticulin with a 3' HA epitope and a KDEL retrieval sequence (Prof Marek Michalak, University of Alberta, Canada), P-, PC-, NP- domains of rabbit calreticulin each with 3' HA epitope and a KDEL retrieval sequence (Prof Marek Michalak, University of Alberta, Canada) and 1-387 amino acid residues of canine calnexin (soluble calnexin) with 3' HA epitope and a KDEL retrieval sequence (Dr David Williams, University of Toronto, Canada) had been previously constructed in pCDNA3 and were a gift from Professor Marek and Dr Williams.

2.11.3 Subcloning

Full-length rabbit calreticulin, and P-, NP- and PC- domains of rabbit calreticulin and soluble calnexin were subcloned into pUB6/V5-His (see Appendix for plasmid map). Briefly, 20 μg of pCDNA3 encoding the gene of interest was sequentially digested with unique restriction enzymes at two ends of the gene of interest according to the guidelines given by the supplier of restriction enzymes (NEB or Promega). The digestion was confirmed by electrophoresis analysis of small amount of digested sample using 1% (w/v) agarose gel buffered with 1 x TBE (0.09 M Tris Borate, 0.002 M EDTA) running at constant voltage (45 V) followed by visualisation using ethidium bromide at a final concentration of 20 mg/ml and ultra-violet (UV) transilluminator (Stratagene, USA). When complete digestion was confirmed, the rest of the digested plasmid was electrophoresed under the same conditions, and the band of interest excised from the gel and purified using the Geneclean DNA purification kit (BIO 101 Inc. Vista USA). The purified fragment was quantified by comparing band intensity on the agarose gel with 200ng DNA from a HindIII digest of λ phage.

PUB6/V5-His was digested using the same sets of restriction enzymes under the same conditions and purified according to the procedure described above. Ligation of the gene fragment and cut pUB6/V5-His was performed overnight at 16^0C using the Ready-To-Go T4 DNA ligase kit (Amersham, Pharmacia Biotech, USA).

2.12 TRANSFORMATION OF CHEMICAL COMPETENT *E COLI* CELLS

Transformation competent DH5α were generated according to the PolyethyleneGlycol/Di-methyl Sulphoxide (PEG/DMSO) method of Chung and

Miller [317] and stored in 50 µl aliquots at –80^{0}C for up to 6 months. Before transformation, competent cells were thawed on ice and mixed gently to ensure the cells were evenly suspended. 10-20ng of the DNA ligation mix was mixed with 50 µl of KCM (5 X stock 0.15 M $CaCl_2$, 0.25 M $MgCl_2$, 0.5 M KCl). 50 µl of DH5α competent cells were added to the DNA mix and incubated on ice for 20 minutes followed by addition of 1 ml LB broth and incubation for1 hr at 37^{0}C (shaking). Following incubation, 100-250 µl of the bacterial culture was plated onto LB agar plates containing 100 µg/ml Ampicillin and left overnight at 37^{0}C. Bacterial colonies were isolated and screened the following day.

2.12.1 Screening for positive colonies

An ampicillin LB plate was divided into numbered grids for replating. Bacterial colonies were individually picked from the overnight plate using sterile pipette tips. After carefully spreading the bacteria inside one grid, the same tip was dipped into a numbered falcon tube (corresponding to the grid number) containing 5 ml LB/Ampicillin bacterial culture media. The bacterial culture was grown overnight at 37^{0}C (with shaking). The following day, plasmid DNA was isolated from bacterial culture by using Qiagen miniprep kit (Qiagen, UK) and restriction digests were performed to check for correct cDNA insertion into the pUB6/V5-His vector. Bacteria expressing the required plasmid were expanded and stocks generated.

2.13 LARGE SCALE PREPARATION OF PLASMID DNA SUITABLE FOR TRANSFECTION

A sterile pipette tip was used to scrape frozen stock of the required plasmid-carrying bacteria and pipette tip carefully dipped into a flask containing 1 litre bacterial culture

media (LB + 100 mg/ml ampicillin) and cultured overnight at 37^0C (with shaking). The following day, the culture was spun down and plasmid extracted from the bacterial pellet using Maxi Prep plasmid purification kit (Promega, USA). The final plasmid pellet was resuspended in sterile distilled water. A small plasmid sample was run on 1% agarose gel in order to quantify the amount of plasmid generated. Sterile plasmid DNA was stored at -20^0C.

2.14 SITE-DIRECTED MUTAGENESIS

Site-directed mutagenesis was carried out to generate glycosylation mutants of HLA-A*0201 using the QuickChange™ site-directed mutagenesis kit (Stratagene, USA). For each mutation, two complementary oligonucleotide primers were designed, containing the desired mutation and a mutation in a flanking codon, which would introduce a novel restriction site without altering the amino acid sequence of the polypeptide chain. Primers were synthesised by Genosys (Sigma, UK).

As suggested in the kit, 125ng of each primer were used in a PCR reaction mixture consisting of 50ng of plasmid template DNA (pCDNA3-HLA-A*0201) (see appendix 2.14), 1 x reaction buffer, dNTP mix (unspecified concentration) and *Pfu Turbo* DNA polymerase (2.5 units) in a final volume of 50 µl. *Pfu Turbo* DNA polymerase was preferred because of its proof-reading capability. For PCR, Hybaid thermocycler was used. PCR reaction was carried out with the following thermal cycling:

Initial denaturation:		95^0C	30 sec
18 amplification-cycles	denaturation	95^0C	30 sec
	annealing	55^0C	1 min
	extension	68^0C	2 min

At the end of the PCR, 10 units of *Dpn* I endonuclease was added directly to the amplification reaction and incubated further for 1 hour at 37^0C to digest parental DNA. 1 μl of *Dpn* I-treated DNA was used to transform 50 μl of DH5'α competent cells according to the procedure described above. After isolation of plasmid DNA, successful mutation was determined by restriction digest and further by DNA sequencing (Department of Biochemistry, University of Oxford, UK).

2.15 VIRUSES

Recombinant vaccinia encoding HLA-A*0201 (vac-A2.1) was a kind gift from Drs J Yewdell and J Bennink. Recombinant vaccinia encoding HLA-A*0201_{T134K} (vac-T134K) was generated by Dr John Lewis in my lab.

2.15.1 Vaccinia expansion by transfection of *tk*-143 cells

Confluent 175cm^2 flasks of *tk*-143 cells (which lack the thymidine kinase gene) were first washed with sterile PBS and infected with 5 x 10^5 Pfu of either vac-A2.1 or vac-T134K in 5 ml virus dilution medium (VDM) (RPMI + 0.1% BSA) for 3 hours at 37^0C. At hour 3, 30 ml of D10 media was added and the cells incubated at 37^0C for 1-3 days. *tk*-143 cells were continuously checked for cytopathic effect. Once good cytopathic effect was evident and just before the cells begin to lift, cells were

harvested, spun at 1800 rpm for 3 minutes, resuspended in 0.5 ml VDM and the virus released from the cells by vortexing and free-thaw cycles using dry ice and methanol. Expansion from one $175cm^2$ typically yielded 0.5-1 $x10^9$ Pfu of total recombinant vaccinia virus.

2.15.2 Infection of cells with recombinant vaccinia virus

C1R cells were harvested and washed in RPMI 1640. Cells were pelleted and infected with a multiplicity of infection (MOI) of 10 with the appropriate recombinant vaccinia (vac-A2.1 or vac-T134K) in VDM. Infected cells were incubated for 90 minutes at 37^0C. Following infection, cells were spun down (1300 rpm for 3 minutes) and the supernatant containing virus particles discarded into 5% Virkon solution. Cells were washed twice in warm R10, resuspended at 5 x 10^5/ml and incubated at 37^0C for a further 4 hours before metabolic labelling.

2.16 STABLE TRANSFECTION OF MOUSE FIBROBLAST CELL LINES

K41 were transfected with either pCDNA3 plasmid containing the P- domain of rabbit calreticulin tagged at 3' end with HA epitope and a KDEL retrieval sequence or with pCDNA3 containing nucleoprotein with the leader sequence (L^+NP). K42 were transfected with pUB6/V5-His plasmid (see appendix 2.14) containing either full-length rabbit calreticulin (amino acids 1-417), or P (amino acids 180-280)-, PC (amino acids 180-417)- or NP (amino acids 1-280)- domains of calreticulin each tagged at 3' end with HA epitope and KDEL retrieval sequence. K42 was also transfected with plasmid pUB6/V5-His containing cDNA encoding residues 1 –387 of cannine calnexin with a carboxy-terminal HA tag followed by KDEL sequence.

Effectene (Qiagen) transfection reagent was used to transfect cells. All transfection were carried out on 60 mm plates and cells were ~ 60% confluent on the day of transfection. Guidelines provided by the kit were followed. Briefly, 1 μg of DNA was added to the DNA condensation buffer (included in the kit) to a total volume of 150 μl. 8 μl of Enhancer (included in the kit) was added to the mix, vortexed briefly and incubated at room temperature for 5 minutes. Finally, 25 μl of the Effectene Transfection reagent was added to the DNA-enhancer mix, vortexed briefly and incubated at room temperature for 10 minutes. In the mean time, cells were washed with sterile PBS and 4 ml of warm R10 added to the plates. Then, 1 ml of R10 was added to the tube containing transfection complexes, mixed thoroughly and added to the cells drop-wise. For transfections with pCDNA3, transfected cells were selected with geneticin (G418) (50 μg/ml) and for transfections with pUB6/V5-His, 5 μg/ml blasticidin was used to select transfected cells. Stably transfected cells were expanded and later cloned by limited dilution (0.3 cell/well) into 96-well plates (200 μl in each well).

2.17 CONFOCAL MICROSCOPY

Adherent fibroblasts (K41 and K42) were plated on poly-lysine deposited microscope slides. Cells were plated such that a 60-70% confluent monolayer would be found on slides in 24 hours. Cells were washed with PBS and fixed with 4% paraformaldehyde in PBS for 45 minutes at room temperature. Following fixation, cells were permeabilised for 10 minutes with permeabilisation solution (1% FCS, 0.03 M sucrose and 1% (w/v) saponin in PBS) for antibody staining. Saponin treatment opens holes in the fixed membranes to allow for antibody movement. Primary antibody (Y3 or anti-calnexin) diluted into wash solution (1% BSA in PBS) (5 μg/ml for Y3 or

1:200 for anti-calnexin) was then added to the slides for 1 hour at room temperature, followed by three washes in permeabilisation solution. For control, non-relevant BB7.2 mAb was used. Secondary FITC-conjugated (Sigma) or TR-conjugated (Molecular Probes) or BODIPY-TR (Molecular Probes) antibody was then added (1:100) for 1 hour followed again by extensive washes. By using Vecta Shield® Mounting solution, cover slips were attached over the slides. These slides were then analysed with Dr Anton Page (Medical Imaging Unit, Southampton General Hospital, UK) by laser scanning confocal microscopy (Leica Microsystems).

2.18 TAP TRANSPORT ASSAY

For the TAP translocation assay, a peptide of the sequence RRYNASTEL was synthesized (Institute of Molecular Medicine, Oxford, UK), and iodinated to a specific activity of 100-150 μCi/μg. K41 and K42 were harvested and washed with incubation buffer (130mM KCl, 10mM NaCl, 1mM $CaCl_2$, 2mM EGTA, 2mM $MgCl_2$, 5mM HEPES, pH 7.3). Cells were then permeabilised by incubating with 100 units of activated Streptolysin-O in incubation buffer for 30 minutes at 37^0C. Radioiodinated RRYNASTEL peptide was then added to the cells in incubation buffer together with 5mM ATP or without ATP (negative control) and incubated for 5 minutes at 37 °C. Translocation was stopped by adding lysis buffer (50mM Tris, 150mM NaCl, 1% (v/v) Triton-X 100, 10mM $MgCl_2$ pH 7.5) and incubated on ice for 1 h. The samples were then centrifuged at 4 °C at 14000rpm for 5 minutes and supernatants transferred to ConA-Sepharose (Amersham Pharmacia Biotech) beads and incubated for 2 h at 4 °C with agitation. Beads were washed four times with large volumes of lysis buffer, and the radioactivity of bound peptides determined using a Beckman 5500 γ-counter.

2.19 PROTEIN DETERMINATION (BRADFORD) ASSAY

For total protein determination, detergent compatible protein determination kit was used (www.bio-rad.com) and total protein concentration was determined by following instruction written in the manual supplied in the kit. Briefly, cells were harvested, counted, washed in PBS twice and lysed in NP40 lysis buffer. Reagent A' was prepared by mixing 20 µl of reagent S to every ml of reagent A (supplied in the kit). Bovine Serum Albumin (BSA- stored at 4^0C) standards were prepared in the range 0.2 mg/ml to 1.5 mg/ml (0.2, 0.4, 0.8, 1.2, 1.5mg/ml) as suggested in the manual.

Cell lysates (samples) were diluted at 1:5 ratio for the assay and experiments done in duplicates. 75 µl of the reagent A' was mixed with 15 µl of the samples or the range of BSA standards and vortexed. 600 µl of reagent B (supplied in the kit) was then added and vortexed. The solution was left to stand at room temperature for 15 minutes and absorbance was read on a spectrophotometer (visible wavelength of 750nm) against a blank prepared without any protein. Absorbance reading was plotted against concentration for standards on an excel sheet and total protein concentration of cell lysates (samples) determined by directly comparing with the standards not forgetting to take into consideration the dilution factor.

2.20 ENZYME-LINKED IMMUNOSPOT (ELISPOT) AND CYTOTOXICITY (CTL) ASSAY

2.20.1 Cell Isolation

Peripheral blood cells (PBMCs) were obtained from normal donors in vials containing EDTA. PBMCs were isolated by density on Lymphoprep (Nycomed, Oslo, Norway). PBMCs were washed 3 times in PBS 1mM EDTA.

2.20.2 T cells

$CD8^+$ T cells were isolated from PBMCs using a MACS bead $CD8^+$ T cells isolation kit (Miltenyi Biotech). This yielded >95% purity of $CD8^+$ T cells.

2.20.3 Dendritic cells

The method for the preparation of mature dendritic cells was based on Larsson *et al.*, [318]. PBMCs were resuspended in RPMI 1640 (Life Technologies-www.invitrogen.com) with 5% pooled human serum (Sigma, UK) and 1 x 10^7 cells were plated in each well of a 6 well tissue culture dishes (Falcon: www.bdbiosciences.com). Cells were allowed to adhere for 2 hours at 37°C. Non-adherent cells were removed by gentle washing. Adherent cells were cultured in RPMI with 1% autologous serum 1000U/ml GM-CSF (Novartis Pharma, Schering-Plough) and 500U/ml IL-4 (R&D systems). Cytokines were added to the cultures on days 0, 2 and 4. On day 5, non-adherent cells were transferred to new plate and half the medium replaced with monocyte-conditioned medium (MCM preparation previously described [319].

Ig coated bacteriological plates (100 mm, Falcon: www.bdbiosciences.com) were prepared by the addition of 5ml of human gamma-globulin (10mg/ml, Sigma, UK). Plates were washed 3 times in PBS before use. $5x10^7$ PBMCs were layered on these plates for 1 hour at 37° in RPMI 5% PHS. Non-adherent cells were washed off and discarded. Adherent cells were incubated for 16 hours in complete medium and the supernatant collected for use as MCM and frozen at -20^0C.

2.20.4 Generation of influenza-specific CTL

Mature Dendritic cells were pulsed for 1 hour with 10mM influenza matrix peptide (GILGFVFTL). Purified $CD8^+$ T cells were added to 96 well plates (Costar Cambridge, MA) at a concentration of $1x10^5$ per well. DCs were washed thoroughly and then added to the wells at a T cell: DC ratio of 30:1. After 10 days the $CD8^+$ T cells were restimulated with matrix peptide-pulsed DCs. On day 13, 20U/ml IL-2 was added to the CTL. After 6 days of restimulation the CTL was used in the cytotoxicity assay. After 10 days of restimulation the CTL was used in the ELISPOT assay.

2.20.5 Influenza A virus infection

HLA-A2 transfectants were washed free of serum and resuspended to 1 x 10^7 in serum-free RPMI 1640. Cells were infected with 1000 haemagglutination U/ml of influenza A strain (A/Japan/305/57) for 1 hour at 37°C. They were then washed three times with RPMI 5% PHS.

2.20.6 ELISPOT assay for IFN-gamma release

The ability of HLA-A2 transfectants to present peptide to the CTL was assessed using the ELISPOT assay. Ninety-six well plates (Millititer, Millipore, Bedford, MA) were coated overnight at 4°C with 5μg/ml of anti-IFN-gamma mAb (Mabtech, Stockholm, Sweden). The Ab-coated plates were washed four times with PBS. HLA-A2 transfectants were pulsed with influenza matrix peptide or control HIV pol peptide (ILKEPVHGV) at varying concentrations. Peptide-pulsed, influenza-infected or untreated HLA-A2 transfectants were added to the Ab-coated wells together with T cells (2-100 x 10^3) and incubated for 6 hours at 37°C. Wells were washed four times with PBS 0.05% Tween-20 (Sigma, UK). 1μg/ml of the secondary antibody, biotin-conjugated anti-IFN-gamma mAb (Mabtech, Stockholm, Sweden) in 0.5% FCS was

added for 4 hours at room temperature . Plates were washed four times with PBS 0.1% Tween-20. 1μg/ml avidin-bound biotinylated ALP (Mabtech, Stockholm, Sweden) in 0.5% FCS was added for 2 hours at room temperature. Plates were washed four times with PBS 0.1% Tween-20. Finally BCIP/NBT substrate (www.zymed.com) was added to each well for 10 minutes. Tap water was added to stop the reaction. Spots were counted using a stereomicroscope under 20x magnification.

2.20.7 Cytotoxicity (CTL) Assay

The ability of CTL generated against the matrix peptide of influenza to kill the HLA-A2 transfectants was tested using the standard 4hour ^{51}Cr release assay. The transfectants were incubated with matrix peptide, influenza or without peptide for 1 hour in the presence of 200 μCi/ml of $Na_2{}^{51}CrO_4$. After thorough washing they were then co-cultured at 37°C with the CTL at different effector to target ratios. After 4 hours the plates were spun at 400g for 5 minutes and the supernatant was collected. Radioactivity was read in a gamma counter (LKB Wallac, Compugamma). Specific lysis was calculated as the mean of triplicate wells according to the standard formula ([(release by CTL – release by targets alone)/(release by 4% Nonidet P-40 – release by targets alone)] x 100%).

2.21 REAL TIME POLYMERASE CHAIN REACTION (RTPCR)

Using the TRIZOL (Gibco-BRL) technique, RNA was extracted from mouse fibroblast cell lines K41 and K41-P. RNA (2 μg) was then reverse transcribed using Omniscript II (Qiagen, Crawley, UK) at 37 °C for 1 h using oligo$(dT)_{15}$ as a primer and the cDNA was then PCR amplified and quantified by Taqman technique. Real-

time detection of PCR was performed using the Perkin Elmer AB1 Prism 7700 Sequence Detection System (Applied Biosystems, Warrington, UK) to determine the expression of K^b using forward primer 5'-CGGCGCTGATCACCAAA-3'; reverse primer 5'-CCAGGTAGGCCCTGAGTCTCT-3'; and FAM-TAMRA probe 5'-AAGTGGGAGCAGGCTGGTGAAGCA -3'. Equal amounts of cDNA were used in triplicate and amplified with the Taqman master mix according to manufacturer's instructions (Applied Biosystems). Thermal cycling conditions were 2 min at 50°C and 10 min at 95°C, followed by 40 cycles of 2-step PCR consisting of 15s at 95°C and 1 min at 60°C. Threshold cycle (C_T) was measured as the cycle number at which the reporter fluorescent emission increased above a threshold level. The amount of mRNA was expressed as fold difference. Amplification efficiencies were validated and normalised against GAPDH (house-keeping gene). For all samples, total RNA that was not reverse transcribed was also analysed to determine genomic DNA contamination, which were found to be negligible.

Chapter 3

EFFECTS OF CALRETICULIN KNOCKOUT ON MHC CLASS I ASSEMBLY AND ANTIGEN PRSENTATION

3.1 BACKGROUND

Calreticulin was discovered about 25 years ago as an abundant calcium-binding protein of the ER [320], and since then, it has been ascribed two major, but potentially overlapping functions [213, 227]. The first function involves calcium homeostasis, a logical role given the presence of calcium-binding sites in the protein [321]. The second function involves a role as a molecular chaperone assisting in the folding and oligomerisation of glycoproteins [231]. Its ability to discriminate between different folding-states of a glycoprotein can be achieved directly via protein-protein interactions as has been shown by Williams and co-workers [272] or indirectly as a result of folding-sensitive reglucosylation of nascent N-linked oligosaccharides as suggested by Helenius and others [322].

The role of calreticulin as a chaperone has been extensively studied in the assembly of MHC class I. It is now well established that peptide loading and hence generation of fully mature and stable class I molecule normally occurs in the peptide loading complex in the ER which comprises of TAP, tapasin, calreticulin [162] and ERp57 [288, 289, 323]. Despite several studies, the function of calreticulin in the class I peptide loading complex is not fully understood. Calreticulin binds to class I molecules only after heavy chain and β2m have assembled and heavy chain has been liberated from calnexin binding [285]. At this stage therefore, class I molecules are properly folded according to most criteria and are recognised by conformation-sensitive monoclonal antibodies.

Recently gene targeting by homologous recombination has been used to generate a calreticulin-deficient mouse and cell line [215, 216]. Calreticulin-deficient mouse embryonic stem cells have also been described [214]. Since the protein is involved in a number of diverse and important functions, it was anticipated that the calreticulin knockout mouse would not be viable. Indeed, the calreticulin-deficient mouse, created by the homologous-recombination technique, is embryonically lethal at 14.5–16.5 days *post coitus* because of impaired cardiac development resulting from downregulated calcium homeostasis [215, 216].

Calreticulin-deficient mouse fibroblast cell line (K42) and its calreticulin-competent counterpart (K41) was a kind gift from Marek Michalak (University of Alberta, Edmonton, Canada). These cells were used to determine whether calreticulin deficiency affected assembly, peptide loading and antigen presentation function of MHC class I. Being a molecular chaperone, it has been suggested that calreticulin is an important factor involved in "quality control" and ensures egress of optimally loaded class I from the ER. K42 was an important tool to dissect this phenomenon.

3.2 CALRETICULIN-DEFICIENT CELLS EXPRESS REDUCED CELL SURFACE LEVELS OF CLASS I MHC

3.2.1 Fewer class I molecules are expressed on the surface of K42

I compared surface expression of H2- D^b and H2- K^b alleles on the calreticulin competent cell line K41 and its calreticulin deficient counterpart K42 by flow-cytometry using conformation-sensitive monoclonal antibodies B22 and Y3 respectively. I found that both H2- D^b and H2- K^b alleles in K42 are expressed at around 25 – 30% of the level observed in K41 (figure 3.2.1).

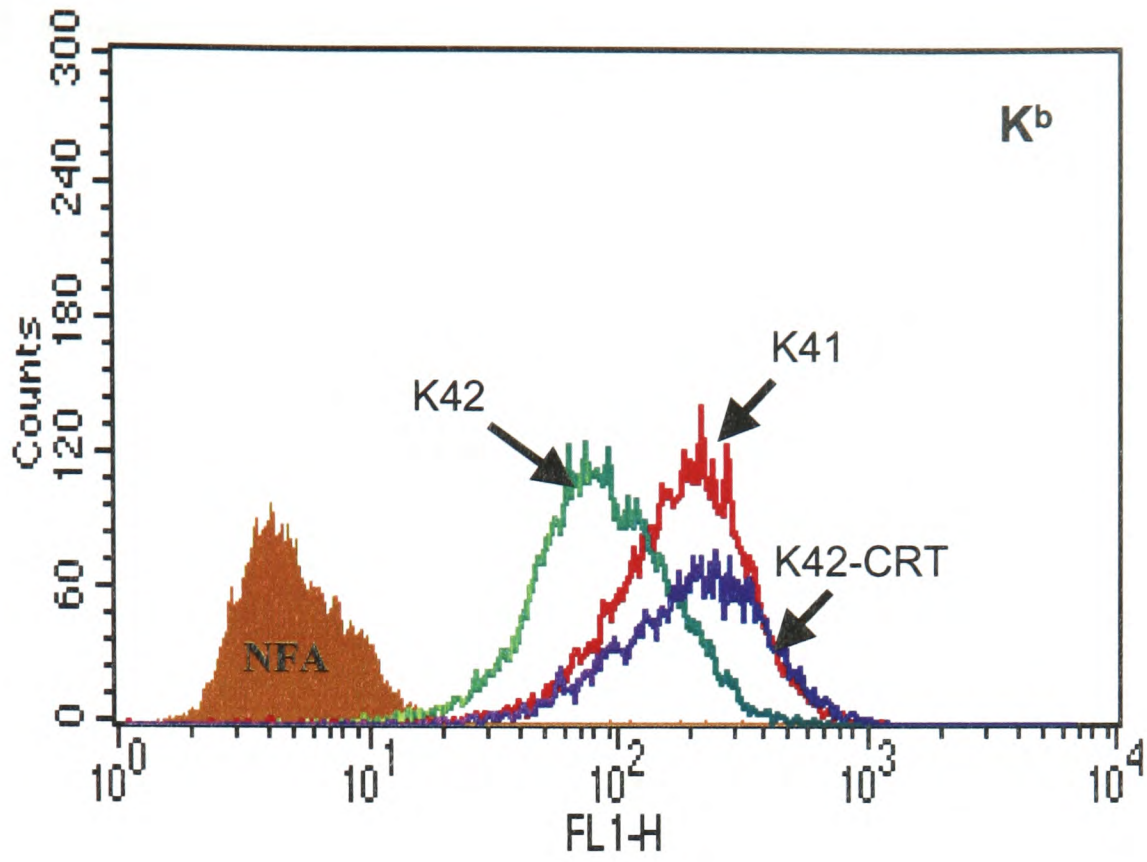

Figure 3.2.1 Reduced expression of MHC class I molecules on the surface of K42 compared to K41

Cell-surface expression of K^b and D^b was detected on the surface of K41 and K42, and K42 transfected with calreticulin (K42-CRT) using monoclonal antibodies Y3 and B22, respectively. NFA, No First Antibody.

3.2.2 Synthesis of class I heavy chain is not affected by the absence of calreticulin

Although cell surface levels of H2- D^b and H2- K^b are low, this does not reflect low levels of synthesis of these alleles in K42. I confirmed this in a western blot assay. 5μg of K41 and K42 lysates were run on a SDS-PAGE and transferred onto a nitrocellulose membrane. Immunoblotting with T18 sera clearly demonstrated class I MHC alleles were synthesised in equivalent amounts in both calreticulin deficient (K42) and calreticulin competent (K41) cells (figure 3.2.2a).

I also tested whether lack of a calreticulin affects the levels of protein synthesis in K42. I measured total amount of protein present in $1x10^7$ K41 and K42 using Bradford protein determination assay. Amount of protein synthesised in K41 and K42 was very similar (figure 3.2.2b). In addition, I pulse labelled equal number of K41 and K42 with ^{35}S methionine and cysteine and subjected to differential lysis protocol to achieve cytosolic, membrane and nuclear fractions. An aliquot of each of the cytosolic, membrane and nuclear fractions was put through β-emission scintillation counting procedure. The results shown in figure 3.2.2c demonstrate similar levels of total cytosolic, nuclear or membrane proteins in K41 and K42.

Therefore, the fact that equal numbers of MHC class I are synthesised in K41 and K42 suggested that a large proportion of class I in calreticulin deficient K42 cells may either a) not assemble with β2m, b) fail to bind peptides and therefore retained in the ER as empty class I molecules, or c) fail to bind and optimise peptides resulting in egress to the cell surface as unstable molecules. I investigated these possibilities further.

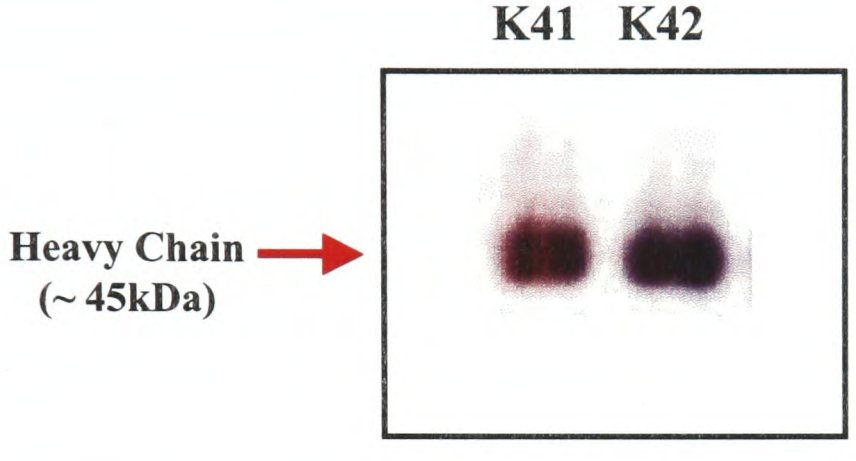

Figure 3.2.2a Expression of MHC class I heavy chain in K41 and K42

Expression of MHC class I heavy chain was detected by western blot using T18 anti-sera, which recognises heavy chains of K^b and D^b molecules.

b

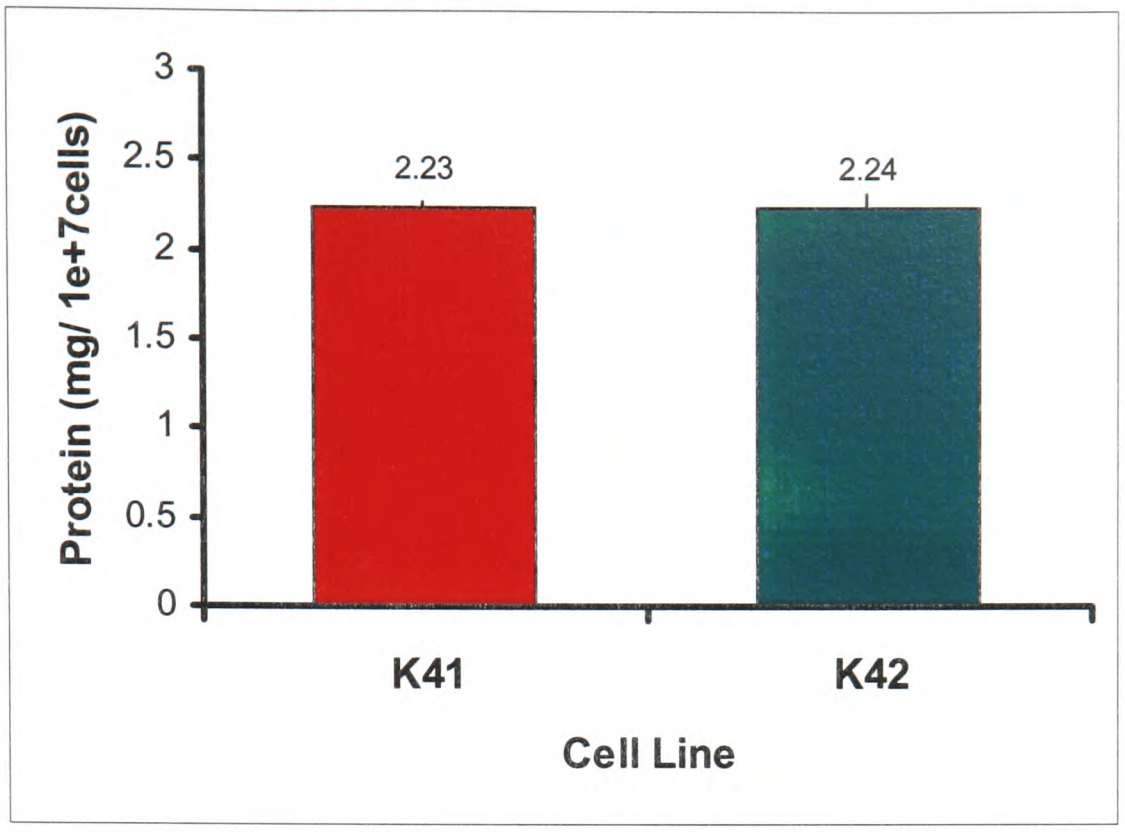

c

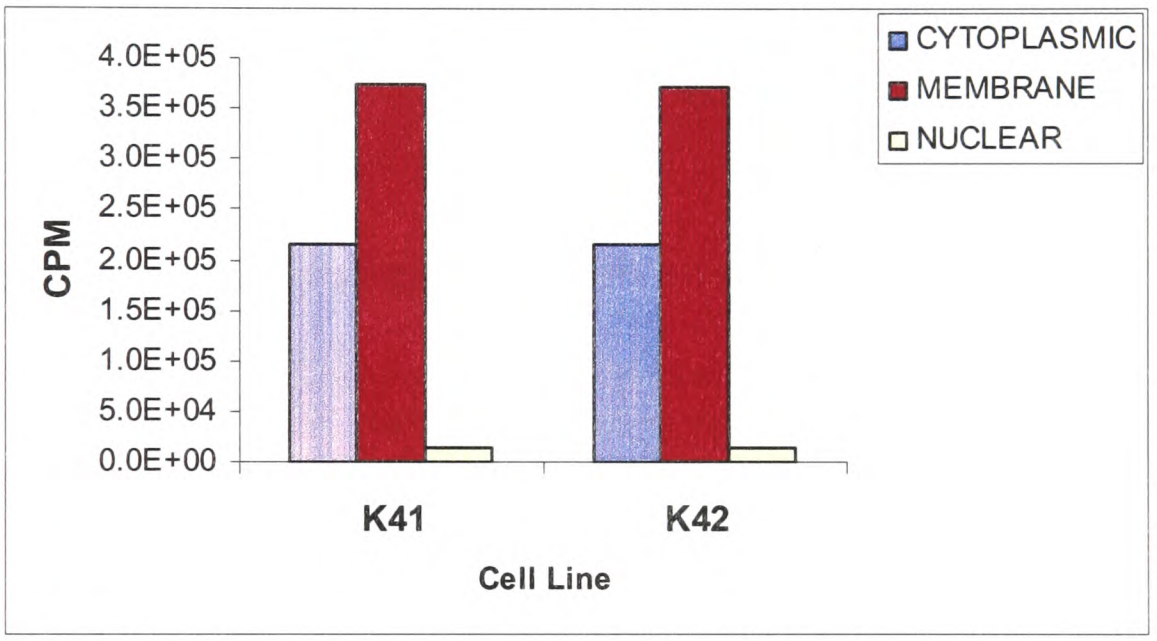

Table 3.2.2 (Contd.) Lack of calreticulin does not alter total protein synthesis

(b) $1x10^7$ K41 and K42 were lysed in of 1% NP40 lysis buffer and small aliquot used to determine total protein concentration using Bradford protein determination assay. Total amount of protein present in $1x10^7$ K41 and K42 is shown above individual bars and standard deviation is represented by the error bars.

(c) Equal number of K41 and K42 cells were pulse labelled with ^{35}S methionine and cysteine and subjected to digitonin lysis followed by differential fractionation to achieve cytosolic, membrane and nuclear fractions.An aliquot of each of the cytosolic,membrane and nuclear fractions was put through β-emission scintillation counter to determine total protein present in each aliquot.

3.2.3 Class I molecules can be stabilised on the surface by incubating K42 with stabilising peptides

To determine whether H2- D^b and H2- K^b molecules in K42 were peptide receptive, I incubated K41 and K42 for 4 hours in the presence of increasing concentrations of the H2-K^b binding peptide SIINFEKL or the H2-D^b binding peptide ASNENMDAM and compared the expression of these alleles by flow cytometry. As shown in figure 3.2.3, both cells gave similar levels of staining with Y3 or B22 monoclonal antibodies at saturation resulting from around a 4.5-fold increase in cell-surface staining in K42 compared to a 1.2-fold increase in K41. Similar results were obtained for five other H2-D^b-binding peptides where the increase in cell surface expression ranged from a 3.8 to 5.6-fold increase in K42 and a 1.1 to 1.6-fold increase in K41. I also found no difference in the binding characteristics of peptides added to K41 and K42 over a range of concentrations (see for example, ASNENMDAM in Figure 3.2.3) suggesting that the peptide receptive molecules released to the cell surface of K42 have the same affinity for peptide ligands as they do in K41. These results tie in with immunoprecipitation studies in which the amount of H2-D^b and H2-K^b that could be recovered with B22 and Y3, respectively, in the absence of stabilising peptide, was lower in K42 than in K41. However, when peptide was added, the total amount of H2-D^b and H2-K^b synthesised and assembled during the pulse-label, was similar in both cells ([324]-manuscript supplied).

In the experiments shown in figure 3.2.3, it is possible that peptide is binding to class I at the cell surface or in the ER since Day *et al.,* have illuminated the retrograde transport of peptides from outside the cell into the ER at 37°C [325]. I attempted to repeat the above experiment at 4°C, where peptides cannot enter the secretory pathway as endocytosis is prevented at this temperature. I observed only a little

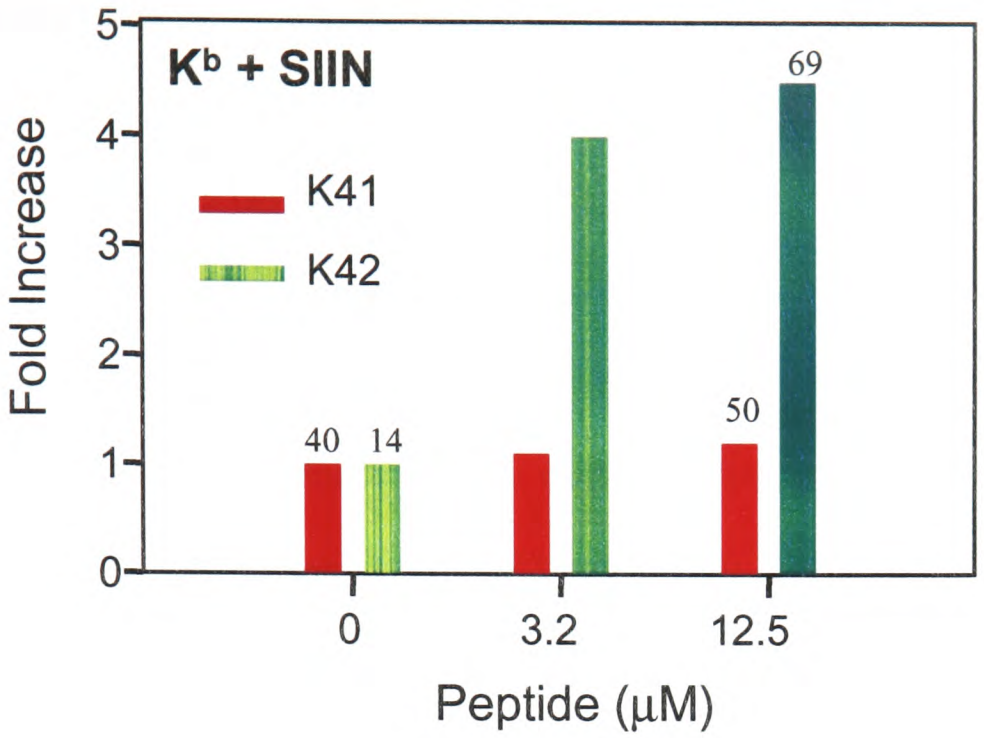

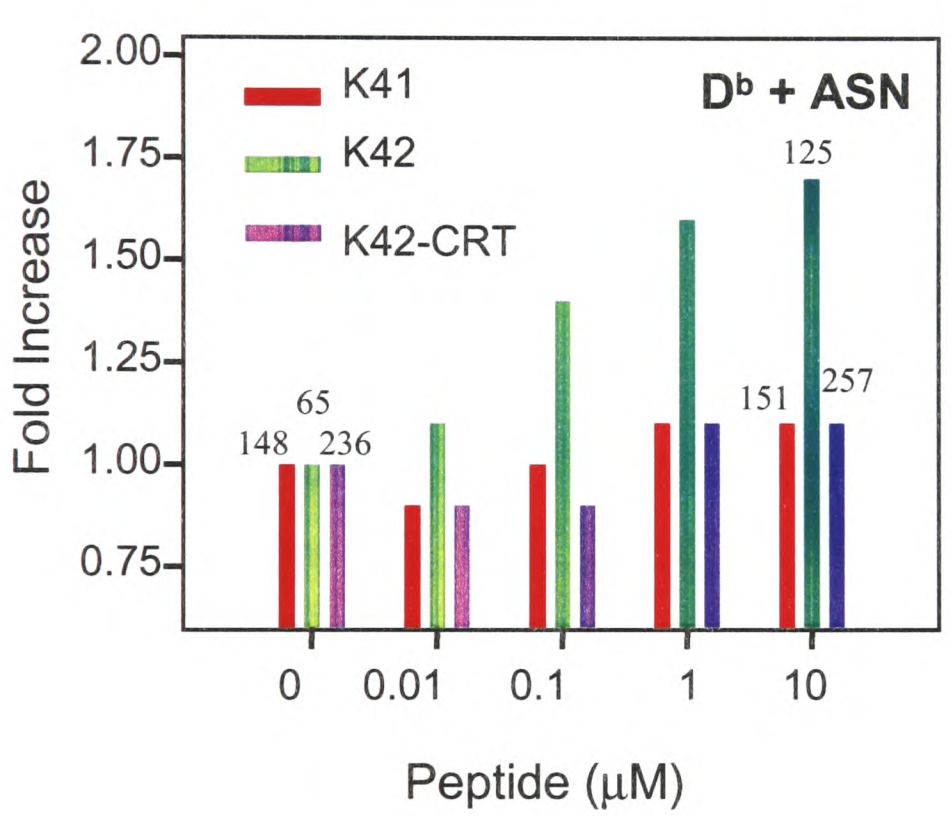

Figure 3.2.3 Stabilising peptides increase cell surface expression of K^b and D^b in a dose-dependent way

K41 and K42 were incubated with K^b binding peptide SIINFEKL (a) and D^b binding peptide ASNENMDAM (b) and class I expression determined by flow cytometry. Results are shown as the fractional increase in expression with increasing amounts of peptide. Actual mean fluorescence value is indicated above individual bars.

increase in cell-surface staining of H2- D^b and H2-K^b molecules by B22 and Y3, respectively (data not shown). I, therefore, concluded that the delivery of peptide-receptive class I molecules to the cell surface is prevented at 4^0C and so there is little increase in cell-surface staining observed.

Overall, these results demonstrate that synthesis of class I molecules is normal in the absence of calreticulin. Moreover, the results also suggest that same number of H2-D^b and H2-K^b molecules are assembled and exported in K41 and K42, but that in the latter, a greater proportion are exported in an unstable, peptide receptive state which "fall apart" at or *en route* to the cell surface unless they encounter exogenous peptides to which they can bind.

3.2.4 Class I molecules can also be stabilised on the surface by incubating K42 with β2m

I next sought to confirm that peptides added exogenously in the above experiment did not gain access to class I molecules in the secretory pathway. I evaluated the number of class I molecules in K41 and K42 that could be stabilised with exogenously added β2m, which is unlikely to have access to the secretory pathway because of its size. I incubated K41 and K42 at 37^0C for four hours with exogenously added β2m. As shown in figure 3.2.4, flow cytometry result of Y3 staining demonstrates dose-dependent stabilisation of cell-surface H2-K^b molecules, resulting in a 3.1-fold increase in K42 and a 1.7 fold increase in K41. At saturating concentrations of β2m, cell surface level of class I on K42 and K41 were equal. These results are consistent with the results shown in figure 3.2.3. This result therefore confirms that whereas the same level of class I synthesis and assembly is observed in K41 and K42, a greater proportion of assembled class I molecules in K42 do not become loaded with

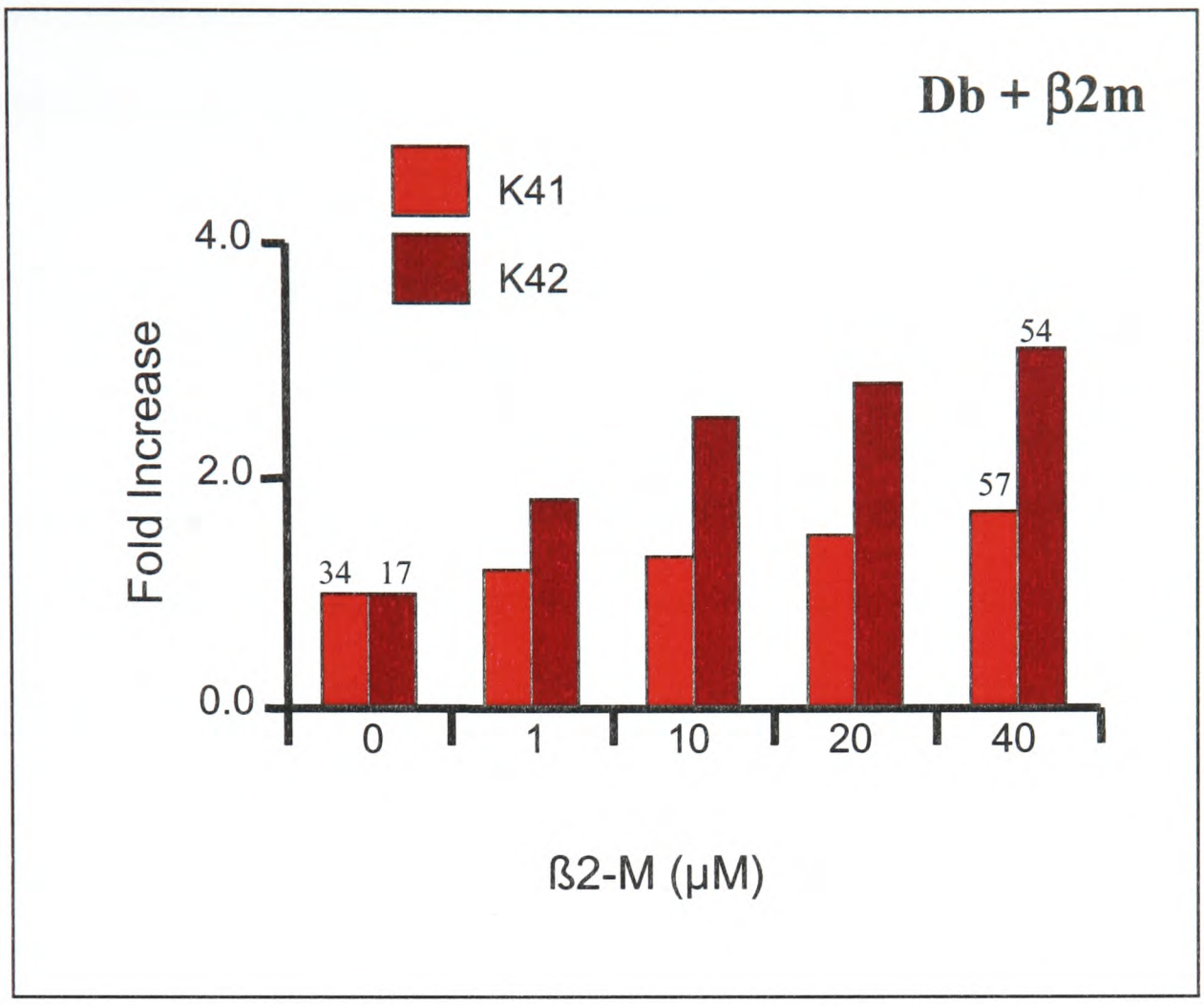

Figure 3.2.4 Stabilisation of surface D^b molecules by β2m in K42

K41 and K42 were incubated with increasing concentrations of β2m and surface D^b expression determined by flow cytometry. Results are shown as the fractional increase in expression with increasing amounts of β2m. Actual mean fluorescence value is indicated above individual bars.

stabilising peptides. In addition, dose-response curves of class I stabilisation with β2m was the same in K41 and K42. This indicates that the affinity of H2-K^b heavy chain for β2m is the same whether the class I molecule is synthesised in the presence or absence of calreticulin.

3.2.5 H2-K^b molecules rapidly traffic to the cell surface in the absence of calreticulin

There is a correlation between the length of time that newly synthesised class I molecules spend in the ER and the extent to which they become loaded with peptides [180]. I carried out a pulse-chase analysis to compare the intracellular maturation of a [^{35}S]-metabolically labelled cohort of H2- K^b molecules expressed in the presence and absence of calreticulin. The rate at which the class I complexes acquire resistance to endoglycosidase-H (endo-H) was used as a measure of egress from the ER to the medial Golgi. At each time point during the chase period, I removed aliquots of cells and lysed them in 0.5% NP40 lysis buffer. The lysates were left to incubate for half an hour at 4^0C before the H2-K^b complexes were immunoprecipitated with conformational sensitive antibody Y3. H2- K^b molecules immunoprecipitated in this way represent total number of (stable and unstable) class I allele present at a particular time point.

The pulse-chases for H2- K^b molecules expressed in K41 and K42 are shown in figure 3.2.5.1a-b after analysis by SDS-PAGE and autoradiography. The intensity of each band, measured as an integrated optical density (IOD) allowed me to compare the intracellular maturation of H2-K^b molecules expressed in calreticulin competent K41 and calreticulin deficient K42 cells. I found that the rate of export of H2-K^b molecules

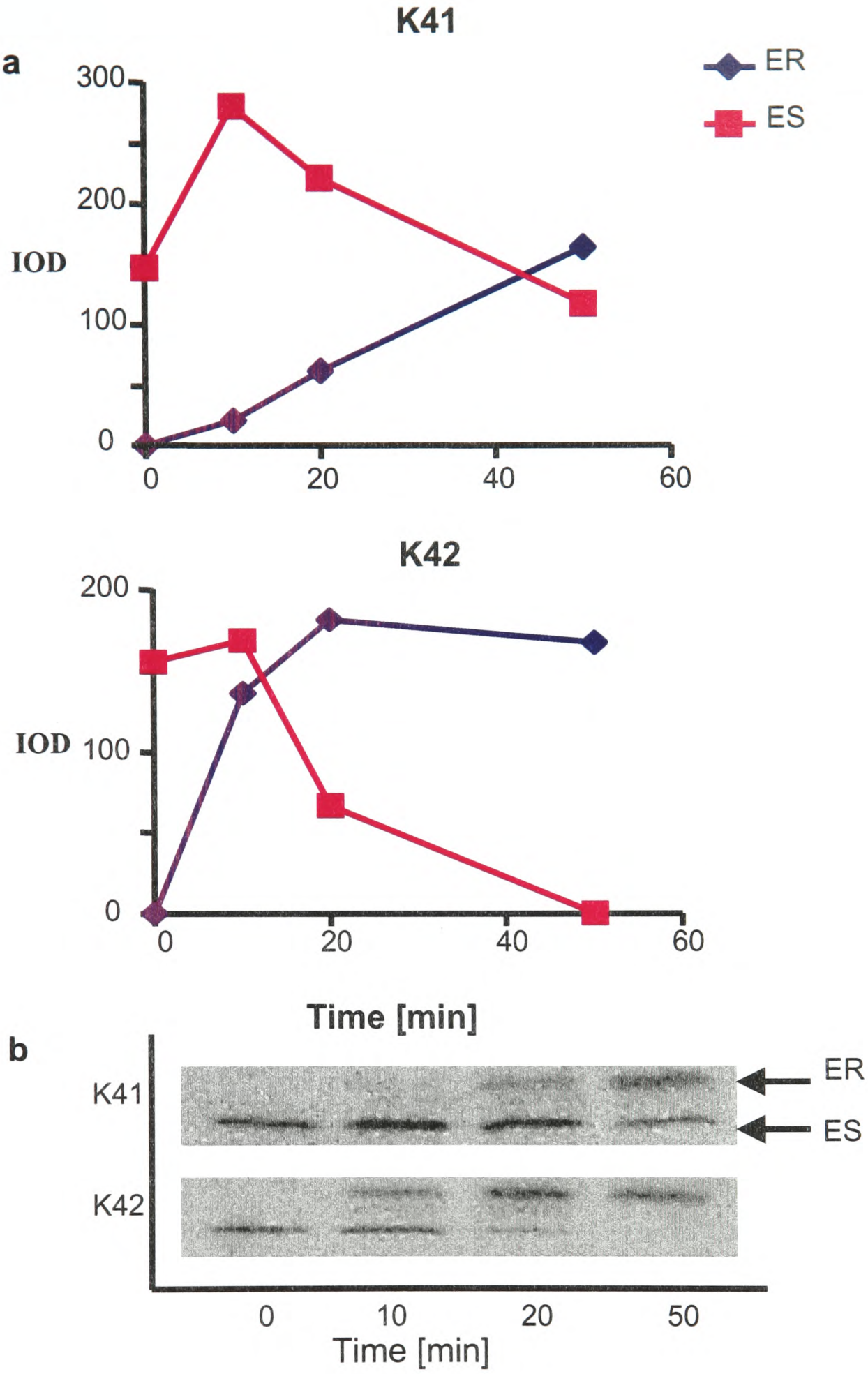

Figure 3.2.5.1 K^b molecules are transported rapidly in the absence of calreticulin

K41 and K42 cells were pulse-labelled for 10 min and chased for the times shown. K^b was immunoprecipitated with Y3, digested overnight with endoglycosidase-H (endo-H), fractionated by SDS-PAGE, and the heavy chain band quantified as Integrated Optical Density (IOD). The band intensity of immature, endo-H sensitive (ES) and mature, endo-H resistant (ER) heavy chains recovered from K41 and K42 was plotted against time of chase. b) Actual image of the pulse-chase experiment to show fraction of ER and ES K^b molecules at each time point.

is considerably enhanced in K42. H2-K^b molecules in K42 mature with half time of around 15 minutes. In contrast, H2-K^b molecules in K41 mature with half time of around 40 minutes. It is to be noted that these figures are calculated from the beginning of the radioactive pulse (which started 5 minutes prior to the chase). This experiment was repeated three times and the results were consistent. Thus, in the absence of calreticulin, H2- K^b molecules exit the ER much faster, and majority of these do so as peptide-receptive complexes.

Interestingly, class I molecules seem to be associated with the TAP complex together with calnexin, ERp57 and tapasin even in the absence of calreticulin. When TAP1 and TAP2 were immunoprecipitated from a digitonin lysates and western blotted for other components of the loading complex, calnexin, Erp57, tapasin and class I HC were identified in coimmunoprecipitates from K42 (figure 3.2.5.2) ([324]- manuscript supplied). This may represent a mixture of preloading complexes and mature loading complexes. These results, therefore, indicate that failure of class I molecules to interact with calreticulin allows them to escape the quality control mechanism operating in the ER.

3.3 ER PEPTIDE SUPPLY IS NOT AFFECTED IN THE ABSENCE OF CALRETICULIN

The defect in peptide loading seen in the absence of calreticulin may be the result of an indirect effect of calreticulin deletion either on proteasomal machinery or on TAP. Defective proteasomal processing may lead to failure to generate optimal peptides. Moreover, failure of TAP to transport peptides generated in the cytosol into the ER may result in defective peptide loading. In order to exclude these possibilities, I did the following experiments.

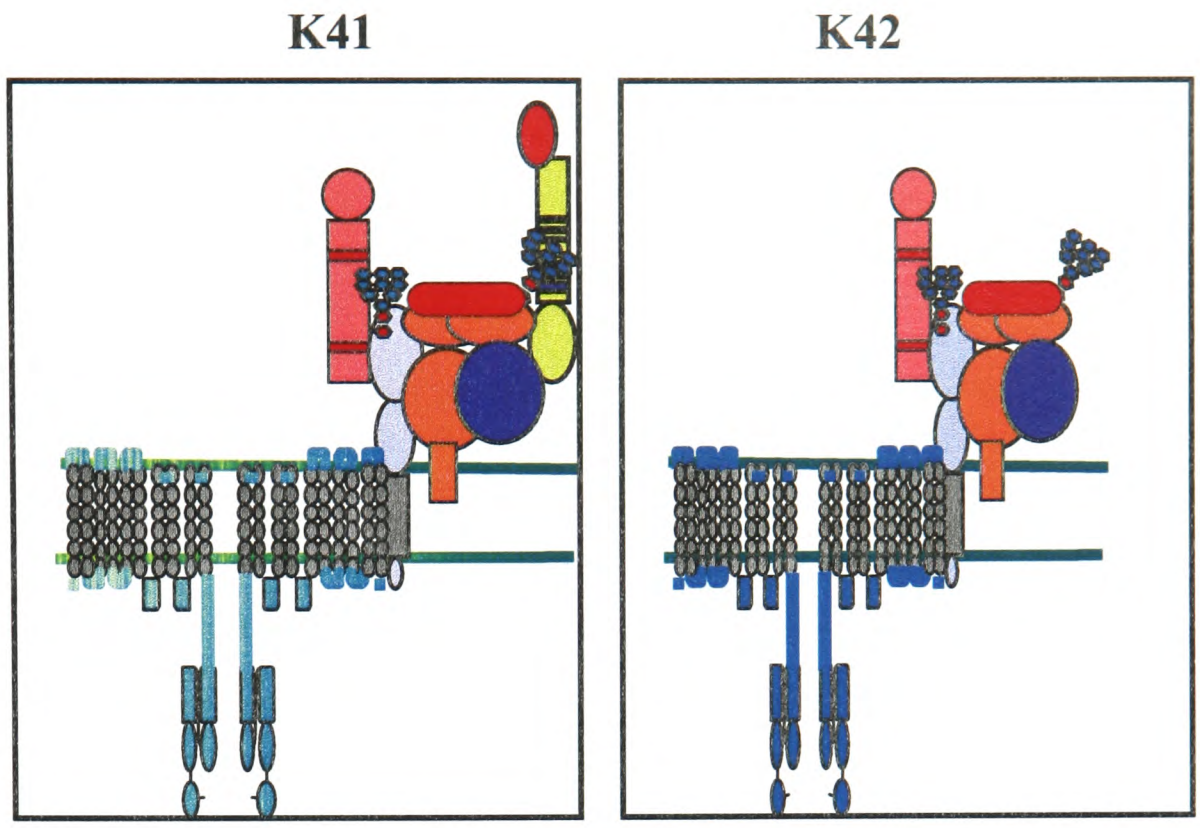

Cofactor/Component	K41	K42
Heavy Chain	++	+
TAP	+	+
Tapasin	+	+
ERp57	+	+
CRT	+	-

Figure 3.2.5.2 Assembly of the peptide loading complex in the absence of calreticulin

Presence of the cofactors of the loading complex in K41 and K42 are shown. Relative abundance is shown by plus (+) sign. For example, **(++)** represents high abundance and (-) represents absence of a cofactor. Calnexin (not shown) is present in the pre-loading complex of K41 and K42, which also includes cofactors TAP, tapasin and ERp57.

3.3.1 Rate of cytosolic degradation of a model antigen is the same in K41 and K42

I used recombinant vaccinia virus encoding influenza A NP tagged with ubiquitin-arginine to infect K41 and K42. Ubiquitin-arginine tag has the advantage that whichever protein it is tagged to, is rapidly degraded. Cells were infected for 90 min and incubated for 3.5 hours to allow for NP antigen expression. I then carried out a pulse-chase analysis similar to that described above to assess the rate of degradation of this model antigen.

It is clear from figure 3.3.1 that the NP antigen is degraded equally well in both the cells and the rate at which the antigen is degraded is also the same. This experiment, therefore, demonstrates that deletion of calreticulin has no affect on the proteasomal activity.

3.3.2 ATP-dependent TAP transport is unaffected in the absence of calreticulin

In order to determine whether absence of calreticulin affected peptide transport by TAP, I assessed the transport of a model peptide RRYQNSTEL into the ER by TAP. I iodinated the model peptide with radioactive ^{125}I. Following permeabilisation of K41 and K42 with activated Streptolysin-O solution, I added iodinated peptides to the permeabilised cell culture. After allowing transport of iodinated peptide across ER membrane by TAP for five minutes, I stopped translocation by placing the cells on ice followed by cell lysis. I centrifuged the lysate to obtain supernatant free of the nuclear debris. TAP transported model peptide will have been glycosylated in the ER as it contains a putative glycosylation site. I recovered the ER transported peptides on ConA-Sepharose and measured radioactivity by gamma-spectrometry. This was done in duplicate and the experiment was repeated twice. The results are shown in figure

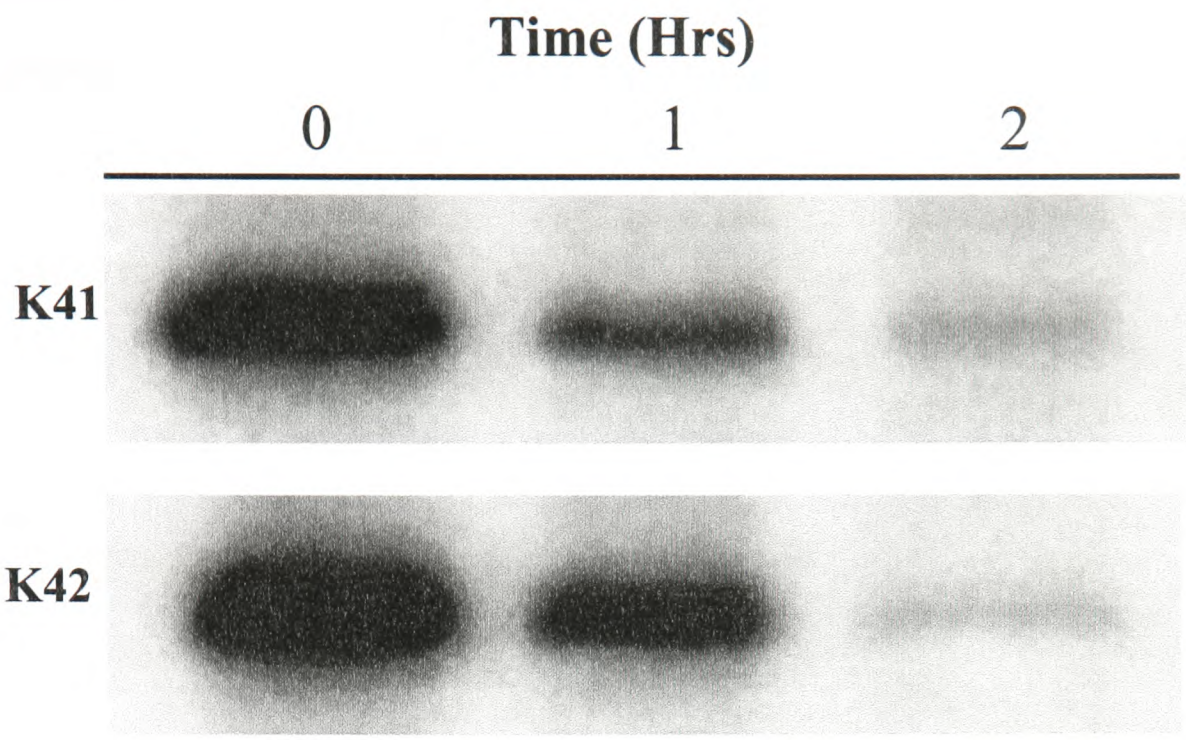

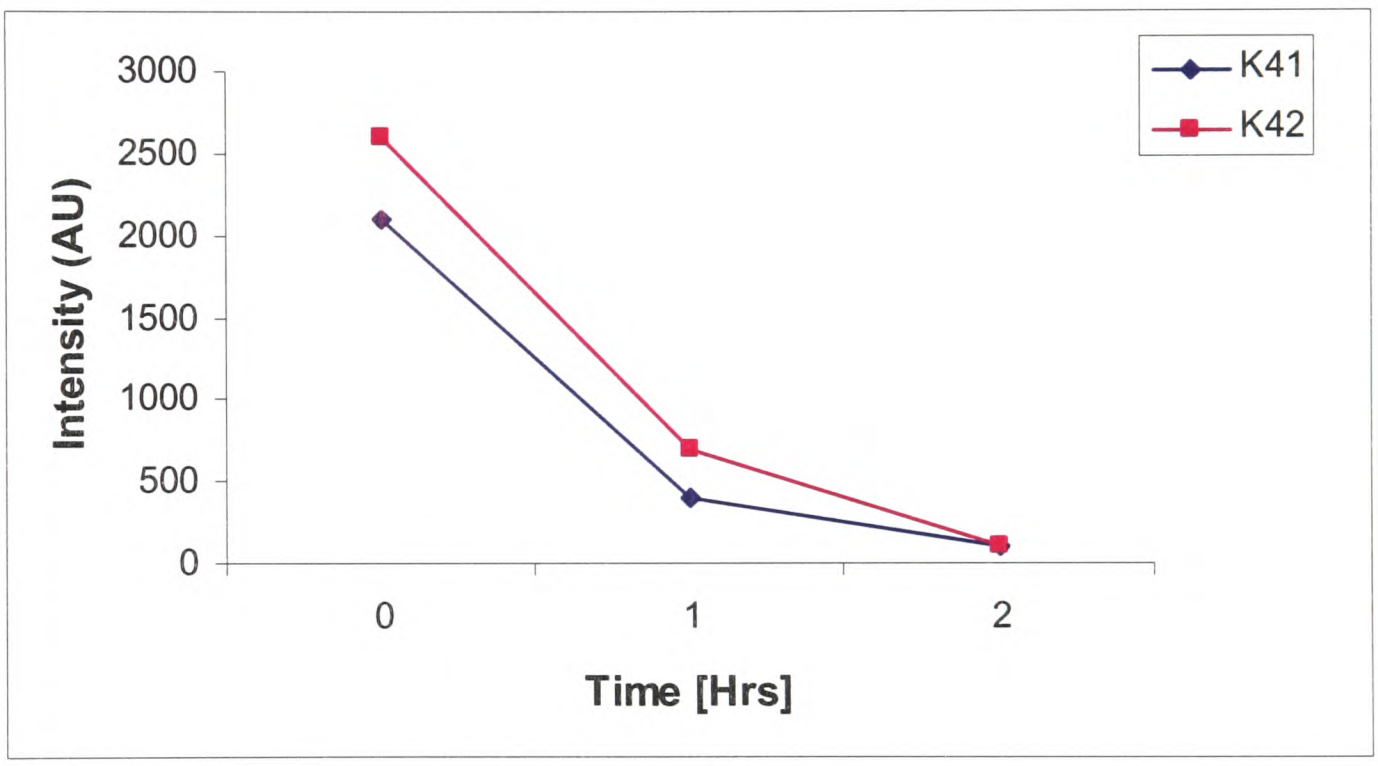

Figure 3.3.1 Rate of cytosolic degradation of a model antigen is the similar in K41 and K42

a) Equal number of K41 and K42 were infected for 90 minutes with vaccinia encoding influenza A nucleoprotein (NP) tagged with ubiquitin-arginine (NP-R-UQ). Vaccinia was removed after 90 minutes and expression of NP-R-UQ allowed for 4 hrs. Cells were then pulse labelled and chased for indicated times. Aliquots of cells were removed at each time point, lysed and immunoprecipitated with anti-NP antibody. Degradation of NP-R-UQ was assessed following SDS-PAGE fractionation and autoradiography. b) NP band on the autoradiograph was quantified by Quantity One software (BIORad Inc, USA) and the intensity of band (expressed as arbitrary units AU) plotted against time (hrs).

3.3.2. and demonstrate that the overall transport of radiolabelled peptide is unaffected in the absence of calreticulin.

3.4 TRANSFECTION OF FULL-LENGTH CALRETICULIN GENE RESTORES CLASS I SURFACE EXPRESSION

In order to establish that the K42 phenotype observed was indeed as a result of lack of calreticulin, I introduced full-length rabbit calreticulin into K42. Rabbit calreticulin was used because the gene was available at the time and that calreticulin is highly conserved between mouse and rabbit. I established a clone of K42 expressing full-length rabbit calreticulin (K42-CRT). I then compared surface expression of H2-D^b and H2-K^b using flow cytometry after staining with B22 and Y3 respectively, in K41, K42 and K42-CRT. As shown in figure 3.2.1, expression of both class I alleles was restored to normal when K42 was transfected with a gene encoding full-length rabbit calreticulin. Moreover, in K42-CRT, not only did cell surface expression of class I increase (figure 3.2.1) but the fold-increase in cell surface expression after incubation with exogenous peptides decreased to that seen for K41 (see for example the ASNENMDAM titration in figure 3.2.3). Together, these results demonstrated that reduced cell surface expression seen in K42 was as a result of lack of calreticulin and introducing full-length rabbit calreticulin into K42 could restore to K41 phenotype.

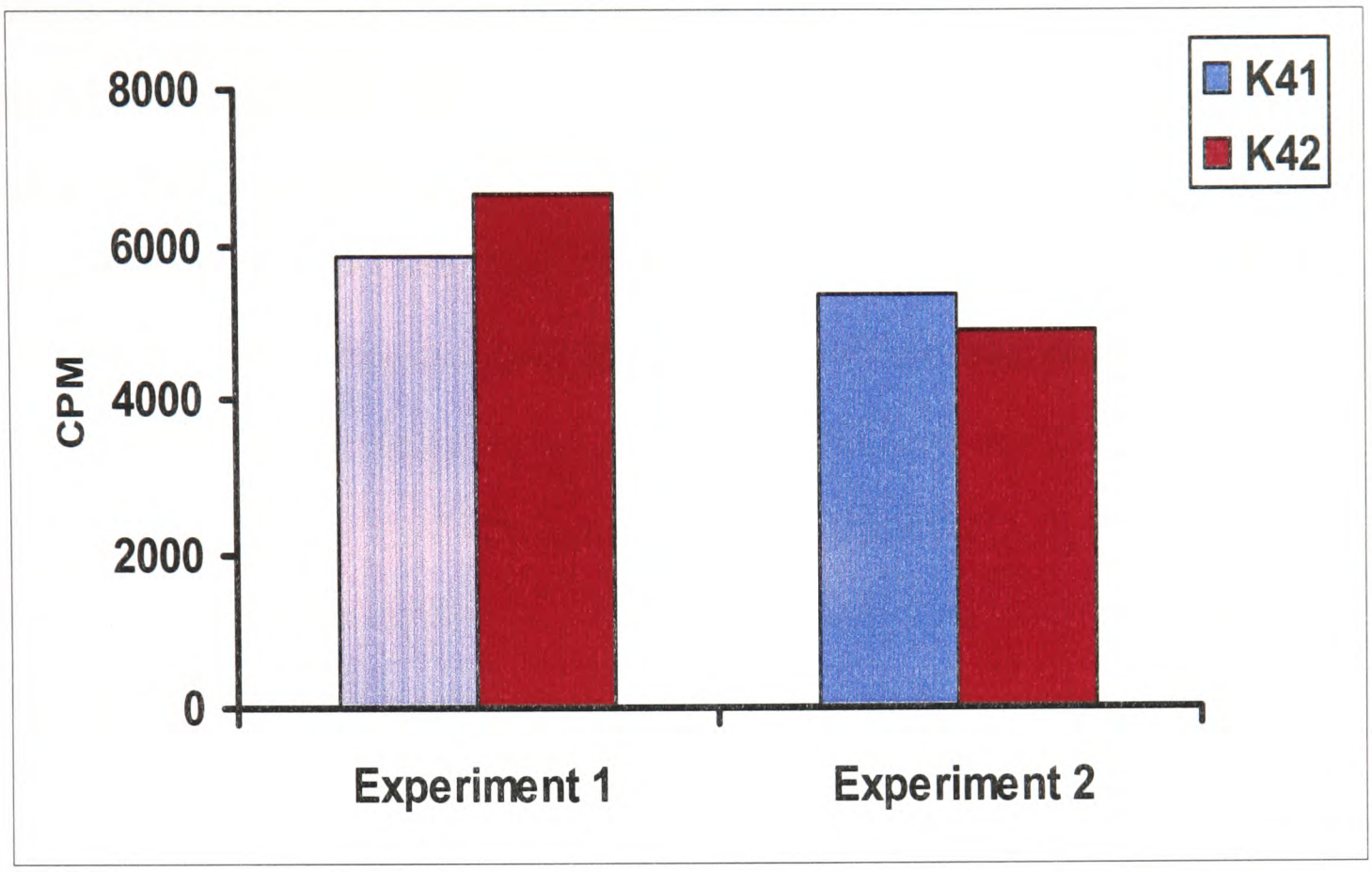

Figure 3.3.2. TAP transport is unaffected in the absence of calreticulin

Transport of an ^{25}I-labelled model peptide RRYQNSTEL into the ER by TAP was determined using the assay described in the materials and method. The extent and ability of TAP to transport the model peptide was largely similar in K41 and K42.

3.5 ANTIGEN PRESENTATION IS IMPAIRED IN K42 CELLS

To determine the extent to which the reduction in intracellular peptide loading in K42 affected the presentation of epitopes at the cell surface, presentation of four viral epitopes was assessed. The results are summarises in table 3.5 (for details, see [324]-manuscript supplied). First, the presentation of epitopes derived from two MCMV-derived proteins to MCMV-specific clones was determined (experiments conducted by Ann Hill and Marielle Gold). One of the clones, clone 96, did not recognise K42 infected with MCMV, whereas another clone, clone 11 (recognising an early protein) did [326, 327]. Second, recognition of vaccinia encoding ovalbumin (vacc-ova) - infected K41 and K42 by T cell hybridoma B3Z, which recognises the SIINFEKL: K^b complex was assessed (experiments conducted by Mark Howarth). Ovalbumin-derived SIINFEKL was presented equally well by K41 and K42 following a 16 hr infection using B3Z to detect presentation. However, presentation of the epitope by K42 was dependent on the duration of vaccinia infection. For example, after 1 hr of infection, there was no presentation by K42 when presentation by K41 was half-maximal, and after 5 hr of infection, by which time presentation by K41 was maximal, presentation by K42 was only half-maximal. Third, presentation of D^b-restricted LCMV gp160-derived epitope KAVYNFATC was assessed. This epitope was not presented by K42 following infection with a vaccinia expressing gp160, although the synthetic peptide was well presented. Both the viral protein and the peptide epitope were well presented by K41. The fact that exogenous peptide-presentation by K42 was normal indicated that the lack of virus-induced sensitisation to lysis was not due to any adverse antigen-independent effects on CTL recognition or killing.

		K41		K42	
	Antigen Source	**Exogenous Peptide supply**	**Endogenous Processing**	**Exogenous Peptide supply**	**Endogenous Processing**
	LCMV gp160 (KAVYNFAC) Vac-gp160	+++	++	+++	-
	Ova (SIINFEKL) Vac-Ova	+++	+++	+++	+/-*
Clone 96	***MCMV (Smith Strain)***	+++	+++	N/A	-
Clone 11	***MCMV (ΔMS94.5)***	+++	+++	N/A	+++

Table 3.5 Antigen presentation function is impaired in the absence of calreticulin

The D^b-restricted LCMV gp160-derived epitope KAVYNFATC was presented by K41 but not by K42 following infection with a vaccinia expressing gp160, although the synthetic peptide epitope was presented well by both K41 and K42. Ovalbumin-derived SIINFEKL was presented equally well by K41 and K42 following a 16 hr infection using the T cell hybridoma B3Z to detect presentation. However, presentation of the epitope by K42 was dependent on the duration of vaccinia infection (+/-*). For example, after 1 hr of infection, there was no presentation by K42 when presentation by K41 was half-maximal, and after 5 hr of infection, by which time presentation by K41 was maximal, presentation by K42 was only half-maximal. Clone 96 (MCMV-*Smith Strain*-derived) did not recognise K42 infected with MCMV, whereas clone 11 (recognising an early protein) did recognise MCMV-infected K42. Both clones recognised epitopes derived from MCMV- proteins following MCMV infection in K41. The sign (+++) indicates good recognition (e.g., 60-80% target cell lysis), (++) indicates moderate recognition (e.g., 20-30% target cell lysis) and (–) indicates no recognition. (N/A): data not available.

3.6 PEPTIDE LOADING OF CLASS I MOLECULES IS A SPECIFIC FUNCTION OF CLARETICULIN

Calnexin and calreticulin are homologous chaperones resident in the ER. There is around 40% identity between calnexin and calreticulin at the amino acid level, with the proline-rich (P) domains being almost identical. Calnexin binds rapidly to newly synthesised heavy chains and remains bound to heavy chains carrying one or more glycosylations in addition to asparagine 86, whereas calreticulin has only ever been detected bound to the class I heavy chain that have assembled with β2m, and uses the asparagines 86 site exclusively [287]. Danilczyk *et al.,* have recently demonstrated considerable redundancy in the function of calreticulin and calnexin in the early biogenesis of class I heavy chain:β2m heterodimers in insect cells [328]. This observation, coupled with the observation made by the same group that calnexin lacking its transmembrane domain has a similar substrate specificity to calreticulin [328] led me to determine whether introducing such a soluble calnexin into K42 could restore normal class I surface expression.

I transfected K42 with the soluble calnexin tagged with HA followed by the ER retrieval sequence KDEL (kindly provided by D.B.Williams, Toronto, Canada) and generated a clone (K42-solCNX). I compared expression of calreticulin (also HA tagged) in K42-CRT and calnexin in K42-solCNX by western blotting using anti-HA tag antibody. Expression of the transfected proteins was similar (see inset to figure 3.6a). Whereas full-length calreticulin was able to restore class I surface expression to that seen in K41 (figure 3.2.1), soluble calnexin was not (figure 3.6a). This construct has been shown to be functional with respect to lectin-binding and chaperone function when expressed in mammalian cells [231].

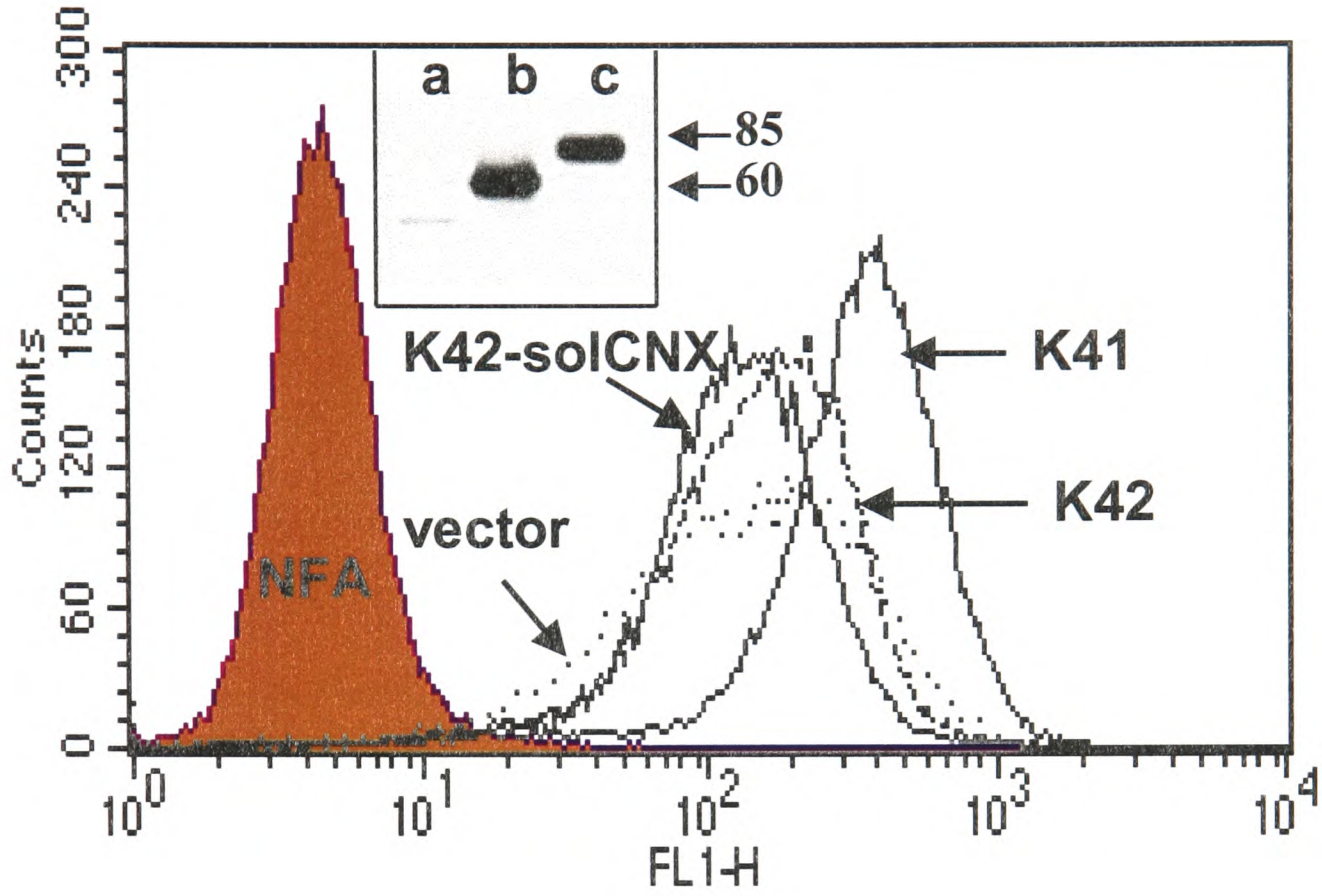

Figure 3.6a. Soluble calnexin does not restore class I expression on the surface of K42

K42 was transfected with soluble calnexin (K42-solCNX) or vector alone. Cell surface expression of K^b was detected with Y3. Expression of soluble calnexin in K42-solCNX (lane c, inset) was confirmed by western blotting against the HA epitope tag, and compared to the expression of calreticulin in K42-CRT cells (lane b, inset) in which class I expression was restored to normal. Lane a (inset) is a blot of K42 lysate with the anti-HA antibody.

It was important to verify that KDEL tag was indeed functional and worked efficiently in K42 as it has been reported to do in the cell lines studied by David Williams [231]. I, therefore, tested whether soluble calnexin was secreted in K42-solCNX I decided to analyse supernatants of K42-solCNX for evidence that calnexin is secreted. I cultured K42-solCNX to high density, harvested supernatant from $1x10^5$ cell equivalents and compared this to a lysate of $1x10^5$ cells for the presence of HA-tagged soluble calnexin by western blotting. As a control, I compared the amount of tapasin present inside $1x10^5$ cells transfected with a soluble version of the molecule and tapasin present in the supernatant of an equivalent number of cells grown to high density. I used rabbit anti-HA tag antibody to detect soluble calnexin and rabbit anti-tapasin antibody to detect soluble tapasin. I could not detect any secreted calnexin whereas it was clearly visible in the cell lysates (figure 3.6b). Moreover, secretion of soluble tapasin was evident in the supernatant. This experiment therefore demonstrated that the C-terminal KDEL tag in soluble calnexin was functional and that soluble calnexin was indeed retained in the ER.

I do not know whether this lack of function arises from a different or absent interaction between soluble calnexin and class I heavy chains, but whichever way, these results indicate that the peptide-loading cofactor function of calreticulin cannot be replaced by a homologous protein with overlapping functions. Consequently this function is probably specific to calreticulin and opens up the intriguing possibility that the functional interaction between calreticulin and class I resides outside the lectin site [272].

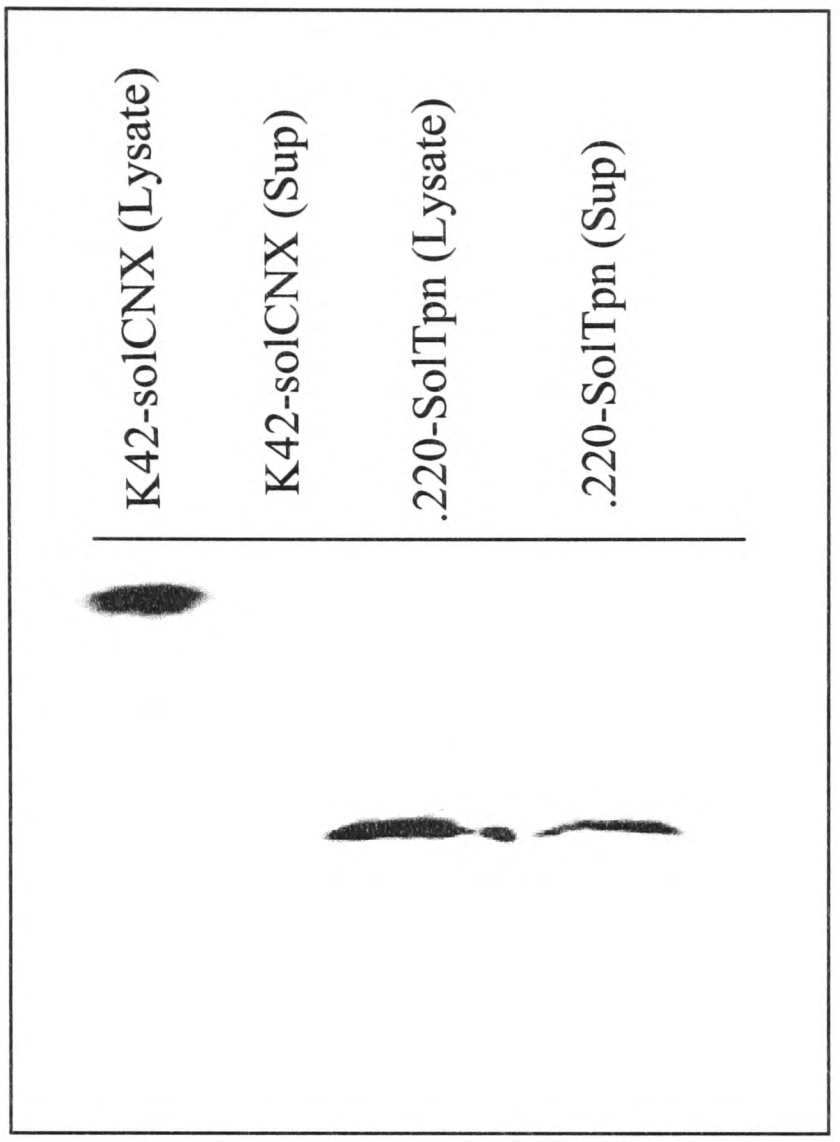

Figure 3.6b. Soluble calnexin is not secreted.

K42-expressing soluble calnexin (K42-solCNX) were grown to high density and supernatant harvested from equivalents of $1x10^5$ cell and was compared this to a lysate of $1x10^5$ cells for the presence of HA-tagged soluble calnexin by western blotting using anti-HA antisera. As control, amount of tapasin present inside $1x10^5$ cells transfected with a soluble version of the molecule and tapasin present in the supernatant of an equivalent number of cells grown to high density was determined using anti-tapasin antibody.

3.7 EXPRESSION, ASSEMBLY AND TRANSPORT OF CLASS I IN CELLS OVEREXPRESSING CALNEXIN AND CALRETICULIN

The primary function of lectin chaperones is to fold glycoproteins efficiently and mediate "quality control" in the ER. Experiments by Jackson *et al.*, [196] using peptide-deficient class I complexes in insect cells and by Rajagopalan *et al.*, [329] using β2m negative cells suggest that calnexin is a major class I retention molecule. Similarly, calreticulin is an important cofactor of the TAP loading complex and plays a major role in the regulated loading of peptides. Moreover, studies have shown correlation between the period of detention of newly synthesised class I molecules in the ER and the extent to which they become loaded with peptides. This led me to ask whether overexpressing calnexin or calreticulin increased dwelling of class I in the ER and consequently increased the number of stable molecules at the cell surface.

I made use of calnexin and calreticulin inducible tet-on HeLa (iHeLa) cells. iHeLa cells were treated with doxycycline at a final concentration of 2 μg/ml and time allowed for overexpression of calnexin and calreticulin. Western blot was carried out to confirm overexpression of lectin chaperones in doxycycline treated cells. Figure 3.7 shows chaperones were induced 3-4-fold in drug treated iHeLa cells.

3.7.1 MHC class I cell surface expression is increased in HeLa cells overexpressing calnexin and calreticulin

HLA-B35 is expressed on HeLa cells endogenously. HLA-B35 expression in doxycycline treated and untreated iHeLa cells were determined by flow cytometry using the conformational-sensitive monoclonal antibody Tu149. Compared to untreated cells, calnexin and calreticulin overexpressing cells expressed 30% and 80%

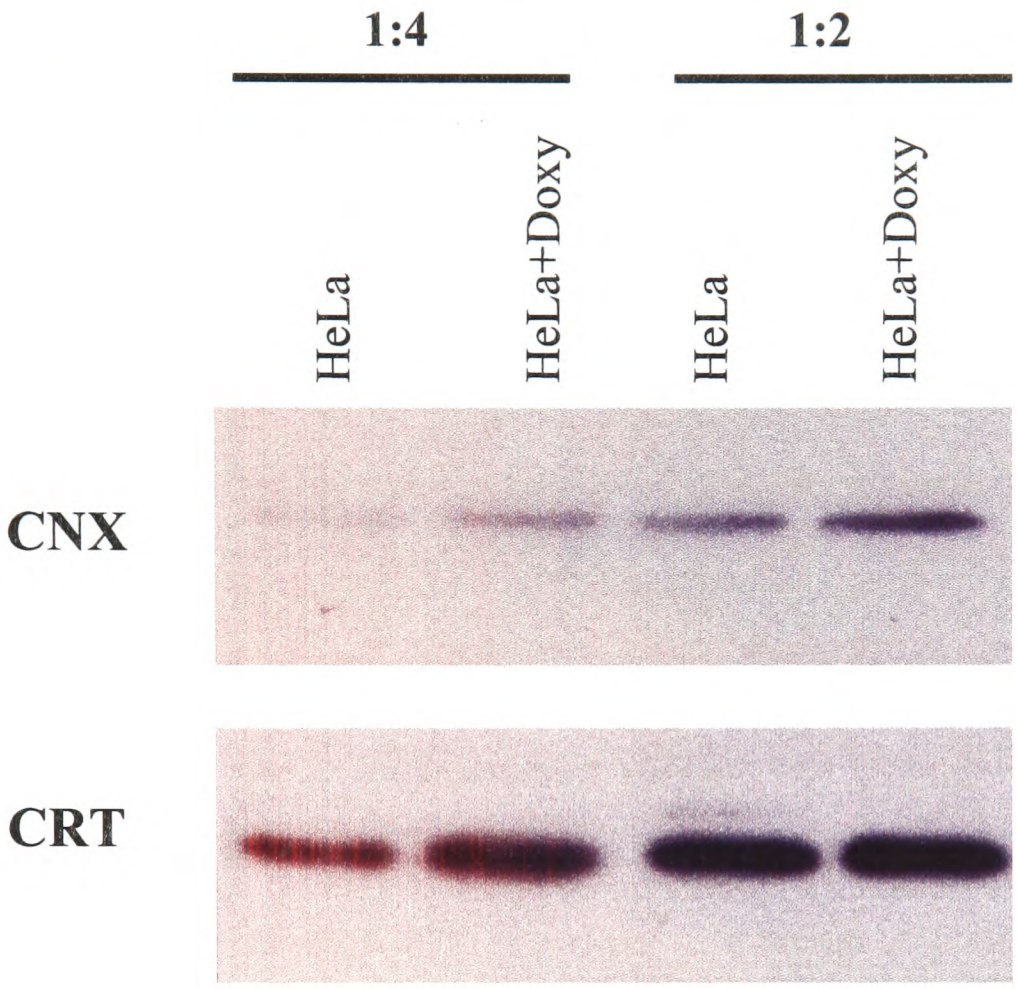

Figure 3.7. Expression of calnexin and calreticulin in doxycycline inducible HeLa cells

Inducible HeLa cells were treated with doxycycline at a final concentration of 2 μg/ml and and time allowed for overexpression of calnexin and calreticulin. Western blot was carried out with anti-calnexin and anti-calreticulin antibodies to determine the level of expression of the chaperones after induction. Dilution of the original lysate (1:2 or 1:4) (10^7 cells per ml of NP 40 lysis buffer) is also indicated.

more HLA-B35, respectively on the cell surface (figure 3.7.1). The increase in cell surface expression of class I in HeLa overexpressing the lectin chaperones, may be a consequence of efficient assembly or loading of class I.

3.7.2 Assembly and export of class I from ER in cells overexpressing calnexin and calreticulin

In order to determine the assembly and ER export of HLA-B35 in HeLa cells overexpressing lectin chaperones, a pulse-chase analysis was carried out. The fraction of class I molecules that assemble and leave the ER at each time point was assessed by immunoprecipitating with the Tu149 and subjecting to endo H treatment to assess their rate of exit from the ER. Figure 3.7.2 shows that the rate of transport of B35 molecules is the same in doxycycline treated as well as untreated cells. This result therefore suggests that overexpression of calnexin and calreticulin does not necessarily lead to longer detention times of class I in the ER. In addition, as Tu149 only recognises fully assembled B35 molecules, the results also suggest that efficiency of assembly is the same irrespective of the amount of calnexin or calreticulin present in these cells.

Fold-increase in the expression of calreticulin and calnexin following induction of iHeLa cells is less than the fold-increase in the cell surface expression of class I molecules at the cell surface (2-4-fold increase in the expression of calreticulin and calnexin resulted in roughly a log increase in the surface expression of B35). This suggests that class I molecules are probably in excess and increased levels of calnexin and calreticulin increases the efficiency of peptide loading onto class I and therefore increase the fraction of stable class I molecules. In light of these results, some reports have suggested calnexin in increasing the efficiency of loading certain peptides. These

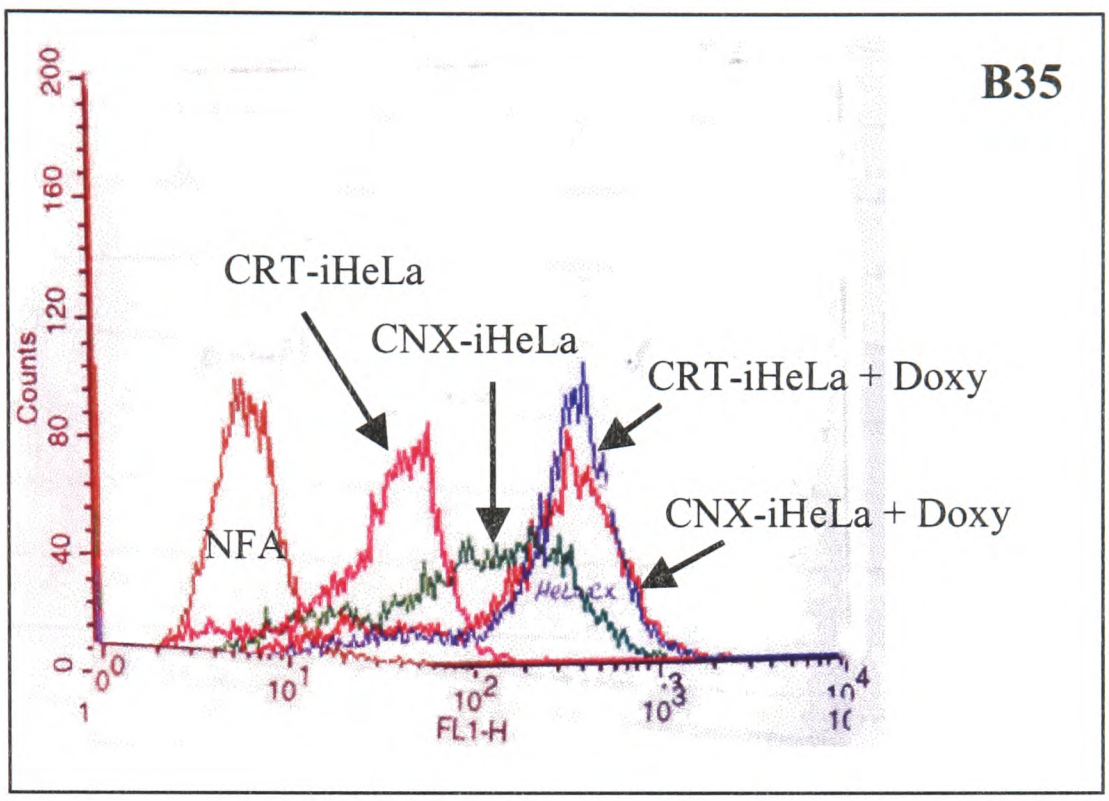

Figure 3.7.1. HLA-B35 (B35) expression is increased in HeLa cells over-expressing calreticulin (CRT) and calnexin (CNX)

Cell-surface expression of HLA-B35 was detected with monoclonal antibody Tu149 in 2mM doxycycline treated (+Doxy) and untreated CRT- and CNX-inducible HeLa (iCRT-HeLa and iCNX-HeLa) cells using flow cytometry. NFA, no first antibody.

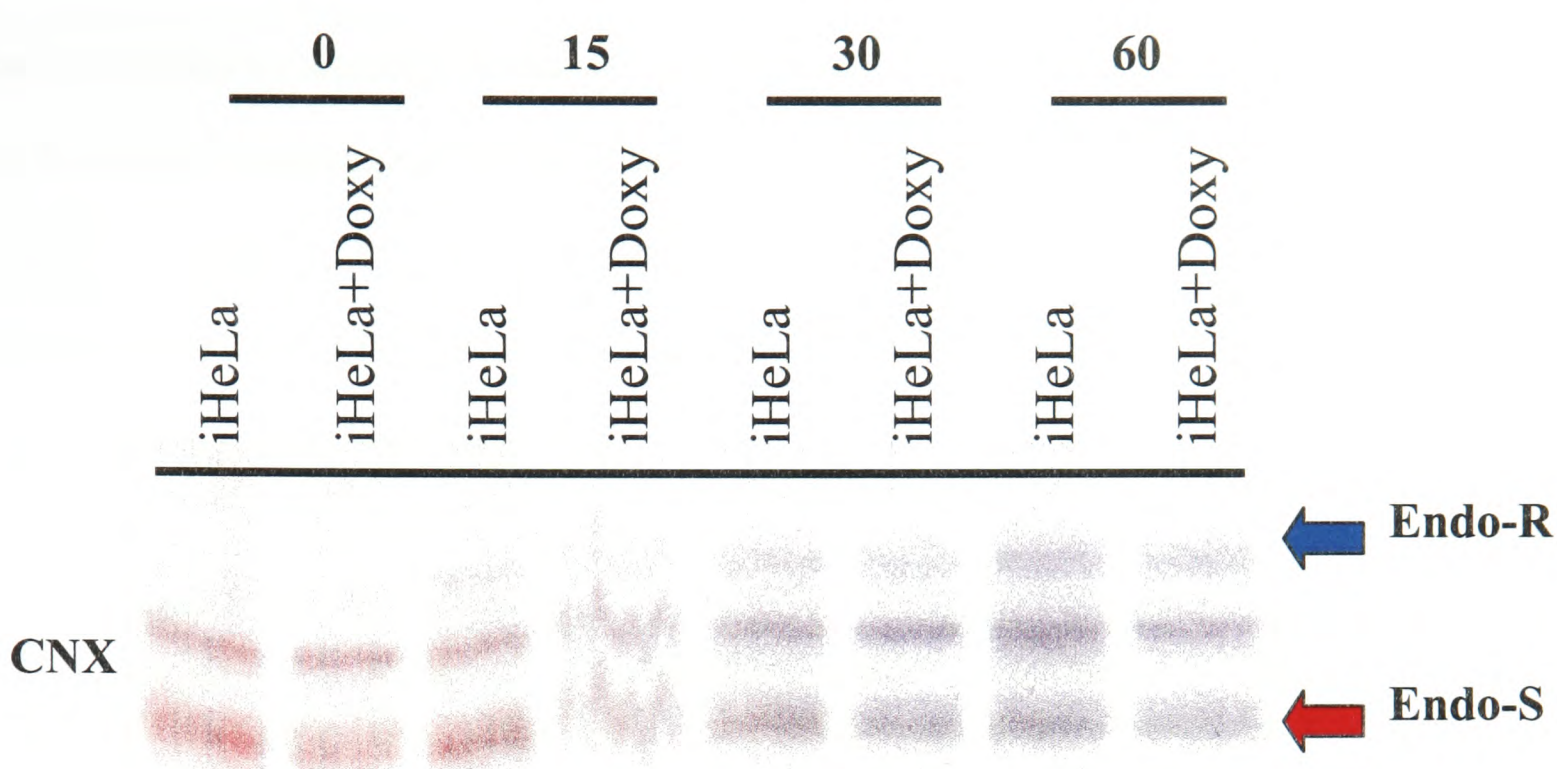

Figure 3.7.2. Assembly and export of class I from ER in cells over expressing calnexin and calreticulin

Pulse-chase analysis was carried out on HLA-B35 synthesised in calreticulin (CRT)- and calnexin (CNX)-inducible doxycycline treated and untreated HeLa (iHeLa) cells. Aliquots of labelled cells were chased up to indicated times and lysed. The lysates were immunoprecipitated with monoclonal antibody Tu149, digested with endoglycosidase H (Endo H) and fractionated by SDS-PAGE. Immature, Endo H-sensitive (Endo-S) and mature Endo H-resistant (Endo-R) bands are indicated by red and green arrowheads, respectively.

may be peptides derived from a certain subset of proteins, e.g., ER proteins, whose degradation may be affected by calnexin [330]. The reason why there is more surface class I in calreticulin compared to calnexin overexpressing iHeLa cells is not clear but may be a direct consequence of increased efficiency of peptide loading by calreticulin compared to calnexin. There was no decrease in the trafficking rate of class I molecules from the ER probably because there is always an excess pool of class I molecules to be peptide-loaded in the ER.

3.8 ASSEMBLY OF CLASS I WHEN INTERACTION OF CALNEXIN AND CALRETICULIN WITH THE CARBOHYDRATE MOIETY IS PHARMACOLOGICALLY BLOCKED

Another way of looking at lectin chaperone interaction with glycoproteins is to use drugs that specifically block interactions of chaperones with the carbohydrate moiety of glycoprotein substrates. Castanospermine (CAS), a naturally occurring alkaloid, is one such drug. CAS inhibits glucosidase-I, one of the enzymes essential in the generation of the monoglucosylated carbohydrate moiety, a prerequisite for calnexin and calreticulin interaction to glycoproteins.

Previous studies have demonstrated that association between lectin chaperones and class I is carbohydrate-dependent [162, 294]. When C1R-A2.1 cells were incubated with CAS, fewer class I molecules were recovered when co-immunoprecipitated with anti-calreticulin antibodies [298]. Moreover, CAS inhibited interactions between class I molecules and TAP [162].

3.8.1 H2-K^b cell surface expression is reduced in the presence of castanospermine

K41 and K42 were treated with 2mM CAS and cell surface expression of H-2K^b determined by FACS in both CAS treated and untreated cells after staining with the conformational specific mAb Y3. Figure 3.8.1a shows that the cell surface expression of K^b in CAS treated K41 is 50-60% of untreated control cells. The reason for occurrence of two populations of CAS-untreated K41 is not clear but I have noticed in other occasions growing cells at higher density leads to the generation of two sub-populations. CAS treatment did not produce significant effect on K^b surface expression in K42.

3.8.2 Peptide loading is impaired in CAS treated cells

It is possible to explain low K^b expression on the surface of CAS treated K41 cells if the class I molecules either failed to assemble with β2m properly or failed to load up with stabilising peptide. In order to determine whether the assembly or intracellular loading of K^b with peptides was indeed impaired in CAS treated cells, I immunoprecipitated a cohort of newly synthesised class I molecules in the presence or absence of added peptide ligand SIINFEKL, using Y3. Figure 3.8.1b shows that the amount of K^b that could be recovered with conformation-sensitive mAb in the presence of added peptides was greater for CAS treated cells compared to untreated cells. This indicates that although total number of K^b molecules synthesised in CAS treated and untreated cells are the same, more peptide-receptive K^b molecules are generated in CAS treated cells compared to untreated cells. And because peptide-receptive molecules are unstable, they "fall apart" when they reach the cell surface and hence we see lower class I surface expression in CAS treated K41 cells, a phenotype that closely resembles K42.

a)

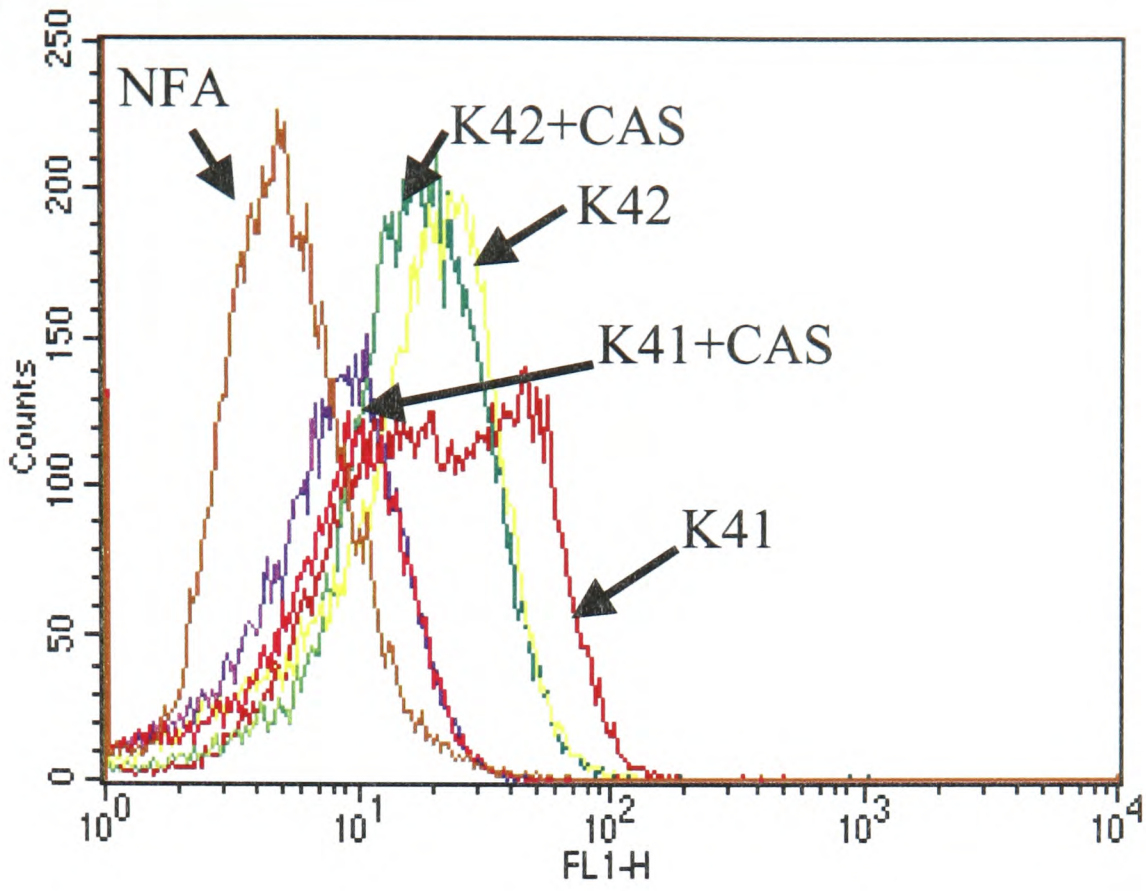

b)

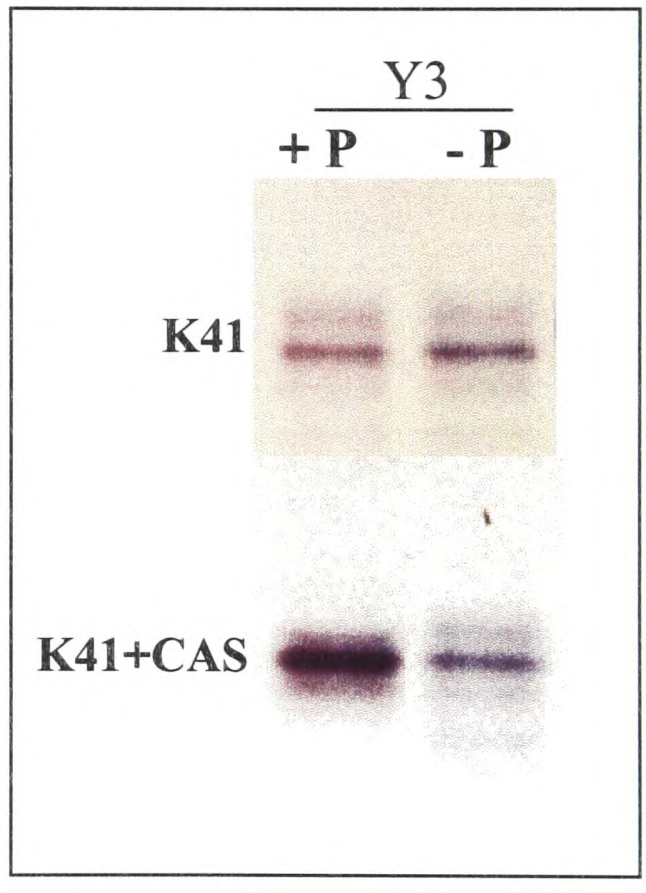

Figure 3.8.1. Cell surface expression and peptide loading of K^b is impaired in castanospermine treated cells

a) K41 and K42 were treated with 2mM castanospermine and cell-surface expression of K^b determined by flow cytometry using monoclonal antibody Y3. NFA, No First Antibody. Pink curve shows K41 treated with 4 mM castanospermine.

b) K41 were treated with 2mM castanospermine and metabolically labelled cohort of K^b were immunoprecipitated in the presence (+P) or absence (-P) of added peptide ligand SIINFEKL (20 μM), using Y3. Immunoprecipitates were analysed by SDS-PAGE fractionation followed by autoradiography.

3.9 INTRACELLULAR DISTRIBUTION OF CLASS I IN CALRETICULIN- DEFICIENT CELLS

The majority of calreticulin detected in cells is localised in the ER. As discussed earlier, the KDEL retrieval sequence located at the C-terminus of calreticulin promotes recycling of proteins from the Golgi to the ER. As calreticulin is associated with class I during its maturation in the ER, I asked whether calreticulin deficiency affected intracellular distribution of class I or differences in the amount of class I present in the Golgi at steady state.

I used confocal microscopy to look directly for the intracellular distribution of class I. I fixed K41 and K42 in 4% paraformaldehyde for 20 min at room temperature, washed three times in PBS, and permeabilised for 15 min in 0.05% Saponin. I then incubated cells in primary antibody (Y3 to stain H2-K^b or anti-C-terminus calnexin antibody to stain ER) for 30 min at room temperature, washed four times, followed by secondary FITC- or Texas Red-conjugated antibody or BODIPY-Texas Red (to stain Golgi) for 30 min at room temperature. After washing for four times, I mounted in Vector Shield on glass slides for analysis by scanning confocal microscopy (1.0μM optical sections).

As shown in figure 3.9a-d, K41 and K42 did not reveal differences in intracellular distribution of class I molecules, or differences in the intensity of staining in the Golgi. Figure 3.9a-b show class I staining (green) on the cell surface as well as in the Golgi (red). At steady-state conditions, majority of class I is localised on the cell surface rather than in the Golgi (figure 3.9a-b) or in the ER (red, figure 3.9c-d).

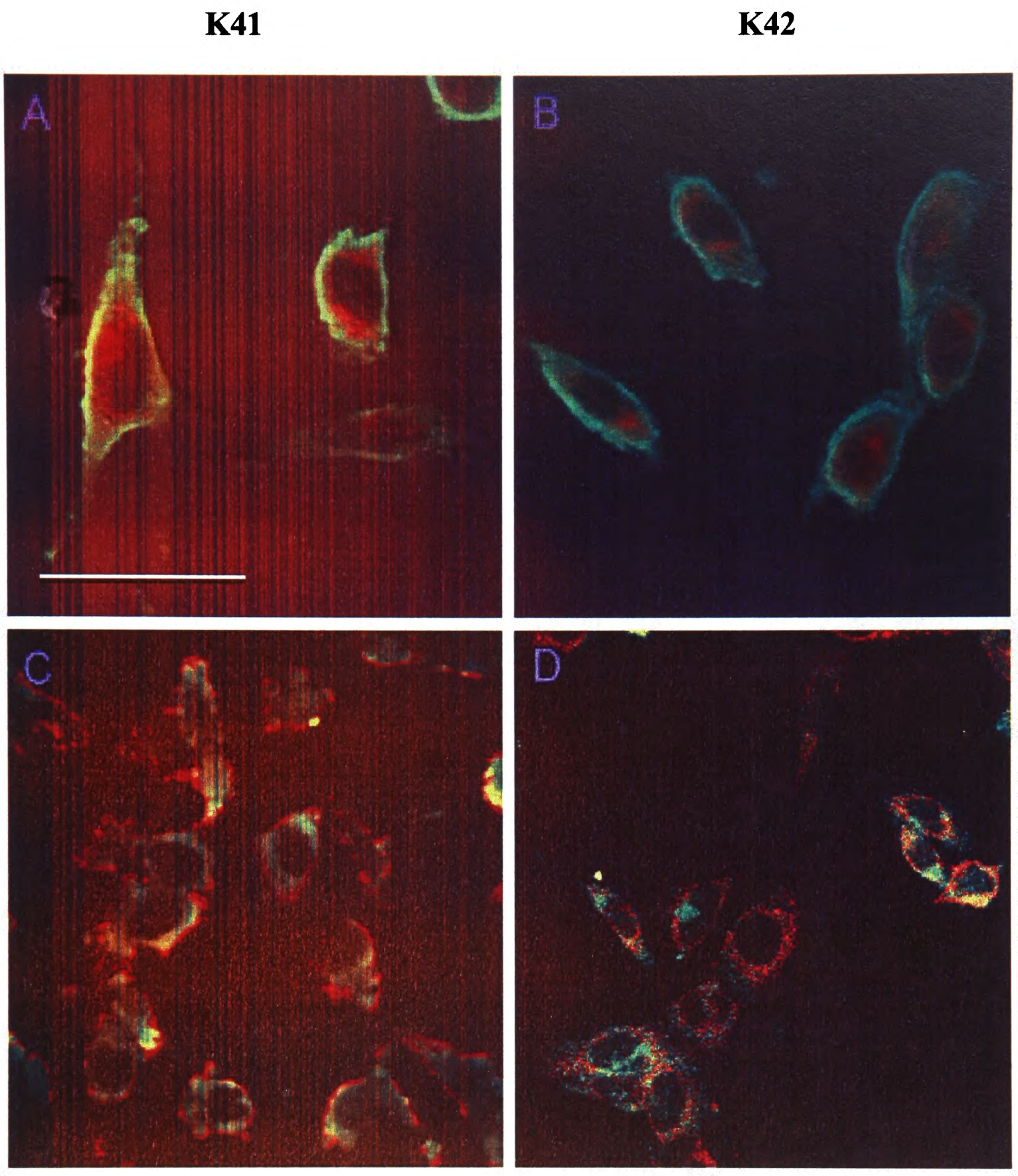

Figure 3.9. Intracellular distribution of class I molecules in K41 and K42

Confocal microscopy was used to look directly at the intracellular distribution of class I in K41 and K42 cells. K41 and K42 were fixed in 4% paraformaldehyde and permeabilized in 0.05% Saponin. Y3 (A-D) was used to stain K^b and anti-C-terminus calnexin antibody was used to stain ER (C, D). FITC (Green) or Texas Red-conjugated antibody (Red) were used as secondary antibodies for Y3 and anti-calnexin antibodies, respectively. BODIPY-Texas Red was used to stain the Golgi apparatus (A, B).

3.10 CHAPTER SUMMARY AND DISCUSSIONS

Antigen presentation function of MHC class I molecules is affected in the absence of calreticulin. Class I molecules expressed in the absence of calreticulin are able to assemble with β2m normally, but their subsequent loading with optimal, stabilising peptides is defective. These unloaded or suboptimally loaded class I molecules escape quality control (i.e. retention in the ER followed by degradation) and are released into the secretory pathway. This occurred despite the ability of newly synthesised class I to interact with the TAP loading complex [324].

The peptide loading efficiency in the absence of calreticulin is approximately reduced by around 50 - 80% of that seen in the presence of calreticulin. The peptide-loading defect in K42 appeared to be specific to calreticulin for two reasons. First, when I transfected K42 with the rabbit calreticulin gene, the surface expression of both H2-D^b and H2-K^b was completely restored. Second, transfection of K42 with the gene encoding lumenal domain of calnexin, failed to restore MHC class I surface expression.

The absence of calreticulin did not affect antigen processing as well as peptide transport by TAP. Moreover, confocal microscopy on K41 and K42 did not reveal differences in intracellular distribution of class I molecules or differences in the intensity of staining in the Golgi, consistent with the delivery of all assembled MHC class I molecules to the cell surface.

Calnexin is another ER resident molecular chaperone. It transiently associates with newly synthesised heavy chains and is proposed to mediate the association between

class I heavy chains and β2m. In the next chapter, using calnexin-deficient cell line, I explore whether calnexin has a role in class I assembly.

Chapter 4

ROLE OF CALNEXIN IN CLASS I ASSEMBLY

4.1 BACKGROUND

In chapter I, I presented evidence for the role of calreticulin in class I peptide loading and antigen presentation. Like calreticulin, calnexin is an abundant calcium-binding ER resident lectin chaperone. In humans, calnexin is proposed to mediate the association between class I heavy chains and β2m. Once class I-β2m heterodimers are formed, calnexin is displaced and the heterodimers physically associate with the TAP loading complex consisting of TAP, tapasin, calreticulin and ERp57 [14, 162]. In mouse, however, class I-β2m heterodimers are found associated with calnexin, and dissociation of calnexin from MHC class I appears to require β2m and peptide [328].

In 1985, a human T lymphoblastoid cell line CEM was subjected to immunoselection by co-culture with peripheral blood mononuclear cells (PBMC) and selected for resistance to natural killer (NK) cell-mediated lysis [306]. This cell line, known as $CEM.NK^R$, also completely lacked mRNA for calnexin [331]. Studies using $CEM.NK^R$ have demonstrated normal cell surface expression and T cell recognition for human and mouse class I alleles [330, 331]. It was suggested that calnexin was not required for cell surface expression of class I molecules or that other ER chaperones could substitute for calnexin in $CEM.NK^R$ [331]. This experiment, however, was not conducted under conditions where expression of other ER chaperones was suppressed. Trafficking rate of class I from ER was also normal in the calnexin deficient cells. However, the study lacked a proper class I assembly assay involving

the use of class I HC specific antibodies to identify HC that fail to assemble. Moreover, exogenous peptides were not added during the overnight preclear step, which would lead to "falling apart" of the assembled but unstable class I molecules. Moreover, the study found some differences in the profiles of the class I-associated peptides in the absence or presence of calnexin suggesting influence of calnexin in the repertoire of peptides loaded onto class I [330].

Jackson *et al.*, have used *Drosophila* Schneider cells to demonstrate the importance of calnexin in class I assembly and transport [196]. In this study, co-expression of calnexin retained free class I heavy chains and peptide-deficient heavy chain-β2m heterodimers in the ER. This result contradicts those in CEM.NK^R where calnexin does not seem to play any role in the surface expression and transport of class I molecules. In CEM.NK^R, there is the possibility that other abundant chaperones like BiP and calreticulin may substitute for calnexin with its role in class I assembly. It is thus important to do experiments under conditions where expression of these highly abundant chaperones is suppressed in order to evaluate the role of calnexin in the assembly and transport of class I in CEM.NK^R cells.

Calnexin and calreticulin are homologous lectin chaperones and highly conserved across species. However, several studies have highlighted the specificities of these chaperones in terms of their interactions with glycoprotein substrates. For example, VSV G-protein, which has two N-linked glycans, binds to calnexin but not calreticulin [261]. T cell receptor α, β, CD3δ and CD3ε bind to calnexin where as only α and β subunits bind to calreticulin, and this for shorter times than they bind to calnexin [332, 333]. Moreover, influenza HA in dog pancreas microsomes associates

initially with calnexin and calreticulin but calreticulin dissociates from the complex earlier [268]. These experiments clearly show that there are differences in the ability of these chaperones to recognise particular substrates. Influenza HA has seven possible consensus sites for glycosylation. Mutation of glycosylation consensus sites in different combination has shown that calreticulin binding to HA depends on three glycans in the top and hinge domain of the protein, where as calnexin binding depends on the four sites in the stem domain. The top domain folds first (oxidises first) than the stem domain, which explains why calreticulin binding ceases earlier than calnexin binding.

In this chapter, I have made use of cells that lack calnexin in order to further explore whether calnexin has a role in class I assembly. Moreover, in order to understand specificities/redundancies of calreticulin and calnexin, I have made use of calnexin-deficient cell line CEM.NK^R infected with vaccinia encoding mutant MHC class I (A2.1T134K), which fails to interact with calreticulin.

4.2 ASSEMBLY OF HLA-A2.1 AND A2.1T134K IN CELLS THAT LACK CALNEXIN

Human HLA-A2.1 (A2.1) that carries a lysine substitution at position 134 (A2.1T134K) interacts with calnexin normally but does not interact with calreticulin and with other cofactors of the peptide-loading complex (PLC) ([180, 291], Simon Powis, submitted). CEM and CEM.NK^R were infected for 90 minutes with vaccinia encoding wild type A2.1 and mutant A2.1T134K at a multiplicity of infection of approximately 10:1. Vaccinia was removed after 90 minutes and CEM and CEM.NK^R were incubated in normal growth media for four hours to allow expression of A2.1

and A2.1T134K molecules. Cells were then labelled by incubating in media containing radiolabelled ^{35}S Methionine and Cysteine for 40 minutes and lysed in the presence or absence of stabilising peptide. The lysates were precleared overnight with normal rabbit serum (NRS) followed by immunoprecipitation with either rabbit polyclonal antibody ABR2 or with mouse monoclonal antibody BB7.2 on protein A Sepharose beads. ABR2 reacts strongly with HLA class I free heavy chains but poorly with β2m associated heavy chains. BB7.2, on the other hand, recognises a conformation dependent epitope on the α1 domain of HLA-A2.1, which is generated after heavy chain assembles with β2m.

4.2.1 Assembly of A2.1 in CEM and CEM.NK^R

Figure 3.2.1a-c shows that 57% of total A2.1 HC synthesised assemble with β2m in CEM and that only 25% assemble CEM.NK^R. The increase in the amount of class I precipitated with BB7.2 in the presence of added peptide (20 μM HIVpol (amino acids 476-484 ILKEPVHGV)) is directly related to the amount of peptide-receptive class I in the cell [180]. Figure 3.2.1a-c shows that out of the 57% that assembled in CEM, 42% were stably loaded whereas 15% were peptide receptive, which would dissociate in the overnight preclearing step in the absence of added stabilising peptide ligand. In contrast, although only 25% of A2.1 assembled in CEM.NK^R, majority of them (22%) were stably loaded. This may be because there are overall fewer assembled molecules in CEM.NK^R, and these get full access to the limited supply of stabilising peptide in the ER. Lower overall assembly in CEM.NK^R was not as a result of increased HC degradation as the total number of HC synthesised in both cells were similar.

a.

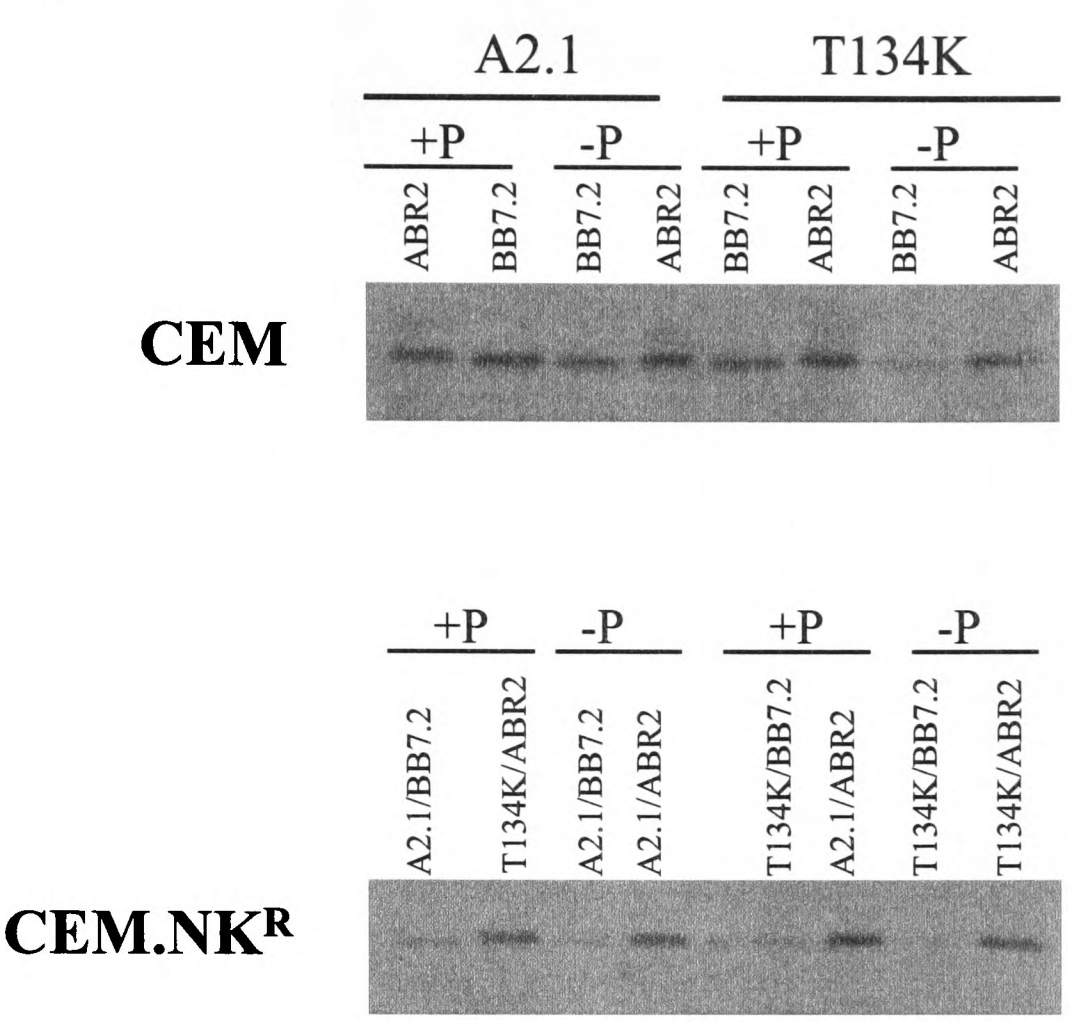

Figure 4.2.1 Assembly of HLA-A*0201 (A2.1) and A2.1T134K in the absence of calnexin

a) Calnexin-positive CEM and calnexin-deficient CEM.NK^R were infected with vaccinia encoding either A2.1 or A2.1T134K for 90 minutes. Vaccinia was then removed and cells incubated for further 4 hrs to allow expression of A2.1 and A2.1T134K. Cells were then metabolically labelled by incubating in growth medium containing ^{35}S-methionine and cysteine for 40 minutes after which cells were lysed in the presence (+P) or absence (-P) of A2.1 stabilising HIV pol peptide ILKEPVHGV (20μM). After overnight preclear, lysates were immunoprecipitated either with ABR2, which recognises A2.1 heavy chain or with BB7.2, which recognises a fully-assembled A2.1, fractionated by SDS-PAGE followed by autoradiography to identify class I heavy chain (HC) bands. HC bands were quantified using Quantity One software (BIArad Inc, USA).

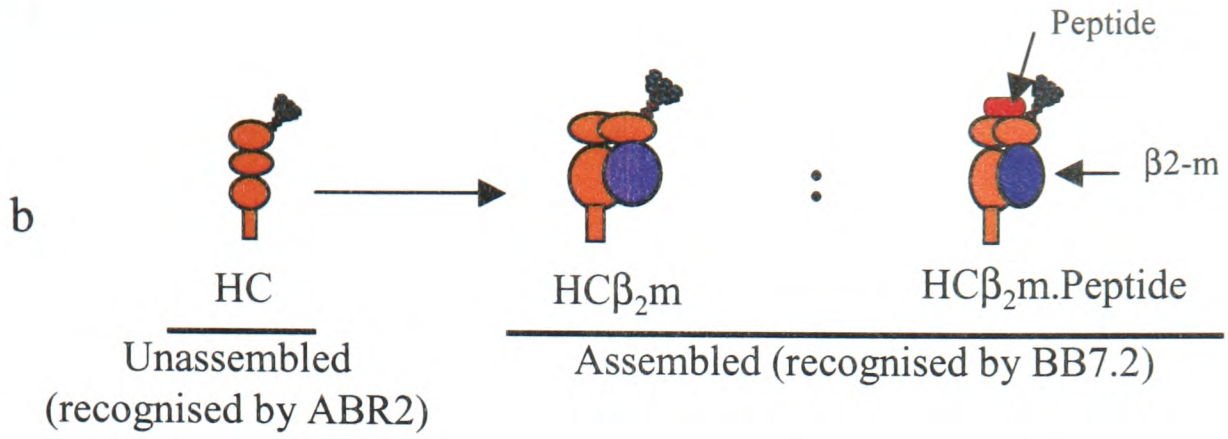

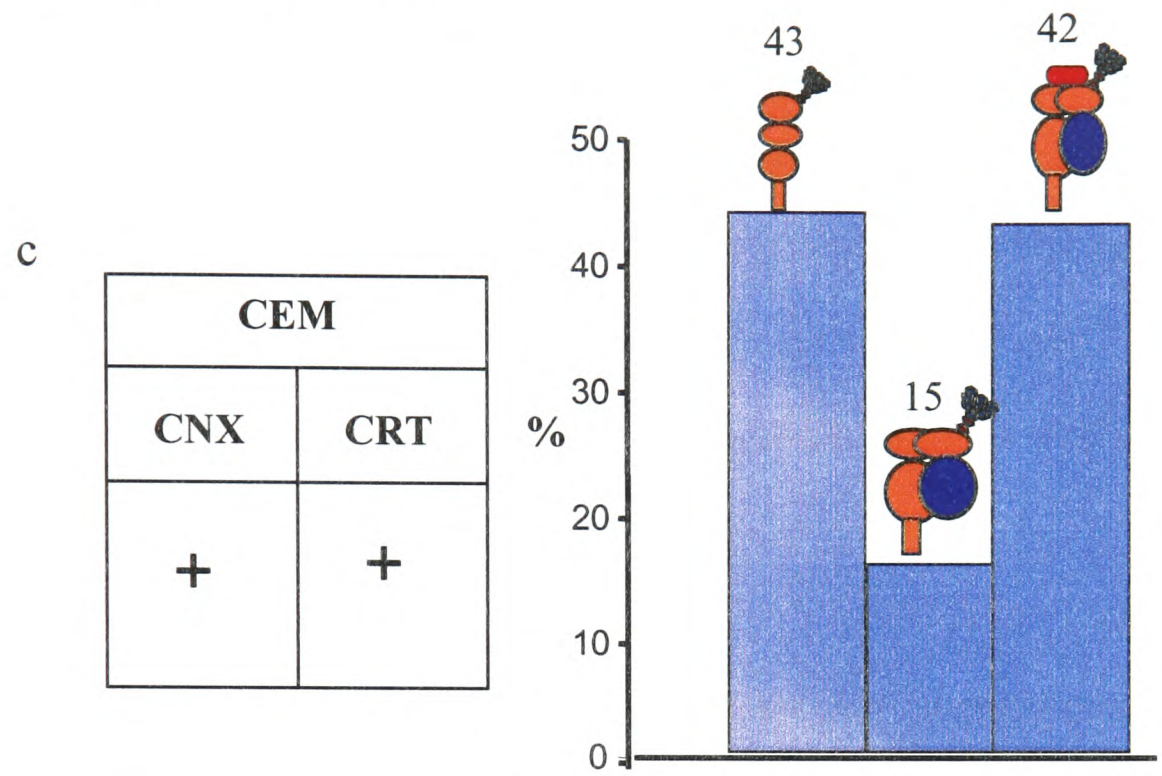

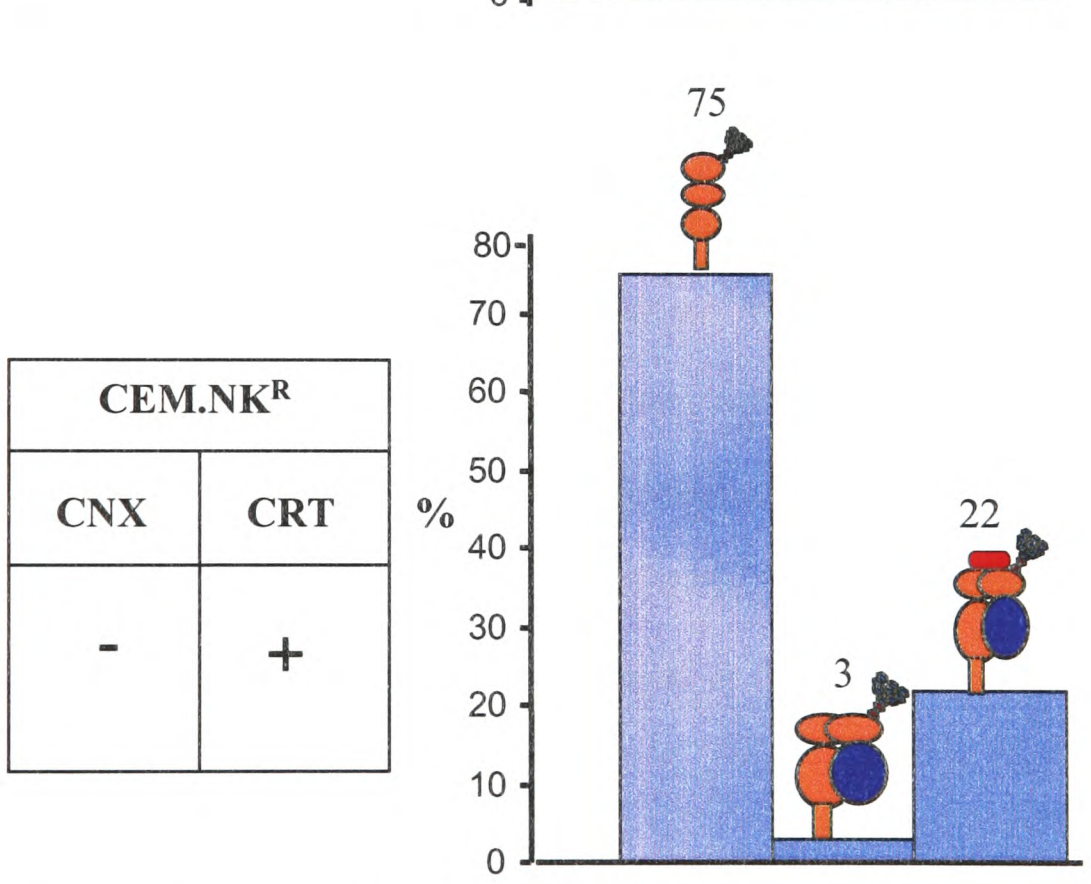

Figure 4.2.1 Assembly of HLA-A*0201 (A2.1) in the absence of calnexin

b) Schematic representation of the assembly of class I heavy chain (HC) with β2-m and peptide. c) Calnexin-positive (CEM) [upper panel] and calnexin-negative (CEM.NK^R) [lower panel] cells expressing A2.1 were pulse labelled, and aliquots were lysed in the presence or absence of 20μM A2.1 binding peptide ILKEPVHGV. Lysates were immunoprecipitated with either antiserum ABR2, which recognises free heavy chains (unassembled A2.1) or monoclonal antibody BB7.2,which recognises folded and assembled A2.1. CEM cells are calnexin and calreticulin positive (+), where as CEM.NK^R are calnexin negative (-) but calreticulin positive (+). The percentage of unassembled, peptide-receptive and peptide-loaded class I molecules is shown above individual bars.

4.2.2 Assembly of A2.1T134K in CEM and CEM.NK^R cells

A2.1T134K fails to interact with calreticulin [and with other cofactors of the peptide loading complex (PLC) including tapasin, Erp57 and TAP] ([291, 294], Simon Powis, submitted). In the absence of interactions with calreticulin (and with the cofactors of the PLC), assembly of the mutant class I molecule is reduced to 45% compared to the assembly of 57% for wild-type A2.1 molecules in the calnexin-positive CEM cells (figure 3.2.1a, b, d). Similarly, in the calnexin-deficient CEM.NK^R cells, assembly of A2.1T134K is just 18% compared to 25% for wild-type A2.1. Therefore, the difference probably reflects contribution from calreticulin (and other cofactors of the PLC) in the assembly of class I.

What is also interesting is that there is greater pool of peptide-receptive class I molecules in the absence of interaction with calreticulin (and with other cofactors of the PLC (compare figures 3.2.1c and 3.2.1d)). In other words, in the absence of interactions with calreticulin (or with the cofactors of the PLC), almost one-third of the HC:β2m heterodimers dissociate during the overnight pre-clear step in the absence of stabilising peptide. This is consistent with the fact that failure to interact with the cofactors of the PLC results in the generation of more peptide-receptive class I molecules. Moreover, lower assembly in CEM.NK^R was not as a result of increased degradation of A2.1T134K HC as the total number of HC synthesised in both cells were similar.

d

CEM	
CNX	CRT
+	-

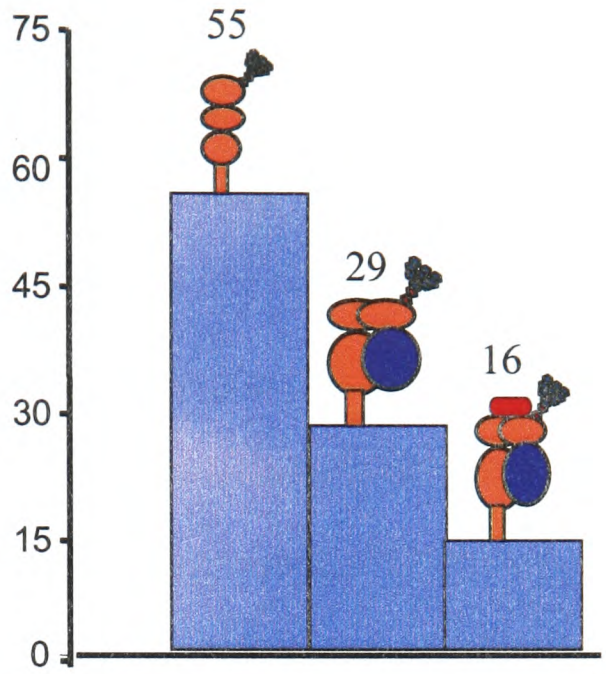

CEM.NK^R	
CNX	CRT
-	-

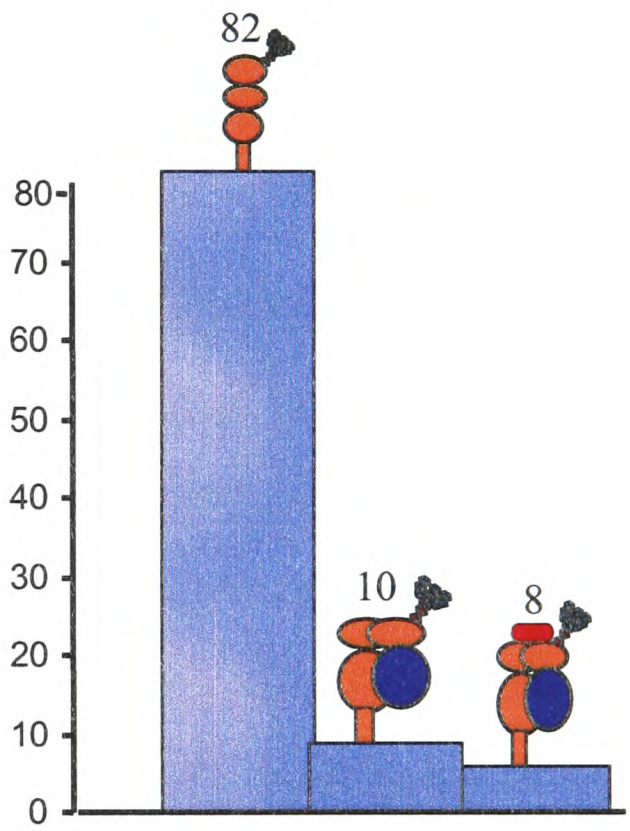

Figure 4.2.1 (contd.) Assembly of HLA-A*0201T134K (A2.1T134K) in the absence of calnexin

d) Calnexin-positive (CEM) [upper panel] and calnexin-negative (CEM.NK^R) [lower panel] cells expressing A2.1 T134K were pulse labelled, and aliquots were lysed in the presence or absence of 20μM A2.1 binding peptide ILKEPVHGV. Lysates were immunoprecipitated either with antiserum ABR2, which recognises unassembled A2.1 or with monoclonal antibody BB7.2, which recognises assembled A2.1. CEM cells are calnexin and calreticulin positive (+), where as CEM.NK^R are calnexin negative (-) but calreticulin positive (+). The percentage of unassembled, peptide-receptive and peptide-loaded class I molecules is shown above individual bars.

Table 3.2.1 suggests that calreticulin (or the cofactors of the PLC) can compensate for lack of calnexin to certain extent. Only 18% of the class I HC:β2m heterodimers assembled in the absence of interactions with both calnexin and the cofactors of the PLC. The number of assembled molecules increased to 25% in the presence of calreticulin (and the cofactors of the PLC). A 1.5 fold increase in calreticulin expression in CEM.NK^R cells was also observed (figure 3.2.2). Taken together, these results demonstrate that although there is some redundancy in the function of calnexin and calreticulin, calreticulin (or indeed other cofactors of the PLC) cannot completely compensate for calnexin function. Therefore, suggestion that the functions of these lectin chaperones are interchangeable [330] and that one chaperone can substitute for another may not be entirely true.

4.3 CHAPTER SUMMARY AND DISCUSSION

The majority of substrates for calnexin and calreticulin overlap. This is not surprising considering their lectin specificities are identical. However, a closer analysis reveals subtle differences in their function. I have used a) a cell line that lacks functional calnexin and b) a human mutant class I that fails to interact with calreticulin to study the chaperone specificity. Wild-type A2.1 fails to assemble properly in calnexin-deficient CEM.NK^R cells. This is despite elevated levels of calreticulin seen in CEM.NK^R (figure 3.2.2). Moreover, A2.1T134K, which fails to interact with calreticulin (and other cofactors of the PLC), assembles poorly in the calnexin-positive CEM cells. Assembly of A2.1T134K is almost completely abolished in CEM.NK^R.

Calreticulin	+	+	-	-
Calnexin	+	-	+	-
% A2.1 Assembled	**57**	**25**	**45**	**18**

Table 4.2.1 Summary of assembled HLA-A*0201 in the presence/ and or absence of calnexin and calreticulin.

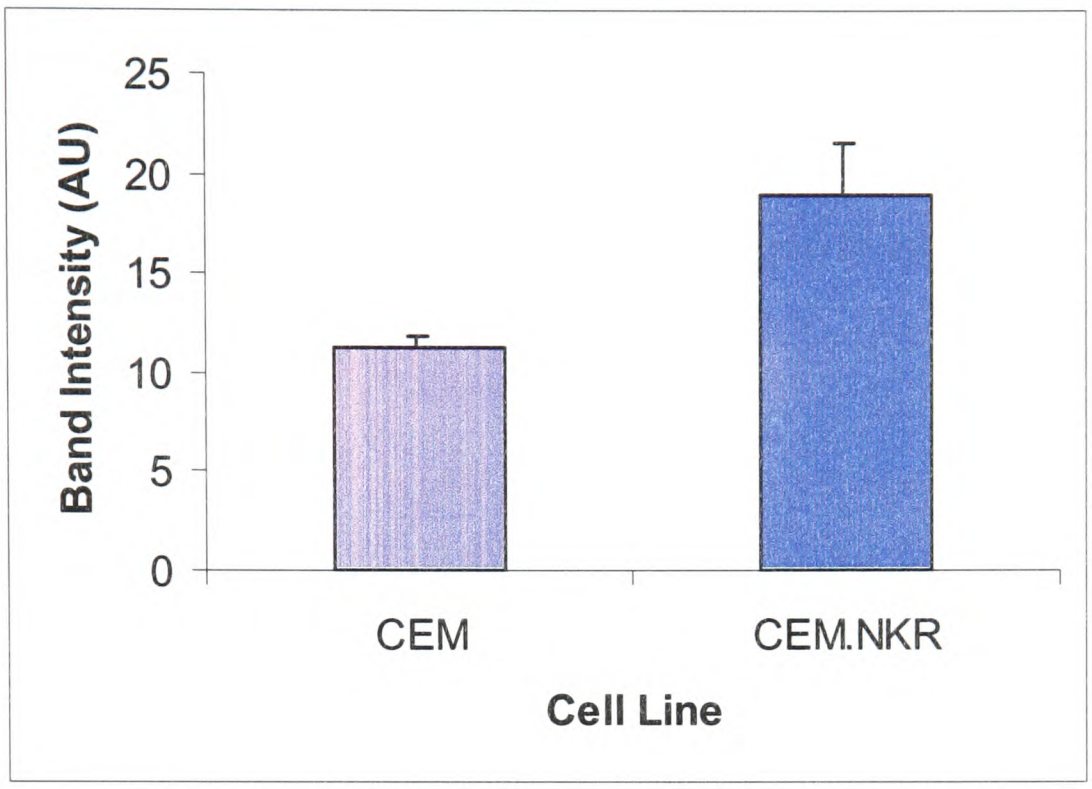

Figure 4.2.2 Expression of calreticulin is increased in calnexin-deficient CEM.NK^R cells

Equal number of calnexin-competent CEM and calnexin-deficient CEM.NK^R cells were lysed and equal volume of aliquots fractionated by SDS-PAGE and immunoblotted with anti-calreticulin serum after transferring onto a nitrocellulose membrane. After detection of the calreticulin band with ECL and autoradiography, the intensity of the bands was quantified and plotted. The experiment was repeated on three different days and on three different lysates and standard deviation is indicated by the error bars.

These results demonstrate calnexin has an important function in class I HC assembly with β2m. Calreticulin (or indeed TAP/tapasin/Erp57) can compensate for lack of calnexin function but only to a certain extent (table 3.2.1). Expression of calreticulin is increased in CEM.NK^R by up to 1.5 fold (figure 3.2.2). It is therefore possible that the compensative action of calreticulin may be a consequent of mass action. In any case, suggestions that the functions of these chaperones are interchangeable and that one chaperone can substitute for another may not be entirely true.

Chapter 5

ROLE OF HEAVY CHAIN GLYCOSYLATION ON CLASS I ASSEMBLY AND ANTIGEN PRESENTATION

5.1 BACKGROUND

Whether N-linked glycans play a significant role in class I assembly and antigen presentation is still controversial. A great deal of work has been done on this subject using both human and mouse class I alleles. Results reported so far range from no effects of N-linked glycosylation on cell surface expression, assembly with β2m and antigen presentation, to having major roles in these processes. These studies have been based on methods that either eliminate or alter glycan moieties in class I heavy chains. Some studies have used drugs either to block glycosylation of heavy chains (e.g., tunicamycin) or to disrupt glycan modifications by inhibiting glucosidases (e.g., with castanospermine, nojirimycin and deoxynojirimycin) [334, 335] or inhibiting mannosidases (e.g., swainsohmine and deoxymannojirimycin) [334]. Other methods have used genetic manipulation in order to alter the number and sites of glycosylation in the class I allele.

5.1.1 Glycosylation and the assembly of class I

In studies using glycosylation inhibitor tunicamycin, the requirement of glycosylation for human class I assembly and cell surface expression has been shown to be dependent on the MHC class I allele [335]. The ability of β2m to assemble with heavy chain alleles was determined by immunoprecipitating either with antibodies that recognise fully assembled class I molecules or with antibodies that are only reactive

to heavy chain or β2m. It was shown that assembly of B alleles were most affected by tunicamycin treatment, although considerable variation was seen within the allelic series of the HLA-A and B loci (see table below). HLA-C assembly with β2m was poor irrespective of tunicamycin treatment. For HLA-A and –B alleles, surface expression in the presence of tunicamycin was directly related to the efficiency of assembly with β2m. In this study, however, tunicamycin treatment resulted in lower overall expression of class I molecules probably as a result of a stress response. In addition, these experiments only visualise the class I HC:β2m:peptide complex and not HC:β2m:peptide complex plus HC:β2m. Moreover, the amount of tunicamycin used failed to completely block glycosylation of class I.

Assembly of human heavy chain alleles with β2m in the presence of tunicamycin

BAD	**INTERMEDIATE**	**GOOD**
A1.1, A30, B5, B35, B8, B13, B44, B37, B60.1, B60.2, B57, B61, B7, B14	B27	A11, A2.1, A2.3, A24.1, A33, A32, A3, A29

Tunicamycin treatment of mouse cells expressing H-2^d alleles reduced the expression of these alleles at the cell surface [334]. Moreover, tunicamycin treatment only moderately affected binding of two antibodies (34-5-8S and 34-2-12S) that recognise the heavy chain:β2m heterodimer. However, binding of a third conformational-sensitive antibody (M1/42), again recognising the heavy chain:β2m heterodimer was disrupted upon tunicamycin treatment. This was probably due to the loss of epitope that this third antibody binds. The result therefore indicates two possibilities: a) β2m probably assembles with H-2^d heavy chains upon tunicamycin treatment but acquires

a slightly different conformation, or b) peptide repertoire is altered following tunicamycin treatment leading to slightly different conformation of class I upon different peptide binding [296].

In contrast to tunicamycin treatment which blocks glycosylation, disruptions of glycan modification processes by inhibiting the enzymes involved have demonstrated no affect on the assembly of both human and mouse heavy chain with β2m. Deoxynojirimycin and swainsonine treatment of Raji cells, which inhibit glucosidases and mannosidases, respectively, had no affect in the assembly of β2m with heavy chains of HLA-A and -B alleles [335, 336]. However, in mouse P815 and EL-4 cells, surface expression of H-2^b and H-2^d was downregulated after treatment of cells with increasing concentrations of deoxynojirimycin and swainsonine [334]. This suggests that either the assembly of class I HC with β2m is low after the treatment or that the inhibitors affect peptide loading of class I.

Therefore, the results using drugs to eliminate or alter glycan moieties suggest that the presence, not composition of glycans is important in the assembly of β2m with class I heavy chain. However, it is to be noted that treatment of cells with drugs affects processing of all carbohydrate moieties of all glycoproteins in the cell and therefore the effect is not specific to class I. In order to understand the effects of class I glycosylation without altering other cellular proteins and to determine whether glycans have importance in class I assembly, glycosylation mutants have been generated with selected omissions or additions of N-linked glycans from the α1, α2 and/or α3 domains of mouse and human class I heavy chain.

Studies done by Miyazaki et al showed that mutations in class I HC to alter glycosylation pattern in L^d heavy chain resulted in downregulation of L^d cell surface expression, although the synthesis of mutant heavy chain determined by western blotting was comparable to the wild type [337]. Using this observation as evidence, they concluded that alterations of glycosylation from normal results in defective transport and this, they suggested, might be because of failure of β2m to assemble with L^d heavy chain. Recently, Harris et al have shown that the removal of the L^d α1 domain glycosylation site at position 86 prevents this mutant from associating with calreticulin and the TAP complex [287]. However, amino acid substitution that prevented glycosylation in the α2domain at position 176 had no such effect. The authors, however, did not study assembly of β2m with the glycosylation mutant L^d heavy chain.

Zhang and Salter have studied the effect of addition of glycosylation in the α2 domain at position 176 of the human allele A*0201 and found reduced cell surface expression of the mutant allele [286]. Moreover, one half of the mutant molecules synthesised were retained in the ER and binding to TAP loading complex was poor [286]. This study, however, did not look at the effects of removal of the glycosylation site at position 86 or additions of two more glycosylation sites at positions 176 (α2 domain) and 256 (α3 domain) so as to directly compare with the mouse alleles. Moreover, the β2m-assembly and antigen presentation function of this glycosylation mutant was not studied.

5.1.2 Glycosylation and antigen Presentation

Using H-2^d anti H-2^b CTL with EL-4 targets and H-2^b anti H-2^d CTL with P815 targets, lysis of both target cell lines was significantly inhibited following treatment with tunicamycin [334]. It was shown that tunicamycin treatment leads to some loss of class I molecules, but not in sufficient amounts to account for the total ablation of lysis. It was concluded that tunicamycin treatment of target cells leads to the loss of the MHC class I epitope required for T cell triggering. In the same study, antigen presentation was not affected by treatment of cells with inhibitors of glucosidases or mannosidases that prevent complex carbohydrate formation [334].

In a separate study done by Hart *et al.*, pretreatment of stimulator cells with tunicamycin downregulated cell surface expression of class I and abrogated the ability of such cells to activate allogeneic thymocytes in a mixed lymphocyte reaction [338]. Moreover, it has been demonstrated that alloreactive epitopes of murine class Ib are defined by the glycosylation state of the molecules. Jenkins *et al.*, have shown that individual CTL clones responsive to different Qa-1 determinants differ with respect to their ability to recognise and lyse tunicamycin treated targets [339].

Shen and Kane have demonstrated the existence of two subsets of H2-K^b molecules, which differ in their ability to stimulate alloreactive CTL [340]. Using Y3 mAb immunoaffinity chromatography to separate the K^b molecules, they found that major difference between these two subsets was in the degree of N-linked glycosylation, with the non-stimulatory subset containing K^b molecules with larger and more complex carbohydrate modifications.

Other studies have suggested that glycosylation of murine MHC class I molecules plays no significant role in antigen recognition by either allo- or syngeneic CTL. Liposomes bearing completely deglycosylated H-$2K^k$ have been shown to trigger the maturation of precursor to effector CTL as effectively as liposomes with wild type H-$2K^k$ in spleen cell cultures initiated from previously primed mice [341].

Miyazaki *et al.*, studied antigen presentation by the mouse allele L^d, which had complete omission and various alterations of N-linked glycans [337]. All glycosylation mutants were recognised by alloreactive CTL clones raised against native antigen and were also able to effectively present foreign (VSV) antigen to MHC I restricted syngeneic CTL. However, the authors mention that the level of recognition of mutants was lower and that they used very high effector to target ratio in all experiments. The level of recognition of mutants may have been lower as a result of lower cell surface expression of class I carrying glycosylation alterations.

The proposal that carbohydrates are not essential for alloantigen specific recognition is further supported by experiments done on HLA-B7 molecules [342]. HLA-B7 molecules were analysed that had N-linked glycans present or absent at those sites that are highly conserved in HLA and H-2 class I antigen, namely positions 86 in humans and positions 86 and 176 in mouse. Transfection of non-glycosylated HLA-B7 (HLA-$B7^{--}$) into mouse L cells resulted in complete loss of cell surface expression whereas it was expressed (albeit at a lower level) at the cell surface when transfected into human RD cells. An N- glycan site added at position 176, the HLA-$B7^{-+}$, did not rescue normal levels of surface expressions. Although cell surface expression of HLA-$B7^{--}$ and HLA-$B7^{-+}$ was reduced, neither of the mutations was seen to affect

recognition by a panel of 12 allospecific CTL clones. These observations thus suggest that the carbohydrate moiety on HLA antigens plays a minimal role in recognition by allospecific CTL clones.

There is still a great deal of controversy in the understanding of the role of glycosylation in the regulated expression, assembly and antigen presentation function of MHC class I. Studies done so far have only looked at the role of N-glycosylation on either assembly or antigen presentation aspect of a particular class I allele. In this study, I have followed through the process of biogenesis of HLA-A2.1 and evaluated the role of N-glycosylation from its expression and assembly through to antigen presentation. Use of drugs either to block glycosylation or prevent formation of complex carbohydrate can affect processing of all glycosyl moieties of all proteins and produce several non-specific effects. I have, therefore, generated a panel of mutants with selected omissions and additions of N-linked glycans from α1, α2 and α3 domains of HLA-A2.1.

5.2 GENERATION OF GLYCOSYLATION MUTANTS

PCR based site directed mutagenesis was used to generate a number of A2.1 mutants. A2.1, in its natural form (A2.1WT), is glycosylated at position 86. The glycosylation consensus sequence was altered at position 86 in A2.1 to generate a non-glycosylated A2.1 (I will refer this as $A2.1^{---}$). Mutagenesis accuracy was confirmed by sequencing. In the process of generating other mutants, two more glycosylation sites were added at amino acid positions 176 and 256 such that A2.1 was similarly glycosylated as mouse H-$2D^b$ (referred as $A2.1^{+++}$). Likewise, H-$2K^b$-like A2.1 was generated by introducing a glycosylation site at position 176 ($A2.1^{++-}$) of wild type A2.1. In addition, the

glycosylation site at position 86 was knocked out of $A2.1^{++}$ to generate another A2.1 mutant ($A2.1^{-+-}$). In order to study the role of glycosylation in the regulated assembly and antigen presentation, the mammalian expression vector pCDNA3 (see Appendix 2.14) carrying these mutants was used to transfect C1R cells and stable lines generated using cloning by limited dilution.

5.3 ROLE OF HEAVY CHAIN GLYCOSYLATION IN THE EXPRESSION OF A2.1 MOLECULES

5.3.1 Reduced cell surface expression of aglycosylated A2.1molecules

As a first step towards evaluating the role of class I heavy chain glycosylation in the regulated class I assembly, I tested the effects of knocking out the glycosylation site at position 86 of A2.1. Cell surface expression of C1R transfected with aglycosylated A2.1 heavy chain ($A2.1^{---}$) was determined by flow-cytometry using conformational-sensitive monoclonal antibody BB7.2. As shown in figure 5.3.1a-b, eliminating the glycosylation site from A2.1 resulted in several fold reduction in cell surface expression of class I. $A2.1^{---}$ surface expression was 78% lower compared to wild-type A2.1.

Western blot was used to determine the level of expression of the aglycosylated heavy chain. Equal number of C1R cells expressing wild type A2.1 and $A2.1^{---}$ were lysed in NP40 lysis buffer. 5μg of lysate was run on SDS-PAG and blotted on a nitrocellulose membrane. A2.1 heavy chain was detected by incubating the membrane with a mouse monoclonal antibody HCA2 (which recognises heavy chain of A2.1 molecules) followed by incubation with secondary horseradish peroxidase antibody and final detection by ECL reagent. As shown in figure 5.3.1c, it is apparent that overall expression of $A2.1^{---}$ is comparable to wild-type A2.1 in C1R cells. The heavy chain

a

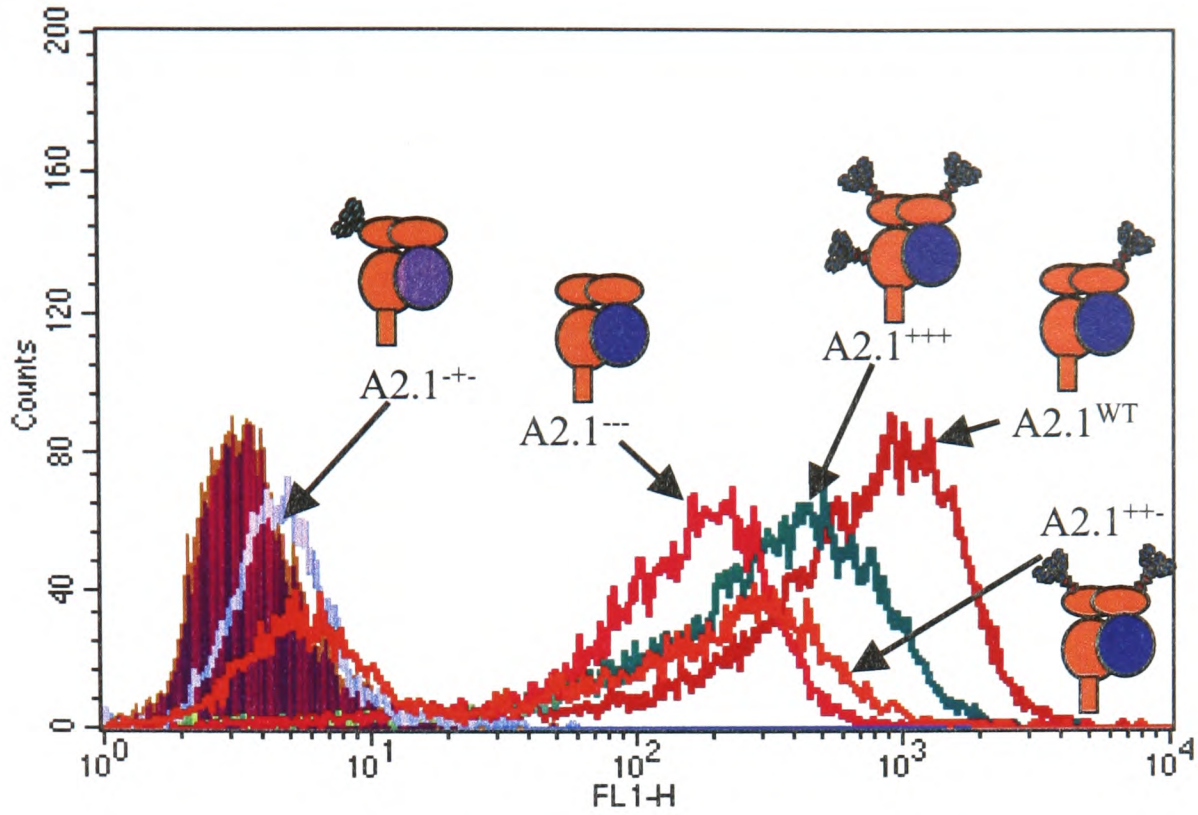

b

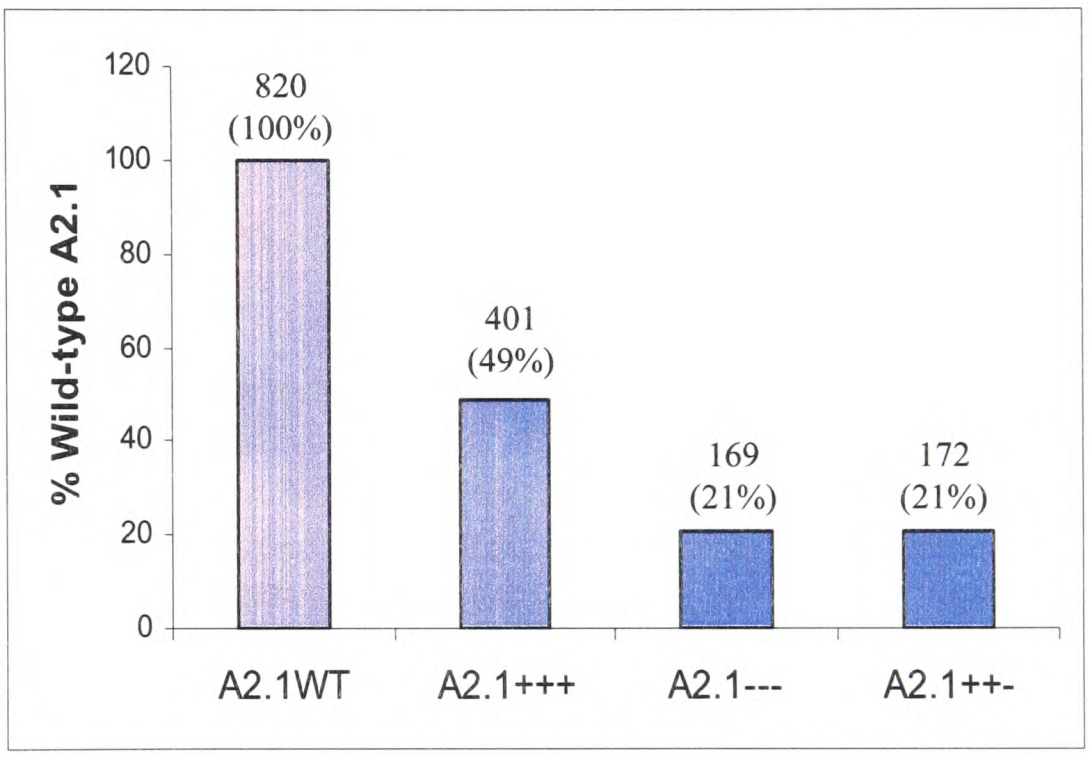

Figure 5.3.1 Expression of MHC class I molecules with altered glycosylation in the heavy chain expressed in C1R cells

a) Cell surface expression of A2.1 heavy chain (HC) glycosylation mutants (see text for explanation of the different HC glycosylations in A2.1) expressed in C1R cells was determined by flow cytometry using monoclonal antibody BB7.2. b) Histogram showing the expression of A2.1 glycosylation mutants on the cell-surface compared as a percentage of that expressed in the wild-type A2.1. The actual mean fluorescence value is indicated above individual bars and the percentage of surface expression compared to the wild-type A2.1 is given in parenthesis above individual bars. Glycosylation mutant A2.1^{-+-} was probably not translated (or transcribed) and was not investigated further.

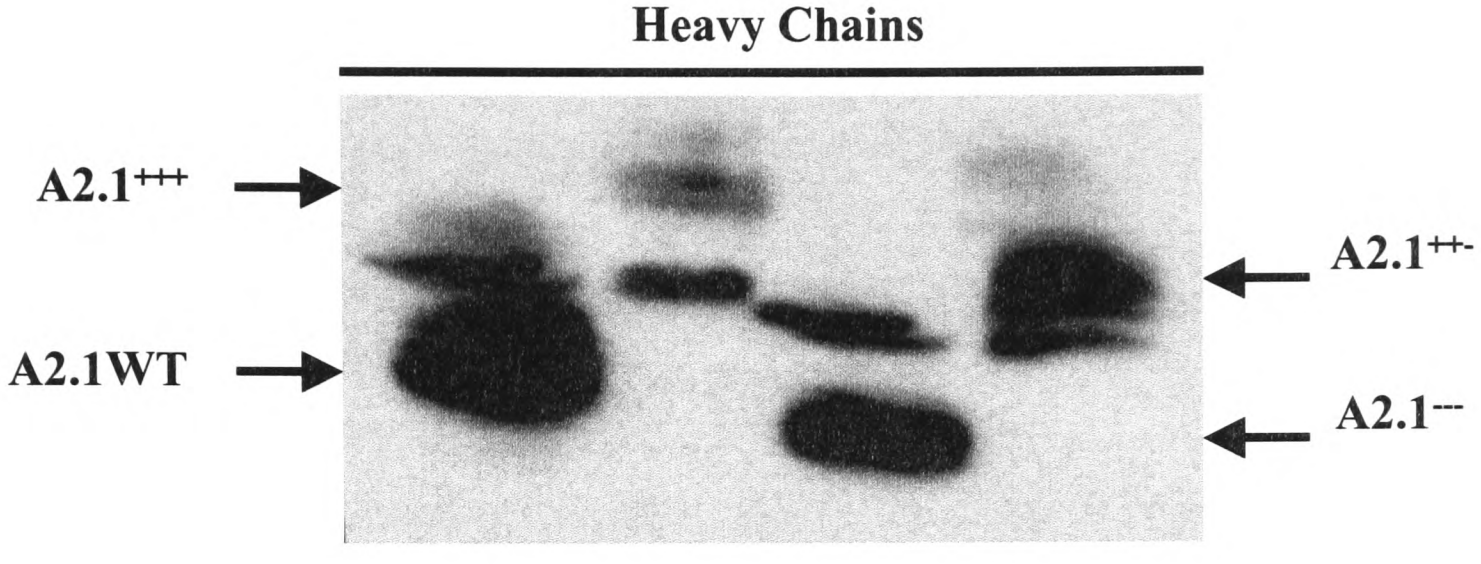

Figure 5.3.1c Expression of the glycosylation mutants in C1R cells

Expression of class I heavy chains with altered glycosylations was detected by western blot using HC10 anti-sera, which recognises heavy chains of A2.1 molecules. The non-specific bands seen may represent some cross reactivity of HCA2 with other proteins in the lysates. There is also some indication of the slight movement of the autoradiograph during exposure.

expression is only slightly reduced in the aglycosylated mutant compared to the wild type. The slight lower recovery of the mutant heavy chain suggests that either the steady-state degradation rate of the mutant is higher compared to wild-type A2.1 or that there is lower transcriptional/ translational turnover of these mutants in C1R cells. In any case, the results demonstrate that the cell surface expression of the aglycosylated mutant is downregulated despite the amount of heavy chain synthesised being roughly the same.

5.3.2 Cell surface expression of di- and tri- glycosylated A2.1

Flow cytometric analysis using BB7.2 antibody on C1R cells transfected with $A2.1^{-+-}$ showed that glycosylation at position 176 reduced cell surface expression by more than 95% compared to wild-type A2.1 (figure 5.3.1a-b). Moreover, the heavy chain for this mutant was barely detectable on the western blot using HCA2 antibody. It is possible that reduced cell surface expression was a result of very poor $A2.1^{-+-}$ HC expression (poor translation or transcription) and was not investigated further.

I transfected C1R cells with $A2.1^{++-}$ and determined cell surface expression of $A2.1^{++-}$ on these cells by flow cytometry using BB7.2. The results show $A2.1^{++-}$ expression was about 25% compared to the wild type molecules (figure 5.3.1a-b). Western blot was carried out to determine the level of overall expression of $A2.1^{++-}$ molecules in C1R cells. Figure 5.3.1c shows that comparable amount of HCA2 reactive material is recovered from C1R cells transfected with either wild type A2.1 heavy chain or $A2.1^{++-}$ heavy chain.

Next, I looked at the phenotype of MHC class I in situation where the heavy chain is tri-glycosylated (at positions 86, 176 and 256) as is the case with some heavy chain alleles in mouse (e.g., H2-K^d, H2-D^b, H2-L^d). Cell surface expression of A2.1^{+++} was determined by flow-cytometry using BB7.2. As shown in figure 5.3.1a-b, addition of two extra glycosylation sites in A2.1 also resulted in the reduction in cell surface expression of class I by almost 50% compared to the wild-type A2.1. Compared to the other glycosylation mutants, A2.1^{+++} surface expression was the highest. However, western blot using mouse monoclonal HCA2 antibody showed that overall expression of A2.1^{+++} heavy chain is reduced (5.3.1c). This may be because the carbohydrate at position 256 affects HCA2 recognition of heavy chain or that A2.1^{+++} is poorly synthesised in the clone.

The reason for the appearance of the non-specific bands is not clear and may represent some cross reactivity of HCA2 with other proteins in the lysates. There is also some indication of the slight movement of the autoradiograph during exposure.

5.4 ASSEMBLY OF A2.1 GLYCOSYLATION MUTANTS

One possible reason for low cell surface expression of A2.1 glycosylation mutants compared to the wild type class I in C1R cells is that the former are less stable at steady state condition and when they reach the cell surface, they "fall apart". In order to assess stability on the cell surface, I looked at the rate of decay of class I molecules from the cell surface.

5.4.1 Glycosylation mutants are unstable at the cell surface

Treatment of C1R cells with the fungal metabolite Brefeldin A (BFA) causes the Golgi complex to collapse into the ER. Typically, 10μM BFA can be used to block egress of class I molecules from the ER. C1R cells expressing wild type and glycosylation A2.1 mutants were treated with BFA for different times and the presence of stable class I was determined by flow-cytometry using BB7.2. As shown in figure 5.4.1a-b, the initial rate of decay for glycosylation mutants is much higher than the wild type A2.1. Less than 10% of the total cell surface molecules are lost from the cell surface in the first five hours of BFA treatment for wild type molecules whereas almost 50% of A2.1 glycosylation mutants disappear from the cell surface during the same treatment time (40% for $A2.1^{+++}$, 42% for $A2.1^{---}$ and 46% for $A2.1^{++-}$).

It can be speculated from figure 5.4.1a-b that there may be greater proportion of glycosylation mutants binding to peptides with higher off-rate (k_{off}) compared to the wild-type (biphasic nature of the curve). A proportion of glycosylation mutants decay at a much faster rate compared wild-type A2.1 molecules. In any case, the results demonstrate that altering the glycosylation pattern in A2.1 reduces their stability on C1R cell surface and once again emphasises the fact that glycosylation is optimal for A2.1 in C1R cells. There are several factors, which may contribute to the instability of the glycosylation mutant molecules on the cell surface. For example, glycosylation mutant molecules may fail to interact or interact less productively with protein factors either en route to the cell surface or at the cell surface. In addition, glycosylation mutant molecules may fail to get loaded with peptides in the ER and be exported in a peptide receptive state, which then "fall apart" at the cell surface.

a

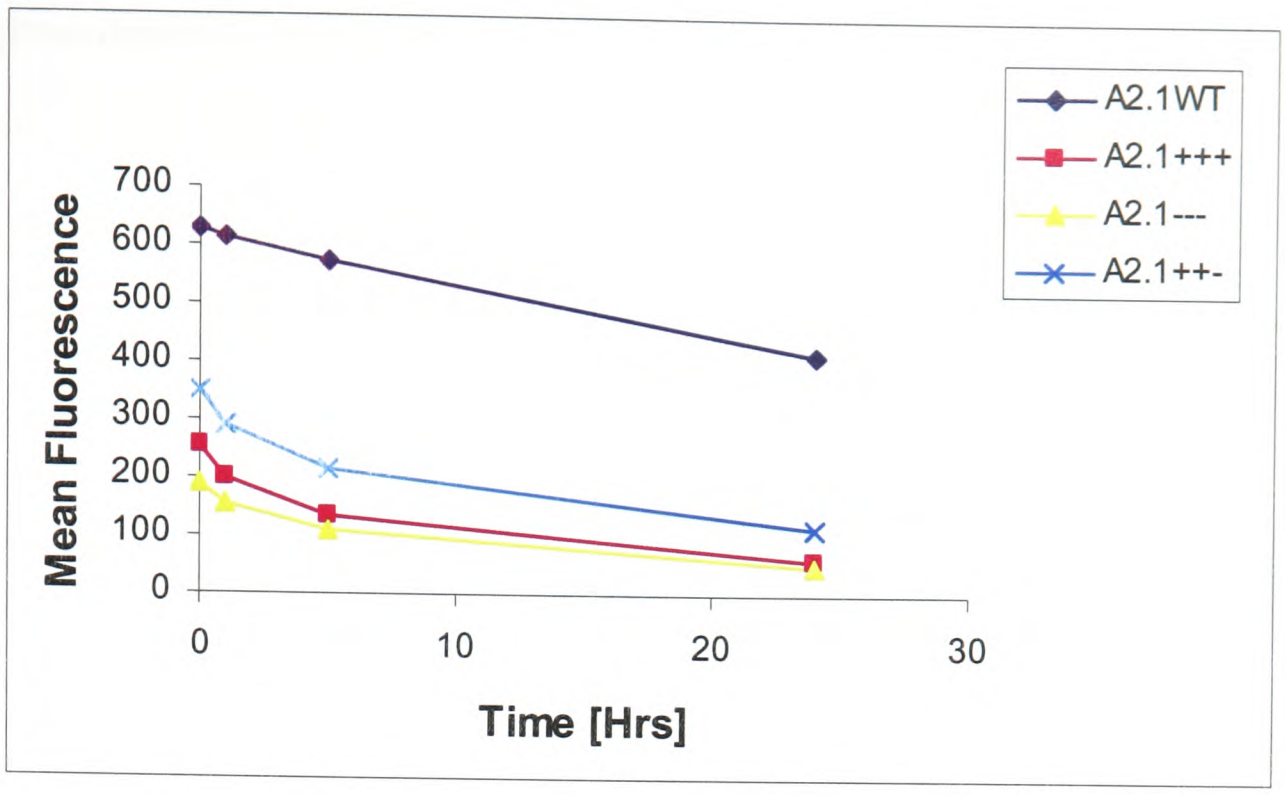

b

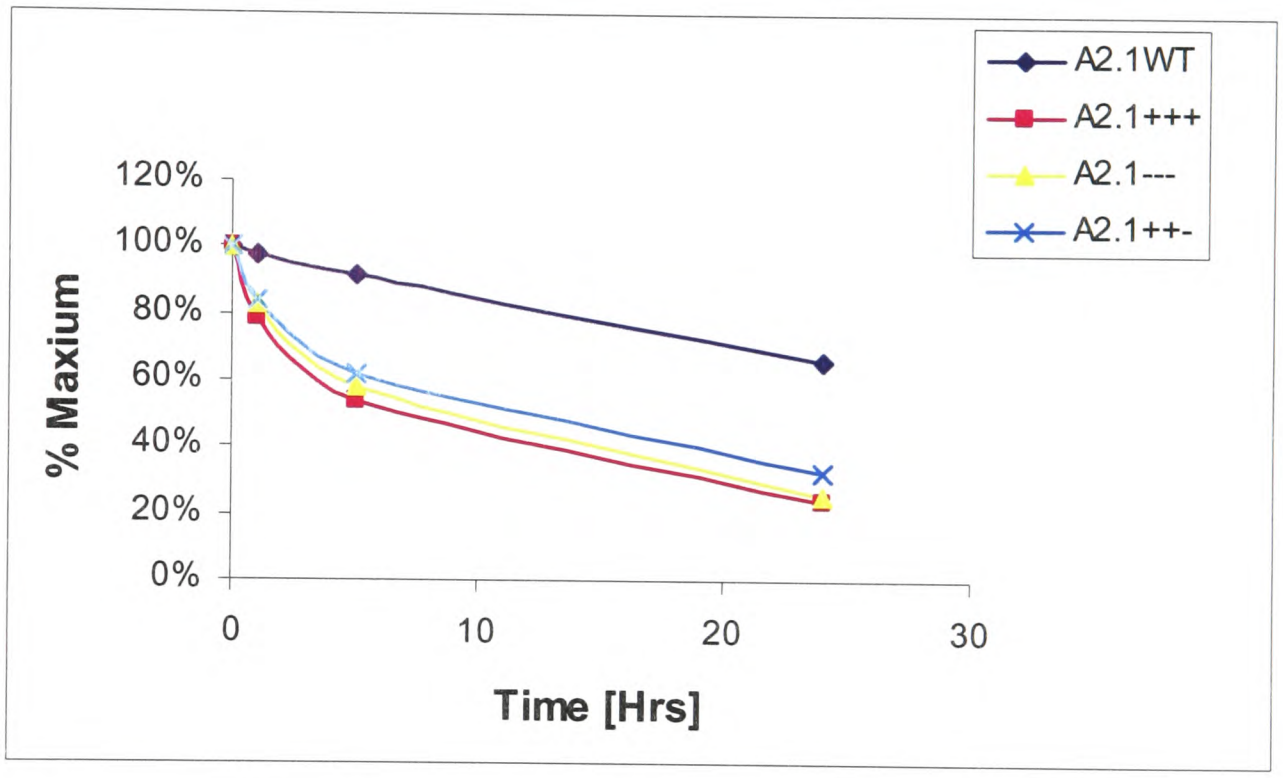

Figure 5.4.1 Glycosylation mutants are unstable at the cell surface

a) C1R cells expressing different glycosylation mutants were treated with 10μM Brefeldin A (BFA) for different times as indicated and the decay of class I cell surface expression was measured by flow cytometry using mAb BB7.2. b) Amount of class I molecules at the cell-surface at a given time point expressed as a percentage of class I molecules on the cell surface at time zero when BFA was just added.

5.4.2 A2.1 glycosylation mutants have loading defect

In order to confirm that A2.1 glycosylation mutants are indeed unstable at the cell surface, I incubated C1R cells expressing wild type or $A2.1^{---}$ or $A2.1^{+++}$ class I molecules with excess of influenza matrix protein derived epitope GILGFVFTL and compared the surface expression of these class I molecules by flow cytometry. As shown in figure 5.4.2a-b, in the absence of exogenous stabilising peptide, the glycosylation mutants only expressed 10-15% of wild-type alleles. However, in the presence of stabilising peptide, there was a big increase in the level of staining and the increase in cell surface expression ranged from 4.11 to 7.21 -fold increase in C1R-$A2.1^{+++}$ and C1R-$A2.1^{---}$, respectively, and a 1.04-fold increase in C1R-A2.1 (figure 5.4.2b). These results clearly demonstrate loading defect in A2.1 glycosylation mutants. This result also suggests that low $A2.1^{+++}$ heavy chain detection by HCA2 on a western blot may partly be a result of blocking of HCA2 epitope by the carbohydrate moiety at position 256.

5.4.3 Glycosylation mutants associate with the TAP loading complex

One important factor which affects the stability of class I molecules on the cell surface is assembly of heavy chain with β2-m and subsequent loading with optimal peptides. Binding of optimal peptides is the final event in the formation of an intact and stable class I complex. Optimal peptide binding normally occurs when class I is in complex with the cofactors of the peptide loading complex which include TAP and calreticulin [162]. Therefore, I determined whether $A2.1^{---}$, $A2.1^{++-}$ and $A2.1^{++-}$ can still associate with TAP. I also asked whether additional glycosylation in A2.1 ($A2.1^{+++}$, $A2.1^{++-}$) increased binding to calnexin.

a

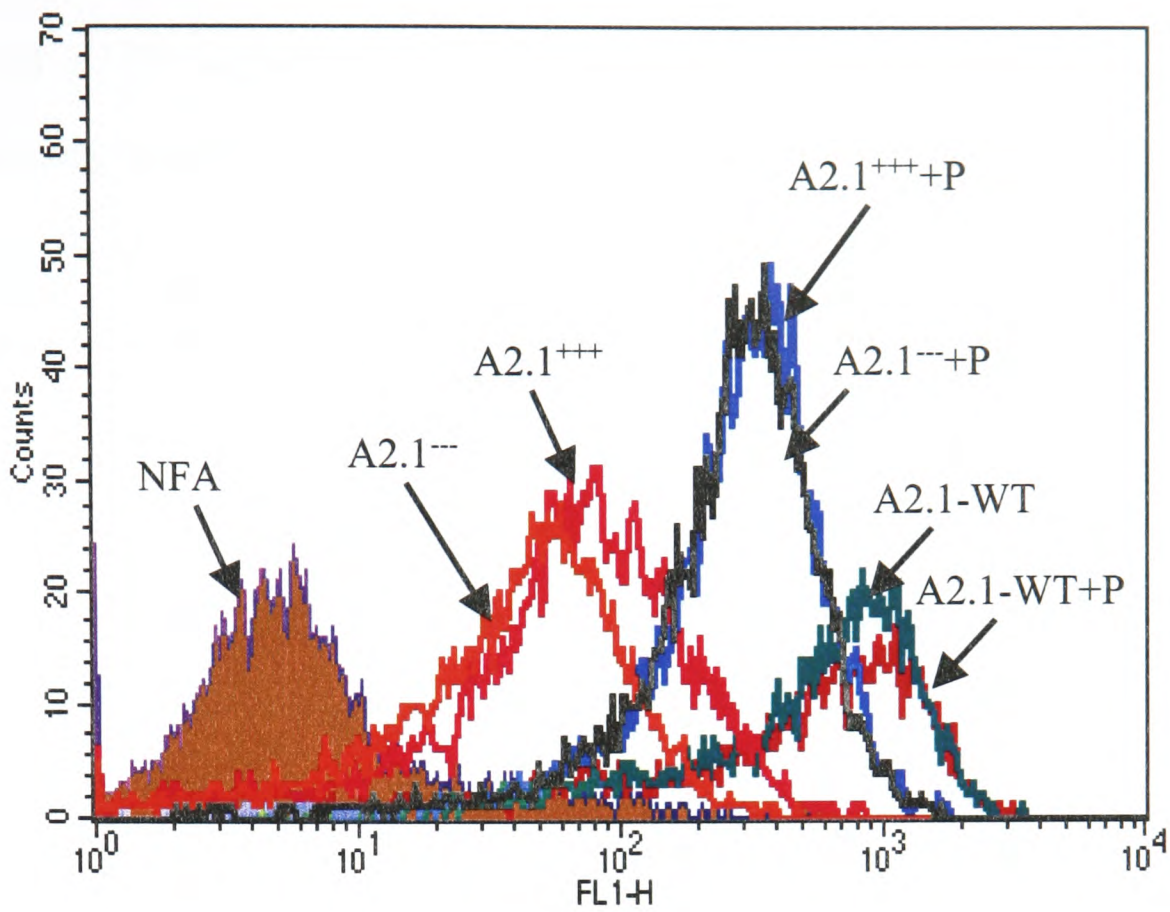

b

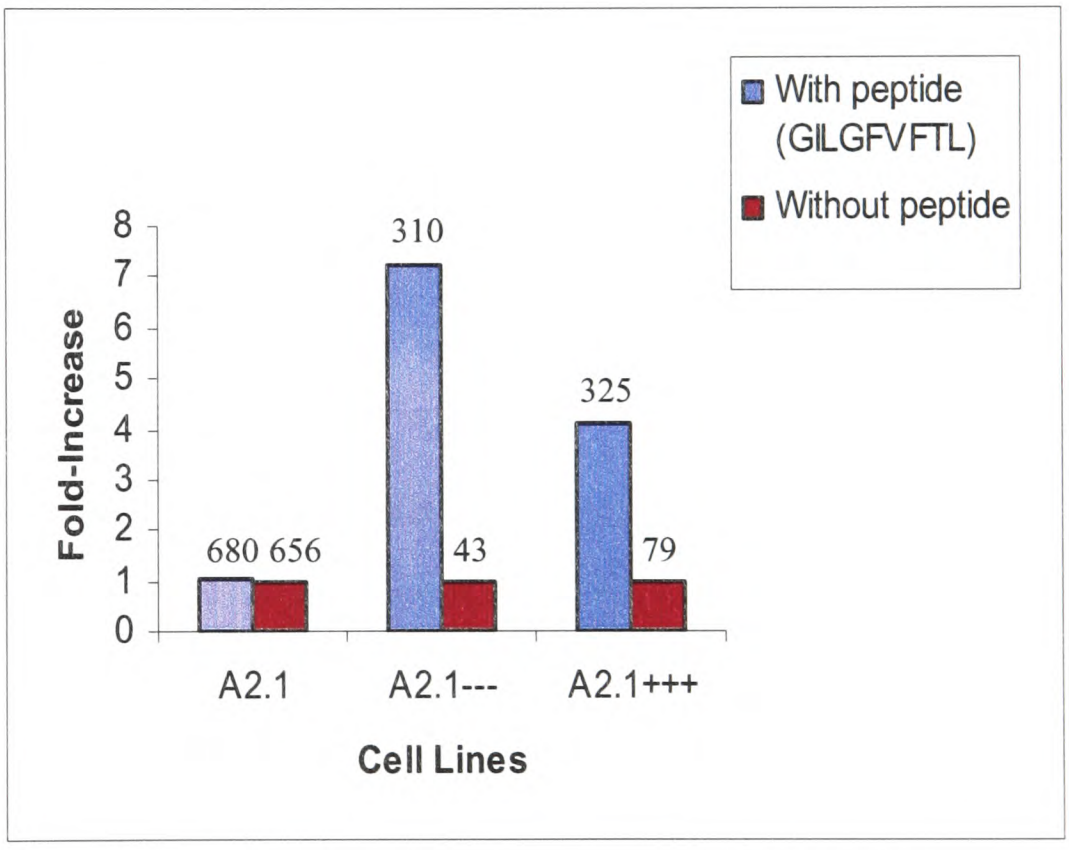

Figure 5.4.2 Glycosylation mutants have a loading defect

a) C1R expressing the glycosylation mutants were incubated in the presence or in the absence of A2.1-binding peptide GILGFVFTL, and cell-surface expression determined by flow cytometry using mAb BB7.2. b) Results are shown as the fractional increase in expression in the presence of peptides. Actual mean fluorescence level is shown above individual bars.

An equal number of C1R cells expressing wild type and glycosylation A2.1 mutant proteins were lysed in 1% digitonin lysis buffer to maintain association between cofactors of the loading complex. The lysates were immunoprecipitated with rabbit anti-TAP antibody. Following co-immunoprecipitation, TAP – associated material was eluted from protein A beads. The individual proteins associated with TAP were immunoblotted with HCA2 antibody, which reacts with A2.1 HC.

The results are shown in figure 5.4.3 and demonstrate that the glycosylation mutants still interact with the TAP complex. It is difficult to say whether the proportion of $A2.1^{---}$, $A2.1^{++-}$ and $A2.1^{+++}$ associated with the TAP complex is lower compared to the wild type. However, if equal amount of class I HC is synthesised in C1R expressing the glycosylation mutants compared to the wild-type A2.1 (figure 5.3.1bc), it is apparent that lower amount of A2.1 glycosylation mutants associate with the TAP complex. The fact that $A2.1^{---}$ co-immunoprecipitates in this experiment clearly demonstrates that glycosylation is not absolutely essential for incorporation into the TAP complex.

The fact that $A2.1^{---}$ is found in the TAP loading complex contradicts earlier reports suggesting no TAP and calreticulin association to class I in the presence of drugs that block either glycosylation (tunicamycin) or terminal glucose trimming (castanospermine) [162, 294, 332]. However, it is to be noted that the drugs used in these experiments affect processing of all glycosyl moieties of all proteins and therefore is not specific for just class I. For example, castanospermine may affect tapasin glycosylation and may in turn affect class I interaction with the TAP complex.

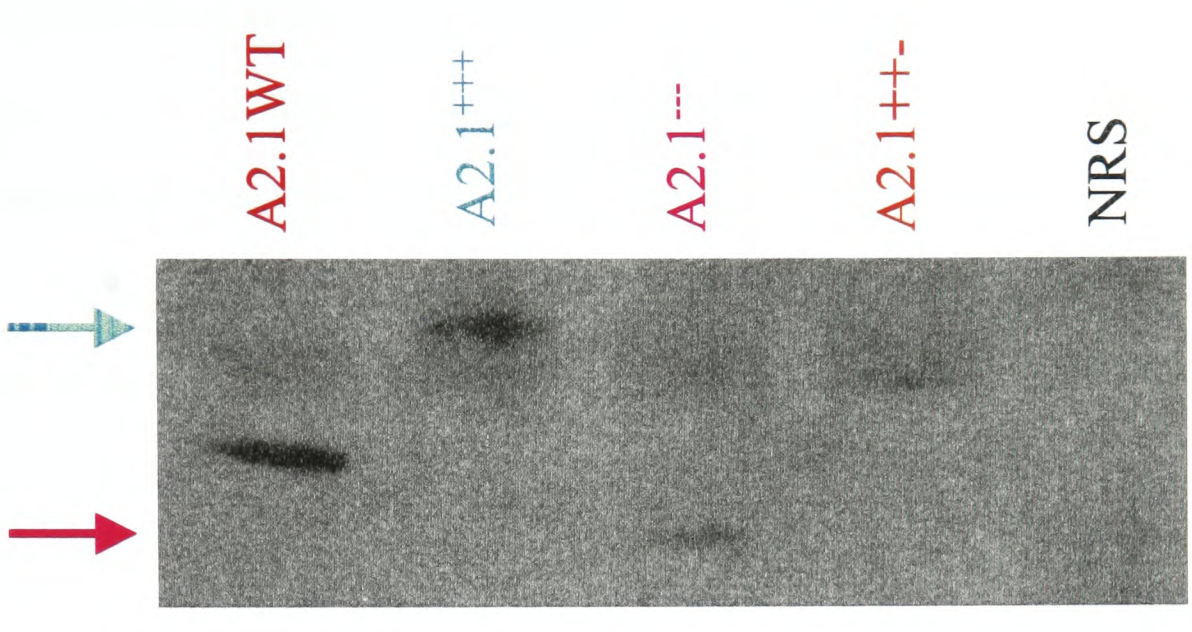

Figure 5.4.3 Glycosylation mutants associate with TAP

Immunoprecipitates of TAP and associated proteins were made from C1R cells expressing different glycosylation mutants, fractionated by SDS-PAGE, and immunoblotted with HCA2, which recognises MHC class I heavy chain (HC). As control, immunoprecipitate of normal rabbit serum (NRS) was made from C1R cells expressing wild-type A2.1, fractionated by SDS-PAGE, and immunoblotted with HCA2. The positions of the HC bands are indicated by coloured arrows.

Moreover, these studies did not use the technique I have used, i.e., co-immunoprecipitation followed by western blot, which is more sensitive.

Human class I molecules associate only transiently with calnexin. While some studies have managed to isolate class I heavy chain in anti-calnexin immunoprecipitate complex, others have failed to so. Using the system described above, I could not detect any A2.1 heavy chain (wild type or glycosylation mutants) in anti-calnexin immunoprecipitates (data not shown). Zhang and Salter, using CHAPS detergent to lyse the cells, managed to show prolonged interaction of $A2.1^{++-}$ with calnexin [286]. However, using digitonin lysis buffer, I could not detect any $A2.1^{++-}$ or $A2.1^{+++}$ heavy chains in anti-calnexin precipitates.

These results demonstrate that glycosylation is not essential for incorporation into the TAP loading complex. It is however, possible that fewer glycosylation mutants are incorporated into the TAP complex.

5.4.4 Existence of a greater proportion of non-transported subpopulation of $A2.1^{+++}$ molecules

Next, I did a pulse-chase analysis to determine the efficiency of $A2.1^{+++}$ heavy chain assembly with β2m and subsequent transport through the Golgi. Following a short period of radiolabeling, cells were incubated for the indicated times in nonradioactive medium before lysis and BB7.2 was used to isolate β2m-associated class I heavy chains. As shown in figure 5.4.4a-b, the entire cohort of wild-type A2.1 molecules exit the ER quickly (t1/2 = 20 min) after assembly with β2m. In contrast, although rate of exit from the ER seems to be the same for $A2.1^{+++}$, only about 20% of the total seem to get out. The remaining are retained in the ER for at least two hours or

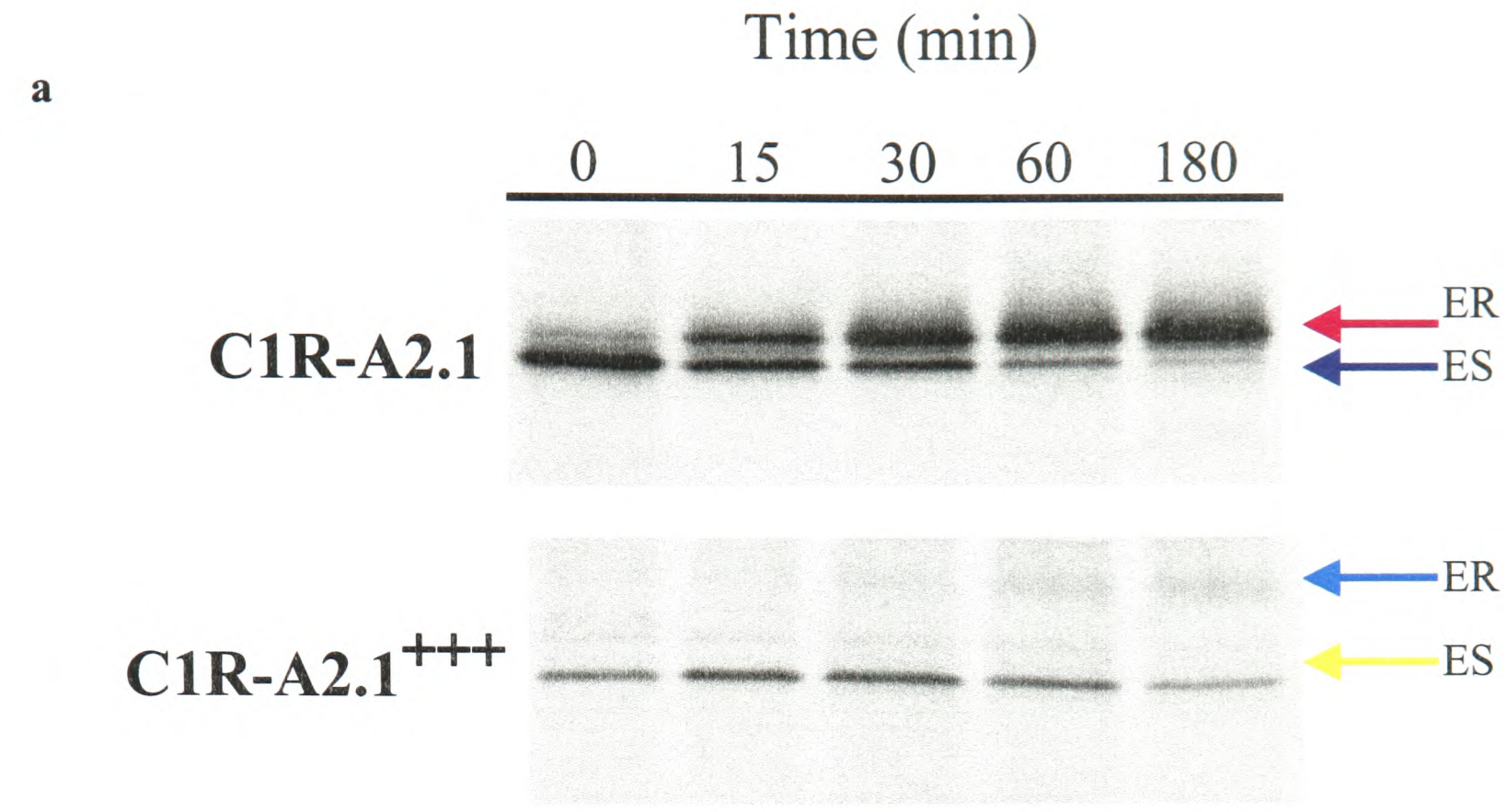

Figure 5.4.4 Existence of greater proportion of non-transported subpopulation of A2.1^{+++} molecules.

a) Pulse-chase analysis was carried out on A2.1 and A2.1^{+++} molecules expressed in C1R cells. Aliquotes of labelled cells were lysed at the time point shown. Immunoprecipitates recognised by BB7.2 were digested with endoglycosidase H (Endo-H), fractionated by SDS-PAGE, and the heavy chain band quantified by Quatity One software (BioRad Inc, USA). b) The intensities of the endo H-sensitive (ES) and Endo H-resistant (ER) heavy chain bands of A2.1 and A2.1^{+++} were plotted against time.c) 2x10^7 C1R expressing either A2.1 or A2.1^{+++} and C1R transfected with vector (pCDNA3) alone were labelled for 30 minutes and immunoprecipitated with mAb BB7.2. Half of the immunoprecipitate was digested with Endo-H. Wild-type A2.1 genomic DNA was used to transfect C1R cells and may contribute to unusual bands seen in immunoprecipitates of the lysates of these cells

possibly more. The fact that the ER resident subpopulation of $A2.1^{+++}$ reacted with BB7.2 suggests that these molecules are associated with β2m.

Together, these experiments demonstrate that $A2.1^{+++}$ molecules are heterogeneous in phenotype, with a small proportion acquiring peptides in the ER and passing through the Golgi, while the majority remain in the ER in a transport-incompetent state, probably due to their failure to load with optimal peptides.

Pulse chase analysis, similar to the one described above, could not be performed for $A2.1^{---}$ molecule. However, an acid strip assay was exploited to look at the trafficking rate for $A2.1^{---}$. The idea is to acid strip all class I molecules from the cell surface and then look at the rate of appearance of new class I molecules using flow cytometry.

5.4.5 Glycosylation mutants appear on the cell surface at a similar rate to wild type A2.1 molecules

C1R cells expressing different glycosylation mutants were subjected to HCl-Phosphate buffer pH3.0 treatment for 90 seconds. The cells were quenched in excess of media followed by several washes. Aliquots of cells were taken at various time points and cell surface expression of A2.1 wild type and glycosylation mutants determined by flow-cytometry using BB7.2 antibody. As shown in figure 5.4.5a-b, the rate at which the glycosylation mutant A2.1 molecules appear at the cell surface is comparable to the appearance of wild type A2.1 at the cell surface. If anything, glycosylation mutant A2.1 molecules appear at a slightly higher rate than the wild type molecules. Almost 95% of surface class I molecules are lost from the surface upon acid treatment. Class I molecules recover on the cell surface after one hour. The

a.

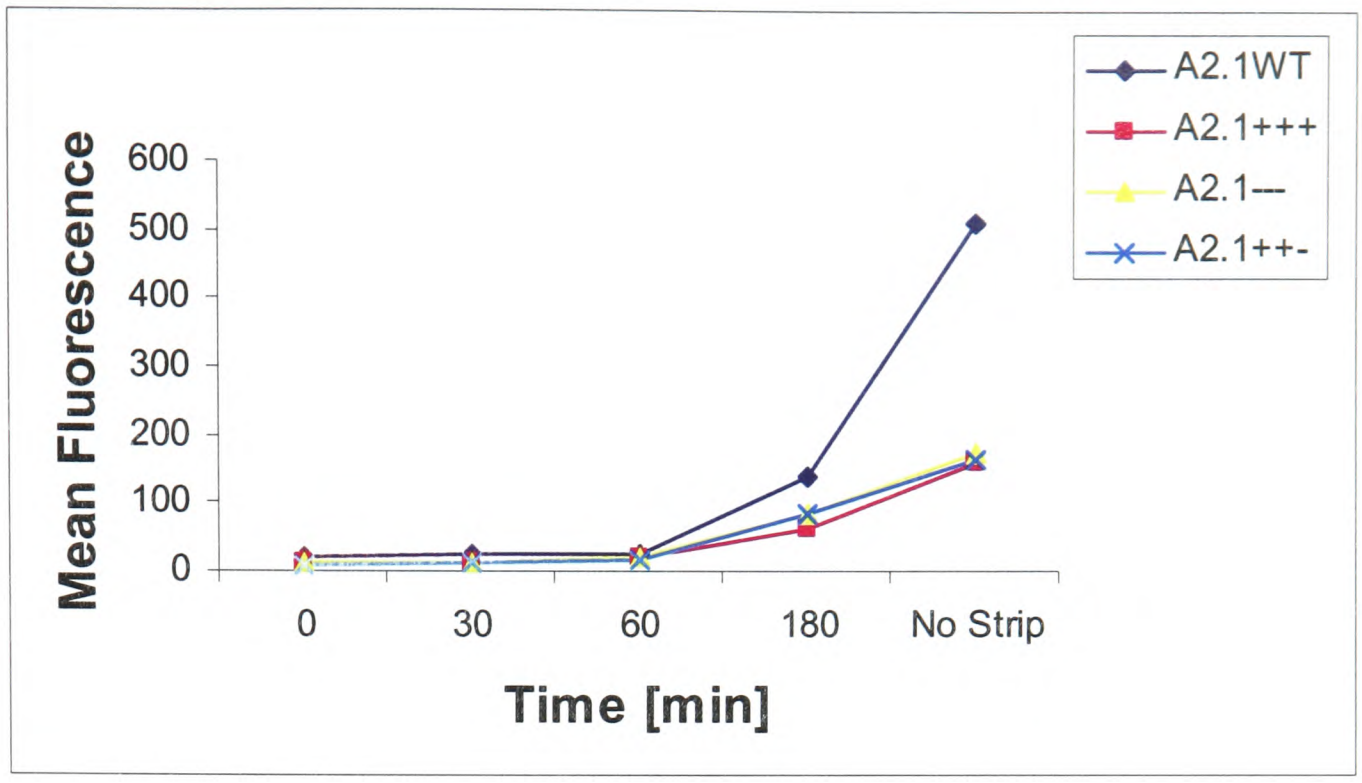

b.

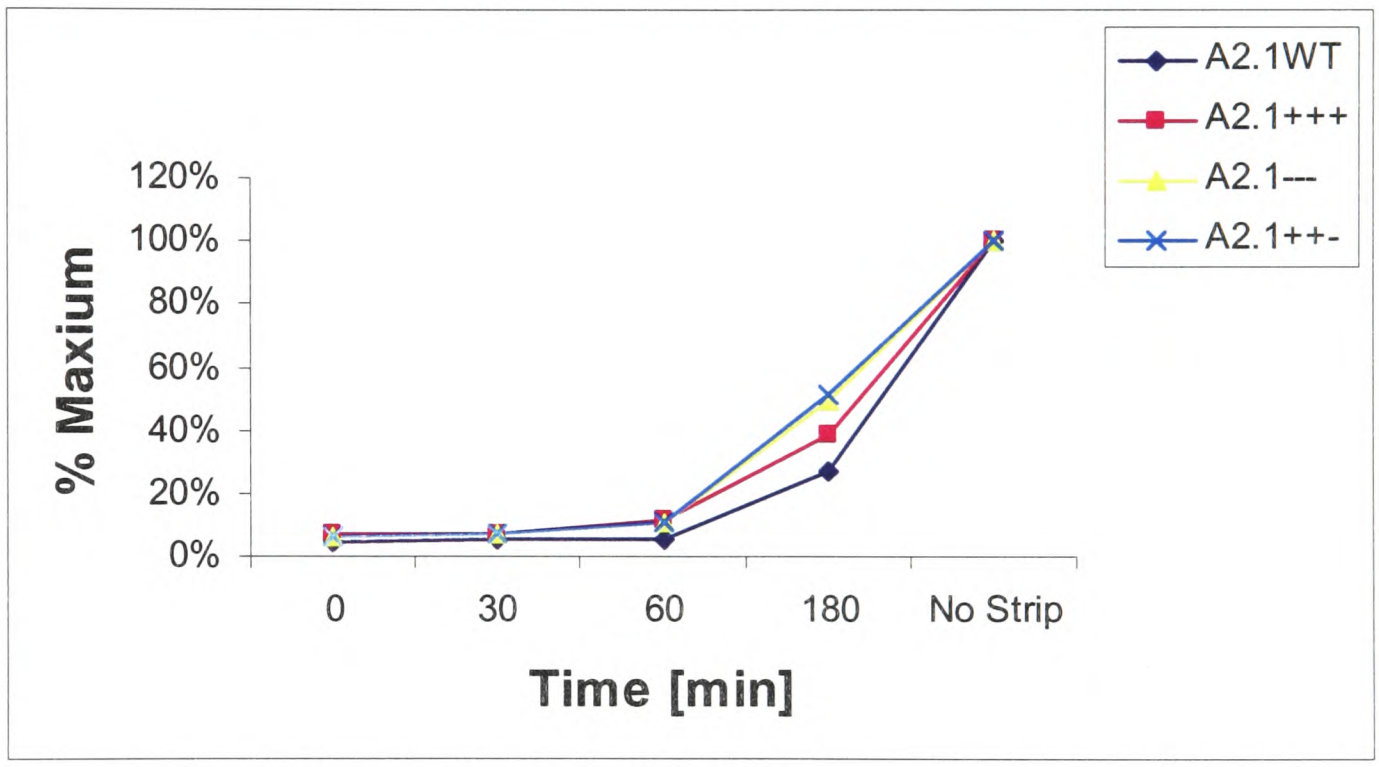

Figure 5.4.5 Glycosylation mutants appear on the cell surface at a similar rate to wild type A2.1 molecules

C1R cells expressing different glycosylation mutants were subjected to pH3.0 acid treatment for 90 seconds. Aliquots of cells were taken at various time points and cell surface expression of A2.1 wild type and glycosylation mutants determined by flow-cytometry using BB7.2 antibody. a) Appearance of class I molecules at the cell surface after acid treatment expressed as mean channel fluorescence. b) Rate of appearance of class I molecules at the cell-surface determined as a percentage by comparing surface expression of class I at given time point with that obtained when cells were not acid-stripped. No Strip, no acid treatment of cells.

initial delay in the cell surface appearance of class I molecules may represent recovery time for cells after acid shock or the limit of BB7.2 sensitivity.

Acid strip results are consistent with the pulse chase analysis described for A2.1^{+++} where mutant molecules acquire Endo H resistance at a similar time as the wild type A2.1 although the number of Endo H resistant wild type molecules is far more at any time compared to the hyperglycosylated A2.1^{+++} mutant molecules. This is again reflected in the flow cytometry profile where we see much more class I at the cell surface for wild type compared to the glycosylation mutants.

5.5 ANTIGEN PRESENTATION BY A2.1 GLYCOSYLATION MUTANTS

To determine the extent to which the differential glycosylation in A2.1 affected the presentation of epitopes at the cell surface, I assessed the presentation of Influenza (A/Japan/305/57) matrix protein derived epitope GILGFVFTL in influenza infected C1R clones expressing different A2.1 glycosylation mutants. Enzyme-linked ImmunoSPOT (ELISPOT) technique was used to assay antigen presentation. ELISPOT is sensitive and allows quantitation of cytokine secretion on a per cell basis.

The results are shown in Figure 5.5. Figure 5.5a and 5.5b show that A2.1 restricted influenza matrix protein derived epitope GILGFVFTL, was presented equally well by both C1R A2.1 and C1R A2.1^{---} following infection with influenza. The result was consistent over two separate CTL concentrations tested. Moreover, presentation of the synthetic matrix peptide epitope was good for both types of cell lines over a range of peptide concentrations (10^{-8} to 10^{-6} M).

a

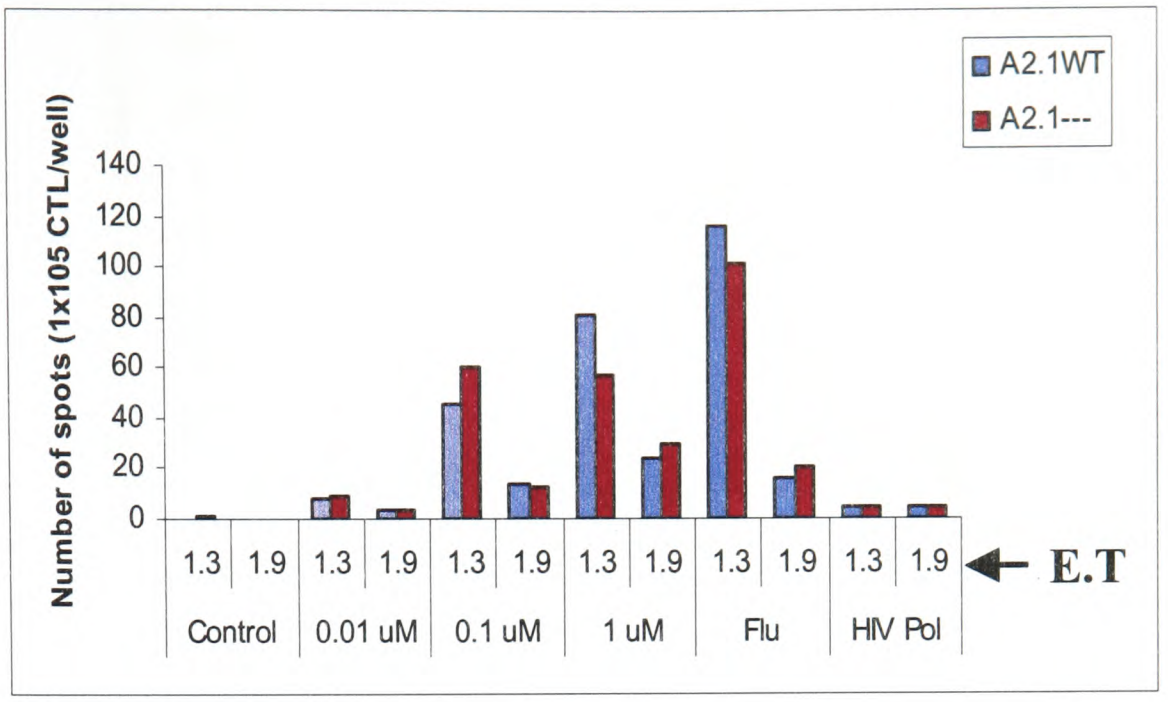

b

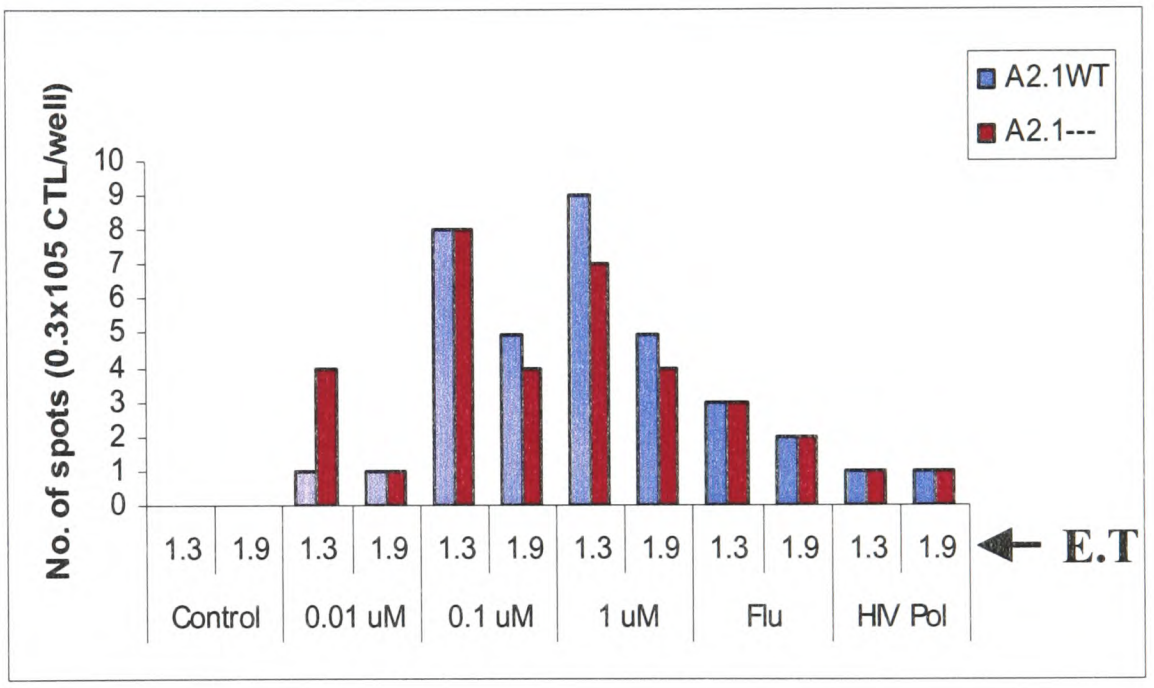

Figure 5.5 Antigen presentation by A2.1^{---}

Recognition of A2.1-restricted Influenza matrix protein epitope GILGFVFTL by cytotoxic T lymphocytes (CTLs) following infection of C1R cells expressing either wild-type A2.1 or glycosylation mutant A2.1^{---} with influenza (flu) (A/Japan/305/57) measured in an ELISPOT assay. Recognition of C1R cells expressing either wild-type A2.1 or A2.1^{---} pulsed with various concentrations of influenza matrix protein derived epitope GILGFVFTL or HIV-pol derived epitope ILKEPVHGV (20μM) are also shown as controls. E.T, effector to target ratio. The experiment was carried out using either 1x10^5 CTLs per well (a) or with 0.3x10^5 CTLs per well (b).

c

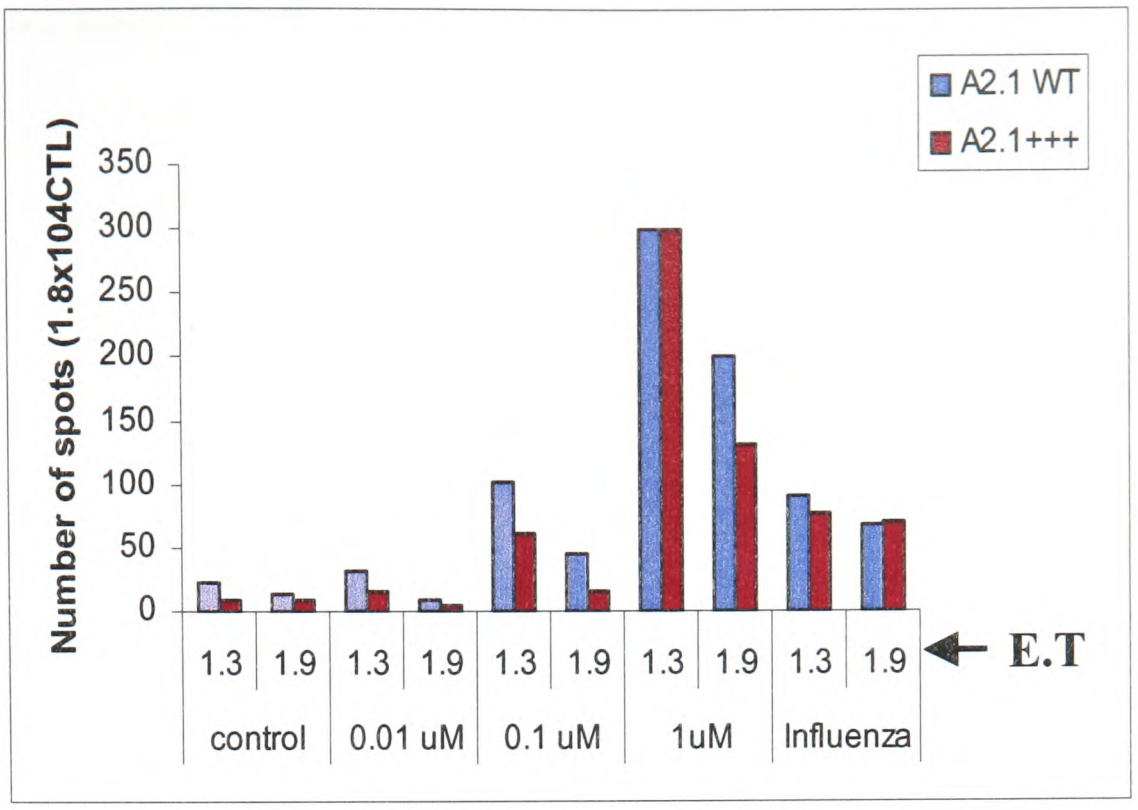

d

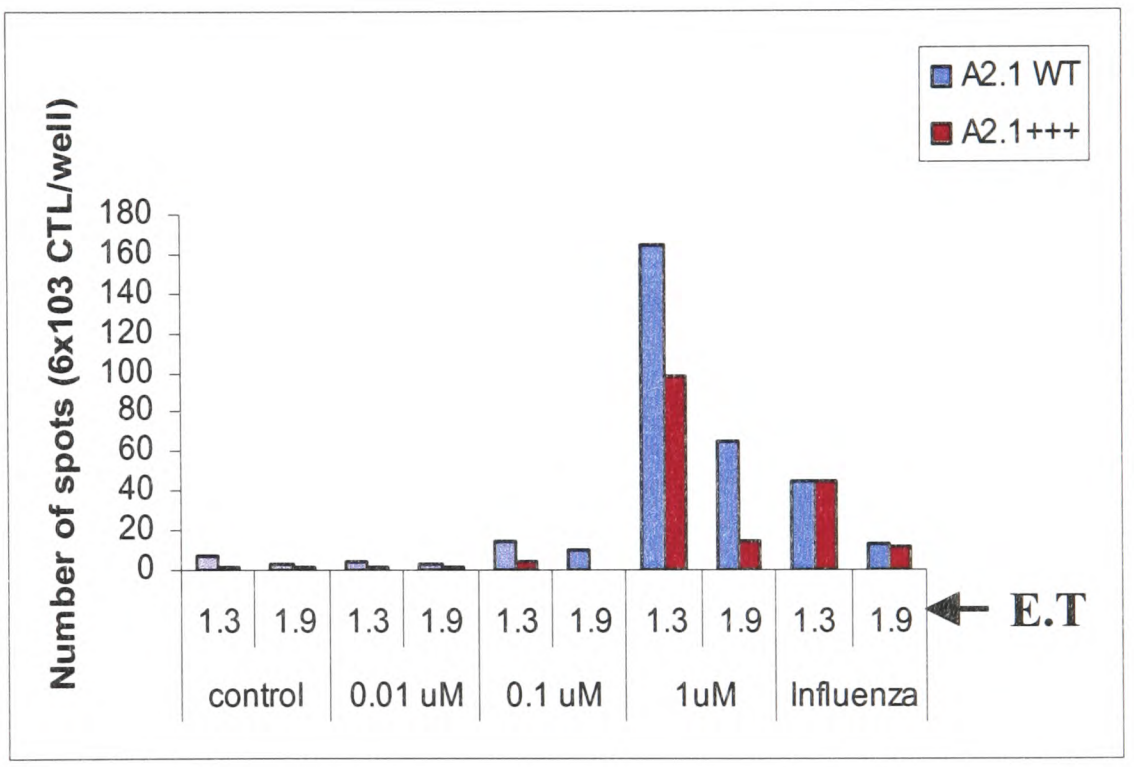

Figure 5.5 (contd.) Antigen presentation by $A2.1^{+++}$

Recognition of A2.1-restricted Influenza matrix protein epitope GILGFVFTL by cytotoxic T lymphocytes (CTLs) following infection of C1R cells expressing either wild-type A2.1 or glycosylation mutant $A2.1^{+++}$ with influenza measured in an ELISPOT assay. Recognition of C1R cells expressing either wild-type A2.1 or $A2.1^{+++}$ pulsed with various concentrations of GILGFVFTL or HIV-pol derived epitope ILKEPVHGV (20μM) are also shown as controls. E:T, effector to target ratio. The experiment was carried out using either $1.8x10^4$ CTLs per well (c) or with $6x10^3$ CTLs per well (d).

Similarly, when C1R cells expressing wild type A2.1 and A2.1^{+++} were infected with Influenza virus (A/Japan/305/57), both were able to process endogenous matrix protein and to be recognised by matrix peptide specific CTL (figure 5.5c and 5.5d). In addition, both cell lines efficiently presented exogenously supplied synthetic matrix peptide epitope. It was observed C1R A2.1 wild type presentation of synthetic peptide was slightly better than C1R A2.1^{---} at lower CTL concentration ($6x10^3$ CTL/well).

Overall the results suggest that absence or alteration of glycosylation in A2.1 does not significantly influence the processing and presentation of the influenza matrix protein derived epitope GILGFVFTL to A2.1 restricted CTL, nor the presentation of exogenous synthetic matrix peptide. Hyperglycosylated C1R A2.1^{+++} presented both endogenous and exogenous supply of matrix peptide epitope as well as the wild type A2.1. Similarly, nonglycosylated A2.1 expressed in C1R was also not impaired in its ability to present both exogenous and endogenous supply of influenza matrix peptide epitope. Presentation was specific for influenza matrix peptide epitope, as exogenous supply of HIV Pol peptide did not elicit IFN-γ release.

These results, however, should be interpreted with some caution as antigen presentation of a highly immunodominant epitope is a crude readout to generalise the role of glycosylation in antigen presentation. It is possible there may be important defects in presentation that may not be evident when looking at just a few immunodominant epitopes.

5.6 NON-GLYCOSYLATED HEAVY CHAIN BINDS TO LECTIN CHAPERONE CALRETICULIN

Identification of nonglycosylated class I molecules in TAP immunoprecipitates suggested an interaction between calreticulin and protein moieties of class I. In order to verify this independently, I used BIAcore to detect real time interaction between calreticulin and nonglycosylated class I heavy chain:β2m heterodimer.

Briefly, BIAcore technique enables detection of biomolecules and monitoring of binding events between two or more molecules, in real time, without the use of labels. It relies on the phenomenon of surface plasmon resonance (SPR), which occurs when surface plasmon waves are excited at a metal/liquid interface (figure 5.6a). Light is directed at, and reflected from, the side of the surface not in contact with sample, and SPR causes a reduction in the reflected light intensity at a specific combination of angle and wavelength. Biomolecular binding events cause changes in the refractive index at the surface layer, which are detected as changes in the SPR signal. In general, the refractive index change for a given change of mass concentration at the surface layer, is practically the same for all proteins and peptides, and is similar for glycoproteins, lipids and nucleic acids.

During a binding analysis SPR changes occur as a solution is passed over the surface of a sensor chip. To perform an analysis, one interactant is captured on a sensor surface. The sensor surface forms one wall of a flow cell. Sample containing the other interactant(s) is injected over this surface in a precisely controlled flow. Fixed wavelength light, in a fan-shaped form, is directed at the sensor surface and biomolecular binding events are detected as changes in the particular angle where

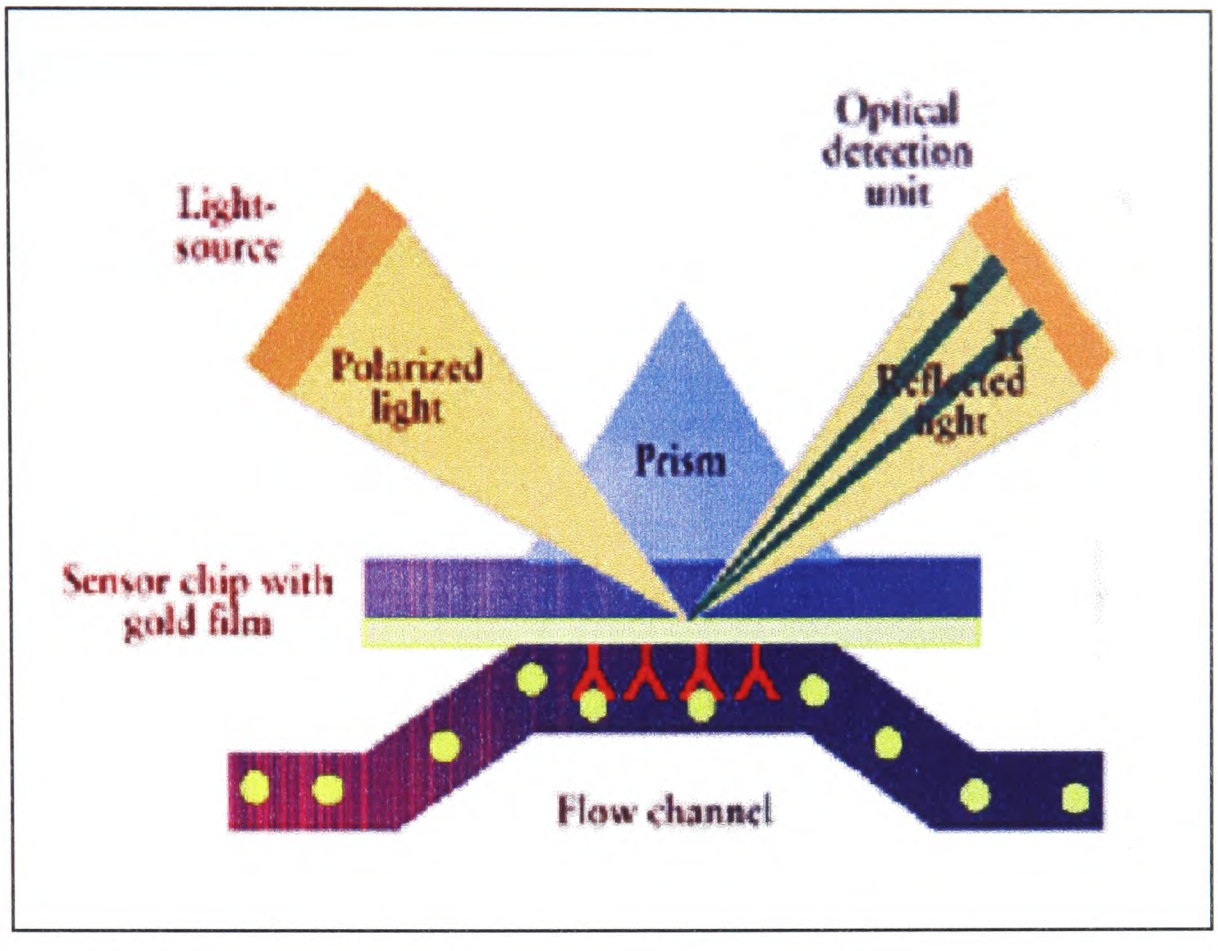

Figure 5.6a A simplified diagram showing the principles of surface plasmon resonance (SPR)

BIAcore can be used to detect real time interaction between two different proteins of interest. The technique relies on the phenomenon of SPR, which occurs when surface plasmon waves are excited at a metal/liquid interface. Receptor molecules (red) are attached to the sensor chip and ligand molecules (yellow) are injected through the flow channel. When a fixed wavelength light (polarised light), in a fan-shaped form, is directed at the sensor surface, depending on the receptor-ligand intaractions, biomolecular binding events are detected as changes in the particular angle where total internal reflection occurs. This change is measured continuously by the optical detection unit to form a graph (sensogram), which provides a complete record of the progress of association or dissociation of the interactions.

SPR creates extinction of light. This change is measured continuously to form a sensorgram, which provides a complete record of the progress of association or dissociation of the interactants.

The experimental set up and results is illustrated in table 5.6. As this experiment was not conclusive and no attempt was made to repeat the experiment, detailed experimental description can be found in appendix 5.6.

	Immobilisation of MHC class I HC:β2m:peptide	**Binding of BB7.2 to class I trimer**	**Elution of peptides (Glycine buffer pH 3)**	**CRT-Binding**	**BBM.1 Binding (after EDTA addition)**
Flow Channel-1 (*Red*)	**X**	**X**	**X**	√ (+)*	**X**
Flow Channel-2 (*Green*)	√	√	**X**	**X**	√
Flow Channel-3 (*Blue*)	√	√	√	√ (+++)	**X**
Flow Channel-4 (*Pink*)	√	√	**X**	**X**	√

*(+ Weaker binding signal
+++ Stronger binding signal)

Table 5.6

The results shown in figure 5.6b clearly indicate a very clear binding of calreticulin with MHC class I dimer in the third flow channel. As expected, calreticulin bound non-specifically to the first flow channel. The true controls were MHC class I trimer in flow channel 2 and 4. The signal for calreticulin binding was weaker than expected. The reason for low binding was probably for the following reasons: a) lowering the pH eluted peptides as well as β2m and hence actual number of HC:β2m dimers were

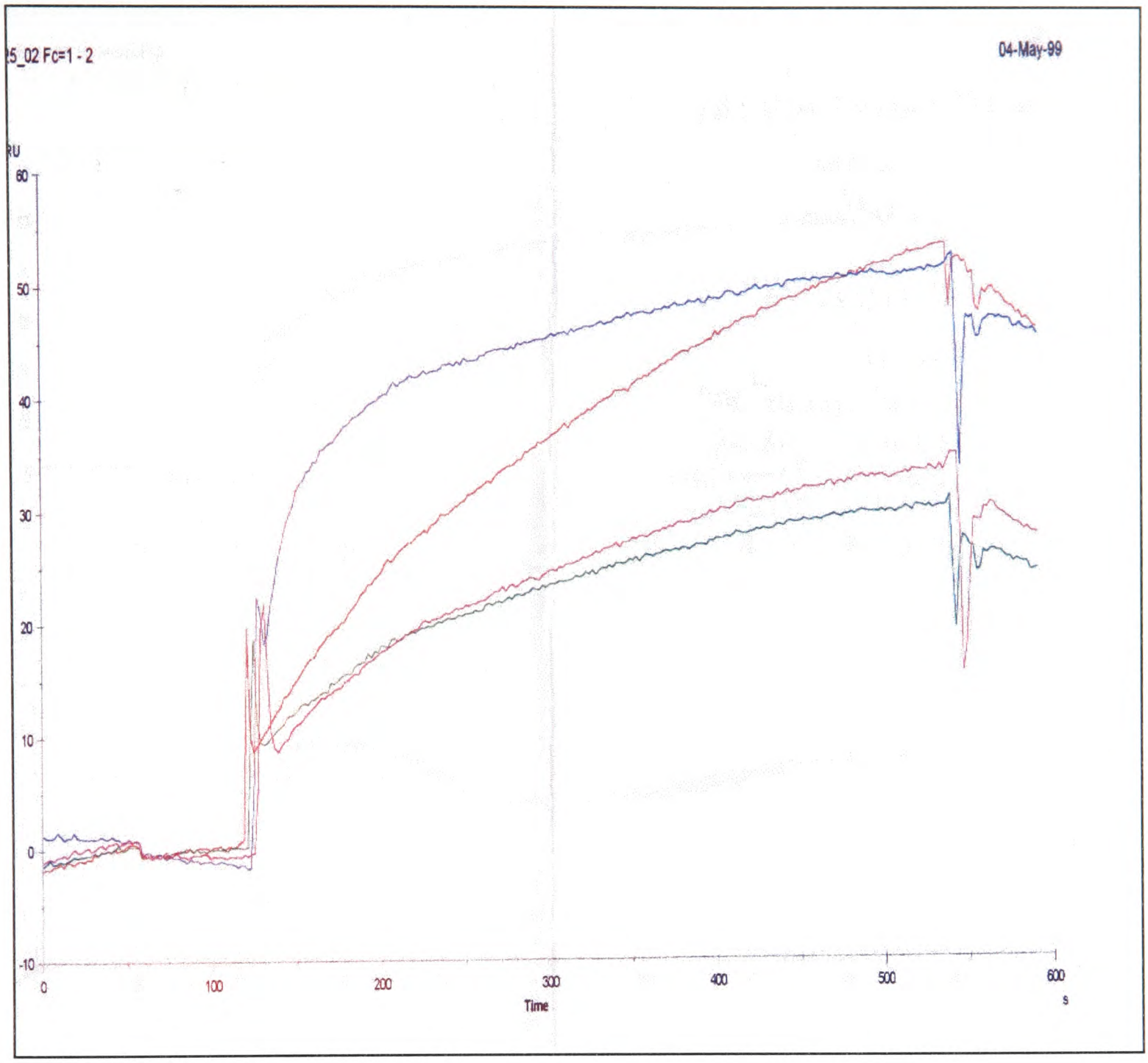

Figure 5.6b Binding of calreticulin to class I heavy chain (HC):β2m heterodimer

HLA-A2.1 heavy chains were immobilised in avidin chip in three flow channels (blue, green and pink) and folded by passing β2m and stabilising peptides. No class I HC was immobilised in the fourth flow channel (red) and was used to detect non-specific binding. Complete folding of class I trimer was confirmed by using conformational-sensitive mAb BB7.2 in the first three flow channels. Glycine Buffer, pH 3.0 was then used to dissociate peptides from the MHC class I trimer complex in second flow channel (blue) followed by injection of calreticulin through the channel. The figure demonstrates interaction of calreticulin to HC:β2M heterodimer (blue). Calreticulin did not bind to the MHC class I trimer in the two flow channels (green and pink). Non-specific binding of calreticulin was observed in the fourth control channel (red).

low, b) protein-protein interaction between calreticulin and HC:β2m dimer may be weaker than lectin interactions. It may be that binding of calreticulin to sugar residues is the initial step in binding to HC:β2m dimer followed by stronger protein-protein interactions. This result, however, provides an initial evidence for protein-protein interaction between calreticulin and class I.

However, the presence of heavy chain:β2m heterodimer in third flow channel could not be confirmed. When I passed BBM.1 antibody, which binds specifically to β2m, there was no antibody binding detected in the third flow channel. This could have been the result of complete dissociation of β2m from heavy chain after release of calreticulin from the dimer complex following EDTA treatment However, it needs to be emphasised that a true control was missing whereby strong acid treatment of the class I trimer would result in just HC remaining in the avidin chip that would fail to bind to calreticulin.

5.7 CHAPTER SUMMARY AND DISCUSSIONS

A number of previous reports have suggested that mouse and human class I molecules differ in their biosynthesis. An important factor contributing to this difference may be the number and position of N-oligosaccharides. My data suggests that glycosylation in human class I heavy chain at position 86 is optimal and any alteration of glycosylation will have an adverse affect on biosynthesis of human A2.1 allele.

Several changes in the biosynthesis of A2.1 glycosylation mutants were observed. Although comparable amount of heavy chains were synthesised by C1R cells expressing either wild type or glycosylation mutant A2.1 molecules, surface

expression of glycosylation mutant molecules was impaired. All glycosylation mutants expressed less than 50% of the wild type A2.1 on the cell surface. Question may arise whether loss of cell-surface expression is indeed due to changes in the amino acid sequence rather than alterations in the carbohydrate moieties. Harris *et al.*, have tested this in mouse allele L^d and verified changes to different amino acids had no effect [287].

Glycosylation mutant molecules were also unstable at the cell surface. This was because they fail to get loaded with stabilising optimal peptides. The loading defect was despite the fact they are able to associate with the TAP complex, although the quality of interaction with the TAP complex may be affected because of altered glycosylation. For example, altered glycosylation may result in slightly different conformation of class I, which could fail to make productive interactions with the TAP complex. Altered conformation of class I due to abnormal glycosylation may also affect the peptide-binding affinity in the peptide-binding groove.

The results also demonstrate a proportion of $A2.1^{+++}$ heavy chains synthesised are retained in the ER (Endo-H sensitive, figure 5.4.4a-b) and these may never get incorporated into the TAP loading complex.

Although not expected for $A2.1^{---}$, I could not identify any $A2.1^{+++}$, $A2.1^{++-}$ or wild type heavy chains in anti-calnexin immunoprecipitates. One report suggests increased binding to calnexin in $A2.1^{++-}$ [286]. Several studies have failed to identify wild type heavy chain in anti-calnexin immunoprecipitate. These differences may be due to the type of assay or antibodies used to detect these associations.

These results thus point to the conclusion that the A2.1 glycosylation mutants fail to load up with peptides in C1R cells. Alteration of N-glycosylation may affect secondary and tertiary structures of mutant molecules, which in turn may affect their productive interaction with the peptide-loading complex.

The A2.1 glycosylation mutants did not have difficulties presenting both endogenous and exogenous CTL specific antigen. Both $A2.1^{---}$ and $A2.1^{+++}$ were able to process and present influenza matrix protein derived epitope like the wild type A2.1 following infection of C1R cells expressing the A2.1 glycosylation mutants. The presentation was also comparable when a synthetic epitope was supplied exogenously. Antigen presentation by mutant class I molecules was comparable to the wild type despite reduced expression of $A2.1^{---}$ and $A2.1^{+++}$ at the cell surface. This could be because fewer number of class I molecules complexed to matix peptide epitope may be sufficient to sensitise the T cells used in the assay. These results support earlier mutational studies done on HLA-B7 molecules where aglycosylated B7 expressing cells were able to process antigens and recognised by allospecific B7-restricted CTL [342]. Moreover, in studies done by Miyazaki *et al.*, nonglycosylated $H\text{-}2L^d$ was unchanged in its overall serological specificities, and was recognised by alloreactive CTL [337]. Further, $H\text{-}2L^d$ was able to mediate cytotoxic activity of VSV-specific T cells. Like A2.1 glycosylation mutants in this study, cell surface expression of non-glycosylated $H\text{-}2L^d$ was also markedly reduced compared to wild type.

The BIAcore data, although not confirmative, suggests interaction of heavy chain:β2m dimer with calreticulin. Furthermore, it highlights the existence of protein-protein interaction between calreticulin and nonglycosylated heavy chain. Although

the data lacks proper controls it does show calreticulin interaction with non-glycosylated substrate in real time.

The results therefore clearly demonstrate that glycosylation of A2.1 heavy chain at position 86 is optimal in human cells. In addition, any alterations in glycosylation, (positions or number) affects the loading steps in class I biogenesis. The loading defect is not absolute as some of the mutant class I molecules manage to assemble properly, incorporate into TAP complex and make their journey to the cell surface.

Chapter 6

P- DOMAIN OF CALRETICULIN DOWNREGULATES PROTEIN EXPRESSION SPECIFICALLY

6.1 BACKGROUND

Structural predictions of calreticulin suggest that the protein has at least three domains [186, 205, 206](see figure 1.6.1.2). Residues 1-180 of the mature protein form the N-domain, which is predicted to form a compact globular structure containing anti-parallel β-strands connected by protein loops [205]. When modeled with the structure of the lumenal domain of homologous protein calnexin, it is likely the N- domain forms the carbohydrate-binding site [184]. This is also the site where the most strongly conserved residues are clustered. Recently, it has been shown that the N- and P- domain together (NP- domain) are sufficient for bradykinin Receptor folding and assembly [343]. Moreover, Holaska *et al.,* have demonstrated nuclear export of the glucocorticoid receptor mediated by calreticulin *in vivo* [237]. This export function was specific to calreticulin and the N- domain region was implicated in binding to the DNA-binding domain (DBD) of the glucocorticoid receptor.

There are several other interactions of the N- domain whose physiological relevance is less clear. For example, *in vitro* studies have shown that N- domain of calreticulin interacts with the DBD of glucocorticoid receptor [232], rubella virus RNA [344], α-integrin tails [345] and with the chaperone protein disulphide isomerase (PDI) [226]. In addition, the N- domain also contains 4 of the 6 E-x-K-x-K peptide motifs which have been implicated in C1q binding and complement inhibition [346]. It is also for these reasons this domain has been implicated in the chaperone activity.

Much interest has been focused in the Proline-rich (P)- domain of calreticulin (amino acids 181-290) for a number of reasons. P- domain contains 17% proline, 6.5% tryptophan and 44% charged residues, and is the most highly conserved region of calreticulin, both across species and with its homologue calnexin. Most striking is the existence of two sequence repeats of 17 [P-x-x-I-x-D-P-D-A-x-K-P-E-D-W-D-x] (type 1) and 14 residues [G-x-W-X-P-P-x-I-x-N-P-x-Y-x] (type 2) (figure 1.6.1.1). Calreticulin comprises three copies of each repeat type in an "111222" arrangement while calnexin has four copies in an "11112222" arrangement.

NMR structure of calreticulin P- domain and X-ray crystallography structure of calnexin P- domain suggests that it probably does not form carbohydrate-binding site, as previously thought [184, 211, 212]. Instead, the protrusion of the P- domain region from the calreticulin core could constitute a protein-ligand binding site. Moreover, the negatively charged amino acid residues decorate the tip of the hairpin loop. This could constitute a binding site for an interacting protein and the inner repeats could serve as "spacers" for positioning the ligand-binding site at a discrete distance from the core of the protein.

The C- domain (residues 291-400) of calreticulin is highly acidic (pI=4). It has been proposed to be responsible for binding calcium [343]. Therefore, this domain is likely to influence calcium-dependent interactions of calreticulin with its substrates [227].

A question that has yet to be answered is whether chaperone activity can be assigned to a particular domain. Several attempts have been made to localize the chaperoning activity to specific domains but the results have been conflicting. Vassilikos et al.,

demonstrated 25% binding of glycosubstrates to lectin- domain (i.e., P- domain with N- and C- terminal extensions) compared to full-length calreticulin [231]. Independent studies by Peterson and Helenius showed that much larger fragment was required for any significant lectin activity to be detected [347]. Recently, it was demonstrated that N- and P-domain together were sufficient to generate a fully folded bradykinin receptor [343].

The MHC class I complex is an excellent example of a molecule, which employs calreticulin and calnexin for proper folding. In chapter three, I described assembly and antigen presenting function of class I in fibroblasts derived from the embryos of mice with a targeted knockout of the calreticulin gene. Optimal peptide loading and antigen presenting function of class I was severely impaired in the absence of calreticulin in mouse fibroblasts. In this chapter, I have gone further to try and reconstitute functional calreticulin in the calreticulin knockout fibroblasts using replacement with various genes encoding different domains of calreticulin and to analyse the role of these domains in MHC class I biogenesis.

6.2 ANALYSIS OF ROLES OF DIFFERENT DOMAINS OF CALRETICULIN ON THE RESTORATION OF MHC CLASS I SURFACE EXPRESSION

In order to establish which region of calreticulin is important in the generation of fully mature MHC class I, I made use of C-terminal HA-tagged calreticulin domain constructs that had been generated by our collaborator (Marek Michalak, University of Alberta, Canada). The constructs included N- and P- domains together (I will refer this construct as NP- domain), P- domain and P- and C- domains together (PC-domain) [figure 6.2.1a]. Note that several laboratories have found it extremely

difficult to independently express N- and C- domains on their own. Our collaborator had therefore, expressed N- and C- domains together with the P- domain. I subcloned the appropriate domains into mammalian expression vector pUB6/V5. I transfected each of these constructs into K42 and generated stable clones. I first examined whether any of these constructs restored cell surface expression in K42.

6.2.1 NP -domain does not restore MHC class I surface expression

NP- domain expresses well in K42 as shown by the western blot with anti-HA tag antibody (figure 6.2.1b, left-hand panel). Some non-specific bands appear in figure 6.2.1b, left-hand panel, which disappear in figure 6.2.1b, right-hand panel (for example compare K42 in both figures). The reason may be non-specific cross reactivity of anti-HA antibody, which may not have been removed during the wash-up steps during Immunoblotting procedure. I compared surface expression of H2- K^b allele on the calreticulin competent cell line K41 and calreticulin-deficient K42 expressing the N- domain of calreticulin (K42-NP) by flow-cytometry using conformation-sensitive monoclonal antibody Y3. I found that H2- K^b in K42-NP is expressed at around 30-40% of the level observed in K41 and similar to the expression of H2-K^b in K42 (figure 6.2.1c-d). Therefore, NP- domain failed to restore MHC class I surface expression in K42. I concluded that NP-domain on its own fails to generate optimally loaded stable MHC class I molecules.

6.2.2 PC- and P- domains downregulate MHC class I surface expression

PC- domain is also expressed well in K42 (figure 6.2.1b, right-hand panel) in contrast to the P- domain, which has a very low expression level (figure 6.2.1b, left-hand panel). The flow-cytometric analysis showed that transfecting both these domains into

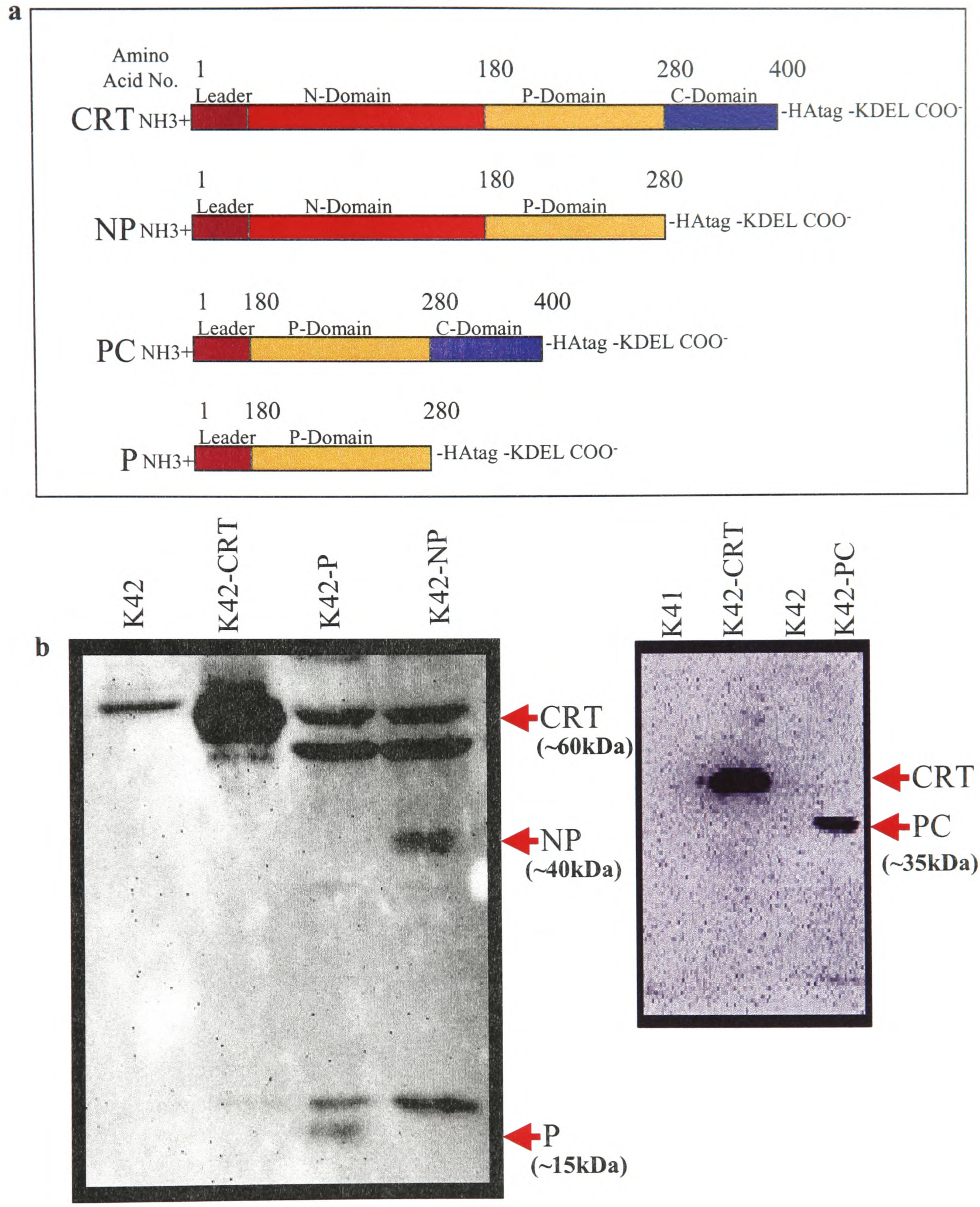

Figure 6.2.1 Expression of calreticulin domains in K42

a) Schematic representation of different calreticulin domain constructs that were used to transfect K42. Each construct has a ER targeting leader sequence at the amino-terminus and a HA-tag followed by the ER retention signal KDEL at the carboxy-terminus. b) K42 was transfected with full-length calreticulin (K42-CRT) and NP- (K42-NP), P- (K42-P) and PC- (K42-PC) domains of calreticulin. Expression was confirmed by western blotting against the HA epitope tag using anti-HA antiserum.

c

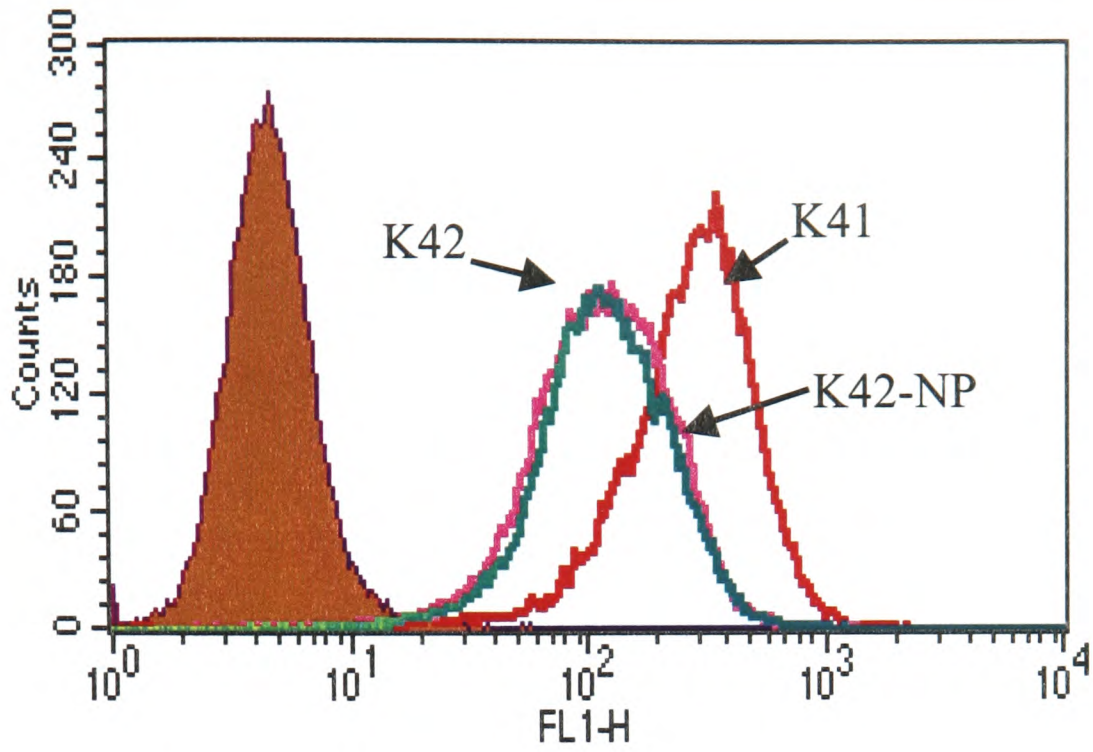

d

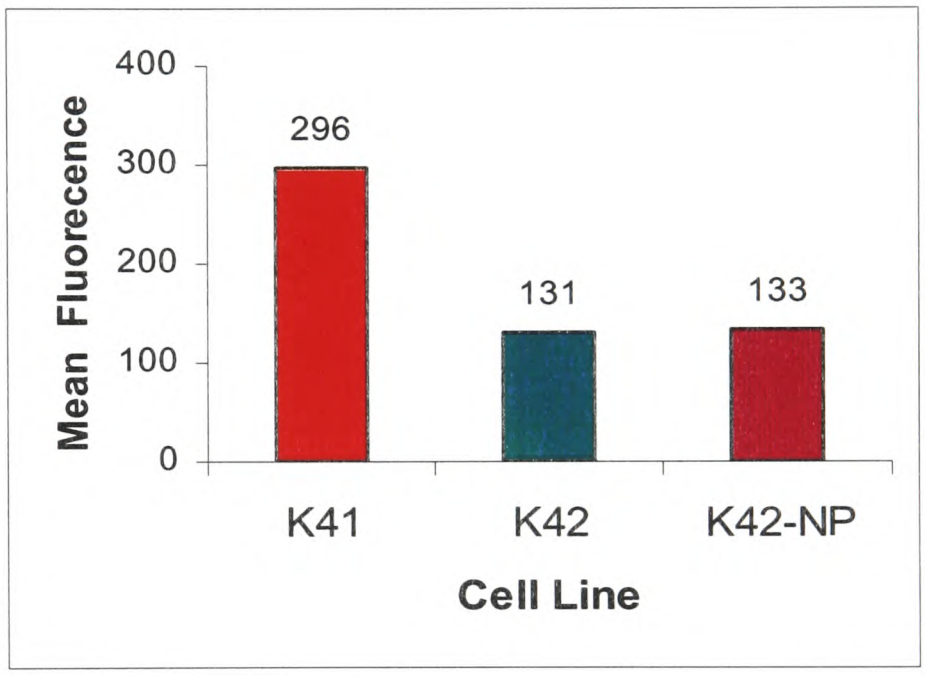

Figure 6.2.1(contd.) NP -domain does not restore MHC class I surface expression

c) Cell-surface expression of K^b was detected on the surfaces of K41, K42 and K42 expressing NP domain of calreticulin (K42-NP) using monoclonal antibody Y3.
d) Results are shown graphically, with actual mean fluorescence value indicated above individual bars.

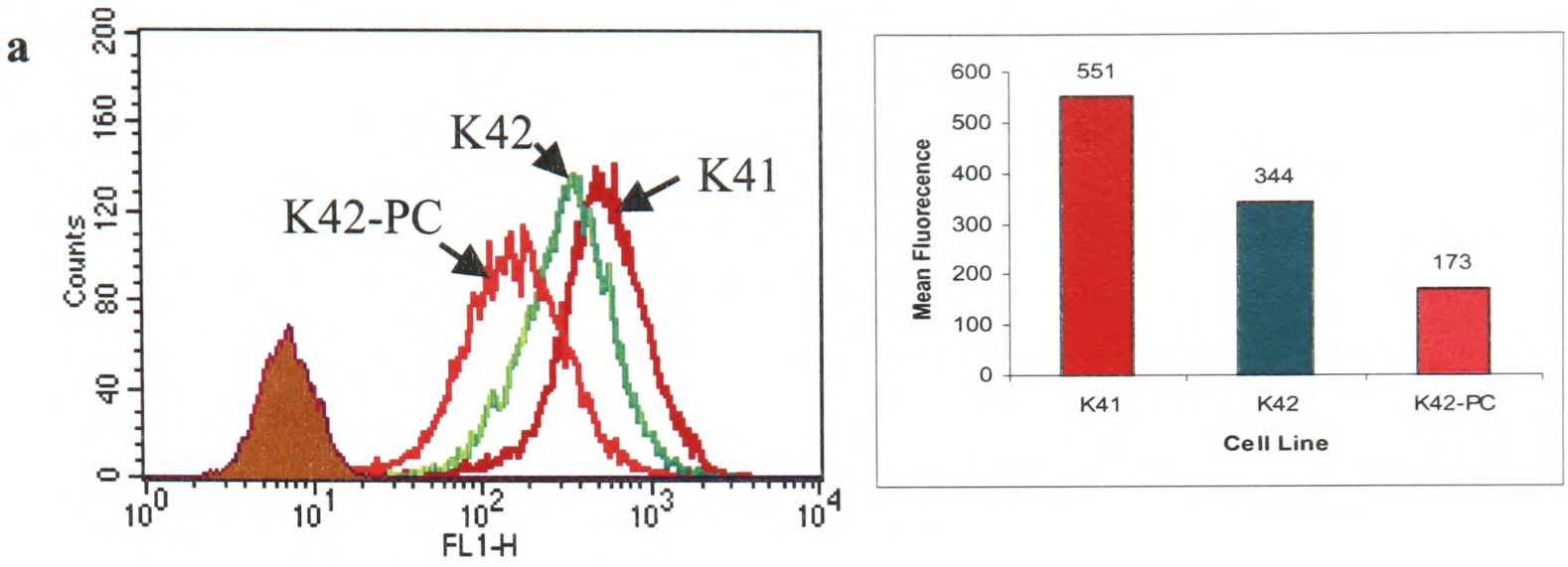

Figure 6.2.2 PC- and P- domains downregulate MHC class I surface expression

a) Cell surface expression of K^b was detected on the surfaces of K41, K42, K42 expressing PC domain of calreticulin (K42-PC) using monoclonal antibody Y3 (left-hand panel). Right-hand panel: histograms showing the mean fluorescence value with the actual value indicated above individual bars. b) Surface expression of K^b on K42 expressing P-domain of calreticulin (K42-P) compared to K41 and K42 (left-hand panel). Histograms showing the mean fluorescence value with the actual value indicated above individual bars (right-hand panel).

K42 produced an unexpected odd negative effect on H2-K^b surface expression. Figure 6.2.2a shows that K42 transfected with the PC-domain (K42-PC) expressed only about 31% of H2-K^b compared to K41 and 50% less compared to K42. The effect was much greater with K42 transfected with just the P-domain (K42-P) where the expression was 21% lower compared to K42 and 10% lower compared to K41 (Figure 6.2.2b). When I incubated K41, K42 and K42-P for two hours in the presence of 20μM of the H2-K^b binding peptide SIINFEKL, K41 and K42 cells gave the same level of staining with Y3 as described earlier. However, K42-P staining remained low compared to K41 and K42 (data not shown). This suggested that less number of K^b molecules were assembled and exported to the cells surface in K42-P.

6.2.3 P-domain has a dominant negative effect on MHC class I expression

Next, I asked whether the effect of the P-domain was dominant. I transfected K41 with the P-domain and generated stable line (K41-P). The expression of the P- domain in K41 was also very low (data not shown). The flow-cytometric analysis showed that transfecting P-domain into K41 produced a similar odd negative effect on H2-K^b surface expression like that seen in K42-P. Figure 6.2.3a-b shows that K41-P expresses only 26% of K^b molecules compared to K41 on the cell surface. Moreover, K41-P expressed 55% of K^b molecules expressed in K42. This experiment therefore suggested that in P- domain expressing cells, either less number of K^b molecules were assembled and exported or overall synthesis of class I molecules was lower. I first did a western blot analysis to determine the level of expression of K^b and D^b in cells transfected with P-domain.

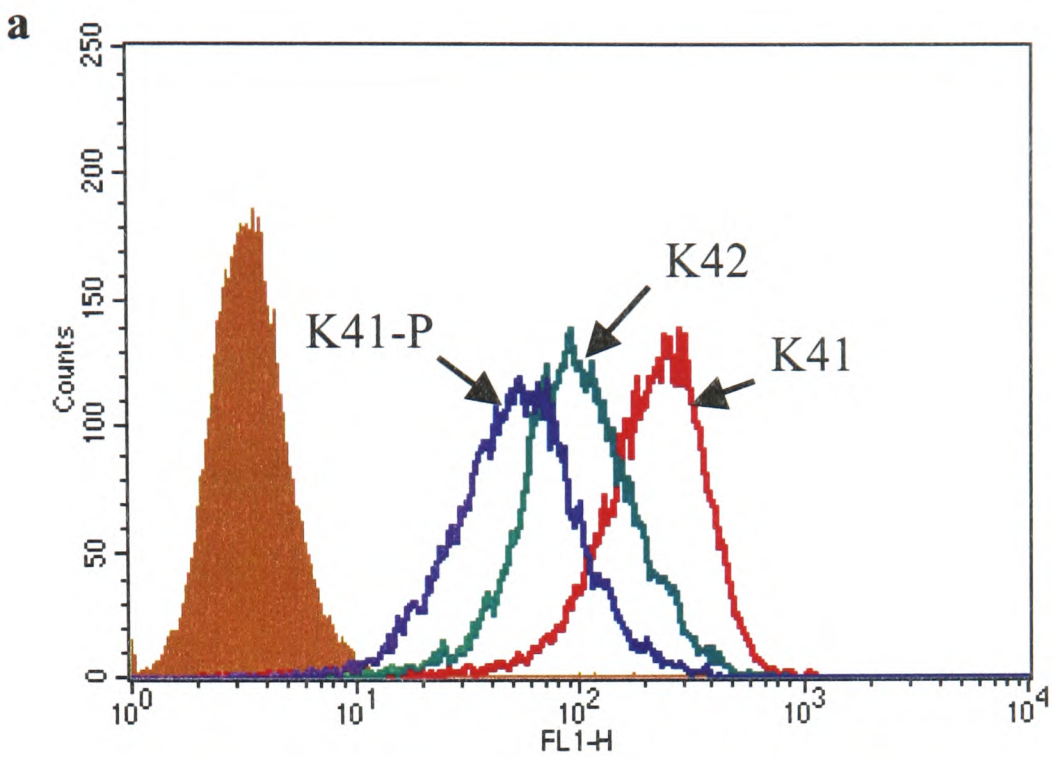

Figure 6.2.3 P-domain has a dominant negative effect on MHC class I expression

a) Cell-surface expression of K^b was detected on the surfaces of K41, K42 and K41 expressing P domain of calreticulin (K41-P) by flow cytometry using monoclonal antibody Y3. b) Results are shown graphically, with actual mean fluorescence value indicated above individual bars.

6.3 P- DOMAIN REDUCES CLASS I HEAVY CHAIN EXPRESSION IN DOMINANT FASHION

I performed western blot analysis on lysate of $1x10^5$ cells using rabbit antisera T18, which recognizes $\alpha2\alpha3$ domain of K^b and D^b. Western blot analysis confirmed a massive reduction on K^b and D^b heavy chain expression in K41-P and K42-P compared to K41 and K42 (figure 6.3). Class I molecules at the cell surface reflected total amount of class I heavy chain synthesized in P- domain transfected cells. I suggested that the down regulation of class I expression could be the result of one or more of the following:

a) P- domain in K42 is not properly folded and so the reduced class I expression is part of the unfolded protein response (UPR)

b) P- domain drives MHC class I into degradative pathway

c) P- domain may affect the transcription of a number of proteins including class I

I investigated each of these possibilities.

6.4 P- DOMAIN DOES NOT PRODUCE AN UNFOLDED PROTEIN RESPONSE

A PKR-like ER kinase (PERK) undergoes phosphorylation to ER stress, also known as an unfolded protein response (UPR). Incubating cells in 10mM Dithiothreitol (DTT) for 30 minutes can induce UPR artificially. I determined the level of phosphorylation of PERK in cells transfected with the P- domain (K41-P and K42-P)

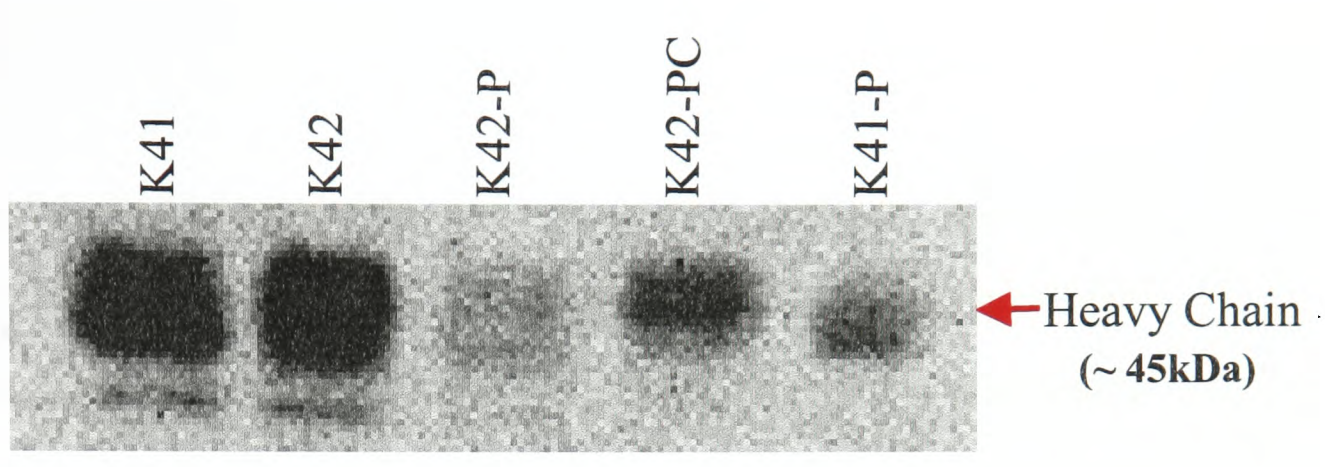

Figure 6.3 Expression of MHC class I heavy chain in K41, K42, K42-P, K42-PC and K41-P

Expression of MHC class I heavy chain was detected by western blot using T18 anti-sera, which recognises heavy chains of K^b and D^b molecules.

as well as in control cells that had been induced an UPR artificially by the addition of DTT. As shown in figure 6.4a, PERK is phosphorylated in cells treated with DTT whereas it remains dephosphorylated in the P-domain transfected cells. This indicated that the P- domain does not lead to an UPR response and that lower level of class I synthesis in P- domain transfected cells was probably not due to an UPR.

In order to confirm this further, I subcloned a fragment of the nucleoprotein (NP) from influenza into a mammalian expression vector pUB6/V5. The NP fragment was tagged with the leader sequence that would direct it to the ER. This NP fragment is known to unfold in the ER (Tim Elliott, unpublished observation). I transfected this construct into K41 and generated a stable clone expressing the NP fragment (K41-np). Western blot analysis confirmed expression of NP fragment in K41. I compared surface expression of H2- K^b alleles on K41, and K41-np by flow-cytometry. I found that there was no difference in cell surface expression of K^b between K41-np and K41 (figure 6.4b). This finding therefore supported the earlier demonstration that the downregulation of class I surface expression on P- domain expressing cells is not the result of an UPR response.

6.5 P- DOMAIN IS FUNCTIONAL IN K42

Although P- domain did not lead to an unfolded protein response, it may be because it is not functional in the P- domain transfected cells. I wanted an independent measurement of P- domain function. One way was to test with antibodies that would recognize only fully folded P- domain. I could not find any such antibodies. During this time, Kim Nakamura (University of Alberta, Edmonton, Canada) had

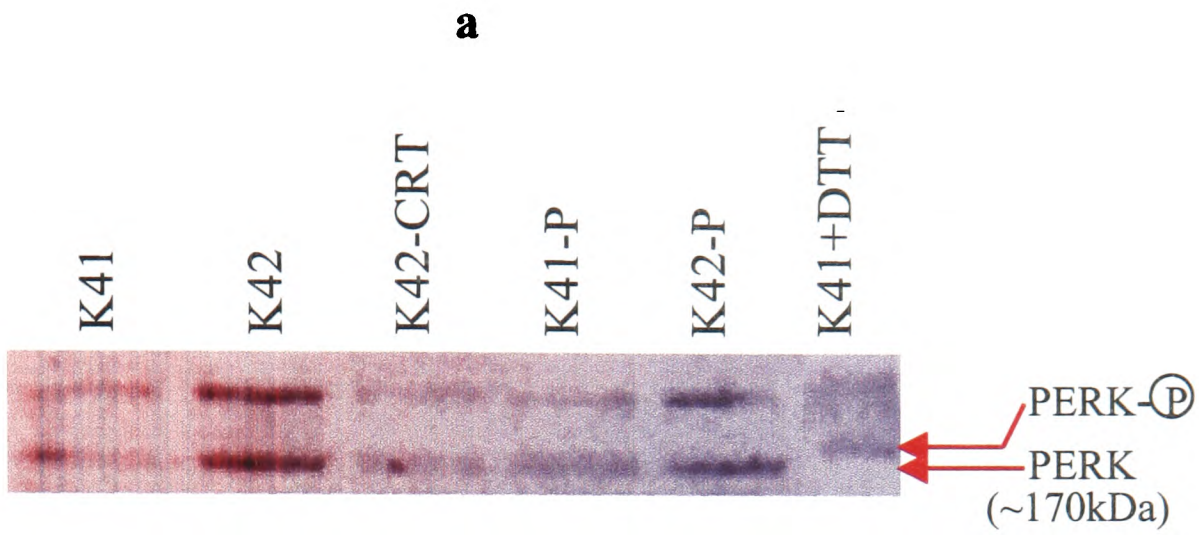

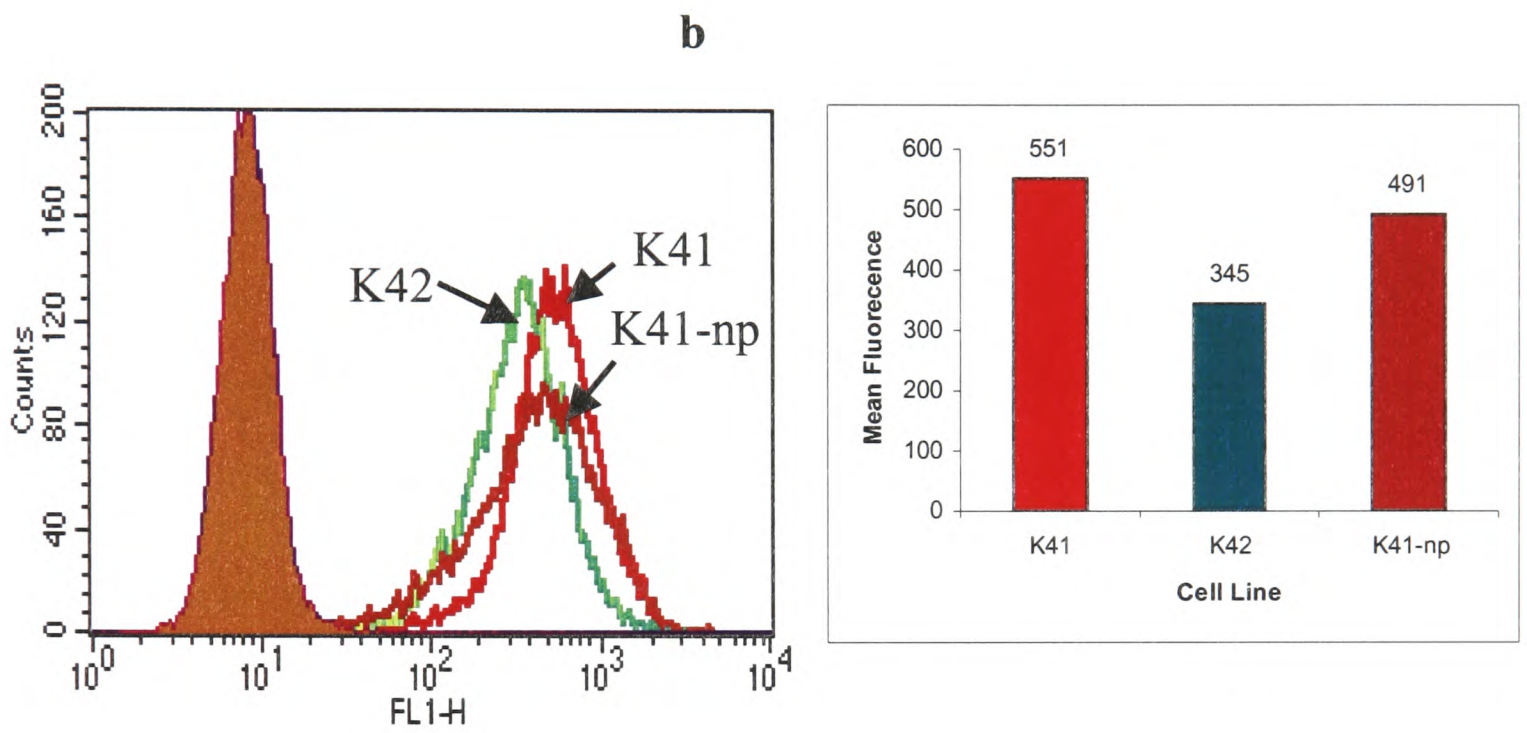

Figure 6.4. P- domain does not produce an unfolded protein response

a) PERK and phosphorylated PERK (PERK-P) was detected by western blot using anti-PERK antibody to determine extent of PERK phosphorylation in K41, K42, K42-expressing different domains of calreticulin. As a positive control, K41 were treated with 10 mM DTT to induce unfolded protein response (UPR).

b) Cell-surface expression of K^b was detected by flow cytometry on the surfaces of K41, K42 and K41 expressing influenza nucleoprotein fragment (np) (K41-np) using monoclonal antibody Y3 (left panel). Results are shown graphically (right panel), with actual mean fluorecence value indicated above individual bars.

demonstrated that basal cytosolic calcium level is raised in K42 compared to K41 (150nM in K42 versus 100nM in K41) [now published in [343]]. This result was obtained by fura-2 based calcium imaging on suspension cells. I, on collaboration with Dr Grant Churchill (Department of Pharmacology, University of Oxford), measured basal cytosolic calcium levels in K41, K42 and K42-P. We also based our analysis on fura-2 calcium imaging method but on adherent conditions, which I believe is more physiological. As shown in figure 6.5, we found that basal cytosolic calcium level (green arrowhead) in K42 was in fact lower (30nM) compared to K41 (100nM). Striking observation we made was that the P- domain had restored the basal cytosolic level of calcium in K42 to that of K41. This meant that the P-domain was functionally significant and was probably folded. It also meant that the P- domain performed an important calcium regulatory function. I do not know how P-domain could restore cytosolic calcium levels in K42, but P- domain could directly or indirectly interact with other calcium storage proteins in the ER or associate with membrane ion channels to produce the effect observed.

Although P-domain restored the basal cytosolic level of calcium in K42, it failed to increase the cytosolic calcium level to that of K41 when treated with thapsigargin (red arrow), a SERCA pump blocker, which causes release of calcium from the stores in the ER. I do not know why this should be the case but one reason could be that P-domain only contains the low capacity calcium-binding site and that the ER calcium store is low in K42 compared to K41 (Marek Michalak, personal communication).

a

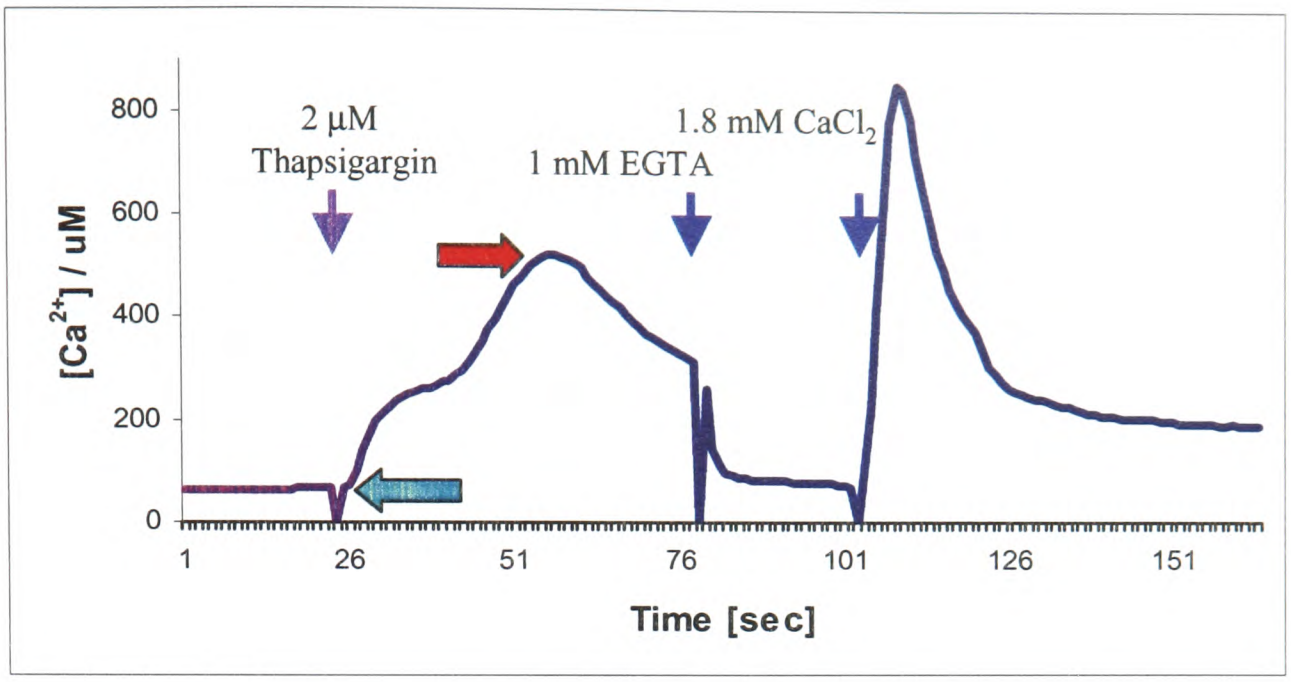

b

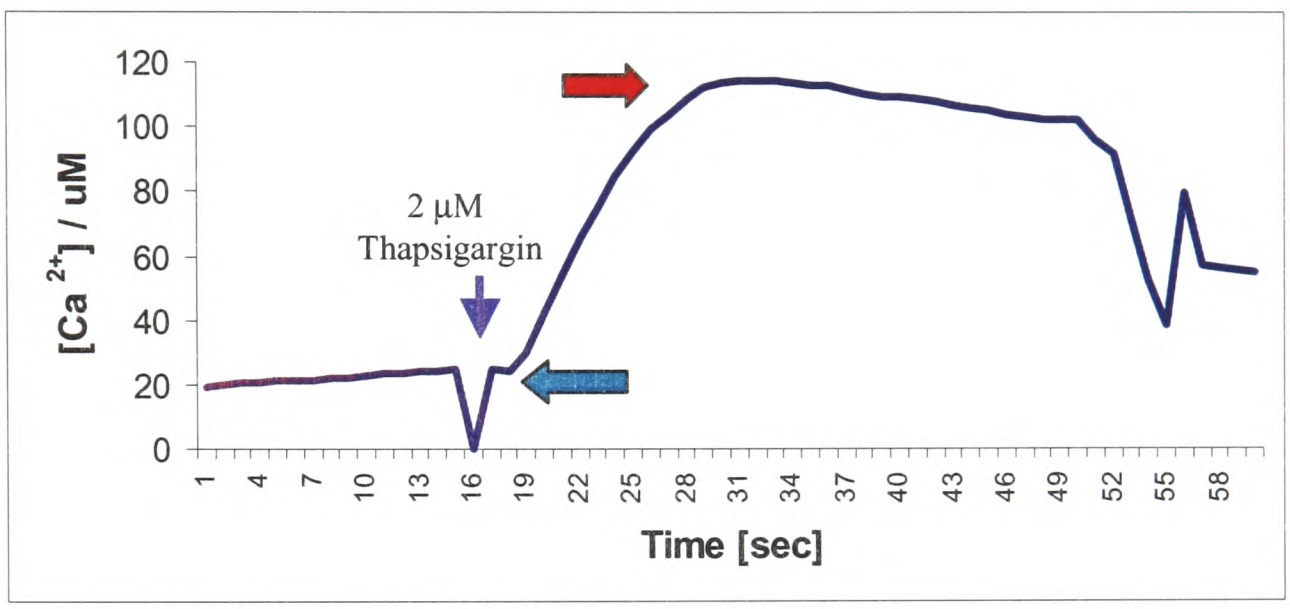

c

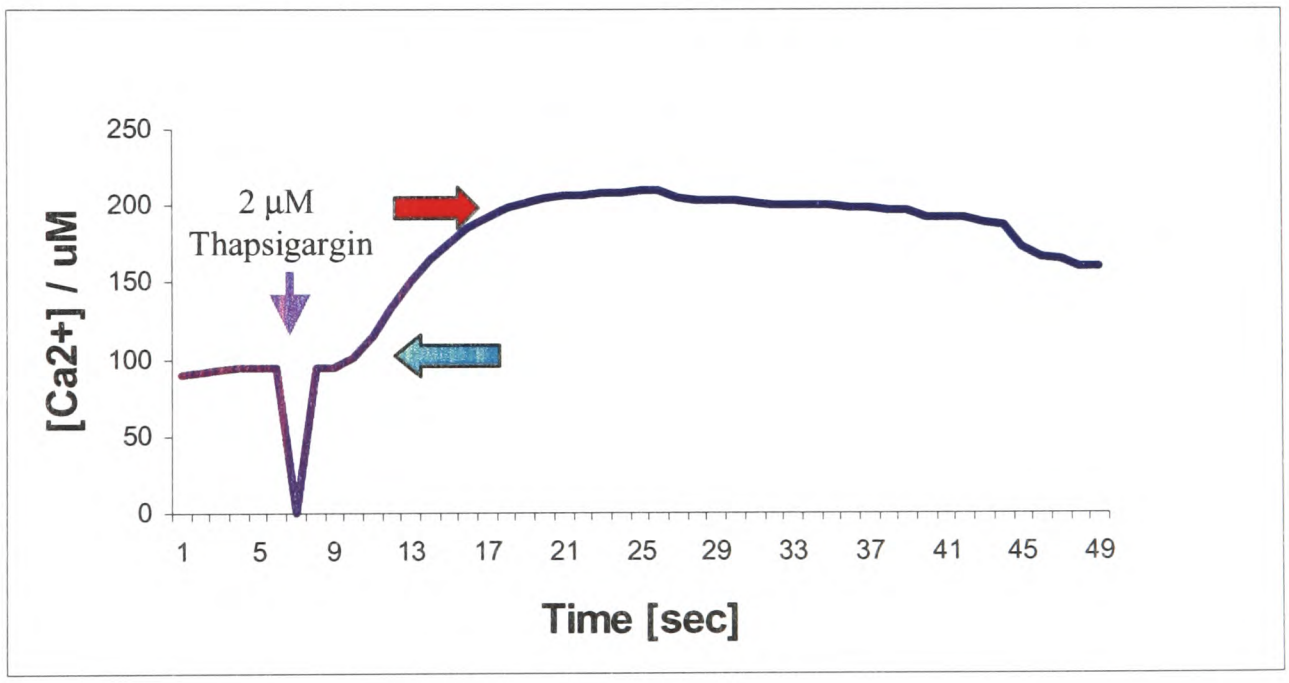

Figure 6.5. P- domain restores basal cytosolic calcium levels in K42

Basal cytosolic calcium levels in K41 (a), K42 (b) and K42-P (c) was determined based on fura-2 calcium imaging method (green arrowhead) . Release of calcium from intracellular stores was measured by treating cells with 2µM thapsigargin (red arrowhead). 1mM EDTA was used to quench cytosolic calcium levels and 1.8mM $CaCl_2$ was to demonstrate uptake of calcium by K41 cells.

6.6 AFFECT OF P- DOMAIN ON PROTEIN SYNTHESIS AND DEGRADATION

6.6.1 P- domain affects the synthesis of membrane proteins

In order to determine whether P- domain affects synthesis of cellular proteins, I subjected K41-P, K42-P and control cells to lysis protocol followed by differential fractionation to achieve cytosolic, membrane and nuclear fractions as described in the materials and methods. I used Bradford protein assay to determine the total protein concentration of an aliquot of each of the cytosolic, membrane and nuclear fractions. In this method, within the linear range of the assay, the more protein present, the intensity of the colour increases, after adding the Bradford reagents, and is read on a spectrophotometer. The protein concentration of a test sample is then determined by comparison to that of a series of protein standards of bovine serum albumin (BSA).

The results shown in figure 6.6.1 demonstrate that amount of protein present in the aliquots of membrane fractions of P- domain expressing cells is lower than that present in the control cells. K41-P expressed only 65% of total membrane proteins compared to K41 and K42-P expressed only 56% compared to K42. It is tempting to speculate that reduction in total proteins in membrane fractions of P- domain expressing cells may be mainly contributed by MHC class I since heavy chain was expressed only about 20% in P- domain expressing cells compared to the control cells (see figure 6.3). The amount of protein in the cytosolic and nuclear fractions was largely unaltered in the P- domain transfected cells compared to the control cells. This experiment therefore suggests that P- domain mostly affects the expression of membrane proteins.

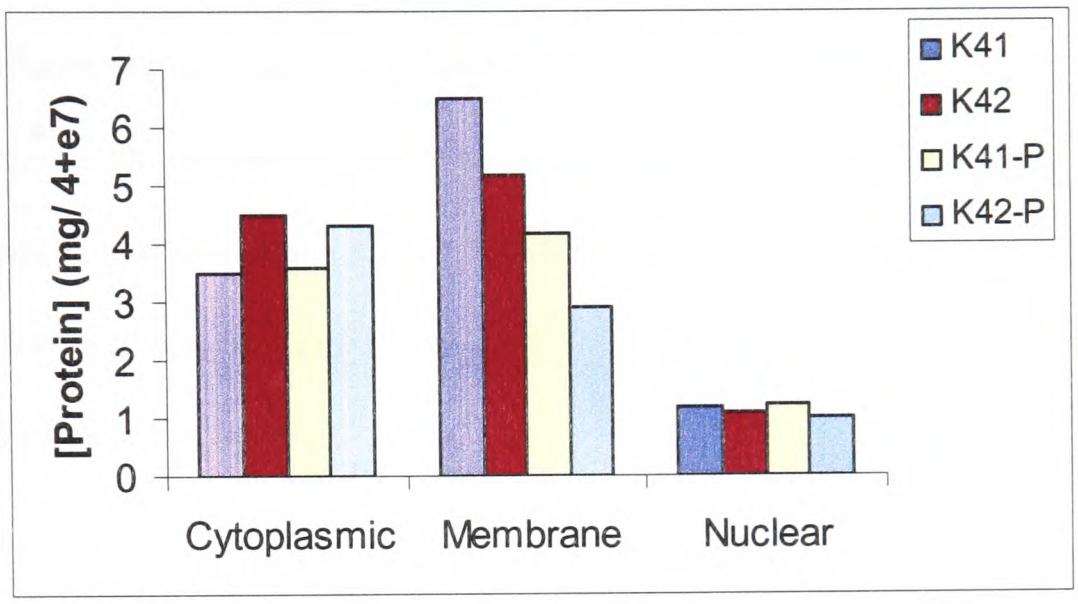

Figure 6.6.1 P- domain affects the synthesis of membrane proteins.

$4x10^7$ each of K41, K42, K41-P and K42-P cells were lysed and subjected to differential fractionation to achieve cytosolic, membrane and nuclear fractions as described in the materials and methods. An aliquot of each of the cytosolic, membrane and nuclear fractions from each of the cell fractions was used to determine total protein concentration using Bradford assay.

6.6.2 P- domain does not affect degradation of membrane proteins

To determine whether P- domain affected the rate of degradation of membrane proteins, I carried out a pulse-chase analysis to compare a cohort of [^{35}S]-labelled membrane proteins in K42-P and in control cells. At each time point during the chase period, I removed aliquots of cells and lysed them followed by differential fractionation to achieve the membrane fraction. An aliquot of membrane fraction from each of the cells was put through β-emission scintillation counter. The result shown in figure 6.6.2 shows that the rate of degradation is the same in all cells as shown by the gradient of the curve. However, the amount of radioactivity incorporated into the cohort of membrane proteins in K42-P is much lower than any other cell lines. These results therefore indicate that P-domain has most affects on synthesis of membrane proteins than on their degradation.

6.6.3 Rate of ER degradation of a model antigen is the same in K41 and K41-P

I used recombinant vaccinia virus encoding influenza A NP tagged with ubiquitin-arginine to infect K41 and K42. NP gene was preceded by ER leader sequence in order for the protein to be directed to the ER. K41 and K41-P were infected with this vaccinia construct as described earlier and time allowed for NP expression (Chapter 3, Section 3.3.1). I then carried out a pulse-chase analysis to assess the rate of degradation of this model antigen.

As shown in figure 6.6.3, the rate of degradation of the model antigen in P-domain expressing K41 was similar to K41. This suggested that degradation probably did not contribute significantly to lower recovery of class I heavy chains observed in cells expressing P- domain. This experiment therefore indicated that P-domain might play a

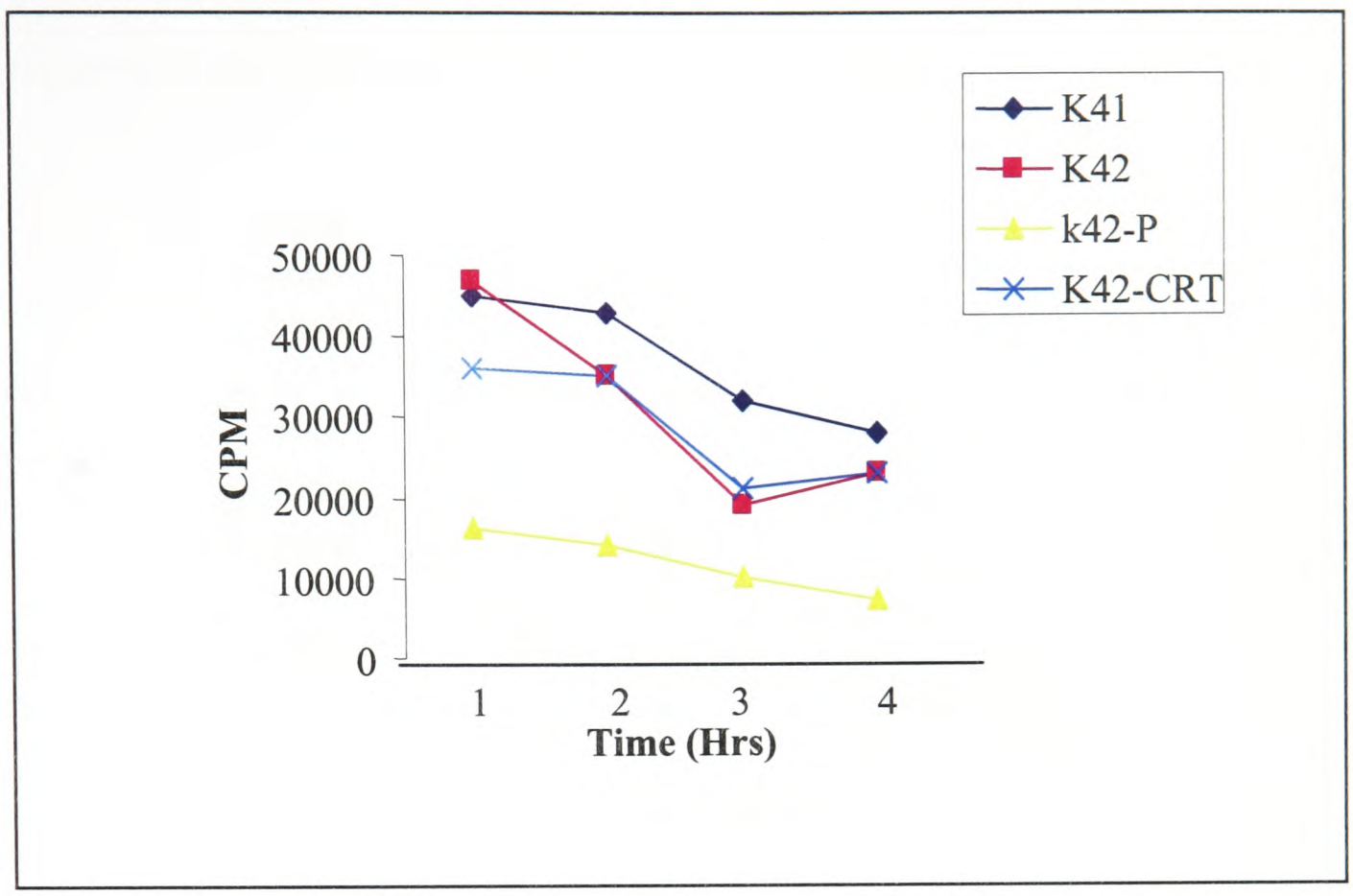

Figure 6.6.2 P- domain probably does not affect degradation of membrane proteins

Equal number of K41, K42, K42-CRT and K42-P cells were pulse labelled with ^{35}S methionine and cysteine and chased for indicated times. At each time point, aliquots of labelled cells were lysed followed by differential fractionation to achieve the membrane fraction as described in materials and methods. Aliquots of membrane fractions at indicated time points from each cell line was put through the β-emission scintillation counter to determine total protein present as counts per minute (CPM), and plotted against time.

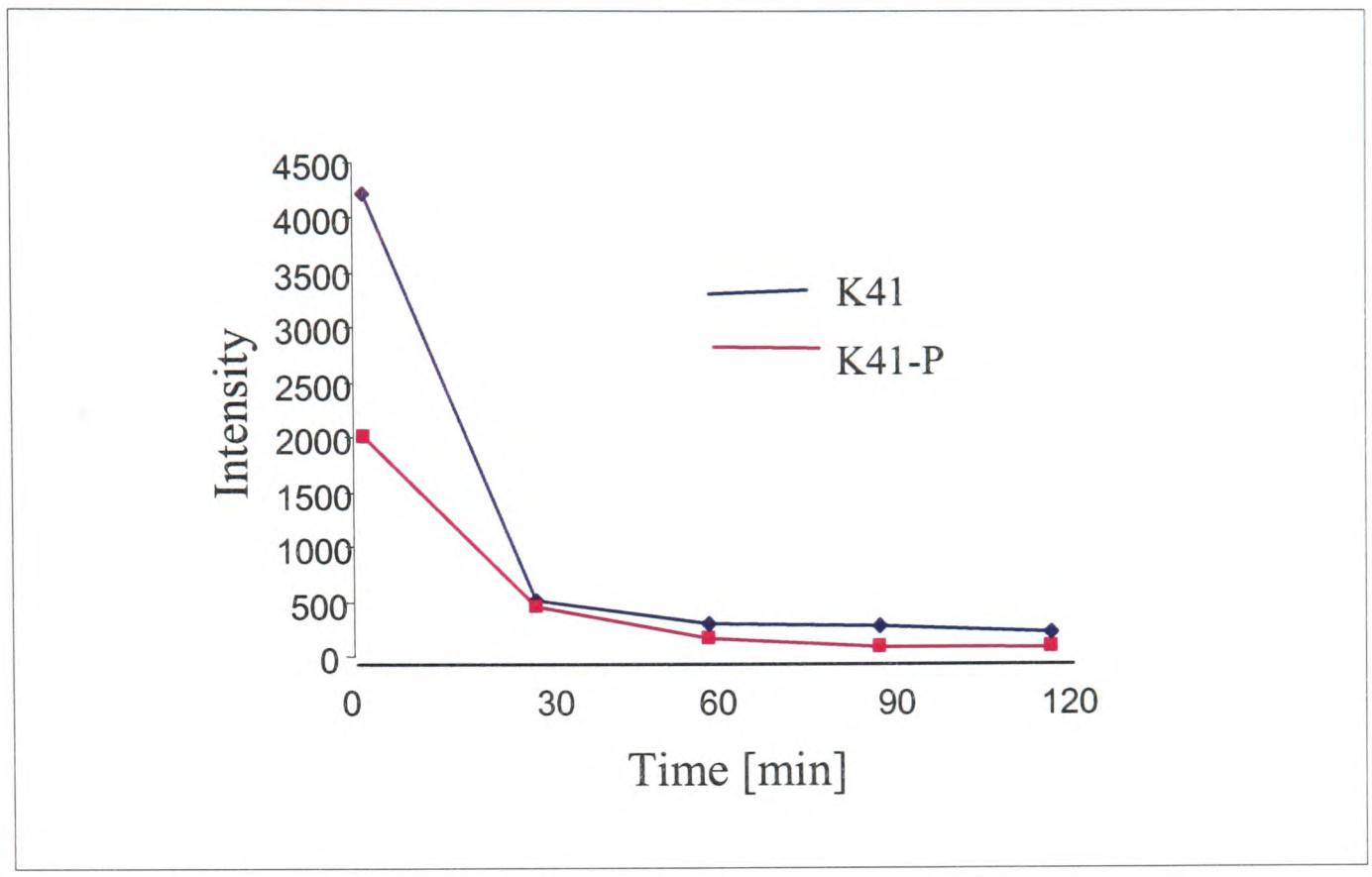

Figure 6.6.3 Rate of cytosolic degradation of a model antigen is the same in K41 and K42

K41 and K41-P were infected for 90 minutes with vaccinia encoding influenza A nucleoprotein (np) containing the ER targeting leader sequence. Vaccinia was removed after 90 minutes and expression of np allowed for further 4 hrs. Cells were then labelled with ^{35}S methionine and cysteine, aliquots removed at indicated times and lysed in NP40 lysis buffer. The lysates were immunoprecipitated with anti-np antibody, fractionated by SDS-PAGE and np band quantified by Quantity One software (BioRad Inc, USA). The intensity of NP band at each time point was plotted against time. Note that the amount of np synthesised in K41-P is half that synthesised in K41.

significant role at the transcriptional level leading to downregulation of class I expression.

6.7 P- DOMAIN DOWNREGULATED EXPRESSION OF SPECIFIC PROTEINS

It was clear that the P- domain was mostly affecting the expression of membrane proteins (figure 6.6.1). It was not clear whether P- domain affected all membrane proteins to the same extent or affected only a subset of proteins. It was also possible for P- domain to affect expression of proteins in microsomal fraction (i.e., proteins of the ER and Golgi complex) where P- domain is expected to be expressed. In order to determine to what extent P- domain affected expression of proteins other than MHC class I, I looked at the expression of some membrane proteins and some ER resident proteins.

6.7.1 Affect of P- domain on the expression of membrane proteins

I looked at the expression of transferrin receptor (TfR), glycoprotein 70 (gp70) and CD44 either by western blotting (TfR and gp70) or by flow cytometry (CD44) on cells expressing P- domain as well as in control cells. P- domain expressing cells and control cells were lysed in NP40 lysis buffer and analysed by western blot for the expression of TfR and gp70, using polyclonal antibodies specific for TfR (anti-CD71, Santa Cruz, California, USA) or gp70 (anti-gp70, kind gift from Dr Denise Golgher, University of Southampton, UK). Moreover, CD44 expression was determined by flow cytometry using anti-CD44 antibody (kind gift from Dr David Jackson, University of Oxford, UK) to stain for surface CD44 in Namalwa cells (positive control) and in cells expressing P-domain. Striking finding was that TfR (figure

6.7.1a) and CD44 (figure 6.7.1b) expressions were not affected by P- domain whereas gp70 expression was downregulated (figure 6.7.1c). I do not know the origin of the non-specific band on the TfR blot but this band seems to be present in all cells tested. I also do not know the origin of two subpopulations of K41 expressing P- domain. I have observed growing fibroblast cells at higher density (~90%) leads to the generation of two subpopulations of the cells. In any case, these results suggest that effect of P- domain is not global but only affects a subset of membrane glycoproteins.

6.7.2 Affect of P- domain on the expression of ER resident proteins

I also looked at the expression of ER resident proteins in P- domain expressing K41 and K42 cells by western blot analysis. I found that calnexin, gp46, UGGT, Erp72 and PDI were expressed more or less at a similar level in P- domain expressing K41 and K42, compared to the control cells (figure 6.7.2). However, other proteins were downregulated to different extent including GRP94, Erp57 and BiP (red arrowhead). It is to be noted that BiP expression is normally upregulated during a stress response. This is another evidence that P- domain expressing cells are probably not under stress. It is not clear why expression of only a subset of proteins was affected, but it is apparent that P- domain also affects the expression of ER resident proteins.

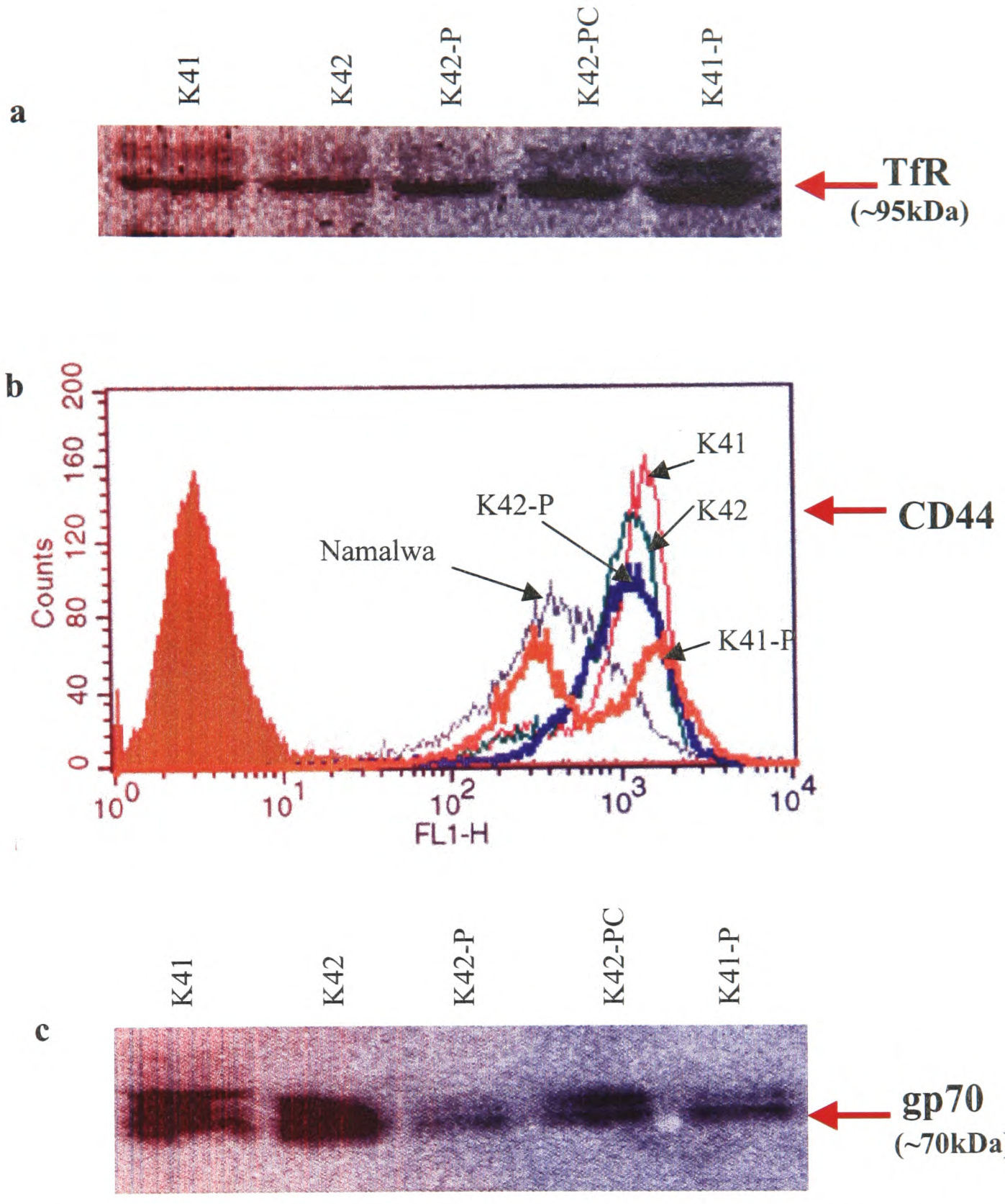

Figure 6.7.1. Affect of P- domain on the expression of membrane proteins

Expression of transferrin receptor (TfR) on various cell lines indicated was determined by western blotting using anti-CD71 antibody (a). Cell-surface expression of CD44 on Namalwa cell line (positive control) and other indicated cell lines was detected by flow Cytometry using monoclonal anti CD44 antibody (b). Expression of gp70 was determined by western blotting on various cell lines as indicated by using anti-gp70 antiserum (c).

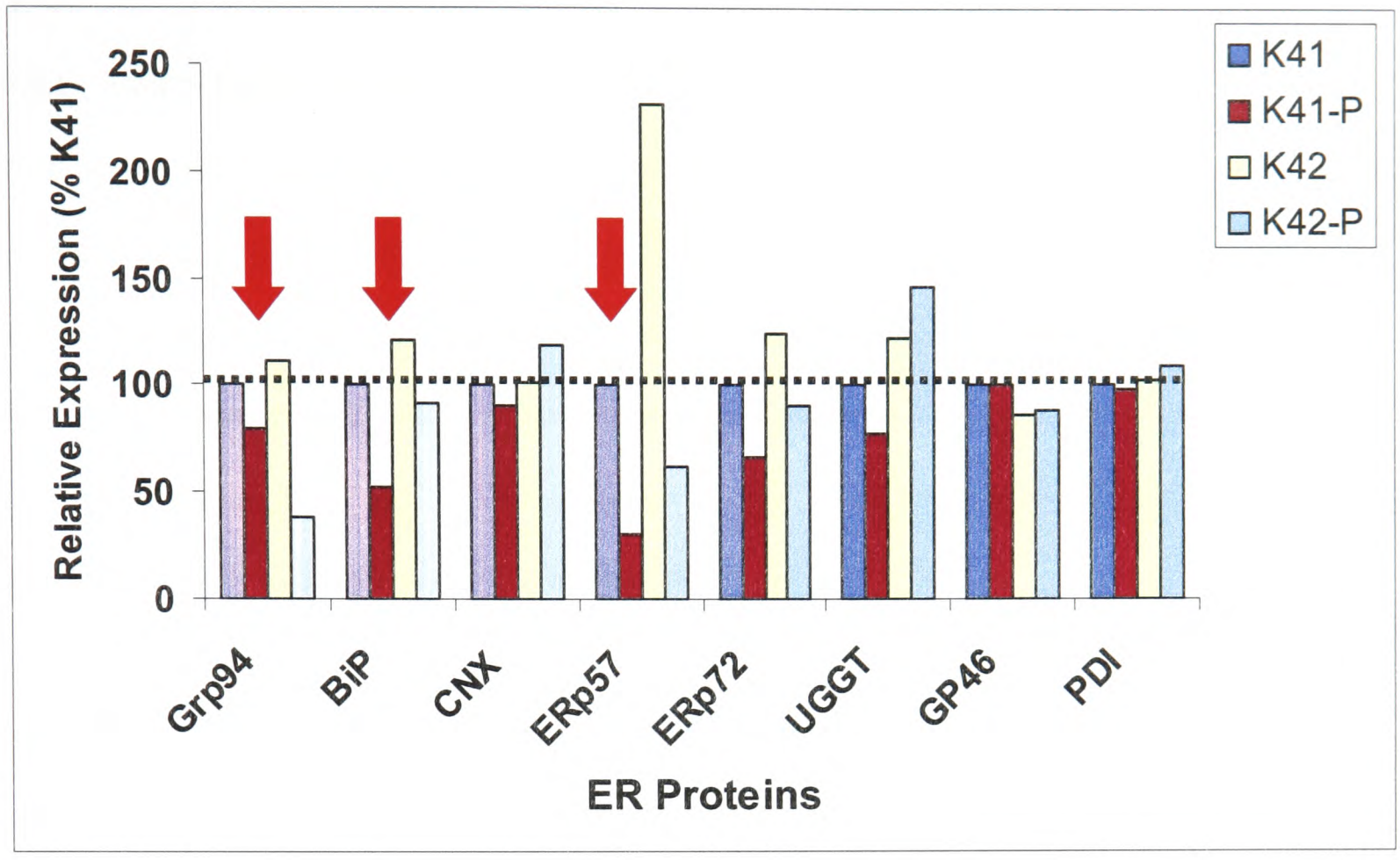

Figure 6.7.2. Affect of P- domain on the expression of ER resident proteins

Level of expression of indicated ER resident proteins was determined in K41, K41-P, K42 and K42-P by Western blotting. Aliquots of lysates (5µg protein determined by Bradford assay) from each of the cell lines was fractionated by SDS-PAGE, western blotted using appropriate antibodies and bands quantified using Quantity One software (BioRad Inc, USA). Expression of ER-resident proteins in various cell lines is shown as percentage expressed in K41 cells (i.e.,expression in K41 is shown as one hundred percent, shown by the dotted line. Red arrows indicate DOWNREGULATED proteins (Grp94, BiP and ERp57) in the P- domain transfected cells.

6.8 MECHANISMS FOR P-DOMAIN DOWNREGULATION OF SPECIFIC PROTEINS

6.8.1 Competition for substrates

It is clear that P- domain restores basal cytosolic calcium level in K42 and most probably upsets free ER calcium. Therefore, it is possible that P- domain may affect calcium-binding function of ER resident proteins like calnexin and calreticulin (in K41-P) and thereby affect calcium-dependent interactions with their glycosubstrates or with other proteins in the ER. In the absence of fruitful interactions with calnexin and/or calreticulin, their substrates will probably sent for degradation.

Although, physiological relevance is less clear, P- domain has been shown to interact with a set of ER proteins including Erp57 and BiP [227]. Both these proteins are downregulated in P- domain expressing cells. It is therefore possible that P- domain may disturb various protein cofactors interacting with either calnexin or calreticulin. For example, P- domain may not allow efficient and sufficient Erp57 binding to calnexin and calreticulin. In this way P- domain may alter the affinity of calnexin and calreticulin for their substrates as well as their chaperoning ability. Moreover, as P-domain is proposed to form a protein-binding site [184, 211, 212], it may compete with substrates of calnexin and calreticulin directly.

In order to determine whether P- domain affected proteins bound to calnexin and calreticulin, I performed coimmunoprecipitation experiments with anti-calnexin and anti-calreticulin antibodies in P- domain expressing K41 cells, and with anti-calnexin antibody in P- domain expressing K42 cells. Equal number of K41 and K41-P were first [^{35}S]-metabolically labelled for 40 minutes. Then immunoprecipitates of calnexin

and calreticulin made in digitonin were fractionated by SDS-PAGE and analysed by autoradiography. It is apparent from figure 6.8.1 that the majority of proteins brought down with either calnexin or calreticulin antibodies were downregulated (red arrowhead) in the P- domain transfected K41 and K42 cells where as expression of some other proteins was unaffected (blue arrowhead) consistent with the results described above. Moreover, the experiment also demonstrates affect on calnexin substrates by the P- domain of calreticulin implying functional homology between P-domains of calnexin and calreticulin. It is possible that P- domain may increase degradation for some proteins by binding to them, which would otherwise be substrates for calnexin and/or calreticulin. In other words P- domain may compete with calnexin and/or calreticulin binding to their substrates. I could not get antibody against P- domain and so I was not able to perform coimmunoprecipitation experiments to see whether any of the downregulated proteins seen on anti-calnexin and anti-calreticulin autoradiograph were binding to the P- domain.

6.8.2 Transcriptional regulation

There are several examples in the literature where calcium signalling has been shown to affect transcriptional regulation. For example, differential calcium signalling has been shown to affect calmodulin function, a protein that is known to phosphorylate the transcription factor NF-AT for its activation [348]. Active phospho form of NF-AT then moves to the nucleus to influence transcription of certain glycoproteins. Therefore, by affecting the functions of proteins like calmodulin, via its affect on calcium signalling, P- domain may regulate expression of various proteins.

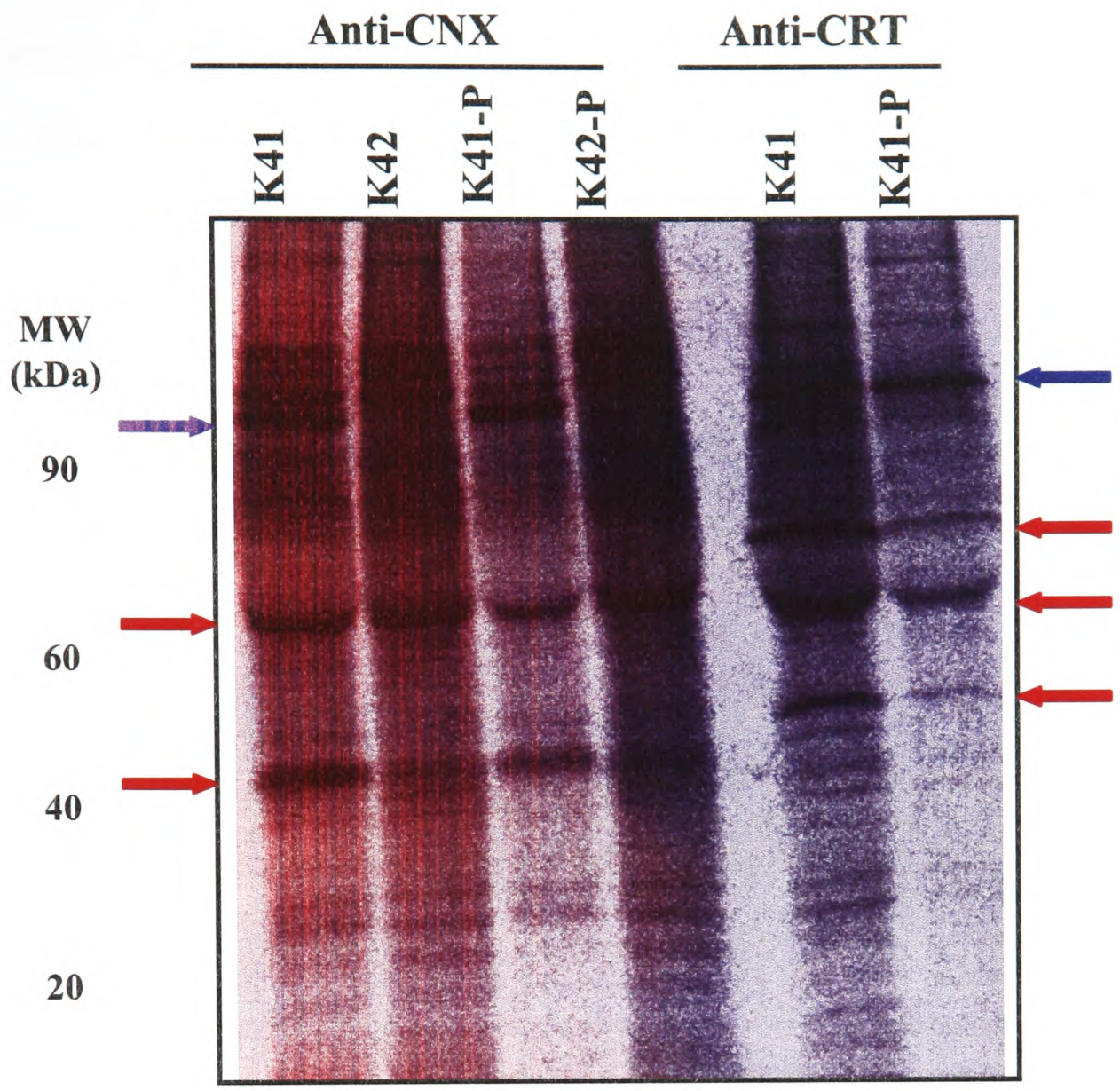

Figure 6.8.1 Calnexin (CNX)- and Calreticulin (CRT)- associated proteins in P- domain transfected K41 and K42 cells

Immunoprecipitates of CNX and CRT were made from K41, K42, K41-P and K42-P (for CNX) and from K41 and K41-P (for CRT), fractionated by SDS-PAGE and analysed by autoradiography. Proteins that are associated less with CNX and CRT in P- domain transfected cells are shown with red arrowhead and proteins that are not affected by the P-domain are shown by blue arrowhead.

Cytosolic calreticulin is involved in the nuclear export of glucocorticoid receptor [237]. Calreticulin is therefore, implicated in regulating the transcriptional activity of steroid hormone receptor. P- domain may also be involved in similar transcriptional regulation. Moreover, as P- domain contains nuclear localization signals [227], it may migrate to the nucleus and once there, could interact with transcription factors to regulate transcription.

In order to determine whether calreticulin P- domain affects synthesis of class I mRNA, I decided to carry out real time quantitative PCR to determine whether P-domain affects class I expression at the level of transcription.

This work was done in collaboration with Dr Zeina Jaffar (University of Southampton, UK). Briefly, real time quantitative PCR is based on the principle that TaqMan® continuously measures PCR product accumulation using a dual-labeled flourogenic oligonucleotide probe. This probe is labeled with two different fluorescent dyes, the 5' terminus reporter dye and the 3' terminus quenching dye. The sequence of the oligonucleotide probe is homologous to an internal target sequence present in the PCR amplicon. When the probe is intact, energy transfer occurs between the two flourophors, and the fluorescent emission is quenched. During the extension phase of PCR, the probe is cleaved by 5' nuclease activity of Taq polymerase. Therefore, the reporter is no longer in proximity to the quencher, and the increase in emission intensity is measured.

RNA was extracted from K41 and K41-P and cDNA generated from a measured quantity of RNA using RT-PCR. The cDNA was then used in the TaqMan® real time

PCR reaction. TaqMan® PCR analysis software was used to examine the fluorescence intensity of reporter and quencher dyes and to calculate the increase in normalized reporter emission intensity over the course of the amplification. To provide precise quantification of initial target in each PCR reaction, the amplification was plotted using a point during the early log phase of product accumulation above background.

The results are shown in figure 6.8.2. The results clearly demonstrate big difference in the amount of K^b mRNA present in K41 and K41-P. There is about 12-fold decrease in the expression of K^b mRNA when K41 expresses the P-domain. This result reflects the western blot data where the class I HC synthesis is down by about 10-fold in P-domain transfected cells. The results clearly suggest P-domain also has an effect at the transcriptional level.

6.9 CHAPTER SUMMARY AND DISCUSSIONS

In this chapter, I have shown that co-operation from all domains of calreticulin is important for calreticulin function in class I surface expression. This is to say although each domain possesses specific biochemical properties, they cannot on their own function as full-length calreticulin. NP- domain on its own was not able to restore class I surface expression in K42. P- and PC- domains not only failed to restore class I surface expression in K42, they downregulated class I expression in K42. This was not a clonal effect as one clone of K42 expressing the P- domain reverted back to the K42 phenotype in terms of class I surface expression. The effect

a.

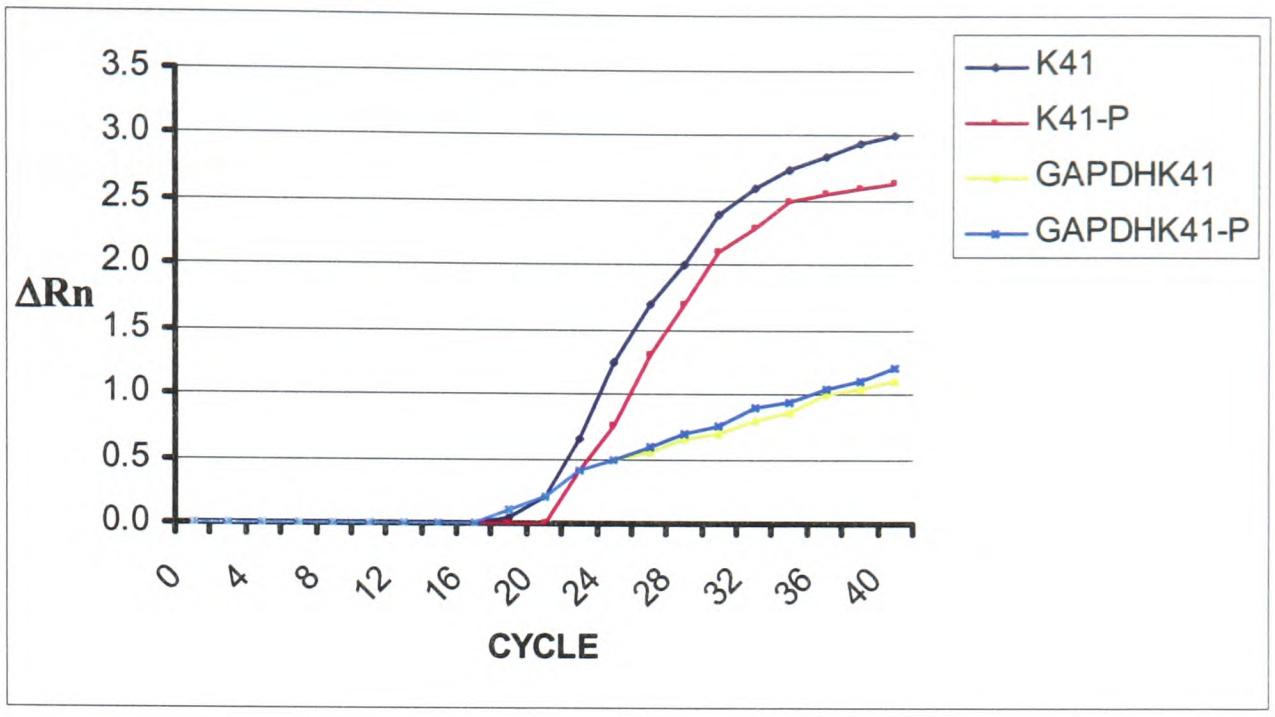

b.

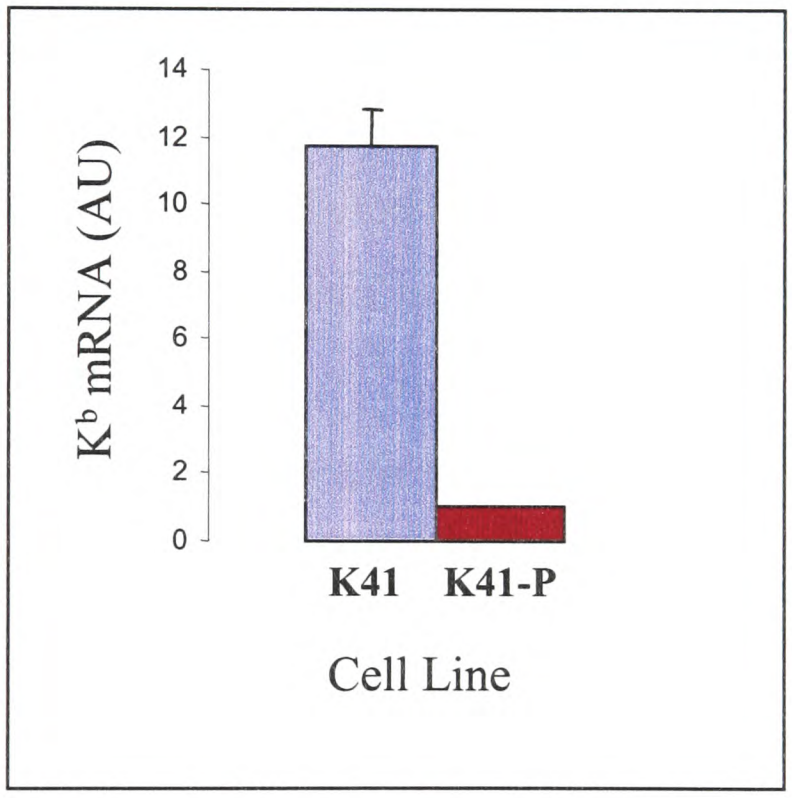

Figure 6.8.2. P- domain controls class I heavy chain expression at the transcriptional level.

K^b mRNA and GAPDH mRNA was extracted from K41 and K41-P and cDNA generated from a measured quantity of RNA using RT-PCR. The cDNA was then used in the TaqMan® real time PCR reaction to determine mRNA expression levels in K41 and K41 expressing the P- domain of calreticulin (K41-P). a) The results are shown as amplification units (ΔRn) versus number of PCR cycles. House keeping GAPDH gene was used as a control. b) Graphical representation of expression of K^b mRNA in K41 (expressed as arbitrary units (AU) compared to the K^b mRNA expression level in K41-P.

of P- domain was dominant as expression of P- domain in K41 resulted in downregulation of class I expression.

Downregulation of class I expression in P- domain expressing cells is probably not because these cells are under stress. ER stress transducer, PERK, normally phosphorylated in stressed cells, in not phosphorylated in K41-P and K42-P. P-domain expressed in K42 seems to be functional as it restored basal cytosolic calcium level in K42. This is also a strong indication that P-domain is properly folded in the ER. In support of this, 3D-structure of rat calreticulin P-domain has been recently determined by NMR [211, 212].

P- domain mostly affected the expression of membrane proteins. Downregulation of protein expression did not seem to be a result of accelerated degradation of proteins in P- domain expressing cells. P- domain affect on protein expression was not global as it affected the expression of only a subset of membrane as well as ER proteins.

The downregulation of protein expression by the P- domain may involve competition for substrates as well as transcriptional control. It is likely P- domain is involved in protein-protein interactions [184, 211, 212]. It is therefore possible that P- domain could compete with calnexin and calreticulin for binding to their substrates. Newly synthesized glycoproteins bound to P- domain in this way may fail to fold properly and may be destined for degradation. Although the rate of degradation of a model antigen was unchanged (figure 6.6.3), the data clearly show decreased calnexin and calreticulin binding to their substrates in cells expressing the P- domain (figure 6.8.1). It is therefore possible that downregulation of expression of certain membrane and ER

proteins is partly contributed by their increased degradation in the presence of the P-domain.

P- domain affected the expression of K^b at the level of transcription. P- domain restores basal cytosolic calcium level in K42. It is likely that the P- domain also influences free ER calcium. It is now known that changes in the free ER calcium affect (and perhaps control) many functions of the ER, including the synthesis of proteins [349], the interactions of chaperones with one another and their substrates [226, 231, 350, 351], and the activation of calcium influx via plasma-membrane channels [352]. Recent reports indicate that free ER calcium influences glucocorticoid-sensitive gene [353] as well as vinculin expression to modulate cell adhesiveness [220]. Therefore, there is a possibility that the P- domain, by affecting the free ER calcium concentrations, affects protein synthesis at the level of transcription.

P- domain contains nuclear localization signal. In regulating gene expression, it is tempting to include a possibility whereby P- domain would migrate to the nucleus and once there it could interact with transcription factors to influence transcription or act as a transcription factor itself to influence transcription of certain proteins including MHC class I.

Chapter 7

SUMMARY AND GENERAL DISCUSSIONS

7.1 CALRETICULIN

My study has demonstrated crucial role for calreticulin in the biogenesis of MHC class I. First, assembly of class I molecules was normal in the absence of calreticulin. Second, class I molecules associated with the "preloading" complex comprising TAP, tapasin, Erp57 and calnexin even in the absence of calreticulin, although the extent of binding may be impaired in the absence of calreticulin. Third, like tapasin [354], calreticulin is involved in peptide loading and optimisation. As a consequence, presentation of several epitopes is impaired in the absence of calreticulin. The assembly and antigen-presentation function of MHC class I molecules expressed in calreticulin-deficient cells share some features with MHC class I molecules expressed either in tapasin-deficient cells or those carrying a non-conservative mutation, which renders them unable to associate with TAP. So, why is calreticulin so critical in MHC class I biogenesis? There are several possible contributions of calreticulin, which lead to successful loading of class I molecules in the ER.

Stability of loading complex Newly assembled class I molecules are likely to be truly empty of peptide ligand and are not competent for export from the ER [290]. The newly assembled class I molecules very soon acquire suboptimal peptides and bind to calreticulin ready to be incorporated into the loading complex. It is possible that calreticulin may stabilise the interaction between class I and the TAP-tapasin complex, as suggested by the observation that aglycosylated A2.1 molecules show

reduced interaction with TAP and that castanospermine (which prevents the generation of the monoglucosyl-glycan recognised by calreticulin) inhibits the interaction between class I molecules and TAP [162, 294].

Assembly of class I Calreticulin may have a role in promoting assembly of class I HC with β2m. In support of this, wild-type A2.1 assembled better (57%) compared to A2.1T134K (45%), which fails to interact with calreticulin (and other cofactors of the peptide loading complex) ([180, 291] and Powis, submitted) in CEM cells. Moreover, slightly lower amount of heavy chain is recovered in calreticulin-deficient K42 cells [324]. However, when exogenous peptides were added, which stabilise only pre-assembled class I molecules and not promote *de novo* assembly [168], similar amount of class I were immunoprecipitated from K42 and K41 cells ([324]- manuscript supplied).

Peptide loading Calreticulin may be directly involved in the loading of peptides delivered through TAP on to the peptide-binding groove of class I. The mechanism of peptide loading by calreticulin is not known but there is evidence from peptide cross-linking experiments that calreticulin can bind to peptides delivered to the ER via TAP [355]. Moreover, two independent studies have demonstrated possibility of CD91 mediated uptake of immunogenic peptides bound to calreticulin, which can be taken up by antigen presenting cell and loaded onto class I for presentation to T cells [356], [357]. In addition, peptides eluted from calreticulin after its purification from tumour cells, also elicit T cell response [357]. It is possible, therefore, that calreticulin could chaperone peptides between TAP and class I, a function normally assigned to tapasin.

Modulation of ER enzyme activities Free ER calcium is reduced in calreticulin-deficient cells [343]. Moreover, free ER calcium has been shown to regulate activities of ER resident chaperones and other proteins [227]. Therefore, it is possible that through calcium regulation, calreticulin may modulate activity of ER-resident proteases which are involved in modification or trimming of longer peptides within the ER. In support of this, ER resident gp96 has been identified as a calcium-dependent aminopeptidase capable of trimming a precursor T cell epitope *in vitro* [155].

Optimisation of peptide cargo It is possible that calreticulin may be involved in peptide optimisation like tapasin [15, 296]. Peptide optimisation could be achieved either by the ability of calreticulin to retain class I molecules in the ER or retrieve them from the early secretory pathway. Pentcheva and Edidin have recently demonstrated that mutated class I molecule that fails to associate with the loading complex (T134K) enters the secretory pathway prematurely at an exit site in the ER that is different for wild-type class I molecules [358]. In doing so, T134K molecules bypass a novel step involved in the selective export of peptide-loaded MHC class I molecules from the ER. Similar situation is possible in calreticulin-deficient calls, where class I molecules may escape peptide optimisation and quality control. Calreticulin may also be involved in recycling of suboptimally loaded class I molecules from ERGIC/Golgi to the ER [301]. Recycling is an important quality control step to ensure proper folding of several glycoproteins and is mediated by the recognition of either a cytoplasmic KKXX motif or a carboxy-terminal KDEL motif. Class I molecules, however, lack these recycling recognition motifs. However, since calreticulin has KDEL retrieval sequence, it is possible that calreticulin can associate

with class I in the Golgi and retrieve them to the ER (figure 7.1). If this is to be the case, calreticulin probably has the ability to distinguish between a class I molecule that is suboptimally loaded and one that is sufficiently stable to exit to the cell surface. In light of this, it is to be noted that Li *et al.*, found that calreticulin predominantly associated with empty class I molecules while tapasin associated with both empty and peptide loaded class I molecules [359]. In support of a possible role for calreticulin in recycling, it has recently been shown that quality control of TCR α chain depends on cycling between the Golgi and the ER via KDEL-dependent retrieval [360].

7.2 CALNEXIN

My study of the calnexin-deficient cell line CEM.NK^R has confirmed the role of calnexin in the assembly of class I HC with β2m. When CEM (calnexin competent) and CEM.NK^R (calnexin-deficient) were infected with recombinant vaccinia virus encoding HLA-A2.1, same amount of class I HC was synthesised in both cells and I did not observe differences in the rate of degradation of class I in these cells. However, using pulse-label followed by overnight pre-clear and immunoprecipitation, the amount of class I that could be recovered with conformational-sensitive antibody in the presence of peptide, and therefore the total amount of class I assembled during the pulse-label, was significantly different in CEM and CEM.NK^R cells. Less than half of A2.1 assembled in CEM.NK^R (25%) compared to CEM (57%). This was despite 1.5 fold increase in calreticulin expression in CEM.NK^R cells. Therefore, this result clearly suggests an important role of calnexin in class I HC assembly with β2m. Calnexin may improve the efficiency of assembly by performing several distinct functions.

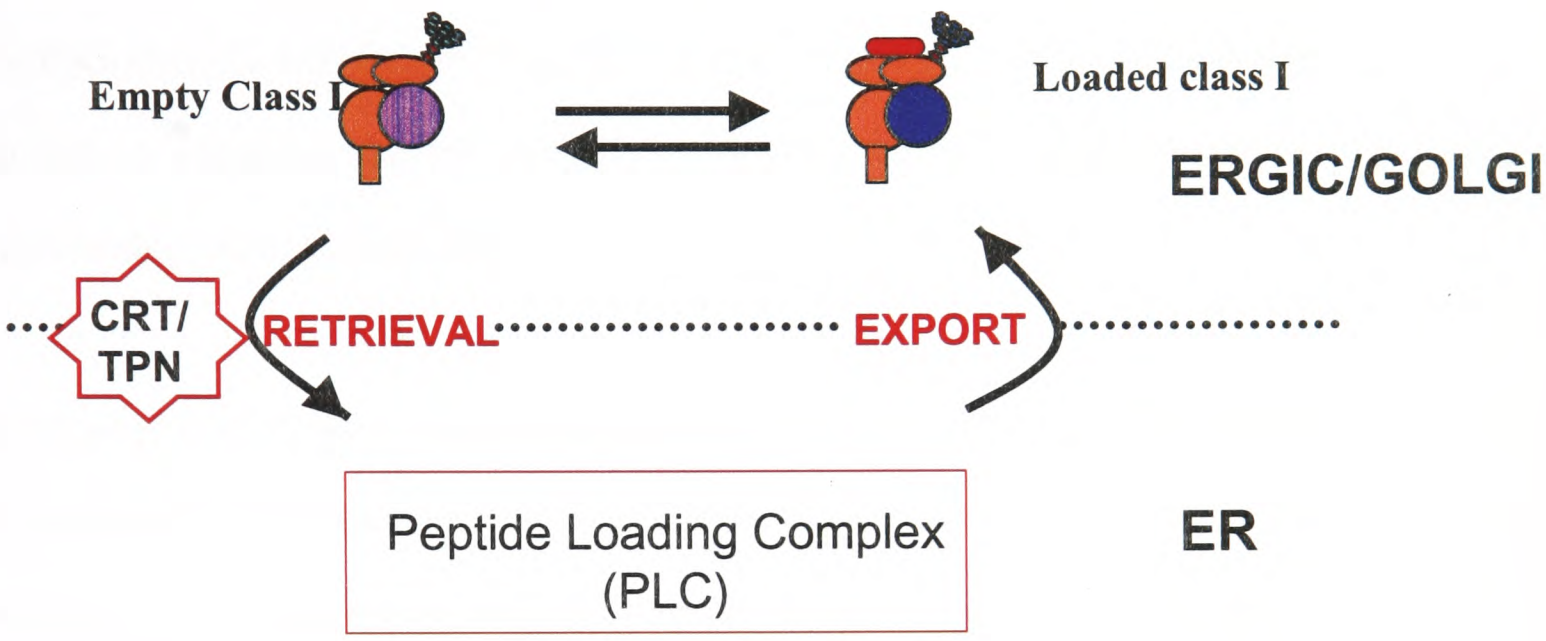

Figure 7.1 Calreticulin may be involved in the retrieval of empty class I from the ERGIC/Golgi compartments into the ER where loading with optimal peptide can occur again. CRT/TPN, Calreticulin/Tapasin

Erp57 recruitment Calnexin is associated with class I HC soon after its synthesis and before the formation of intra-chain disulfide bonds within the α2 and α3 domains. Several studies have used cross-linking approach to identify ERp57 as a partner that interacted with glycoproteins including class I forming a complex with calnexin [361], [283, 362, 363]. The interaction of ERp57 with a nondisulphide-bonded population at earlier time points suggests a role for ERp57, in association with calnexin, in the folding and disulfide bond formation of heavy chain [285]. Moreover, it has been demonstrated that only the fully disulfide-bonded form of HC is assembled with β2m, emphasizing that the formation of disulfide bonds is a requirement for correct folding and assembly [364].

Prevention of degradation Calnexin may have a pivotal role in stabilising class I HC and prevent from premature degradation [365]. When heavy chain is expressed in *Drosophila* cells in the presence of β2m, assembly occurs; however, co-expression of calnexin prevents heavy chain degradation and thereby increases the yield of MHC Class I molecules [366]. Co-expression of calnexin with K^b and D^b in *Drosophila* cells has been shown to extend half-lives class I molecules by four- and fivefold, respectively, again suggesting that calnexin protects the heavy chains from rapid intracellular degradation [196]. A more direct evidence for the role of calnexin in prevention of degradation of class I HC has come from mammalian semipermeabilized (SP) cell system pioneered by Wilson *et al.*, that faithfully reconstitutes the proteasome-mediated degradation of class I heavy chain [198]. In their study, the authors translated heavy chain in SP cells derived from either calnexin-competent (CEM) or calnexin-deficient (CEM-NK^R) cell line and added. When the SP cells were isolated from the translation mix and added to the untreated

reticulocyte lysates (does not contain haemin which interferes with proteasomal activity), very rapid degradation of heavy chain was observed for those derived from CEM-NK^R, which could be blocked by lactacystine, a specific inhibitor of proteasome. Rapid degradation was also observed for heavy chain products translated in the presence of castanospermine (a drug that prevents generation of monoglucosylated glycoproteins to which calnexin and calreticulin bind), and added to the untreated reticulocyte lysates in the presence of castanospermine [198].

A recent experiment by Paulsson *et al.* has explored the relationship between calnexin association, β2-m association and HC degradation [197]. A pulse-labelled cohort of newly synthesised HC in a β2-m-negative cell line dissociated from calnexin with a half-life of 10 minutes (whereupon it was rapidly degraded), whereas in cells that expressed β2-m but lacked TAP (.174), HC dissociation from calnexin had a half-time of 30 min. (whereupon it assembled with β2-m). None of the HC bound to calnexin was also bound to β2-m. This observation suggests therefore that binding of HC to β2-m protects it from intracellular degradation – allowing it to rebind to calnexin upon dissociation of β2-m thereby apparently prolonging the interaction between HC and calnexin. As we have already mentioned, binding of HC to calnexin also protects it from degradation. It is unclear whether HC binds to β2-m while it is associated with calnexin leading to its rapid dissociation, or whether β2-m binds only to free HC, but the overall effect seems to be to sequester free HC from degradation.

Peptide optimisation It is possible calnexin may play an indirect role in peptide optimisation of class I molecules. I determined cell surface expression of HLA-B35 molecules in calnexin and calreticulin over expressing HeLa cells. There was a

significant (20-40%) increase in the number of stable class I molecules expressed in calnexin or calreticulin overexpressing HeLa cells compared normal HeLa cells suggesting a role of calnexin in peptide loading and optimisation. Moreover, Sadasivan *et al.*, eluted peptides from MHC class I expressed on CEM and CEM.NK^R cells [330]. Their data showed differences in the HPLC profiles of peptides eluted from MHC class I molecules expressed on CEM and CEM.NK^R cells suggesting differential loading of peptides in calnexin-positive and calnexin-negative cells. How calnexin may mediate peptide optimisation is unclear but as a calcium-binding protein, it may modulate calcium-dependent trimmases in the ER. ER resident gp96 has recently been identified as a calcium-dependent aminopeptidase capable of trimming long precursor peptides *in vitro* [155]. Some studies have also suggested trimming of polypeptides by Erp57 *in vitro* [367-369]. As Erp57 is found in complexes with calnexin, it is possible that calnexin may regulate trimming function of Erp57.

7.3 HEAVY CHAIN GLYCOSYLATION

I have followed through the process of expression and assembly to the antigen presentation by aglycosylated and differentially glycosylated HLA-A2.1 molecules to evaluate role of glycosylation at each stage. The results indicate that glycosylation in human class I HC is optimal and any alteration from normal glycosylation impairs loading (and perhaps some assembly) of MHC class I molecules with optimal peptide cargo. Similar amounts of HCs were recovered in cells expressing A2.1 with altered glycosylations of the HC. Peptide loading was impaired in class I with altered glycosylation despite being able to associate with the TAP complex. Cell surface expression of class I molecules with altered glycosylation could never reach the level

of wild-type class I molecules even in the presence of exogenous supply of stabilising peptides although the synthesis of HC was comparable suggesting a defect in the assembly of HC (with altered glycosylation) with β2m. There are several possible contributions of glycosylation at position 86 of human class I HC to the observed phenotype.

Assembly In the absence or in abnormal glycosylation of class I heavy chain, calnexin may not be able to interact to the heavy chain efficiently to promote assembly with β2m.

Interaction with the loading complex: Altered glycosylation of the HC, although allowing TAP interaction, may destabilise qualitative interactions between class I and the TAP-tapasin complex for efficient loading of peptides onto class I. Alterations in the glycosylation patterns of class I HC may alter the conformation of the assembled class I, which may affect qualitative interactions with the TAP complex. While I observed interactions of aglycosylated class I with the TAP complex, some studies have shown that castanospermine treatment, which prevents the generation of the monoglucosyl-glycan, inhibits interactions between class I molecules and TAP [162, 294]. In this regard, it needs to be noted that treatment of cells with castanospermine has global affect on all glycosylated proteins rather than a specific affect on class I.

Antigen presentation: Although aglycosylated as well as hyperglycosylated HLA-A2.1 were able to process and present influenza matrix protein derived epitope like the wild type HLA-A2.1 to A2.1 restricted CTL, these data, however, should be interpreted with caution. It is possible there may be important defects in presentation

that may not be evident when looking at just a few immunodominant epitopes. Moreover, there is accumulating evidence that T cells recognise MHC class I:glycopeptide complex [370, 371].

7.4 A MODEL FOR MHC CLASS I ASSEMBLY

A model is proposed which incorporates major experimental data demonstrating the pivotal role of calnexin and calreticulin in the generation of fully assembled class I molecules (figure 7.4). In the early stage of class I assembly, calnexin binds to newly synthesised class I HC and protects from degradation allowing HC folding. Calnexin also recruits Erp57, which promotes disulfide bond formation within the HC. Calnexin remains associated with HC until β2m binds. Upon β2m binding, at least in human class I alleles, which have just one glycosylation site at asparagine 86, class I undergoes a conformational change [168] and calnexin dissociates from class I HC and is replaced by calreticulin. At this stage majority of class I molecules are competent to egress from the ER and are loaded with suboptimal peptides that bind to class I peptide-binding groove with low affinity. Class I molecules and calreticulin then bind to the "preloading" complex comprising of TAP, tapasin, Erp57 and calnexin which results in the displacement of calnexin (in human cells) forming the "loading" complex [372]. It is here that class I molecules loaded with "sub-optimal" (low-affinity) peptide cargo are exchanged for "optimal" peptides which have high-affinity of binding, a function given to tapasin [354] and now also to calreticulin [324]. Optimally loaded class I molecules then egress to the cell surface for presentation to the T cells, and those, which are sub-optimally loaded are destined for degradation.

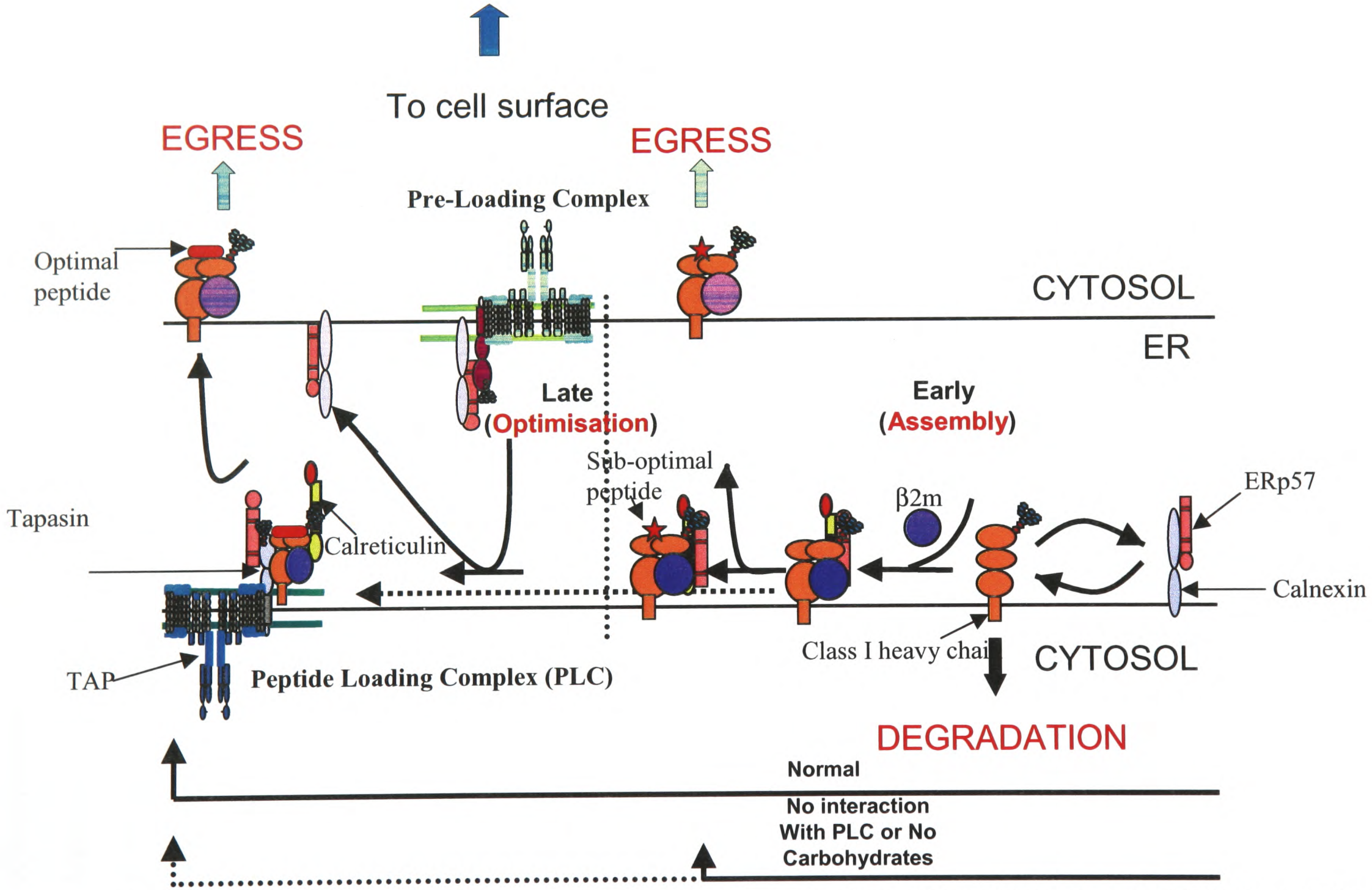

Figure 7.4 A model for the assembly of class I MHC molecules in the ER, which has been divided into an early assembly and late optimisation stages. Calnexin plays an important role in the early assembly of class I heavy chain with β2m. Calreticulin is important in the optimisation of peptide cargo in the later stages of class I assembly. Note that optimisation is also prevented when class I heavy chain has altered glycosylations, or when class I is prevented from interacting with the peptide loading complex.

A bigger picture on the role of calnexin and calreticulin in class I assembly is beginning to emerge. Calnexin increases the efficiency of class I assembly by preventing class I HC from degradation and recruiting Erp57 to promote disulfide bond formation. On the other hand, calreticulin is involved in peptide loading and optimisation, which results in the generation of fully assembled and optimally loaded class I molecule that is competent to display bound peptide on the surface of antigen presenting cells to T cells. It is interesting to note that calreticulin associates with folded class I HC-β2m heterodimer and therefore recognises conformational-sensitive determinants and not unfolded determinants. In this regard, it is different to calreticulin association during folding of vesicular stomatitis virus G (VSVG) protein and hemagglutinin (HA). Moreover, it is unclear whether calreticulin associated class I HC-β2m heterodimer is a substrate for UDP-Glucose:glycoprotein glucosyltransferase (UGGT), but if it is, it will be interesting to find out why a folded class I HC-β2m heterodimer can be a substrate for UGGT. UGGT may be able to detect particular environment around asparagine 86 of class I HC that allows it to sense a subtle conformational change in class I molecule when an optimal peptide is bound. It thus appears that during evolution class I has utilised calreticulin not as a classical chaperone to assist in its folding but to assist in peptide loading and optimisation.

7.5 WHAT MAY BE THE FUNCTION OF P- DOMAIN?

The three dimensional structure of rat calreticulin P- domain, encompassing residues 189-288, has now been determined using NMR [211, 212]. The structure of the lumenal domain of calnexin has also been solved by X-ray crystallography [184]. The structural features of the P- domain region of calnexin are similar to the structure of

calreticulin P- domain determined by NMR [184, 211, 212]. These structures have demonstrated that the long held view that P- domain may form carbohydrate-binding site may not be entirely true. Instead, it has been suggested that the protrusion of the P- domain region from the calreticulin core could constitute a protein-ligand binding site. Moreover, the negatively charged amino acid residues decorate the tip of the hairpin loop. This could constitute a binding site for an interacting protein and the inner repeats could serve as "spacers" for positioning the ligand-binding site at a discrete distance from the core of the protein.

The downregulation of protein expression by the P- domain may involve competition for binding to substrates. For example, it is possible that P- domain could compete with calnexin and calreticulin for binding to their substrates. Newly synthesized glycoproteins bound to P- domain in this way may fail to fold properly and may be destined for degradation. Although the rate of degradation of a model antigen was unchanged (figure 6.6.3), the data clearly show decreased calnexin and calreticulin binding to some of their substrates in cells expressing the P- domain (figure 6.8.1). It is therefore possible that downregulation of expression of certain membrane and ER proteins is partly contributed by their increased degradation in the presence of the P-domain.

P- domain affects class I expression at the level of transcription. It may do so for other proteins as well. It restores basal cytosolic calcium level in K42. P- domain may also influence free ER calcium either directly or indirectly via its ability to interact with other calcium-binding proteins or with proteins that are involved in calcium regulation. For example, site-directed mutagenesis and truncation studies have shown

that residue N-1036 of SERCA2b and the P- domain are essential for calreticulin-dependent effects on SERCA2b function [224]. Therefore, it is possible for P- domain to modulate SERCA function, which are involved in the uptake of calcium into the ER. It is now known that changes in the free ER calcium affects (and perhaps control) many functions of the ER [226], including the synthesis of proteins [349], the interactions of chaperones with one another and their substrates [226, 231, 350, 351], and the activation of calcium influx via plasma-membrane channels [352]. Moreover, several reports indicate that free ER calcium influences glucocorticoid-sensitive gene expression [353] as well as vinculin expression to modulate cell adhesiveness [220]. Therefore, there is a possibility that the P- domain, by affecting the free ER calcium concentrations, could modulate gene expression from within the ER. It is to be noted that other ER-resident proteins, such as BiP and Erp61 (a PDI) homologue, have also been shown to regulate gene expression [353].

More recently, Holaska *et al.,* have demonstrated the existence of cytosolic calreticulin [237]. Cytosolic calreticulin interacts with the DNA-binding domain (DBD) of glucocorticoid receptor (GR), and this interaction has been shown to be functional as a nuclear export signal (NES). By preventing DBD interaction with the DNA response elements of a particular gene, these protein–protein interactions underlie a nuclear export–based mechanism for antagonizing the transcriptional activation potential of GR, and may represent an important regulatory step for other nuclear receptors as well. It is possible that P- domain may regulate gene expression of a variety of proteins in a similar manner.

Finally, P- domain has been suggested to contain nuclear localization signal. In regulating gene expression, it is tempting to include a possibility whereby P- domain would migrate to the nucleus and once there it could interact with transcription factors to influence transcription or act as a transcription factor itself to influence transcription of certain proteins including MHC class I. Nuclear localisation of P-domain could be tested with a GFP-tagged P- domain. Moreover, microarray analysis of P- domain expressing cells could yield information on selective regulation of proteins by the P- domain. Moreover, analysis of P- domain expressing and control cells at a particular point in their cell cycle could yield information on the regulation by P- domain of proteins involved in cell growth and proliferation.

7.6 CONCLUDING REMARKS

Immunity is controlled by immunodominance. Selection of particular peptide epitopes from a big repertoire and their presentation by dendritic cells or any other antigen presenting cells is a major influencing factor on immunodominance. Therefore, anything that affects this process has a potential to affect immunodominance.

A great deal of progress has been made in the elucidation of many of the key processes involved in MHC class I assembly and peptide optimisation recently and we are now in a position to appreciate how the increasing number of cofactor molecules work together to produce a fully assembled and optimally loaded class I molecules for presentation to T cells. Understanding the process of peptide "optimisation" in greater depth has potential to identify targets for immunoinvasion and consequently open up avenues for immunotherapy.

However, there is still great deal to be understood about the processes that occur within the ER and in the Golgi, which lead to peptide optimisation. One suggestion is that calreticulin (or indeed tapasin and Erp57) promotes recycling of suboptimally loaded class I molecules from the ERGIC/Golgi to the ER [301, 324]. This could be tested by the use of inhibitors of retrograde transport and compared to K42. A recent paper has suggested existence of two exit sites for class I molecules from the ER [358]. Calreticulin has been suggested to control distribution of newly assembled class I molecules between these two exit sites of the ER, only one of which has access to TAP-tapasin [324]. Expressing T134K and wild-type class I tagged with different fluorescent labels and comparing their distribution in K41 and in K42 could allow better understanding of the role of calreticulin in the distribution of class I molecules in these two subdomains of the ER.

Function of Erp57 remains largely unclear. It can be found in the TAP complex in the absence of calreticulin, suggesting it interacts with the loading complex directly [324, 373]. Moreover, it forms disulphide bond with tapasin [373]. Erp57 has been implicated to be involved in disulphide bond isomerisation in MHC class I molecules bound to the peptide loading complex, which may allow efficient peptide loading and peptide editing by tapasin [373]. Recently, gp96 was identified as an ER peptidase [155]. More work is required to identify and characterise ER trimmases. It is clear that viruses can evolve very quickly and acquire strategies to prevent presentation of their peptides and thus avoid recognition by T cells. It is only by understanding fully the exact nature of class I assembly and peptide optimisation at molecular level that we will be able to address immune-invasion and design targets for immune-therapy.

APPENDIX 2.14

Map of pCDNA3

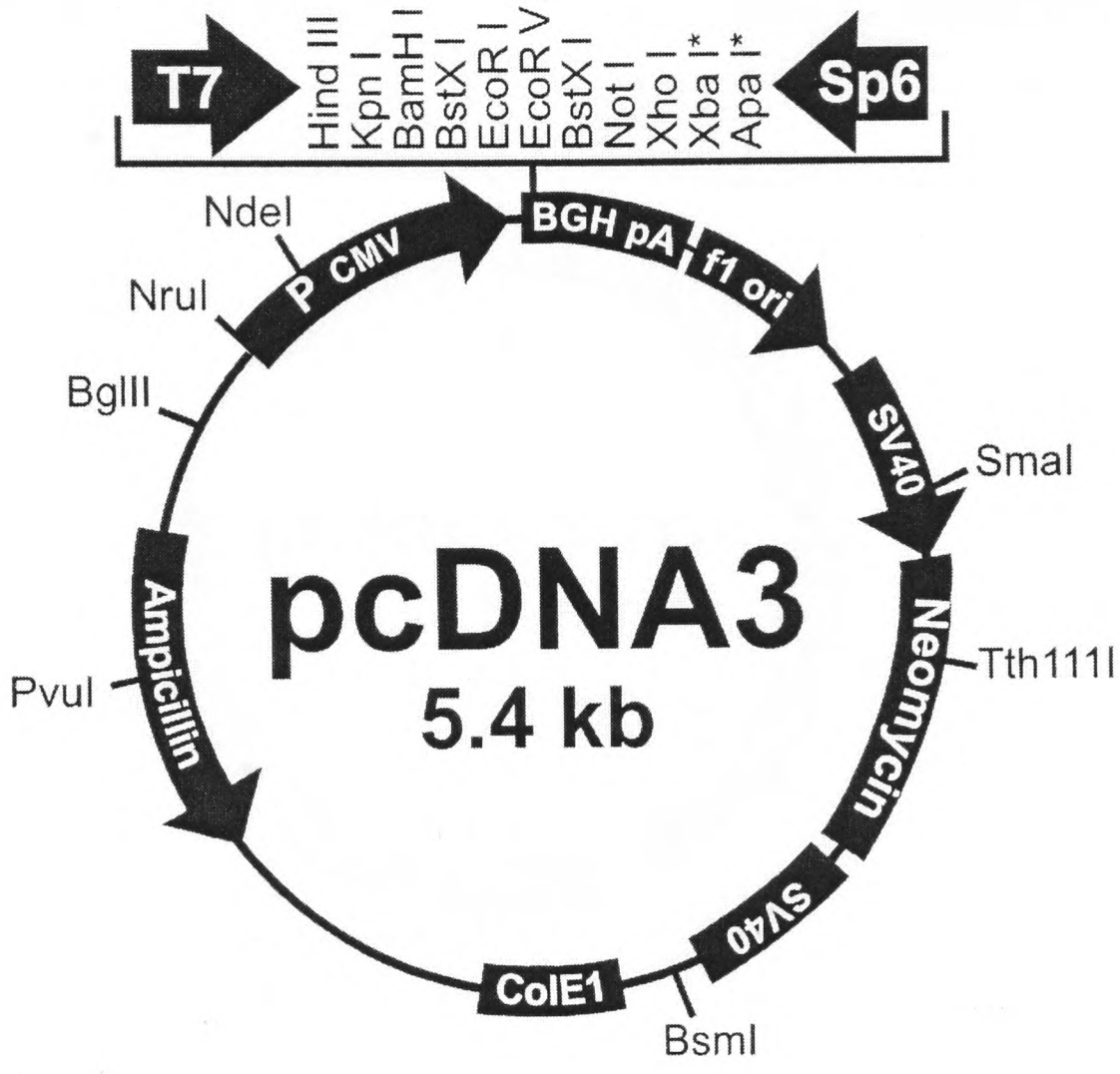

Map of pUB6/V5

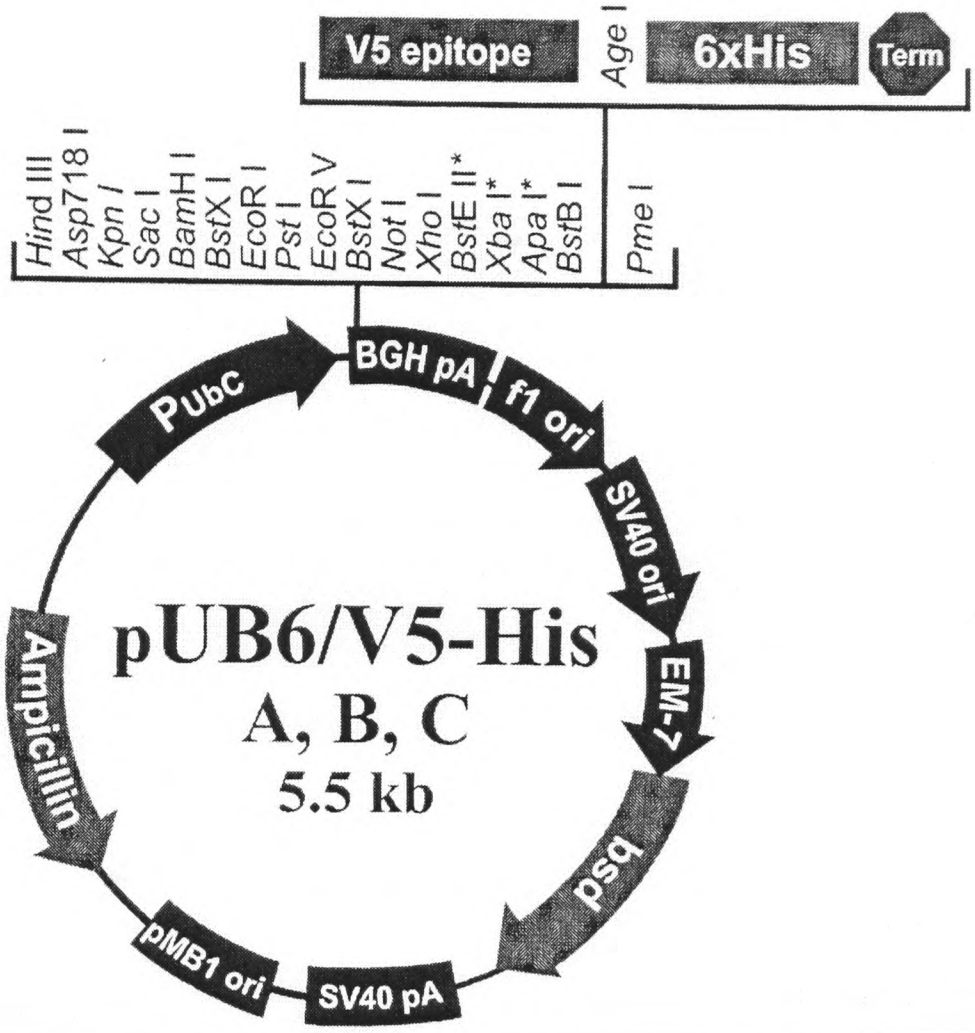

APPENDIX 5.6

Investigation into Binding of BB7.2, Calreticulin and BBM.1 to MHC class I components.

Reagents

Fully folded Biotin-labelled Class I heavy chain + β2m + peptide

- Flow Cell-1 (FC-1) was used as blank throughout the experiment: Red Line curve
- FC-2 fully folded MHC class I was immobilised: Green line curve
- FC-3 Fully folded class I was immobilised: Blue line curve
- FC-4 Fully folded class I was immobilised: Pink line curve

Experiment 1: *Immobilisation of MHC class I on FC-1 to FC-4*

Reagents: MHC class I, 100μl of 50μg/ml concentration was used. Temp 25C. Injection speed was 5μl/min. Measured over 7 minutes

Results

- A clear binding of biotinylated class I trimer to the avidin chip was observed
- It was concluded however that the binding signal was lower than expected. Has to be in the thousands rather than hundreds (about 250 RU). The reason for the observed binding could have been single rather than multiple biotinylation of the heavy chain. It was suggested multiple biotinylation of either HC or β2m for future experiments.
- It was unclear why MHC class I trimer binding in FC-2 was different from binding in the other two FCs. It was suggested free biotin in the solution could compete with biotin in HC of Class I for binding to the Avidin Chip.

Experiment 2: *Binding of BB7.2 to fully folded MHC class I*

Reagents: BB7.2 used 100μl (50μg/ml). Speed 5μl/min. Temp 25C BB7.2 was injected in FC-1 and FC-2. Measured over 7 minutes

Results

- Antibody binding to fully folded MHC class I was clearly observed (compared to the blank) although again the signal intensity was not that great (300 RU)
- BB7.2 seems to have 2 on rates and a single off rate. Result of divalent binding
- The slow dissociation of the antibody from MHC class I was observed over time

Experiment 3: *Elution of Peptides from folded MHC class I trimer*

Reagents: Glycine buffer, pH 3.0. 35µl of buffer was injected over FC-3 over a period of 7 minutes

Results

- Slow exponential decrease in the earlier curve of FC-3 was observed indicating elution of peptides (and some β2m) from MHC class I trimer.

Experiment 4: *Binding of full length Calreticulin (CRT) to MHC class I dimer*

Reagents: 100 µl of CRT (50µg/ml) was injected over FC-1 to FC-4 over a period of 7 minutes. Calreticulin was only expected to bind to MHC class I dimer in FC-3 and possibly in FC-1 (non-specific binding of CRT)

Results

- A very clear binding (although again the signal was weak) was seen with MHC class I dimer in FC-3. As expected, CRT bound non-specifically to blank FC-1. The true controls were MHC class I trimer in FC-2 and FC-4.
- After the best fit, the $K_{(association)}$ was calculated to be 9.48×10^3 [ka in 1/Ms] and $K_{(dissociation)}$ to be 1.36×10^3 [kd in 1/s]
- The reason for low binding was probably for the following reasons
  - Lowering the pH eluted peptide as well as β2m hence actual number of HC-β2m dimers were low
  - It could be protein-protein interation between CRT and HC-β2m less important than carbohydrate recognition by CRT. It may be that binding of CRT to sugar residues is the initial step in binding to HC-β2m dimer. This result however provides an evidence for protein-protein interaction [the CRT used for the experiment was glycosylated- produced in yeast]

Experiment 5: *Dissociation of CRT following addition of EDTA*

Reagents: 35µl EDTA buffer was injected into FC-1 to FC-4

Results

- The addition of EDTA [Ca^{2+} chealater] brought back FC-3 curve in line with other curves confirming the dissociation of CRT from HC-β2m dimer in FC-3

Experiment 6: *Binding of BBM.1 to folded MHC class I complex*

Reagents: 100µl of BBM.1 (50µg/ml) was injected into all flow cells over a duration of 7 minutes

Results

- Binding was detected in flow cells 2 and 4 and not in FC-3 and FC-1 as expected.

Experiment 7: *Reassociation of β2m with HC*

Reagents: 100 µl of β2m (50µg/ml) was injected into FC-1 to FC-4 over a period of 7 minutes.

Results

- Although expected, binding and thus increase in the FC-3 curve didn't happen. This may be because it takes longer time for folding into HC-β2m heterodimer.

Two further experiments were carried out. Glycine pH3.0 buffer was used to elute peptide and BB7.2 from FC-2 and FC-4. All curves roughly came to the baseline but addition of full-length calreticulin didn't shift up the curve lines, as was expected for FC-2, (FC-3) and FC-4.

REFERENCES

1. Paul, W., *Fundamental Immunology*. 3rd ed. 1993, New York: Raven Press.
2. Kuby, J. Immunology, ed. W. Freeman. 1997, New York. 335-355.
3. Koopmann, J.O., G.J. Hammerling, and F. Momburg, Generation, intracellular transport and loading of peptides associated with MHC class I molecules. *Curr Opin Immunol*, 1997. 9(1): p. 80-8.
4. Germain, R.N., MHC-dependent antigen processing and peptide presentation: providing ligands for T lymphocyte activation. *Cell*, 1994. 76(2): p. 287-99.
5. Germain, R.N. and D.H. Margulies, The biochemistry and cell biology of antigen processing and presentation. *Annu Rev Immunol*, 1993. 11: p. 403-50.
6. Heemels, M.T. and H. Ploegh, Generation, translocation, and presentation of MHC class I-restricted peptides. *Annu Rev Biochem*, 1995. 64: p. 463-91.
7. York, I.A. and K.L. Rock, Antigen processing and presentation by the class I major histocompatibility complex. *Annu Rev Immunol*, 1996. 14: p. 369-96.
8. Bouteiller Le, P., HLA class I chromosomal region, genes and products: facts and questions. *Crit Rev Immunol*, 1994. 14: p. 89-129.
9. Albertella, M.R., et al., Localization of eight additional genes in the human major histocompatibility complex, including the gene encoding the casein kinase II beta subunit (CSNK2B). *Genomics*, 1996. 36(2): p. 240-51.
10. Milner, C.M. and R.D. Campbell, Genes, genes and more genes in the human major histocompatibility complex. *Bioessays*, 1992. 14(8): p. 565-71.
11. Parham, P., E.J. Adams, and K.L. Arnett, The origins of HLA-A,B,C polymorphism. *Immunol Rev*, 1995. 143: p. 141-80.
12. Belich, M.P., et al., Proteasome components with reciprocal expression to that of the MHC- encoded LMP proteins. *Curr Biol*, 1994. 4(9): p. 769-76.
13. Pamer, E. and P. Cresswell, Mechanisms of MHC class I--restricted antigen processing. *Annu Rev Immunol*, 1998. 16: p. 323-58.
14. Ortmann, B., et al., A critical role for tapasin in the assembly and function of multimeric MHC class I-TAP complexes. *Science*, 1997. 277(5330): p. 1306-9.
15. Lehner, P.J. and J. Trowsdale, Antigen presentation: coming out gracefully. *Curr Biol*, 1998. 8(17): p. R605-8.
16. Herberg, J.A., et al., Genomic analysis of the Tapasin gene, located close to the TAP loci in the MHC. *Eur J Immunol*, 1998. 28(2): p. 459-67.
17. Kaufman, J., et al., The chicken B locus is a minimal essential major histocompatibility complex. *Nature*, 1999. 401(6756): p. 923-5.
18. Bjorkman, P.J. and P. Parham, Structure, function, and diversity of class I major histocompatibility complex molecules. *Annu Rev Biochem*, 1990. 59: p. 253-88.
19. Rosenthal, A.S. and E.M. Shevach, Function of macrophages in antigen recognition by guinea pig T lymphocytes. I. Requirement for histocompatible macrophages and lymphocytes. *J Exp Med*, 1973. 138(5): p. 1194-212.
20. Zinkernagel, R.M. and P.C. Doherty, Restriction of in vitro T cell-mediated cytotoxicity in lymphocytic choriomeningitis within a syngeneic or semiallogeneic system. *Nature*, 1974. 248(450): p. 701-2.
21. Blanden, R.V., et al., Genes required for cytotoxicity against virus-infected target cells in K and D regions of H-2 complex. *Nature*, 1975. 254(5497): p. 269-70.

22. Zinkernagel, R.M. and P.C. Doherty, Immunological surveillance against altered self components by sensitised T lymphocytes in lymphocytic choriomeningitis. *Nature*, 1974. 251(5475): p. 547-8.
23. Zinkernagel, R.M. and P.C. Doherty, H-2 compatability requirement for T-cell-mediated lysis of target cells infected with lymphocytic choriomeningitis virus. Different cytotoxic T- cell specificities are associated with structures coded for in H-2K or H-2D. *J Exp Med*, 1975. 141(6): p. 1427-36.
24. Zinkernagel, R.M. and P.C. Doherty, MHC-restricted cytotoxic T cells: studies on the biological role of polymorphic major transplantation antigens determining T-cell restriction-specificity, function, and responsiveness. *Adv Immunol*, 1979. 27: p. 51-177.
25. Zinkernagel, R.M. and K.L. Rosenthal, Experiments and speculation on antiviral specificity of T and B cells. *Immunol Rev*, 1981. 58: p. 131-55.
26. Klein, J., *Natural History of the Major Histocompatability Complex.* 1986, Chichester: Wiley.
27. Townsend, A.R. and J.J. Skehel, Influenza A specific cytotoxic T-cell clones that do not recognize viral glycoproteins. *Nature*, 1982. 300(5893): p. 655-7.
28. Bennink, J.R., J.W. Yewdell, and W. Gerhard, A viral polymerase involved in recognition of influenza virus-infected cells by a cytotoxic T-cell clone. *Nature*, 1982. 296(5852): p. 75-6.
29. Townsend, A. and H. Bodmer, Antigen recognition by class I-restricted T lymphocytes. *Annu Rev Immunol*, 1989. 7: p. 601-24.
30. Townsend, A.R., et al., Cytotoxic T cell recognition of the influenza nucleoprotein and hemagglutinin expressed in transfected mouse L cells. *Cell*, 1984. 39(1): p. 13-25.
31. Townsend, A.R., F.M. Gotch, and J. Davey, Cytotoxic T cells recognize fragments of the influenza nucleoprotein. *Cell*, 1985. 42(2): p. 457-67.
32. Townsend, A.R., et al., Cytotoxic T lymphocytes recognize influenza haemagglutinin that lacks a signal sequence. *Nature*, 1986. 324(6097): p. 575-7.
33. Townsend, A.R., et al., The epitopes of influenza nucleoprotein recognized by cytotoxic T lymphocytes can be defined with short synthetic peptides. *Cell*, 1986. 44(6): p. 959-68.
34. Gotch, F., et al., Cytotoxic T lymphocytes recognize a fragment of influenza virus matrix protein in association with HLA-A2. *Nature*, 1987. 326(6116): p. 881-2.
35. Bastin, J., et al., Use of synthetic peptides of influenza nucleoprotein to define epitopes recognized by class I-restricted cytotoxic T lymphocytes. *J Exp Med*, 1987. 165(6): p. 1508-23.
36. Maryanski, J.L., et al., H-2-restricted cytolytic T cells specific for HLA can recognize a synthetic HLA peptide. *Nature*, 1986. 324(6097): p. 578-9.
37. Gotch, F., A. McMichael, and J. Rothbard, Recognition of influenza A matrix protein by HLA-A2-restricted cytotoxic T lymphocytes. Use of analogues to orientate the matrix peptide in the HLA-A2 binding site. *J Exp Med*, 1988. 168(6): p. 2045-57.
38. Bjorkman, P.J., et al., Structure of the human class I histocompatibility antigen, HLA-A2. *Nature*, 1987. 329(6139): p. 506-12.
39. Bjorkman, P.J., et al., The foreign antigen binding site and T cell recognition regions of class I histocompatibility antigens. *Nature*, 1987. 329(6139): p. 512-8.

40. Garrett, T.P., et al., Specificity pockets for the side chains of peptide antigens in HLA-Aw68. *Nature*, 1989. 342(6250): p. 692-6.
41. Madden, D.R., et al., The structure of HLA-B27 reveals nonamer self-peptides bound in an extended conformation. *Nature*, 1991. 353(6342): p. 321-5.
42. Young, A.C., et al., The three-dimensional structure of H-2Db at 2.4 A resolution: implications for antigen-determinant selection. *Cell*, 1994. 76(1): p. 39-50.
43. Saper, M.A., P.J. Bjorkman, and D.C. Wiley, Refined structure of the human histocompatibility antigen HLA-A2 at 2.6 A resolution. *J Mol Biol*, 1991. 219(2): p. 277-319.
44. Barber, L.D. and P. Parham, Peptide binding to major histocompatibility complex molecules. *Annu Rev Cell Biol*, 1993. 9: p. 163-206.
45. Parham, P., et al., Nature of polymorphism in HLA-A, -B, and -C molecules. *Proc Natl Acad Sci U S A*, 1988. 85(11): p. 4005-9.
46. Fremont, D.H., et al., Crystal structures of two viral peptides in complex with murine MHC class I H-2Kb. *Science*, 1992. 257(5072): p. 919-27.
47. Smith, K.J., et al., An altered position of the alpha 2 helix of MHC class I is revealed by the crystal structure of HLA-B*3501. *Immunity*, 1996. 4(3): p. 203-13.
48. Young, A.C., S.G. Nathenson, and J.C. Sacchettini, Structural studies of class I major histocompatibility complex proteins: insights into antigen presentation. *Faseb J*, 1995. 9(1): p. 26-36.
49. Madden, D.R., The three-dimensional structure of peptide-MHC complexes. *Annu Rev Immunol*, 1995. 13: p. 587-622.
50. Latron, F., et al., A critical role for conserved residues in the cleft of HLA-A2 in presentation of a nonapeptide to T cells. *Science*, 1992. 257(5072): p. 964-7.
51. Rohren, E.M., et al., Polymorphisms in pockets of major histocompatibility complex class I molecules influence peptide preference. *J Exp Med*, 1993. 177(6): p. 1713-21.
52. McMichael, A.J., et al., Effect of mutations and variations of HLA-A2 on recognition of a virus peptide epitope by cytotoxic T lymphocytes. *Proc Natl Acad Sci U S A*, 1988. 85(23): p. 9194-8.
53. Robbins, P.A., et al., Comparison between two peptide epitopes presented to cytotoxic T lymphocytes by HLA-A2. Evidence for discrete locations within HLA-A2. *J Immunol*, 1989. 143(12): p. 4098-103.
54. Colbert, R.A., et al., Allele-specific B pocket transplant in class I major histocompatibility complex protein changes requirement for anchor residue at P2 of peptide. *Proc Natl Acad Sci U S A*, 1993. 90(14): p. 6879-83.
55. Van Bleek, G.M. and S.G. Nathenson, Isolation of an endogenously processed immunodominant viral peptide from the class I H-2Kb molecule. *Nature*, 1990. 348(6298): p. 213-6.
56. Falk, K., et al., Allele-specific motifs revealed by sequencing of self-peptides eluted from MHC molecules. *Nature*, 1991. 351(6324): p. 290-6.
57. Rotzschke, O., et al., Isolation and analysis of naturally processed viral peptides as recognized by cytotoxic T cells. *Nature*, 1990. 348(6298): p. 252-4.
58. Falk, K., et al., Identification of naturally processed viral nonapeptides allows their quantification in infected cells and suggests an allele-specific T cell epitope forecast. *J Exp Med*, 1991. 174(2): p. 425-34.

59. Rammensee, H.G., K. Falk, and O. Rotzschke, Peptides naturally presented by MHC class I molecules. *Annu Rev Immunol*, 1993. 11: p. 213-44.
60. Elliott, T., Peptide selection by class I molecules of the major histocompatibility complex. *Current Biology*, 1993. 3(12): p. 854-866.
61. Madden, D.R., et al., The three-dimensional structure of HLA-B27 at 2.1 A resolution suggests a general mechanism for tight peptide binding to MHC. *Cell*, 1992. 70(6): p. 1035-48.
62. Madden, D.R., D.N. Garboczi, and D.C. Wiley, The antigenic identity of peptide-MHC complexes: a comparison of the conformations of five viral peptides presented by HLA-A2. *Cell*, 1993. 75(4): p. 693-708.
63. Matsumura, M., et al., Emerging principles for the recognition of peptide antigens by MHC class I molecules. *Science*, 1992. 257(5072): p. 927-34.
64. Guo, H.C., et al., Different length peptides bind to HLA-Aw68 similarly at their ends but bulge out in the middle. *Nature*, 1992. 360(6402): p. 364-6.
65. Silver, M.L., et al., Atomic structure of a human MHC molecule presenting an influenza virus peptide. *Nature*, 1992. 360(6402): p. 367-9.
66. Hunt, D.F., et al., Characterization of peptides bound to the class I MHC molecule HLA-A2.1 by mass spectrometry. *Science*, 1992. 255(5049): p. 1261-3.
67. Chen, Y., et al., Naturally processed peptides longer than nine amino acid residues bind to the class I MHC molecule HLA-A2.1 with high affinity and in different conformations. *J Immunol*, 1994. 152(6): p. 2874-81.
68. Ruppert, J., et al., Prominent role of secondary anchor residues in peptide binding to HLA- A2.1 molecules. *Cell*, 1993. 74(5): p. 929-37.
69. Gould, K., et al., A 15 amino acid fragment of influenza nucleoprotein synthesized in the cytoplasm is presented to class I-restricted cytotoxic T lymphocytes. *J Exp Med*, 1989. 170(3): p. 1051-6.
70. Sweetser, M.T., et al., Recognition of pre-processed endogenous antigen by class I but not class II MHC-restricted T cells. *Nature*, 1989. 342(6246): p. 180-2.
71. Townsend, A., et al., Association of class I major histocompatibility heavy and light chains induced by viral peptides. *Nature*, 1989. 340(6233): p. 443-8.
72. Townsend, A., et al., Recognition of influenza virus proteins by cytotoxic T lymphocytes. *Philos Trans R Soc Lond B Biol Sci*, 1989. 323(1217): p. 527-33.
73. Townsend, A. and J. Trowsdale, The transporters associated with antigen presentation. *Semin Cell Biol*, 1993. 4(1): p. 53-61.
74. Trowsdale, J., et al., Sequences encoded in the class II region of the MHC related to the 'ABC' superfamily of transporters. *Nature*, 1990. 348(6303): p. 741-4.
75. Spies, T., et al., A gene in the human major histocompatibility complex class II region controlling the class I antigen presentation pathway. *Nature*, 1990. 348(6303): p. 744-7.
76. Goldberg, A.L. and K.L. Rock, Proteolysis, proteasomes and antigen presentation. *Nature*, 1992. 357(6377): p. 375-9.
77. Rivett, A.J., Proteasomes: multicatalytic proteinase complexes. *Biochem J*, 1993. 291(Pt 1): p. 1-10.
78. Schubert, U., et al., Rapid degradation of a large fraction of newly synthesized proteins by proteasomes. *Nature*, 2000. 404(6779): p. 770-4.

79. Yewdell, J.W., U. Schubert, and J.R. Bennink, At the crossroads of cell biology and immunology: DRiPs and other sources of peptide ligands for MHC class I molecules. *J Cell Sci*, 2001. 114(Pt 5): p. 845-51.
80. Yewdell, J.W., L.C. Anton, and J.R. Bennink, Defective ribosomal products (DRiPs): a major source of antigenic peptides for MHC class I molecules? *J Immunol*, 1996. 157(5): p. 1823-6.
81. Goldberg, A.L., Functions of the proteasome: the lysis at the end of the tunnel. *Science*, 1995. 268(5210): p. 522-3.
82. Townsend, A., et al., Defective presentation to class I-restricted cytotoxic T lymphocytes in vaccinia-infected cells is overcome by enhanced degradation of antigen. *J Exp Med*, 1988. 168(4): p. 1211-24.
83. Michalek, M.T., et al., A role for the ubiquitin-dependent proteolytic pathway in MHC class I- restricted antigen presentation. *Nature*, 1993. 363(6429): p. 552-4.
84. Driscoll, J. and D. Finley, A controlled breakdown: antigen processing and the turnover of viral proteins. *Cell*, 1992. 68(5): p. 823-5.
85. Ciechanover, A., The ubiquitin-proteasome proteolytic pathway. *Cell*, 1994. 79(1): p. 13-21.
86. Rock, K.L., et al., Inhibitors of the proteasome block the degradation of most cell proteins and the generation of peptides presented on MHC class I molecules. *Cell*, 1994. 78(5): p. 761-71.
87. Harding, C.V., et al., Novel dipeptide aldehydes are proteasome inhibitors and block the MHC-I antigen-processing pathway. *J Immunol*, 1995. 155(4): p. 1767-75.
88. Hughes, E.A., et al., The protease inhibitor, N-acetyl-L-leucyl-L-leucyl-leucyl-L- norleucinal, decreases the pool of major histocompatibility complex class I-binding peptides and inhibits peptide trimming in the endoplasmic reticulum. *J Exp Med*, 1996. 183(4): p. 1569-78.
89. Cerundolo, V., et al., The proteasome-specific inhibitor lactacystin blocks presentation of cytotoxic T lymphocyte epitopes in human and murine cells. *Eur J Immunol*, 1997. 27(1): p. 336-41.
90. Fenteany, G., et al., Inhibition of proteasome activities and subunit-specific amino-terminal threonine modification by lactacystin. *Science*, 1995. 268(5211): p. 726-31.
91. Yang, B., et al., The requirement for proteasome activity class I major histocompatibility complex antigen presentation is dictated by the length of preprocessed antigen. *J Exp Med*, 1996. 183(4): p. 1545-52.
92. Niedermann, G., et al., The proteolytic fragments generated by vertebrate proteasomes: structural relationships to major histocompatibility complex class I binding peptides. *Proc Natl Acad Sci U S A*, 1996. 93(16): p. 8572-7.
93. Kuckelkorn, U., et al., Incorporation of major histocompatibility complex--encoded subunits LMP2 and LMP7 changes the quality of the 20S proteasome polypeptide processing products independent of interferon-gamma. *Eur J Immunol*, 1995. 25(9): p. 2605-11.
94. Glynne, R., et al., A proteasome-related gene between the two ABC transporter loci in the class II region of the human MHC. *Nature*, 1991. 353(6342): p. 357-60.
95. Kelly, A., et al., Second proteasome-related gene in the human MHC class II region. *Nature*, 1991. 353(6345): p. 667-8.

96. Ortiz-Navarrete, V., et al., Subunit of the '20S' proteasome (multicatalytic proteinase) encoded by the major histocompatibility complex. *Nature*, 1991. 353(6345): p. 662-4.
97. Brown, M.G., J. Driscoll, and J.J. Monaco, Structural and serological similarity of MHC-linked LMP and proteasome (multicatalytic proteinase) complexes. *Nature*, 1991. 353(6342): p. 355-7.
98. Martinez, C.K. and J.J. Monaco, Homology of proteasome subunits to a major histocompatibility complex- linked LMP gene. *Nature*, 1991. 353(6345): p. 664-7.
99. Driscoll, J., et al., MHC-linked LMP gene products specifically alter peptidase activities of the proteasome. *Nature*, 1993. 365(6443): p. 262-4.
100. Gaczynska, M., K.L. Rock, and A.L. Goldberg, Gamma-interferon and expression of MHC genes regulate peptide hydrolysis by proteasomes. *Nature*, 1993. 365(6443): p. 264-7.
101. Rammensee, H.G., T. Friede, and S. Stevanoviic, MHC ligands and peptide motifs: first listing. *Immunogenetics*, 1995. 41(4): p. 178-228.
102. Benham, A.M. and J.J. Neefjes, Proteasome activity limits the assembly of MHC class I molecules after IFN-gamma stimulation. *J Immunol*, 1997. 159(12): p. 5896-904.
103. Chu-Ping, M., et al., Identification, purification, and characterization of a high molecular weight, ATP-dependent activator (PA700) of the 20 S proteasome. *J Biol Chem*, 1994. 269(5): p. 3539-47.
104. Knowlton, J.R., et al., Structure of the proteasome activator REGalpha (PA28alpha). *Nature*, 1997. 390(6660): p. 639-43.
105. Groettrup, M., et al., Peptide antigen production by the proteasome: complexity provides efficiency. *Immunol Today*, 1996. 17(9): p. 429-35.
106. Dick, T.P., et al., Coordinated dual cleavages induced by the proteasome regulator PA28 lead to dominant MHC ligands. *Cell*, 1996. 86(2): p. 253-62.
107. Groettrup, M., et al., A role for the proteasome regulator PA28alpha in antigen presentation. *Nature*, 1996. 381(6578): p. 166-8.
108. Stoltze, L., et al., Two new proteases in the MHC class I processing pathway. *Nat Immunol*, 2000. 1(5): p. 413-8.
109. Stoltze, L., et al., The function of the proteasome system in MHC class I antigen processing. *Immunol Today*, 2000. 21(7): p. 317-9.
110. Johnson, G.V. and R.P. Guttmann, Calpains: intact and active? *Bioessays*, 1997. 19(11): p. 1011-8.
111. Ljunggren, H.G., et al., Molecular analysis of H-2-deficient lymphoma lines. Distinct defects in biosynthesis and association of MHC class I heavy chains and beta 2- microglobulin observed in cells with increased sensitivity to NK cell lysis. *J Immunol*, 1989. 142(8): p. 2911-7.
112. Karre, K., et al., Selective rejection of H-2-deficient lymphoma variants suggests alternative immune defence strategy. *Nature*, 1986. 319(6055): p. 675-8.
113. DeMars, R., et al., Homozygous deletions that simultaneously eliminate expressions of class I and class II antigens of EBV-transformed B-lymphoblastoid cells. I. Reduced proliferative responses of autologous and allogeneic T cells to mutant cells that have decreased expression of class II antigens. *Hum Immunol*, 1984. 11(2): p. 77-97.

114. DeMars, R., et al., Mutations that impair a posttranscriptional step in expression of HLA-A and -B antigens. *Proc Natl Acad Sci U S A*, 1985. 82(23): p. 8183-7.
115. Salter, R.D. and P. Cresswell, Impaired assembly and transport of HLA-A and -B antigens in a mutant TxB cell hybrid. *Embo J*, 1986. 5(5): p. 943-9.
116. Kelly, A., et al., Assembly and function of the two ABC transporter proteins encoded in the human major histocompatibility complex. *Nature*, 1992. 355(6361): p. 641-4.
117. Cerundolo, V., et al., Presentation of viral antigen controlled by a gene in the major histocompatibility complex. *Nature*, 1990. 345(6274): p. 449-52.
118. Hosken, N.A. and M.J. Bevan, Defective presentation of endogenous antigen by a cell line expressing class I molecules. *Science*, 1990. 248(4953): p. 367-70.
119. Whitehead, A.S., et al., Localization of the human MHC-linked complement genes between HLA-B and HLA-DR by using HLA mutant cell lines. *J Immunol*, 1985. 134(1): p. 641-3.
120. Higgins, C.F., ABC transporters: from microorganisms to man. *Annu Rev Cell Biol*, 1992. 8: p. 67-113.
121. Spies, T., et al., Presentation of viral antigen by MHC class I molecules is dependent on a putative peptide transporter heterodimer. *Nature*, 1992. 355(6361): p. 644-6.
122. Kleijmeer, M.J., et al., Location of MHC-encoded transporters in the endoplasmic reticulum and cis-Golgi. *Nature*, 1992. 357(6376): p. 342-4.
123. Elliott, T., Transporter associated with antigen processing. *Adv Immunol*, 1997. 65: p. 47-109.
124. Howard, J.C., Supply and transport of peptides presented by class I MHC molecules. *Curr Opin Immunol*, 1995. 7(1): p. 69-76.
125. Muller, K.M., C. Ebensperger, and R. Tampe, Nucleotide binding to the hydrophilic C-terminal domain of the transporter associated with antigen processing (TAP). *J Biol Chem*, 1994. 269(19): p. 14032-7.
126. Momburg, F., et al., Residues in TAP2 peptide transporters controlling substrate specificity. *J Immunol*, 1996. 156(5): p. 1756-63.
127. Armandola, E.A., et al., A point mutation in the human transporter associated with antigen processing (TAP2) alters the peptide transport specificity. *Eur J Immunol*, 1996. 26(8): p. 1748-55.
128. Deverson, E.V., et al., Functional analysis by site-directed mutagenesis of the complex polymorphism in rat transporter associated with antigen processing. *J Immunol*, 1998. 160(6): p. 2767-79.
129. Powis, S.J., et al., Effect of polymorphism of an MHC-linked transporter on the peptides assembled in a class I molecule. *Nature*, 1992. 357(6375): p. 211-5.
130. Gileadi, U. and C.F. Higgins, Membrane topology of the ATP-binding cassette transporter associated with antigen presentation (Tap1) expressed in Escherichia coli. *J Biol Chem*, 1997. 272(17): p. 11103-8.
131. Vos, J.C., et al., Membrane topology and dimerization of the two subunits of the transporter associated with antigen processing reveal a three-domain structure. *J Immunol*, 1999. 163(12): p. 6679-85.
132. Lapinski, P.E., et al., Pairing of the nucleotide binding domains of the transporter associated with antigen processing. *J Biol Chem*, 2000. 275(10): p. 6831-40.

133. Newitt, S. and S.J. Powis, Interactions formed by truncated transporter associated with antigen- processing polypeptides. *Transplant Proc*, 1999. 31(3): p. 1519-21.
134. Vos, J.C., et al., Head-head/tail-tail relative orientation of the pore-forming domains of the heterodimeric ABC transporter TAP. *Curr Biol*, 2000. 10(1): p. 1-7.
135. Velarde, G., et al., Three-dimensional structure of transporter associated with antigen processing (TAP) obtained by single Particle image analysis. *J Biol Chem*, 2001. 276(49): p. 46054-63.
136. Neefjes, J.J., F. Momburg, and G.J. Hammerling, Selective and ATP-dependent translocation of peptides by the MHC- encoded transporter. *Science*, 1993. 261(5122): p. 769-71.
137. Androlewicz, M.J., K.S. Anderson, and P. Cresswell, Evidence that transporters associated with antigen processing translocate a major histocompatibility complex class I-binding peptide into the endoplasmic reticulum in an ATP-dependent manner. *Proc Natl Acad Sci U S A*, 1993. 90(19): p. 9130-4.
138. Shepherd, J.C., et al., TAP1-dependent peptide translocation in vitro is ATP dependent and peptide selective. *Cell*, 1993. 74(3): p. 577-84.
139. Obst, R., et al., TAP polymorphism does not influence transport of peptide variants in mice and humans. *Eur J Immunol*, 1995. 25(8): p. 2170-6.
140. Momburg, F., et al., Peptide size selection by the major histocompatibility complex-encoded peptide transporter. *J Exp Med*, 1994. 179(5): p. 1613-23.
141. Schumacher, T.N., et al., Peptide length and sequence specificity of the mouse TAP1/TAP2 translocator. *J Exp Med*, 1994. 179(2): p. 533-40.
142. Androlewicz, M.J. and P. Cresswell, Human transporters associated with antigen processing possess a promiscuous peptide-binding site. *Immunity*, 1994. 1(1): p. 7-14.
143. Heemels, M.T. and H.L. Ploegh, Substrate specificity of allelic variants of the TAP peptide transporter. *Immunity*, 1994. 1(9): p. 775-84.
144. Koopmann, J.O., et al., Translocation of long peptides by transporters associated with antigen processing (TAP). *Eur J Immunol*, 1996. 26(8): p. 1720-8.
145. Momburg, F., et al., Selectivity of MHC-encoded peptide transporters from human, mouse and rat. *Nature*, 1994. 367(6464): p. 648-51.
146. Joly, E., et al., The distribution of Tap2 alleles among laboratory rat RT1 haplotypes. *Immunogenetics*, 1994. 40(1): p. 45-53.
147. Heemels, M.T., et al., Peptide translocation by variants of the transporter associated with antigen processing. *Science*, 1993. 262(5142): p. 2059-63.
148. Powis, S.J., The major histocompatibility complex class II-linked *cim* locus controls the kinetics of intracellular transport of a classical class I molecule. *J. Exp. Med.*, 1991. 173: p. 913-921.
149. Livingstone, A.M., Powis, S.J., Diamond, A.G., Butcher, G. W. and Howard, J.C., A *trans*-acting major histocompatibility complex-linked gene whose alleles determine gain and loss changes in the antigenic structure of a classical class I molecule. *J. Exp. Med.*, 1989. 170: p. 777-195.
150. Powis, S.J., et al., The rat cim effect: TAP allele-dependent changes in a class I MHC anchor motif and evidence against C-terminal trimming of peptides in the ER. *Immunity*, 1996. 4(2): p. 159-65.

151. Neefjes, J., et al., Analysis of the fine specificity of rat, mouse and human TAP peptide transporters. *Eur J Immunol*, 1995. 25(4): p. 1133-6.
152. Neisig, A., et al., Major differences in transporter associated with antigen presentation (TAP)-dependent translocation of MHC class I-presentable peptides and the effect of flanking sequences. *J Immunol*, 1995. 154(3): p. 1273-9.
153. Snyder, H.L., J.W. Yewdell, and J.R. Bennink, Trimming of antigenic peptides in an early secretory compartment. *J Exp Med*, 1994. 180(6): p. 2389-94.
154. Elliott, T., et al., Processing of major histocompatibility class I-restricted antigens in the endoplasmic reticulum. *J Exp Med*, 1995. 181(4): p. 1481-91.
155. Menoret, A., et al., An endoplasmic reticulum protein implicated in chaperoning peptides to major histocompatibility of class I is an aminopeptidase. *J Biol Chem*, 2001. 276(36): p. 33313-8.
156. Serwold, T., S. Gaw, and N. Shastri, ER aminopeptidases generate a unique pool of peptides for MHC class I molecules. *Nat Immunol*, 2001. 2(7): p. 644-51.
157. Brouwenstijn, N., T. Serwold, and N. Shastri, MHC class I molecules can direct proteolytic cleavage of antigenic precursors in the endoplasmic reticulum. *Immunity*, 2001. 15(1): p. 95-104.
158. Ortmann, B., M.J. Androlewicz, and P. Cresswell, MHC class I/beta 2-microglobulin complexes associate with TAP transporters before peptide binding. *Nature*, 1994. 368(6474): p. 864-7.
159. Suh, W.K., et al., Interaction of MHC class I molecules with the transporter associated with antigen processing. *Science*, 1994. 264(5163): p. 1322-6.
160. Powis, S.J., Major histocompatibility complex class I molecules interact with both subunits of the transporter associated with antigen processing, TAP1 and TAP2. *Eur J Immunol*, 1997. 27(10): p. 2744-7.
161. Li, S., et al., Cloning and functional characterization of a subunit of the transporter associated with antigen processing. *Proc Natl Acad Sci U S A*, 1997. 94(16): p. 8708-13.
162. Sadasivan, B., et al., Roles for calreticulin and a novel glycoprotein, tapasin, in the interaction of MHC class I molecules with TAP. *Immunity*, 1996. 5(2): p. 103-14.
163. Solheim, J.C., et al., Prominence of beta 2-microglobulin, class I heavy chain conformation, and tapasin in the interactions of class I heavy chain with calreticulin and the transporter associated with antigen processing. *J Immunol*, 1997. 158(5): p. 2236-41.
164. Grandea, A.G., 3rd, et al., Regulation of MHC class I heterodimer stability and interaction with TAP by tapasin. *Immunogenetics*, 1997. 46(6): p. 477-83.
165. Lehner, P.J., M.J. Surman, and P. Cresswell, Soluble tapasin restores MHC class I expression and function in the tapasin-negative cell line .220. *Immunity*, 1998. 8(2): p. 221-31.
166. Suh, W.K., et al., Interaction of murine MHC class I molecules with tapasin and TAP enhances peptide loading and involves the heavy chain alpha3 domain. *J Immunol*, 1999. 162(3): p. 1530-40.
167. Townsend, A., et al., Assembly of MHC class I molecules analyzed in vitro. *Cell*, 1990. 62(2): p. 285-95.
168. Elliott, T., et al., Peptide-induced conformational change of the class I heavy chain. *Nature*, 1991. 351(6325): p. 402-6.

169. Schumacher, T.N., et al., Direct binding of peptide to empty MHC class I molecules on intact cells and in vitro. *Cell*, 1990. 62(3): p. 563-7.
170. Elliott, T., How does TAP associate with MHC class I molecules? *Immunol Today*, 1997. 18(8): p. 375-9.
171. Lie, W.R., et al., Peptide ligand-induced conformation and surface expression of the Ld class I MHC molecule. *Nature*, 1990. 344(6265): p. 439-41.
172. Cerundolo, V., et al., The binding affinity and dissociation rates of peptides for class I major histocompatibility complex molecules. *Eur J Immunol*, 1991. 21(9): p. 2069-75.
173. Cerundolo, V., et al., Association of the human invariant chain with H-2 Db class I molecules. *Eur J Immunol*, 1992. 22(9): p. 2243-8.
174. Smith, J.D., et al., Disparate interaction of peptide ligand with nascent versus mature class I major histocompatibility complex molecules: comparisons of peptide binding to alternative forms of Ld in cell lysates and the cell surface. *J Exp Med*, 1992. 175(1): p. 191-202.
175. Bluestone, J.A., et al., Peptide-induced conformational changes in class I heavy chains alter major histocompatibility complex recognition. *J Exp Med*, 1992. 176(6): p. 1757-61.
176. Kozlowski, S., et al., Excess beta 2 microglobulin promoting functional peptide association with purified soluble class I MHC molecules. *Nature*, 1991. 349(6304): p. 74-7.
177. Catipovic, B., et al., Analysis of the structure of empty and peptide-loaded major histocompatibility complex molecules at the cell surface. *J Exp Med*, 1994. 180(5): p. 1753-61.
178. Neefjes, J.J., G.J. Hammerling, and F. Momburg, Folding and assembly of major histocompatibility complex class I heterodimers in the endoplasmic reticulum of intact cells precedes the binding of peptide. *J Exp Med*, 1993. 178(6): p. 1971-80.
179. Elvin, J., et al., A method to quantify binding of unlabeled peptides to class I MHC molecules and detect their allele specificity. *J Immunol Methods*, 1993. 158(2): p. 161-71.
180. Lewis, J.W., et al., Point mutations in the alpha 2 domain of HLA-A2.1 define a functionally relevant interaction with TAP. *Curr Biol*, 1996. 6(7): p. 873-83.
181. Christinck, E.R., et al., Peptide binding to class I MHC on living cells and quantitation of complexes required for CTL lysis. *Nature*, 1991. 352(6330): p. 67-70.
182. Springer, S., et al., Fast association rates suggest a conformational change in the MHC class I molecule H-2Db upon peptide binding. *Biochemistry*, 1998. 37(9): p. 3001-12.
183. Bergeron, J.J., et al., Calnexin: a membrane-bound chaperone of the endoplasmic reticulum. *Trends Biochem Sci*, 1994. 19(3): p. 124-8.
184. Schrag, J.D., et al., The Structure of calnexin, an ER chaperone involved in quality control of protein folding. *Mol Cell*, 2001. 8(3): p. 633-44.
185. Degen, E. and D.B. Williams, Participation of a novel 88-kD protein in the biogenesis of murine class I histocompatibility molecules. *J Cell Biol*, 1991. 112(6): p. 1099-115.
186. Michalak, M., et al., Calreticulin. *Biochem J*, 1992. 285(Pt 3): p. 681-92.
187. Wada, I., et al., SSR alpha and associated calnexin are major calcium binding proteins of the endoplasmic reticulum membrane. *J Biol Chem*, 1991. 266(29): p. 19599-610.

188. Galvin, K., et al., The major histocompatibility complex class I antigen-binding protein p88 is the product of the calnexin gene. *Proc Natl Acad Sci U S A*, 1992. 89(18): p. 8452-6.
189. Ahluwalia, N., et al., The p88 molecular chaperone is identical to the endoplasmic reticulum membrane protein, calnexin. *J Biol Chem*, 1992. 267(15): p. 10914-8.
190. David, V., et al., Interaction with newly synthesized and retained proteins in the endoplasmic reticulum suggests a chaperone function for human integral membrane protein IP90 (calnexin). *J Biol Chem*, 1993. 268(13): p. 9585-92.
191. Ou, W.J., et al., Association of folding intermediates of glycoproteins with calnexin during protein maturation. *Nature*, 1993. 364(6440): p. 771-6.
192. Hochstenbach, F., et al., Endoplasmic reticulum resident protein of 90 kilodaltons associates with the T- and B-cell antigen receptors and major histocompatibility complex antigens during their assembly. *Proc Natl Acad Sci U S A*, 1992. 89(10): p. 4734-8.
193. Gelman, M.S., et al., Role of the endoplasmic reticulum chaperone calnexin in subunit folding and assembly of nicotinic acetylcholine receptors. *J Biol Chem*, 1995. 270(25): p. 15085-92.
194. Lenter, M. and D. Vestweber, The integrin chains beta 1 and alpha 6 associate with the chaperone calnexin prior to integrin assembly. *J Biol Chem*, 1994. 269(16): p. 12263-8.
195. Anderson, K.S. and P. Cresswell, A role for calnexin (IP90) in the assembly of class II MHC molecules. *Embo J*, 1994. 13(3): p. 675-82.
196. Jackson, M.R., et al., Regulation of MHC class I transport by the molecular chaperone, calnexin (p88, IP90). *Science*, 1994. 263(5145): p. 384-7.
197. Paulsson, K.M., et al., Distinct differences in association of MHC class I with endoplasmic reticulum proteins in wild-type, and beta 2-microglobulin- and TAP- deficient cell lines. *Int Immunol*, 2001. 13(8): p. 1063-73.
198. Wilson, C.M., M.R. Farmery, and N.J. Bulleid, Pivotal role of calnexin and mannose trimming in regulating the endoplasmic reticulum-associated degradation of major histocompatibility complex class I heavy chain. *J Biol Chem*, 2000. 275(28): p. 21224-32.
199. Tharin, S., et al., Widespread tissue distribution of rabbit calreticulin, a non-muscle functional analogue of calsequestrin. *Cell Tissue Res*, 1992. 269(1): p. 29-37.
200. Milner, R.E., et al., Calreticulin, and not calsequestrin, is the major calcium binding protein of smooth muscle sarcoplasmic reticulum and liver endoplasmic reticulum. *J Biol Chem*, 1991. 266(11): p. 7155-65.
201. Smith, M.J., Nucleotide sequence of a Drosophila melanogaster gene encoding a calreticulin homologue. *DNA Seq*, 1992. 3(4): p. 247-50.
202. Smith, M.J., A C. elegans gene encodes a protein homologous to mammalian calreticulin. *DNA Seq*, 1992. 2(4): p. 235-40.
203. Joshi, M., et al., Isolation and characterization of Leishmania donovani calreticulin gene and its conservation of the RNA binding activity. *Mol Biochem Parasitol*, 1996. 81(1): p. 53-64.
204. Denecke, J., et al., The tobacco homolog of mammalian calreticulin is present in protein complexes in vivo. *Plant Cell*, 1995. 7(4): p. 391-406.
205. Smith, M.J. and G.L. Koch, Multiple zones in the sequence of calreticulin (CRP55, calregulin, HACBP), a major calcium binding ER/SR protein. *Embo J*, 1989. 8(12): p. 3581-6.

206. Fliegel, L., et al., Molecular cloning of the high affinity calcium-binding protein (calreticulin) of skeletal muscle sarcoplasmic reticulum. *J Biol Chem*, 1989. 264(36): p. 21522-8.
207. Fliegel, L., et al., The high-affinity calcium binding protein of sarcoplasmic reticulum. Tissue distribution, and homology with calregulin. *Biochim Biophys Acta*, 1989. 982(1): p. 1-8.
208. Krause, K.H. and M. Michalak, Calreticulin. *Cell*, 1997. 88(4): p. 439-43.
209. Baksh, S. and M. Michalak, Expression of calreticulin in Escherichia coli and identification of its Ca2+ binding domains. *J Biol Chem*, 1991. 266(32): p. 21458-65.
210. Tjoelker, L.W., et al., Human, mouse, and rat calnexin cDNA cloning: identification of potential calcium binding motifs and gene localization to human chromosome 5. *Biochemistry*, 1994. 33(11): p. 3229-36.
211. Ellgaard, L., et al., NMR structure of the calreticulin P-domain. *Proc Natl Acad Sci U S A*, 2001. 98(6): p. 3133-8.
212. Ellgaard, L., et al., Three-dimensional structure topology of the calreticulin P-domain based on NMR assignment. *FEBS Lett*, 2001. 488(1-2): p. 69-73.
213. Michalak, M., et al., Calreticulin: one protein, one gene, many functions. *Biochem J*, 1999. 344 Pt 2: p. 281-92.
214. Coppolino, M.G., et al., Calreticulin is essential for integrin-mediated calcium signalling and cell adhesion. *Nature*, 1997. 386(6627): p. 843-7.
215. Mesaeli, N., et al., Calreticulin is essential for cardiac development. *J Cell Biol*, 1999. 144(5): p. 857-68.
216. Rauch, F., et al., Heart, brain, and body wall defects in mice lacking calreticulin. *Exp Cell Res*, 2000. 256(1): p. 105-11.
217. Bastianutto, C., et al., Overexpression of calreticulin increases the Ca2+ capacity of rapidly exchanging Ca2+ stores and reveals aspects of their lumenal microenvironment and function. *J Cell Biol*, 1995. 130(4): p. 847-55.
218. Liu, N., et al., Decreasing calreticulin expression lowers the Ca2+ response to bradykinin and increases sensitivity to ionomycin in NG-108-15 cells. *J Biol Chem*, 1994. 269(46): p. 28635-9.
219. Mery, L., et al., Overexpression of calreticulin increases intracellular Ca2+ storage and decreases store-operated Ca2+ influx. *J Biol Chem*, 1996. 271(16): p. 9332-9.
220. Opas, M., et al., Calreticulin modulates cell adhesiveness via regulation of vinculin expression. *J Cell Biol*, 1996. 135(6 Pt 2): p. 1913-23.
221. Clapham, D.E. and J. Sneyd, Intracellular calcium waves. *Adv Second Messenger Phosphoprotein Res*, 1995. 30: p. 1-24.
222. Clapham, D.E., Intracellular calcium. Replenishing the stores. *Nature*, 1995. 375(6533): p. 634-5.
223. Clapham, D.E., Calcium signaling. *Cell*, 1995. 80(2): p. 259-68.
224. John, L.M., J.D. Lechleiter, and P. Camacho, Differential modulation of SERCA2 isoforms by calreticulin. *J Cell Biol*, 1998. 142(4): p. 963-73.
225. Roderick, H.L., J.D. Lechleiter, and P. Camacho, Cytosolic phosphorylation of calnexin controls intracellular Ca(2+) oscillations via an interaction with SERCA2b. *J Cell Biol*, 2000. 149(6): p. 1235-48.
226. Corbett, E.F., et al., Ca2+ regulation of interactions between endoplasmic reticulum chaperones. *J Biol Chem*, 1999. 274(10): p. 6203-11.
227. Corbett, E.F. and M. Michalak, Calcium, a signaling molecule in the endoplasmic reticulum? *Trends Biochem Sci*, 2000. 25(7): p. 307-11.

228. Meldolesi, J. and T. Pozzan, The heterogeneity of ER Ca2+ stores has a key role in nonmuscle cell signaling and function. *J Cell Biol*, 1998. 142(6): p. 1395-8.
229. Meldolesi, J., Calcium signalling. Oscillation, activation, expression. *Nature*, 1998. 392(6679): p. 863, 865-6.
230. Meldolesi, J. and T. Pozzan, The endoplasmic reticulum Ca2+ store: a view from the lumen. *Trends Biochem Sci*, 1998. 23(1): p. 10-4.
231. Vassilakos, A., et al., Oligosaccharide binding characteristics of the molecular chaperones calnexin and calreticulin. *Biochemistry*, 1998. 37(10): p. 3480-90.
232. Burns, K., et al., Modulation of gene expression by calreticulin binding to the glucocorticoid receptor. *Nature*, 1994. 367(6462): p. 476-80.
233. Dedhar, S., et al., Inhibition of nuclear hormone receptor activity by calreticulin. *Nature*, 1994. 367(6462): p. 480-3.
234. Burns, K., M. Opas, and M. Michalak, Calreticulin inhibits glucocorticoid- but not cAMP-sensitive expression of tyrosine aminotransferase gene in cultured McA-RH7777 hepatocytes. *Mol Cell Biochem*, 1997. 171(1-2): p. 37-43.
235. Shago, M., et al., Modulation of the retinoic acid and retinoid X receptor signaling pathways in P19 embryonal carcinoma cells by calreticulin. *Exp Cell Res*, 1997. 230(1): p. 50-60.
236. Wheeler, D.G., et al., Calreticulin inhibits vitamin D3 signal transduction. *Nucleic Acids Res*, 1995. 23(16): p. 3268-74.
237. Holaska, J.M., et al., Calreticulin Is a receptor for nuclear export. *J Cell Biol*, 2001. 152(1): p. 127-40.
238. Fadel, M.P., et al., Calreticulin affects focal contact-dependent but not close contact- dependent cell-substratum adhesion. *J Biol Chem*, 1999. 274(21): p. 15085-94.
239. Matlack, K.E., W. Mothes, and T.A. Rapoport, Protein translocation: tunnel vision. *Cell*, 1998. 92(3): p. 381-90.
240. Andrin, C., et al., Interaction between a Ca2+-binding protein calreticulin and perforin, a component of the cytotoxic T-cell granules. *Biochemistry*, 1998. 37(29): p. 10386-94.
241. Fraser, S.A., et al., Perforin lytic activity is controlled by calreticulin. *J Immunol*, 2000. 164(8): p. 4150-5.
242. Arosa, F.A., et al., Calreticulin is expressed on the cell surface of activated human peripheral blood T lymphocytes in association with major histocompatibility complex class I molecules. *J Biol Chem*, 1999. 274(24): p. 16917-22.
243. Malhotra, R., et al., Structure and homology of human C1q receptor (collectin receptor). *Immunology*, 1993. 78(3): p. 341-8.
244. Eggleton, P., A.J. Tenner, and K.B. Reid, C1q receptors. *Clin Exp Immunol*, 2000. 120(3): p. 406-12.
245. Kishore, U., et al., The systemic lupus erythematosus (SLE) disease autoantigen-calreticulin can inhibit C1q association with immune complexes. *Clin Exp Immunol*, 1997. 108(2): p. 181-90.
246. Ben-Chetrit, E., R. Fischel, and A. Rubinow, Anti-SSA/Ro and anti-SSB/La antibodies in serum and saliva of patients with Sjogren's syndrome. *Clin Rheumatol*, 1993. 12(4): p. 471-4.
247. Boehm, J., et al., Systemic lupus erythematosus is associated with increased auto-antibody titers against calreticulin and grp94, but calreticulin is not the Ro/SS-A antigen. *Eur J Clin Invest*, 1994. 24(4): p. 248-57.

248. Lieu, T.S., et al., Molecular characterization of human Ro/SS-A antigen. Amino terminal sequence of the protein moiety of human Ro/SS-A antigen and immunological activity of a corresponding synthetic peptide. *J Clin Invest*, 1988. 82(1): p. 96-101.
249. Verreck, F.A., et al., DR4Dw4/DR53 molecules contain a peptide from the autoantigen calreticulin. *Tissue Antigens*, 1995. 45(4): p. 270-5.
250. Sanchez, D., et al., Occurrence of IgA and IgG autoantibodies to calreticulin in coeliac disease and various autoimmune diseases. *J Autoimmun*, 2000. 15(4): p. 441-9.
251. Routsias, J.G., et al., Calreticulin synthetic peptide analogues: anti-peptide antibodies in autoimmune rheumatic diseases. *Clin Exp Immunol*, 1993. 91(3): p. 437-41.
252. Eggleton, P., et al., Fine specificity of autoantibodies to calreticulin: epitope mapping and characterization. *Clin Exp Immunol*, 2000. 120(2): p. 384-91.
253. Zhang, J.X., et al., Quality control in the secretory pathway: the role of calreticulin, calnexin and BiP in the retention of glycoproteins with C-terminal truncations. *Mol Biol Cell*, 1997. 8(10): p. 1943-54.
254. Hebert, D.N., et al., The number and location of glycans on influenza hemagglutinin determine folding and association with calnexin and calreticulin. *J Cell Biol*, 1997. 139(3): p. 613-23.
255. Lingappa, V.R., et al., Coupled cell-free synthesis, segregation, and core glycosylation of a secretory protein. *Proc Natl Acad Sci U S A*, 1978. 75(5): p. 2338-42.
256. Kornfeld, R. and S. Kornfeld, Assembly of asparagine-linked oligosaccharides. *Annu Rev Biochem*, 1985. 54: p. 631-64.
257. Elbein, A.D., Glycosidase inhibitors: inhibitors of N-linked oligosaccharide processing. *Faseb J*, 1991. 5(15): p. 3055-63.
258. Moremen, K.W., R.B. Trimble, and A. Herscovics, Glycosidases of the asparagine-linked oligosaccharide processing pathway. *Glycobiology*, 1994. 4(2): p. 113-25.
259. Ware, F.E., et al., The molecular chaperone calnexin binds Glc1Man9GlcNAc2 oligosaccharide as an initial step in recognizing unfolded glycoproteins. *J Biol Chem*, 1995. 270(9): p. 4697-704.
260. Hebert, D.N., B. Foellmer, and A. Helenius, Glucose trimming and reglucosylation determine glycoprotein association with calnexin in the endoplasmic reticulum. *Cell*, 1995. 81(3): p. 425-33.
261. Hammond, C. and A. Helenius, Folding of VSV G protein: sequential interaction with BiP and calnexin. *Science*, 1994. 266(5184): p. 456-8.
262. Kearse, K.P., D.B. Williams, and A. Singer, Persistence of glucose residues on core oligosaccharides prevents association of TCR alpha and TCR beta proteins with calnexin and results specifically in accelerated degradation of nascent TCR alpha proteins within the endoplasmic reticulum. *Embo J*, 1994. 13(16): p. 3678-86.
263. Parodi, A.J., et al., Evidence that transient glucosylation of protein-linked Man9GlcNAc2, Man8GlcNAc2, and Man7GlcNAc2 occurs in rat liver and Phaseolus vulgaris cells. *J Biol Chem*, 1984. 259(10): p. 6351-7.
264. Parodi, A.J., D.H. Mendelzon, and G.Z. Lederkremer, Transient glucosylation of protein-bound Man9GlcNAc2, Man8GlcNAc2, and Man7GlcNAc2 in calf thyroid cells. A possible recognition signal in the processing of glycoproteins. *J Biol Chem*, 1983. 258(13): p. 8260-5.

265. Sousa, M.C., M.A. Ferrero-Garcia, and A.J. Parodi, Recognition of the oligosaccharide and protein moieties of glycoproteins by the UDP-Glc:glycoprotein glucosyltransferase. *Biochemistry*, 1992. 31(1): p. 97-105.
266. Trombetta, S.E. and A.J. Parodi, Purification to apparent homogeneity and partial characterization of rat liver UDP-glucose:glycoprotein glucosyltransferase. *J Biol Chem*, 1992. 267(13): p. 9236-40.
267. Trombetta, S.E., S.A. Ganan, and A.J. Parodi, The UDP-Glc:glycoprotein glucosyltransferase is a soluble protein of the endoplasmic reticulum. *Glycobiology*, 1991. 1(2): p. 155-61.
268. Hebert, D.N., B. Foellmer, and A. Helenius, Calnexin and calreticulin promote folding, delay oligomerization and suppress degradation of influenza hemagglutinin in microsomes. *Embo J*, 1996. 15(12): p. 2961-8.
269. Rodan, A.R., et al., N-linked oligosaccharides are necessary and sufficient for association of glycosylated forms of bovine RNase with calnexin and calreticulin. *Embo J*, 1996. 15(24): p. 6921-30.
270. Ritter, C. and A. Helenius, Recognition of local glycoprotein misfolding by the ER folding sensor UDP-glucose:glycoprotein glucosyltransferase. *Nat Struct Biol*, 2000. 7(4): p. 278-80.
271. Molinari, M. and A. Helenius, Chaperone selection during glycoprotein translocation into the endoplasmic reticulum. *Science*, 2000. 288(5464): p. 331-3.
272. Saito, Y., et al., Calreticulin functions in vitro as a molecular chaperone for both glycosylated and non-glycosylated proteins. *Embo J*, 1999. 18(23): p. 6718-29.
273. Danilczyk, U.G. and D.B. Williams, The lectin chaperone calnexin utilizes polypeptide-based interactions to associate with many of its substrates in vivo. *J Biol Chem*, 2001. 276(27): p. 25532-40.
274. Ihara, Y., et al., Calnexin discriminates between protein conformational states and functions as a molecular chaperone in vitro. *Mol Cell*, 1999. 4(3): p. 331-41.
275. Dunphy, W.G. and J.E. Rothman, Compartmental organization of the Golgi stack. *Cell*, 1985. 42(1): p. 13-21.
276. Dunphy, W.G., R. Brands, and J.E. Rothman, Attachment of terminal N-acetylglucosamine to asparagine-linked oligosaccharides occurs in central cisternae of the Golgi stack. *Cell*, 1985. 40(2): p. 463-72.
277. Hirschberg, C.B. and M.D. Snider, Topography of glycosylation in the rough endoplasmic reticulum and Golgi apparatus. *Annu Rev Biochem*, 1987. 56: p. 63-87.
278. Barber, L.D., et al., Unusual uniformity of the N-linked oligosaccharides of HLA-A, -B, and - C glycoproteins. *J Immunol*, 1996. 156(9): p. 3275-84.
279. Seong, R.H., et al., Rescue of Daudi cell HLA expression by transfection of the mouse beta 2- microglobulin gene. *J Exp Med*, 1988. 167(2): p. 288-99.
280. Claesson, M.H., et al., Antibodies directed against monomorphic and evolutionary conserved self epitopes may be generated in 'knock-out' mice. Development of monoclonal antibodies directed against monomorphic MHC class I determinants. *Scand J Immunol*, 1994. 40(2): p. 257-64.
281. Claesson, M.H. and M.H. Nissen, Binding of human beta 2-microglobulin to murine EL4 thymoma cells upregulates MHC class I heavy-chain epitopes, inhibits IL-2 secretion and induces resistance to killing by natural killer cells. *Immunol Lett*, 1994. 39(2): p. 195-202.

282. Perarnau, B., et al., Beta 2-microglobulin restriction of antigen presentation. *Nature*, 1990. 346(6286): p. 751-4.
283. Tector, M. and R.D. Salter, Calnexin influences folding of human class I histocompatibility proteins but not their assembly with beta 2-microglobulin. *J Biol Chem*, 1995. 270(33): p. 19638-42.
284. Zapun, A., et al., Enhanced catalysis of ribonuclease B folding by the interaction of calnexin or calreticulin with ERp57. *J Biol Chem*, 1998. 273(11): p. 6009-12.
285. Farmery, M.R., et al., The role of ERp57 in disulfide bond formation during the assembly of major histocompatibility complex class I in a synchronized semipermeabilized cell translation system. *J Biol Chem*, 2000. 275(20): p. 14933-8.
286. Zhang, Q. and R.D. Salter, Distinct patterns of folding and interactions with calnexin and calreticulin in human class I MHC proteins with altered N-glycosylation. *J Immunol*, 1998. 160(2): p. 831-7.
287. Harris, M.R., et al., Calreticulin and calnexin interact with different protein and glycan determinants during the assembly of MHC class I. *J Immunol*, 1998. 160(11): p. 5404-9.
288. Morrice, N.A. and S.J. Powis, A role for the thiol-dependent reductase ERp57 in the assembly of MHC class I molecules. *Curr Biol*, 1998. 8(12): p. 713-6.
289. Lindquist, J.A., et al., ER-60, a chaperone with thiol-dependent reductase activity involved in MHC class I assembly. *Embo J*, 1998. 17(8): p. 2186-95.
290. Townsend, A., et al., A mutant cell in which association of class I heavy and light chains is induced by viral peptides. *Cold Spring Harb Symp Quant Biol*, 1989. 54(Pt 1): p. 299-308.
291. Yu, Y.Y., et al., An extensive region of an MHC class I alpha 2 domain loop influences interaction with the assembly complex. *J Immunol*, 1999. 163(8): p. 4427-33.
292. Peace-Brewer, A.L., et al., A point mutation in HLA-A*0201 results in failure to bind the TAP complex and to present virus-derived peptides to CTL. *Immunity*, 1996. 4(5): p. 505-14.
293. Day, P.M., et al., Effect of TAP on the generation and intracellular trafficking of peptide-receptive major histocompatibility complex class I molecules. *Immunity*, 1995. 2(2): p. 137-47.
294. Lewis, J.W. and T. Elliott, Evidence for successive peptide binding and quality control stages during MHC class I assembly. *Curr Biol*, 1998. 8(12): p. 717-20.
295. Grandea, A.G., 3rd, et al., Dependence of peptide binding by MHC class I molecules on their interaction with TAP. *Science*, 1995. 270(5233): p. 105-8.
296. Peh, C.A., et al., HLA-B27-restricted antigen presentation in the absence of tapasin reveals polymorphism in mechanisms of HLA class I peptide loading. *Immunity*, 1998. 8(5): p. 531-42.
297. Schoenhals, G.J., et al., Retention of empty MHC class I molecules by tapasin is essential to reconstitute antigen presentation in invertebrate cells. *Embo J*, 1999. 18(3): p. 743-53.
298. Lewis, J.W., et al., HLA-A*0201 presents TAP-dependent peptide epitopes to cytotoxic T lymphocytes in the absence of tapasin. *Eur J Immunol*, 1998. 28(10): p. 3214-20.

299. Knittler, M.R., et al., Nucleotide binding by TAP mediates association with peptide and release of assembled MHC class I molecules. *Curr Biol*, 1999. 9(18): p. 999-1008.
300. Knittler, M.R., et al., MHC class I molecules compete in the endoplasmic reticulum for access to transporter associated with antigen processing. *J Immunol*, 1998. 161(11): p. 5967-77.
301. Hsu, V.W., et al., A recycling pathway between the endoplasmic reticulum and the Golgi apparatus for retention of unassembled MHC class I molecules. *Nature*, 1991. 352(6334): p. 441-4.
302. Storkus, W.J., et al., NK susceptibility varies inversely with target cell class I HLA antigen expression. *J Immunol*, 1987. 138(6): p. 1657-9.
303. Edwards, P.A., et al., A human-hybridoma system based on a fast-growing mutant of the ARH-77 plasma cell leukemia-derived line. *Eur J Immunol*, 1982. 12(8): p. 641-8.
304. Zemmour, J., et al., The HLA-A,B "negative" mutant cell line C1R expresses a novel HLA-B35 allele, which also has a point mutation in the translation initiation codon. *J Immunol*, 1992. 148(6): p. 1941-8.
305. Matsui, M., et al., Genetic evidence for difference between intracellular and extracellular peptides in influenza A matrix peptide-specific CTL recognition. *J Immunol*, 1995. 154(3): p. 1088-96.
306. Howell, D.N., et al., Natural killing target antigens as inducers of interferon: studies with an immunoselected, natural killing-resistant human T lymphoblastoid cell line. *J Immunol*, 1985. 134(2): p. 971-6.
307. Parham, P., Monoclonal antibodies against two separate alloantigenic sites of HLA- B40. *Immunogenetics*, 1981. 13(6): p. 509-27.
308. Little, A.M., E. Nossner, and P. Parham, Dissociation of beta 2-microglobulin from HLA class I heavy chains correlates with acquisition of epitopes in the cytoplasmic tail. *J Immunol*, 1995. 154(10): p. 5205-15.
309. Parham, P., C.J. Barnstable, and W.F. Bodmer, Use of a monoclonal antibody (W6/32) in structural studies of HLA- A,B,C, antigens. *J Immunol*, 1979. 123(1): p. 342-9.
310. Barnstable, C.J., et al., Production of monoclonal antibodies to group A erythrocytes, HLA and other human cell surface antigens-new tools for genetic analysis. *Cell*, 1978. 14(1): p. 9-20.
311. Hammerling, G.J., U. Hammerling, and L. Flaherty, Qat-4 and Qat-5, new murine T-cell antigens governed by the Tla region and identified by monoclonal antibodies. *J Exp Med*, 1979. 150(1): p. 108-16.
312. Ortiz-Navarrete, V. and G.J. Hammerling, Surface appearance and instability of empty H-2 class I molecules under physiological conditions. *Proc Natl Acad Sci U S A*, 1991. 88(9): p. 3594-7.
313. Rigney, E., et al., A soluble major histocompatibility complex class I peptide-binding platform undergoes a conformational change in response to peptide epitopes. *J Biol Chem*, 1998. 273(23): p. 14200-4.
314. Tsomides, T.J., B.D. Walker, and H.N. Eisen, An optimal viral peptide recognized by CD8+ T cells binds very tightly to the restricting class I major histocompatibility complex protein on intact cells but not to the purified class I protein. *Proc Natl Acad Sci U S A*, 1991. 88(24): p. 11276-80.
315. Walker, B.D., et al., Long-term culture and fine specificity of human cytotoxic T-lymphocyte clones reactive with human immunodeficiency virus type 1. *Proc Natl Acad Sci U S A*, 1989. 86(23): p. 9514-8.

316. Ishioka, G.Y., et al., Failure to demonstrate long-lived MHC saturation both in vitro and in vivo. Implications for therapeutic potential of MHC-blocking peptides. *J Immunol*, 1994. 152(9): p. 4310-9.
317. Chung, C.T. and R.H. Miller, A rapid and convenient method for the preparation and storage of competent bacterial cells. *Nucleic Acids Res*, 1988. 16(8): p. 3580.
318. Larsson, M., et al., Requirement of mature dendritic cells for efficient activation of influenza A-specific memory CD8+ T cells. *J Immunol*, 2000. 165(3): p. 1182-90.
319. Reddy, A., et al., A monocyte conditioned medium is more effective than defined cytokines in mediating the terminal maturation of human dendritic cells. *Blood*, 1997. 90(9): p. 3640-6.
320. Ostwald, T.J. and D.H. MacLennan, Isolation of a high affinity calcium-binding protein from sarcoplasmic reticulum. *J Biol Chem*, 1974. 249(3): p. 974-9.
321. Camacho, P. and J.D. Lechleiter, Calreticulin inhibits repetitive intracellular Ca2+ waves. *Cell*, 1995. 82(5): p. 765-71.
322. Trombetta, E.S. and A. Helenius, Lectins as chaperones in glycoprotein folding. *Curr Opin Struct Biol*, 1998. 8(5): p. 587-92.
323. Hughes, E.A. and P. Cresswell, The thiol oxidoreductase ERp57 is a component of the MHC class I peptide-loading complex. *Curr Biol*, 1998. 8(12): p. 709-12.
324. Gao, B., et al., Assembly and Antigen-Presenting Function of MHC Class I Molecules in Cells Lacking the ER Chaperone Calreticulin. *Immunity*, 2002. 16(1): p. 99-109.
325. Day, P.M., Yewdell, J.W., Porgador, A., Germain, R.N. and Bennink, J.R., Direct delivery of exogenous MHC class I molecule-binding oligopeptides to the endoplasmic reticulum by viable cells. *Proc Natl Acad Sci U S A*, 1997. 94: p. 8064-8069.
326. Kavanagh, D.G., et al., The multiple immune-evasion genes of murine cytomegalovirus are not redundant: m4 and m152 inhibit antigen presentation in a complementary and cooperative fashion. *J Exp Med*, 2001. 194(7): p. 967-78.
327. Kavanagh, D.G., U.H. Koszinowski, and A.B. Hill, The murine cytomegalovirus immune evasion protein m4/gp34 forms biochemically distinct complexes with class I MHC at the cell surface and in a pre-Golgi compartment. *J Immunol*, 2001. 167(7): p. 3894-902.
328. Danilczyk, U.G., M.F. Cohen-Doyle, and D.B. Williams, Functional relationship between calreticulin, calnexin, and the endoplasmic reticulum luminal domain of calnexin. *J Biol Chem*, 2000. 275(17): p. 13089-97.
329. Rajagopalan, S. and M.B. Brenner, Calnexin retains unassembled major histocompatibility complex class I free heavy chains in the endoplasmic reticulum. *J Exp Med*, 1994. 180(1): p. 407-12.
330. Sadasivan, B.K., et al., Assembly, peptide loading, and transport of MHC class I molecules in a calnexin-negative cell line. *Cold Spring Harb Symp Quant Biol*, 1995. 60: p. 267-75.
331. Scott, J.E. and J.R. Dawson, MHC class I expression and transport in a calnexin-deficient cell line. *J Immunol*, 1995. 155(1): p. 143-8.
332. Van Leeuwen, J.E. and K.P. Kearse, The related molecular chaperones calnexin and calreticulin differentially associate with nascent T cell antigen

receptor proteins within the endoplasmic reticulum. *J Biol Chem*, 1996. 271(41): p. 25345-9.
333. van Leeuwen, J.E. and K.P. Kearse, Calnexin associates exclusively with individual CD3 delta and T cell antigen receptor (TCR) alpha proteins containing incompletely trimmed glycans that are not assembled into multisubunit TCR complexes. *J Biol Chem*, 1996. 271(16): p. 9660-5.
334. Bagriacik, E.U., A. Kirkpatrick, and K.S. Miller, Glycosylation of native MHC class Ia molecules is required for recognition by allogeneic cytotoxic T lymphocytes. *Glycobiology*, 1996. 6(4): p. 413-21.
335. Neefjes, J.J. and H.L. Ploegh, Allele and locus-specific differences in cell surface expression and the association of HLA class I heavy chain with beta 2-microglobulin: differential effects of inhibition of glycosylation on class I subunit association. *Eur J Immunol*, 1988. 18(5): p. 801-10.
336. Ploegh, H.L., Human histocompatibility antigens. *Hamatol Bluttransfus*, 1983. 28: p. 447-53.
337. Miyazaki, J., et al., Expression and function of a nonglycosylated major histocompatibility class I antigen. *J Exp Med*, 1986. 163(4): p. 856-71.
338. Hart, G.W., The role of asparagine-linked oligosaccharides in cellular recognition by thymic lymphocytes. Effects of tunicamycin on the mixed lymphocyte reaction. *J Biol Chem*, 1982. 257(1): p. 151-8.
339. Jenkins, R.N., et al., Oligosaccharide-dependent and independent Qa-1 determinants. *J Immunol*, 1985. 134(5): p. 3218-25.
340. Shen, L. and K.P. Kane, Differential ability of isolated H-2 Kb subsets to serve as TCR ligands for allo-specific CTL clones: potential role for N-linked glycosylation. *J Exp Med*, 1995. 181(5): p. 1773-83.
341. Goldstein, S.A. and M.F. Mescher, Carbohydrate moieties of major histocompatibility complex class I alloantigens are not required for their recognition by T lymphocytes. *J Exp Med*, 1985. 162(4): p. 1381-6.
342. Barbosa, J.A., et al., Site-directed mutagenesis of class I HLA genes. Role of glycosylation in surface expression and functional recognition. *J Exp Med*, 1987. 166(5): p. 1329-50.
343. Nakamura, K., et al., Functional specialization of calreticulin domains. *J Cell Biol*, 2001. 154(5): p. 961-72.
344. Atreya, C.D., N.K. Singh, and H.L. Nakhasi, The rubella virus RNA binding activity of human calreticulin is localized to the N-terminal domain. *J Virol*, 1995. 69(6): p. 3848-51.
345. Leung-Hagesteijn, C.Y., et al., Cell attachment to extracellular matrix substrates is inhibited upon downregulation of expression of calreticulin, an intracellular integrin alpha-subunit-binding protein. *J Cell Sci*, 1994. 107(Pt 3): p. 589-600.
346. Kovacs, H., et al., Evidence that C1q binds specifically to CH2-like immunoglobulin gamma motifs present in the autoantigen calreticulin and interferes with complement activation. *Biochemistry*, 1998. 37(51): p. 17865-74.
347. Peterson, J.R. and A. Helenius, In vitro reconstitution of calreticulin-substrate interactions. *J Cell Sci*, 1999. 112(Pt 16): p. 2775-84.
348. Santini, M.P., et al., Cross talk among calcineurin, Sp1/Sp3, and NFAT in control of p21(WAF1/CIP1) expression in keratinocyte differentiation. *Proc Natl Acad Sci U S A*, 2001. 98(17): p. 9575-80.

349. Sambrook, J.F., The involvement of calcium in transport of secretory proteins from the endoplasmic reticulum. *Cell*, 1990. 61(2): p. 197-9.
350. Lodish, H.F., N. Kong, and L. Wikstrom, Calcium is required for folding of newly made subunits of the asialoglycoprotein receptor within the endoplasmic reticulum. *J Biol Chem*, 1992. 267(18): p. 12753-60.
351. Baksh, S., et al., Interaction of calreticulin with protein disulfide isomerase. *J Biol Chem*, 1995. 270(52): p. 31338-44.
352. Putney, J.W., Jr. and R.R. McKay, Capacitative calcium entry channels. *Bioessays*, 1999. 21(1): p. 38-46.
353. Michalak, M., et al., Endoplasmic reticulum form of calreticulin modulates glucocorticoid- sensitive gene expression. *J Biol Chem*, 1996. 271(46): p. 29436-45.
354. Androlewicz, M.J., The role of tapasin in MHC class I antigen assembly. *Immunol Res*, 1999. 20(2): p. 79-88.
355. Spee, P. and J. Neefjes, TAP-translocated peptides specifically bind proteins in the endoplasmic reticulum, including gp96, protein disulfide isomerase and calreticulin. *Eur J Immunol*, 1997. 27(9): p. 2441-9.
356. Basu, S. and P.K. Srivastava, Calreticulin, a peptide-binding chaperone of the endoplasmic reticulum, elicits tumor- and peptide-specific immunity. *J Exp Med*, 1999. 189(5): p. 797-802.
357. Nair, S., et al., Calreticulin displays in vivo peptide-binding activity and can elicit CTL responses against bound peptides. *J Immunol*, 1999. 162(11): p. 6426-32.
358. Pentcheva, T. and M. Edidin, Clustering of peptide-loaded MHC class I molecules for endoplasmic reticulum export imaged by fluorescence resonance energy transfer. *J Immunol*, 2001. 166(11): p. 6625-32.
359. Li, S., et al., Peptide-bound major histocompatibility complex class I molecules associate with tapasin before dissociation from transporter associated with antigen processing. *J Biol Chem*, 1999. 274(13): p. 8649-54.
360. Yamamoto, K., et al., The KDEL receptor mediates a retrieval mechanism that contributes to quality control at the endoplasmic reticulum. *Embo J*, 2001. 20(12): p. 3082-91.
361. Oliver, J.D., et al., Interaction of the thiol-dependent reductase ERp57 with nascent glycoproteins. *Science*, 1997. 275(5296): p. 86-8.
362. Rupp, K., et al., Effects of CaBP2, the rat analog of ERp72, and of CaBP1 on the refolding of denatured reduced proteins. Comparison with protein disulfide isomerase. *J Biol Chem*, 1994. 269(4): p. 2501-7.
363. Oliver, J.D., et al., ERp57 functions as a subunit of specific complexes formed with the ER lectins calreticulin and calnexin. *Mol Biol Cell*, 1999. 10(8): p. 2573-82.
364. Wang, H., et al., Ab initio association with beta 2-microglobulin during biosynthesis of the H-2Ld class I major histocompatibility complex heavy chain promotes proper disulfide bond formation and stable peptide binding. *J Biol Chem*, 1994. 269(35): p. 22276-81.
365. Williams, D.B. and T.H. Watts, Molecular chaperones in antigen presentation. *Curr Opin Immunol*, 1995. 7(1): p. 77-84.
366. Vassilakos, A., et al., The molecular chaperone calnexin facilitates folding and assembly of class I histocompatibility molecules. *Embo J*, 1996. 15(7): p. 1495-506.

367. Otsu, M., et al., A possible role of ER-60 protease in the degradation of misfolded proteins in the endoplasmic reticulum. *J Biol Chem*, 1995. 270(25): p. 14958-61.
368. Urade, R. and M. Kito, [Protein degradation in endoplasmic reticulum]. *Tanpakushitsu Kakusan Koso*, 1997. 42(14 Suppl): p. 2342-7.
369. Urade, R., et al., Functions of characteristic Cys-Gly-His-Cys (CGHC) and Gln-Glu-Asp-Leu (QEDL) motifs of microsomal ER-60 protease. *J Biochem (Tokyo)*, 1997. 122(4): p. 834-42.
370. Glithero, A., et al., Crystal structures of two H-2Db/glycopeptide complexes suggest a molecular basis for CTL cross-reactivity. *Immunity*, 1999. 10(1): p. 63-74.
371. Speir, J.A., et al., Crystal structure of an MHC class I presented glycopeptide that generates carbohydrate-specific CTL. *Immunity*, 1999. 10(1): p. 51-61.
372. Diedrich, G., et al., A role for calnexin in the assembly of the MHC class I loading complex in the endoplasmic reticulum. *J Immunol*, 2001. 166(3): p. 1703-9.
373. Dick, T.P. and P. Cresswell, Thiol oxidation and reduction in Major Histocompatibility Complex class I-restricted antigen processing and presentation. *Methods Enzymol*, 2002. 348: p. 49-54.